UNIVERSIDADE DA BEIRA INTERIOR
Engenharia

Clear-water scour at single piers and pile groups

Rui Miguel Madeira Lança

Tese para obtenção do Grau de Doutor em
Engenharia Civil
(3º ciclo de estudos)

Orientadora: Professora Doutora Cristina Maria Sena Fael
Co-orientador: Professor Doutor António Heleno Cardoso

Covilhã, Fevereiro de 2013

Acknowledgements

I express special appreciation to my advisors, Professor Cristina Fael and Professor António Cardoso, for their assistance, guidance and supervision during this research. Thanks to the members of the research project "Experimental study of local scour at complex bridge piers", Fernando Veloso Gomes, João Rocha, João Pêgo, Lúcia Couto, Mário Moreno, Rodrigo Maia and also to Roger Bettess for their help during the development of the study.

Sincere acknowledge is given to the Portuguese Foundation for Science and Technology for the financial support through the PhD grant SFRH/BD/49296/2008 and the research project PTDC/ECM/101353/2008.

Special thanks are extended to Jorge Barros, Hydraulics Laboratory technician, for the assistance during experimental tests.

The author also wishes to thank his family, for their continuous encouragement and moral support in many ways.

This study would not have been possible without the encouragement, patience, support and dedication of all those mentioned above.

Abstract

The major damage to bridges at river crossings occurs during floods. Damage is caused for various reasons, one of the main reasons being the riverbed scour at bridge foundations. Local scour is induced by the flow field generated around piers typically inserted in movable bed rivers. In Portugal, the tragic accident of Entre-os-Rios was mostly due to scour at one of the bridge piers.

Physical and economic reasons lead to bridge foundations composed of a pier column founded on a pile cap, supported by an array of piles. Piers of this configuration are known as complex piers. Frequently the pile cap is completely buried, or in opposition, above the water, being the column or the pile group respectively the only structural element interacting with the flow and causing local scour. In modern bridges it is also common to find structural solutions where the deck is supported directly by pile groups composed of only one alignment, without pile cap. For scouring proposes the structural elements may be considered as single piers, pile groups and pier alignments.

The construction of new bridges and the maintenance of thousands of bridges built before the main developments in local scour prediction, amount to costs of billions of Euro and justifies a rigorous prediction of the scour depth, both for economic and safety of human lives reasons.

The present study develops an extensive research to systematically map equilibrium scour at single cylindrical piers and pile groups and relate the observations with the characteristic variables of the tests. Special attention is given to the effect of time, relative sediment size and relative approach flow depth at single cylindrical piers and spacing, skew-angle, number of columns and time at pile groups. The pertinence of considering the effect of viscosity it is also assessed.

Using dimensional analysis, the following major conclusions are achieved. Regarding single cylindrical piers, it is discussed the required duration of the laboratory tests to render reliable equilibrium scour depths and it is confirmed that equilibrium scour depth decreases with the relative sediment size. It is suggested a predictor for the equilibrium scour depth at single cylindrical piers, function of relative sediment size and relative approach flow depth. The parameters of the equation suggested by Franzetti *et al.* (1982) are fully characterized rendering a predictor of the scour depth time evolution. Regarding pile groups and pier alignments, it is assessed the effect of the test duration on the equilibrium scour depth and it is confirmed that the spacing factor and the factor for the number of aligned rows recommended in the predictors commonly used in engineering practice are reliable since the scour depth at single cylindrical piers and pile groups remain essentially self-similar in time.

The prediction of the equilibrium scour depth at pile groups is improved by the suggestion of a aggregate pile group factor, function of the pile spacing, skew-angle and number of parallel pile alignments. Finally it is revealed that the viscosity may affect scouring in laboratory tests.

Keywords

piers, pile groups, pier alignments, complex pier, scour depth, time, flow shallowness, sediment coarseness.

Resumo

Os principais danos em pontes ocorrem em cenários de cheias. Os danos são causados por diversas razões, sendo a principal a erosão do leito do rio no local das fundações da ponte. A erosão localizada é induzida pelo campo de escoamento gerado em torno dos pilares, tipicamente localizados em fundos de leito móvel. Em Portugal, o acidente de Entre-os-Rios, ocorreu em parte devido à erosão localizada em um dos pilares.

Razões físicas e económicas determinam que com frequência os pilares de pontes sejam compostos por coluna, maciço de encabeçamento e grupo de estacas. Pilares com esta configuração são designados por pilares complexos. É comum encontrar casos onde o maciço de encabeçamento está completamente enterrado, ou em oposição, está acima da superfície do escoamento, com a coluna ou o grupo de estacas, respectivamente, sendo o único elemento estrutural interagindo com o escoamento e provocando erosões localizadas. Nas pontes modernas também é comum encontrar soluções estruturais em que o tabuleiro é suportado directamente por grupos de estacas compostos por um único alinhamento, sem o maciço de encabeçamento. Para a analise da erosão os elementos estruturais são considerados pilares isolados, grupos de estacas e alinhamentos de pilares, respectivamente.

A construção de novas pontes e a manutenção de milhares de pontes construídas antes dos principais desenvolvimentos na previsão da profundidade de cavidades de erosão, somam custos de biliões de Euros e justificam a previsão rigorosa da profundidade de erosão, por razões económicas e de segurança de vidas humanas.

O presente estudo apresenta uma extensa campanha experimental que sistematicamente caracteriza as profundidades de equilíbrio da cavidade de erosão em pilares isolados e grupos de estacas, relacionando as observações com as variáveis características dos ensaios. É dada atenção à caracterização do efeito do tempo, tamanho relativo do sedimento e profundidade relativa do escoamento de aproximação em pilares cilíndricos isolados e ao efeito do espaçamento, enviesamento, numero de colunas e tempo em grupos de estacas. Também é analisada a importância de considerar o efeito da viscosidade.

Com base na analise dimensional, são obtidas as seguintes conclusões. No âmbito dos pilares cilíndricos isolados, é analisada a duração mínima de ensaios laboratoriais para obter com rigor as profundidades de equilíbrio das cavidades de erosão e é comprovado que a profundidade de equilíbrio decresce com o aumento da dimensão relativa do sedimento. É proposto um modelo de previsão da profundidade de equilíbrio da cavidade de erosão, função da dimensão relativa do sedimento e da profundidade relativa do escoamento de aproximação. A previsão da evolução temporal é conseguida pela caracterização dos parâmetros da equação de Franzetti *et al.* (1982). Em relação aos grupos de estacas e

alinhamentos de pilares, é analisado o efeito da duração dos ensaios na profundidade de equilíbrio da cavidade de erosão e confirma-se que o coeficiente do espaçamento e do número de linhas recomendados pelos métodos mais utilizados na prática da engenharia são fiáveis porque a profundidade de erosão em pilares cilíndricos isolados e em grupos de estacas é aproximadamente semelhante no tempo. É dado um contributo na previsão da profundidade de erosão em grupos de estacas através da proposta de um coeficiente agregado função do espaçamento entre estacas, ângulo de enviesamento e numero de colunas. Finalmente é revelado que a viscosidade pode influenciar o processo erosivo em ensaios laboratoriais.

Palavras-chave

pilares, grupo de estacas, alinhamento de pilares, pilar complexo, profundidade de erosão, tempo, profundidade relativa do escoamento, dimensão relativa do sedimento.

Table of contents

List of figures

List of Tables

List of symbols

a_1, a_2	Franzetti *et al.* (1989) model coefficients;
b_1, b_2	constants;
B	channel width;
B'	constant of integration of the logarithm law of the wall;
C_1, C_2, C_3	constants;
d	approach flow depth;
d_s	scour depth at instant t;
d_{se}	equilibrium scour depth;
d_{se1}	equilibrium scour depth at an isolated pile or pier subjected to the same hydrodynamic conditions;
d_{sg}	maximum scour at pier or pile group at instant t;
d_{sge}	pier or pile group equilibrium scour depth;
D_p	pier or pile diameter;
D_{pg}	pier or pile group equivalent diameter;
D_x	diameter for which x% by weight of a sediment mixture is smaller than that a given mesh size of the mechanical sieve;
$D_{15.9}$	diameter for which 15.9% by weight of a sediment mixture is smaller than that a given mesh size of the mechanical sieve;
D_{50}	median grain size;
$D_{84.1}$	diameter for which 84.1% by weight of a sediment mixture is smaller than that a given mesh size of the mechanical sieve;
Fr	Froude number;
Fr_d	densimetric Froude number;
$Fr_{d\beta}$	densimetric particle Froude number of scour entrainment;
g	acceleration of gravity;
g'	submerged specific weight;
G	free space between piles;
k	height of grain roughness;
K_3	factor for bed condition;
K_4	factor for armouring;
K_d	relative flow depth factor;
K_{dDp}	flow shallowness factor according to Richardson and Davis (2001);
K_{dpg}	pile group submergence ratio factor;
K_{D50}	relative sediment size factor;
K_g	factor describing the geometry of the channel cross-section;
K_{gs}	pile group shape factor;
$K_{g\alpha}$	skew-angle factor for a group of piles;
K_I	flow intensity factor;
K_m	factor describing the number of piles aligned with the approach flow;
K_{pg}	pile group factor;
K_{pgw}	pile group factor associated with W_g;
K_s	pile or pier shape factor;
K_{sp}	pile group spacing factor;
K_{smn}	factor to correct the scour depth predictions at pile groups according Ataie-Ashtiane and Beheshti (2006);
K_α	pier skew-angle factor;
K_t	time factor;
$K\sigma_D$	factor for the effect of sediment gradation;
L	pier length;
m	number of piers in the alignment or rows in the pile group;
n	number of pile alignments (or columns) in the group;
N	pier shape factor;
p_1, p_2, p_3, p_4, p_5 and p_6	parameters obtained by regression analysis;
Q	flow-discharge;
r	determination coefficient;

R	hydraulic radius;
Re	Reynolds number;
Re_p	pier Reynolds number;
Re_s	shear Reynolds number;
Re_U	approach velocity sediment Reynolds number;
s	pier or pile spacing;
S_f	slope of the energy line;
S_0	channel bottom slope;
t	time;
t_C	time to equilibrium according Cardoso and Bettess (1999);
t_d	test duration;
t_F	time to equilibrium according Franzetti *et al.* (1994);
t_G	time to equilibrium according Grimaldi (2005);
t_K	time to equilibrium according Kothyary *et al.* (2007);
t_M	time to equilibrium according Melville and Chiew (1999);
t_r	truncated test duration;
T	non-dimensional time or temperature;
T_e	non-dimensional time at which equilibrium is attained;
u	approach flow velocity;
u_*	approach flow friction velocity;
u_{*c}	critical bed shear velocity for sediment entrainment;
U	average approach flow velocity;
U_c	average approach flow velocity for the threshold condition of sediment entrainment;
W_g	sum of the non-overlapping individual pile widths projected on a plane normal to the approach flow;
Z	dimensionless scour depth according to Oliveto and Hager (2002, 2005);
z_R	reference scour depth according to Oliveto and Hager (2002, 2005);
α	skew-angle;
β'	Coriolis coefficient;
β, β_w, γ, γ_w, δ and δ_w	constants;
χ	parameter function of k/δ';
δ'	thickness of the viscous sub-layer;
Δ	submerged density of the bed material;
Δd_s	increment of scour depth;
ΔK_{pg}	relative deviation of the pile group factor;
Δp	pressure change;
γ	fluid specific weight;
φ, φ_1, φ_2, φ_3	function;
ν	kinematic viscosity;
ρ	fluid density;
ρ_s	sediment density;
σ_D	gradation coefficient of the bed material;
τ_0	average total bed shear stress;
τ_c	average critical bed shear stress of initiation of sediment motion;
ξ	constant.

1. INTRODUCTION

1.1 Background

Local scour is defined as the erosion of the streambed around an obstruction inserted in a flow field over mobile bed. This phenomenon may affect the structural integrity of bridges and hydraulic structures, causing failure by foundation undermining and structural instability.

Local scour around bridge piers continues to be one of the most common causes of bridge failures. The presence of a bridge pier in the flow modifies the velocity field, increases the sediment entrainment capacity and originates scour. The combined effects of 3D flow patterns and time-dependent scour development make the phenomenon complex and difficult to assess.

The high number of structures on alluvial beds, most of them built before the most recent advances on local scour prediction, leads to an increasing number of bridge failures. In the United States of America there are approximately 500 000 bridges and, since 1950, approximately 1000 have collapsed. Sixty percent of those failures were due to streambed instability: long-term streambed aggradation or degradation, general scour, local scour or lateral migration. The following important cases of bridge failures due to scour can be reported in the USA: *i*) bridge over the Arroyo Pasajero, California – seven people were killed in 1955 due to the bridge collapse; *ii*) Thruway bridge, crossing Schoharie Creek, New York State – collapsed in 1987 with the loss of ten lives; *iii*) bridge over the Hatchie River near Covington, Tennessee – failed in 1989 and eight people were killed; *iv*) Great Miami River bridge, Miamitown, Ohio – two people were killed in 1989 due to the collapse of the spans. The 1993 flood in the upper Mississippi basin caused 23 bridge failures and an estimated damage of 15 million USD. The total loss of the Georgia Department of Transportation was approximately 130 million USD because more than 100 bridges had to be replaced and repaired due to flooding from tropical storm Alberto, in Georgia, in 1994.

In New Zealand, several bridge failures due to scour have been reported: *i*) Bulls road bridge crossing the Rangitikei River – opened in 1949 and failed due to local scour in 1973; *ii*) Mahitahi river road bridge, crossing river Mahitahi – failed due to contraction and confluence scour in 1955; *iii*) Blackmount road bridge, crossing river Mararoa – failed due to local scour in 1980.

In Portugal, scouring has also been a cause of bridge failure. The following cases can be mentioned in recent years: *i*) Penacova bridge, Penacova – the displacement of the central pier in 1983 caused the partial failure of the steel bridge roadway; *ii*) Gafanha bridge, Aveiro – local scour on central piers in 1994; *iii*) EN122 bridge over Foupana stream – pier displacement due to local scour in 2000; *iv*) Bridge over Sorraia River – abutment failure in 2001; *v*) Hintze Ribeiro bridge, Entre-os-Rios – pier and tray failure due to scour, causing 59 casualties in 2001.

Failure prevention of bridge foundations is the motivation to better understand the scouring process and achieve better accuracy in scour prediction. Under-prediction of scour depth may lead to bridge failure while over-prediction usually leads to waste of resources.

Many studies on scour at single piers have been concluded since the pioneer research of Chabert and Engeldinger (1956), but some aspects are yet to be resolved, as shown by the various contradictions reported in the literature. Raudkivi and Ettema (1983) and Hoffmans and Verheij (1997) pointed out that structural design of bridges is well established, but in contrast, there is no unifying theory, at present, and the designer can not predict, with confidence, the scour depth at bridge piers. In spite of the high number of theoretical and experimental studies, some problems remain unsolved due to difficulties in characterizing scouring mechanisms and scaling laboratory tests. Scouring depends on many variables and the available knowledge on the effect of each one differs with the type of obstacle and the variable itself. At present, a major concern is the definition of the equilibrium scour depth and the time required to attain the equilibrium state. Since the work of Chabert and Engeldinger (1956) it is accepted that the equilibrium scour depth is attained asymptotically with time; however, the concept of equilibrium scour depth is subjective and different authors suggest different definitions. For this reason, the pertinence of existing approaches to assess the onset of the equilibrium phase of scour at single cylindrical piers in experimental studies is investigated.

Another research concern is the understanding for the reason why the predictions of the equilibrium scour depth, based on formulations developed through laboratory experiments, tend to over-estimate the field values. One possible reason is the effect of the relative sediment size or sediment coarseness. For decades, most investigators (*e.g.* Ettema 1980; Melville and Coleman 2000) reported that the relative sediment size had no influence on scour depth for values of this parameter greater than ~25 – 50. Recently, Sheppard *et al.* (1995, 1999, 2004) carried out laboratory tests for very low values of the relative sediment size and concluded for a drastic influence of this parameter on the equilibrium scour depth. In the present study, the effects of the flow shallowness, relative sediment size and time on the scour depth time evolution are investigated.

For major river crossings, there is increasing use of bridge foundations that consist of a number of piles supporting a pile cap. The foundations of the piles are often deep but if the piles rely on skin friction, rather than end-loading, to support the weight of the bridge, the foundations can

be vulnerable to scour. There have been a number of recent bridge failures caused by scour at pile groups. This study focuses on local scour at pile groups whose piles are only partly submerged, *i.e.*, at complex piers whose pile caps are out of the water. Pile groups may be composed of one or more alignments – or columns – of piles. Pile groups composed of only one such column are frequently used, without pile cap, to directly sustain bridge decks. For this reason, this special group configuration is also named pier alignment herein.

The number of studies on scouring at pile groups is comparatively small and most of them have used fine sand, prone to the formation of ripples in the approach flow reach, and have reported short duration tests where the equilibrium state may not have been attained. Since the pioneer studies of Laursen and Toch (1956) and Hannah (1978), few sound scour depth predictors have been suggested. Among them, there are those authored by Melville and Coleman (2000), Richardson and Davis (2001) and Sheppard and Renna (2005, 2010). However, these predictors have been developed on the basis of tests with rather short duration as compared to the time needed to sufficiently approach the equilibrium scour depth. Consequently, the conclusions from the mentioned studies on scouring at pile groups may not guarantee accurate predictions of the equilibrium scour depth. For this reason, the effects of pile spacing, skew-angle and number of rows per column or alignment of the pile group on the maximum scour depth are investigated herein, special attention being given to the effect of time.

During the last few decades, most authors considered that the flow inside scour holes is fully rough and viscosity does not play any important role in the scouring process. Consequently, the Reynolds number is usually eliminated from the list of non-dimensional parameters in scour studies. However pioneer studies of Shen *et al.* (1966, 1969) and Nicollet and Ramette (1971) seem to indicate that some effects of viscosity may prevail in laboratory studies. Possibly due to difficulties associated with the small size of laboratory facilities, this effect may have been overlooked. For this reason, the effect of viscosity is revisited in this work.

1.2 Objectives

The general objective of this study is to contribute for the understanding and characterization of local scour at single cylindrical piers as well as at pile groups. These objectives are detailed as follows:

i) production of high quality data on clear-water local scour at single cylindrical piers and pile groups;

ii) investigation on the pertinence of existing approaches to assess the onset of the equilibrium phase of scour at single cylindrical piers in experimental studies;

iii) revision of the influence of the relative sediment size and flow shallowness on equilibrium scour depth at single cylindrical piers;

iv) improvement of the scour depth time evolution modelling at single cylindrical piers;

v) characterization of the effect of pile spacing, skew-angle, time and number of pile group columns on the maximum scour depth at pile groups composed of four cylindrical pile rows;

vi) improvement of the scour depth modelling at groups of cylindrical piles;

vii) assessment of the effect of viscosity on the scouring process.

1.3 Synopsis

This thesis is organized in nine chapters – including the Introduction – and three appendices. Chapters 1, 2, 3 and 9 are written according to the classical thesis format; chapters 4 and 6 reproduce the contents of two conference papers; chapters 5 and 7 are written in paper format and have already been submitted to a prestigious scientific journal; chapter 8 is the embryo of a future paper to be completed and submitted after special experiments are made. The contents of the chapters and appendices are described next.

Chapter 2 (Literature review) is an attempt to present the current state of the art on local scour at single cylindrical piers and pile groups, with special emphasis on the flow structure, characteristic variables and non-dimensional parameters affecting local scouring and scour depth prediction at single cylindrical piers and pile groups.

Chapter 3 (Experimental setup, measuring equipment and procedure), describes two experimental facilities (two flumes) and the measuring equipment used in the present study. It also includes the adopted procedures in the study. The contents of this chapter are partly reproduced in chapters 5 to 8 since these are self contained papers, where experimental details are unavoidable. It should be noticed here that a third flume was used for a small number (five) of experiments exploited in the dissertation through made before. For this reason, the short description of the third flume is restricted to chapter 4, where the corresponding results are presented and discussed.

Chapter 4 (Assessing equilibrium clear-water scour around single cylindrical piers) presents the results of long-lasting tests[(1)] used to investigate the pertinence of existing approaches to assess the onset of the equilibrium phase of scour at single cylindrical piers in laboratory tests. This chapter corresponds to the conference paper whose reference is Lança, R., Fael, C. and Cardoso, A. H. (2010) — "Assessing equilibrium clear-water scour around single cylindrical piers", *Proceedings of River Flow 2010*, Dittrich *et al.* (editors), 1207 – 1213.

[(1)] The used tests were run in a small flume of the University of Beira Interior (UBI) and correspond to existing data that had not been analysed or published. The brief description of the UBI small flume is included in Chapter 4.

In Chapter 5 (Clear-water scour at comparatively large cylindrical piers), the results of thirty eight tests on scouring at single cylindrical piers, run for the present study, are analysed with the objective of investigating the effect of the relative sediment size and flow shallowness on the equilibrium scour depth. A predictor of equilibrium scour depth is suggested and the scour depth time evolution modelling is improved by making use of the exponential function suggested by Franzetti *et al.* (1982). This chapter was submitted to the Journal of Hydraulic Engineering under the title "Clear-water scour at comparatively large cylindrical piers".

In Chapter 6 (Effect of spacing and skew-angle on clear-water scour at pier alignments), the results of twenty six laboratory tests (run in this study) are used to describe the scour depth time evolution at pier alignments. The effect of the skew-angle and pier spacing is established and the dependence of the traditional group factor on the same variables is defined. The predictions of two methods used in engineering practice are evaluated. This chapter corresponds to the conference paper whose reference is Lança, R., Fael, C., Maia, R., Pêgo, J. and Cardoso, A. H. (2012) — "Effect of spacing and skew-angle on clear-water scour at pier alignments", *Proceedings of River Flow 2012*, Muñoz, R. (editor), 927 – 933.

Chapter 7 (Clear-water scour at pile groups) deals with the results of seventy five long-lasting laboratory tests on scouring at pile groups and five reference tests at single piers. All these tests were run with the propose of *i*) characterizing the impact of the test duration on the scour depth, *ii*) assessing the precision of coefficients involved in current predictors, *iii*) identifying the most unfavourable skew-angle, *iv*) characterizing the behaviour of "collapsed" pile groups, *v*) identifying the maximum scour depth at pile groups composed of a single column (pier alignment) and testing the performance of two current predictors of scour depth at pile groups. Two formulations of a predictor for the calculation of an aggregated pile group factor are suggested. This chapter was also submitted to the Journal of Hydraulic Engineering under the title "Clear-water scour at pile groups".

Chapter 8 (Effect of viscosity on the equilibrium scour depth at single cylindrical piers) investigates the viscous effects on scouring at single piers by making use of five tests specially designed to vary the approach flow Reynolds number (and others forms of non-dimensional viscosity), while the other non-dimensional parameters are kept constant. This chapter is written in the form of a future technical note to be completed after another three laboratory tests and two full scale tests are performed.

Chapter 9 (Conclusions and future works) summarizes the most relevant conclusions of the present study, identifies additional open questions and recommends topics for future research.

One of the specific objectives of the present work was the production of high quality scour data. These data are available in three appendices. Each appendix reports the characteristic control variables, the equilibrium scour depth, the scour depth time evolution records and the scour

hole patterns of the laboratory tests. Appendix A includes data of scour tests at single cylindrical piers, Appendix B reports the data on scouring at pile groups and Appendix C covers the scour tests specially designed to isolate the effect of viscosity.

2. LITERATURE REVIEW

2.1 Introduction

This chapter presents the review of the most relevant literature on local scour at single piers and pile groups. The text includes the state of the art on the flow structure and the effect of characteristic variables on the scour process and describes the most up-to-date predictors of local scour at single cylindrical piers and pile groups.

2.2 Flow structure around single cylindrical piers

When a unidirectional flow is partially obstructed by a bridge pier, the flow patterns near the pier is significantly modified. The shear stress distribution around the pier is strongly changed, potentially resulting in scour around the pier, which, in turn, also changes the flow and shear stress patterns.

Detailed investigations of the flow patterns around a single cylindrical pier have been reported by Hjorth (1975), Melville (1975), Dargahi (1987), Dey and Raikar (2007), among others. The main features of the flow field are the bow wave, down-flow, horse-shoe vortex and wake vortices. The flow stagnation in front of the pier changes the pressure gradient and produces the down-flow. At the pier base, the down-flow separates and rolls up to form a large helical flow, named the horse-shoe vortex, which bends along the sides of the pier and keeps the maximum down-flow velocity inside the scour hole close to the pier (Raudkivi 1986). A bow wave appears in the free surface adjacent to the pier at the upstream side, rotating in the opposite direction of the horse-shoe vortex. The stagnation pressure gradient also accelerates the flow past the cylinder, resulting in flow separation at the sides of the cylinder and creating wake vortices at the interface with the undisturbed approach flow (Dey *et al.* 1992). Increased velocities in front and sides of the pier increase the flow capacity to entrain sediment particles and produce the scour hole. Figure 2.1 presents the approach flow pressure distribution and velocity field in modification in front of a pier. In the figure, d = approach flow depth; u = approach flow velocity; g = acceleration of gravity; β' = Coriolis coefficient; ρ = fluid density; γ = fluid specific weight; Δp = pressure change).

Behind the pier, wake vortices are convected downstream and sediment particles are lifted due to pressure fluctuations (Melville 1975). The intensity of wake vortices strongly diminishes with the downstream distance from the pier, causing material deposition downstream.

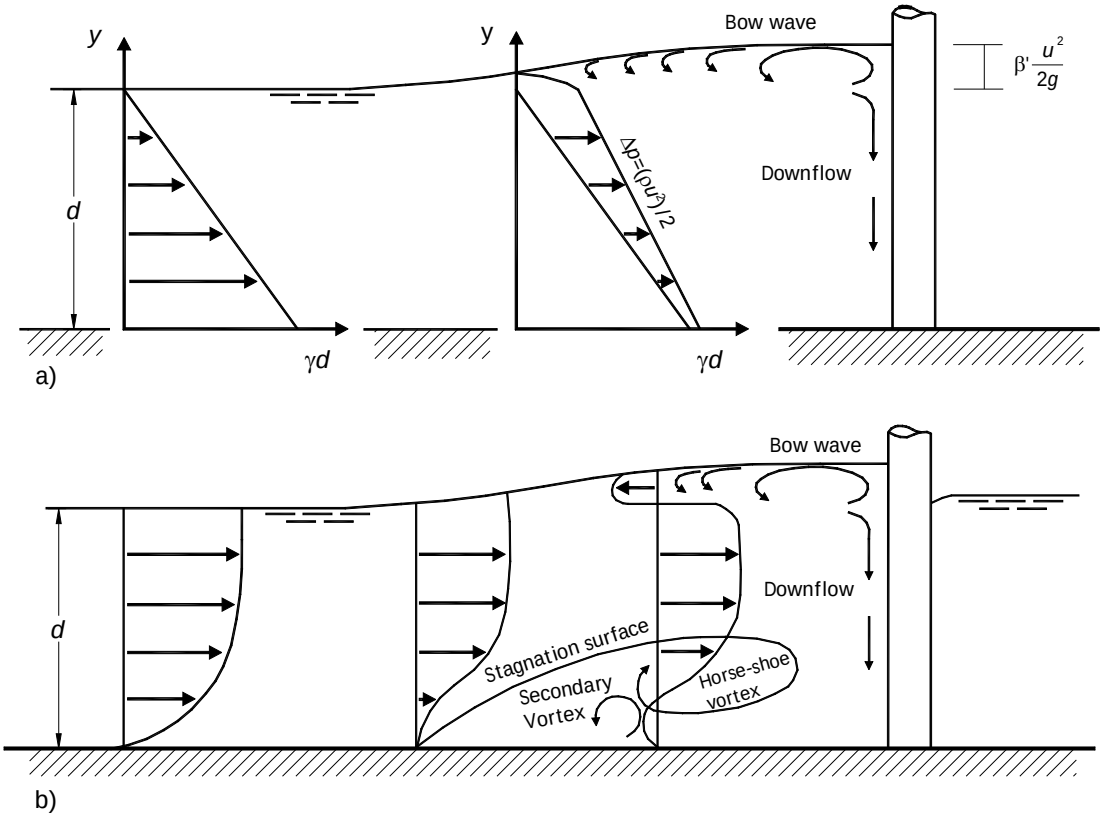

Figure 2.1 – Approach flow in front of a pier: a) pressure; b) velocity

2.3 Flow structure and local scour at pile groups

Local scouring at submerged and partly submerged pile groups has already been addressed in the past. Pile groups are composed of matrical arrangements of *n* columns and *m* rows. The piers are spaced of *s* (center to center) and the pile group may display a skew-angle to the approach flow, α. The diameter of each elemental pile is D_p (*cf.* Figure 2.2). For $n = 1$, non-submerged pile groups constitute pier alignments that can be used to directly support a bridge deck.

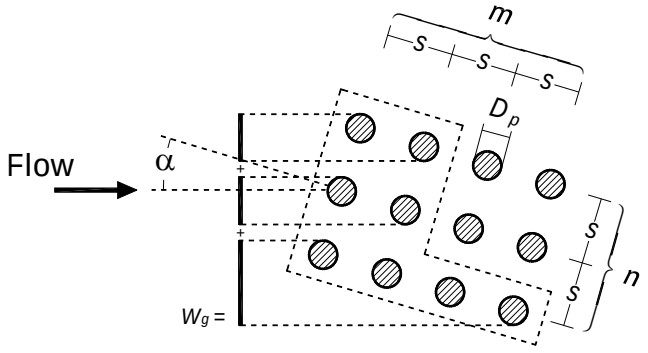

Figure 2.2 – Characteristic variables of a pile group

Laursen and Toch (1956) carried out pioneer studies on the scour interference at two piers. They have concluded that when two piers are placed one in front of the other, or with small skew-angles to the approach flow ($0^o \leq \alpha \leq 10^o$), the rear pier is sheltered by the front pier and, consequently, a smaller scour depth is observed at the rear pier (see Figure 2.3). As the angle increases, the protection is lost and the downstream pier is exposed to the wake vortices from the upstream pier. This shifts the region of deepest scour to the downstream hole. Then, at higher angles, the interference practically disappears. The observations of Laursen and Toch (1956) were based on experiments lasting 3 hours, where equilibrium scour depth could not be attained. However, they are a comparative measure of scour patterns as a function of the relative positioning of the piers.

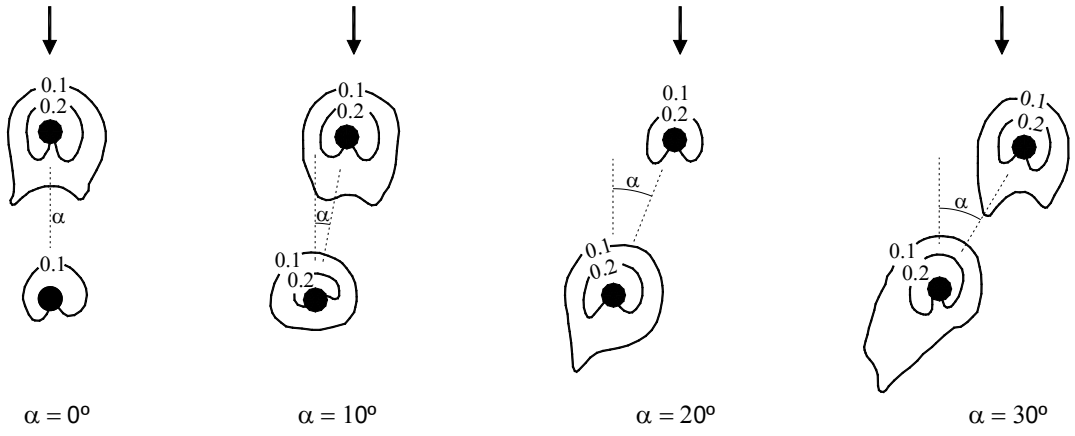

Figure 2.3 – Scour hole at two cylindrical piers with interference, after Laursen and Torch (1956)

Hannah (1978) conducted experiments on a pier alignment (n = 1) with various spacings and with different skew-angles. The experiments lasted 7 hours, after which the author claimed that 80% of the equilibrium scour depth was attained. Figures 2.4 and 2.5 illustrate four processes, first identified by Hannah (1978), that are not present in scouring at a single piers:

i) Scour reinforcement, in which case sediment particles lifted from the base of the first scour hole but not entrained, are easily entrained by the flow when the scour hole near the rear pier deepens the bed level at the rear of the front pier. As the pier spacing increases, the reinforcing effect diminishes. This process is illustrated in Figure 2.4 at time, $t = t_2$.

ii) Sheltering: the front pier causes the reduction of the approach velocity at the rear pier. This reduction weakens the horse-shoe vortex at the rear pier and reduces its scour hole depth. Sheltering may also occur when the bed material dislodged from scour hole at front piers is deposited in front of a rear pier and the flow streamlines are deflected upwards, as illustrated in Figure 2.4 at time, $t = t_1$. This process diminishes the strength and effectiveness of the horse-shoe vortex. As pier spacing increases the sheltering effect tends to become negligible.

iii) Wake vortices interaction, which occurs due to the convection of wake vortices from the front piers. If the rear pier is close, the velocity of the vortices and pressure distribution may lead to sediment lifting at the rear pier. The scouring caused by the wake vortices is a function of convection speed and distance between the vortices path and the downstream piers. At specific skew-angles, the rear piers are closer to the most energetic paths traced by the wake vortices from the front piers and scour increases.

iv) Compressed horse-shoe vortices: in pier alignments transverse to the approach flow, except at very close spacing, each pier has its own horse-shoe vortex. As pier spacing decreases, the inner arms of the horse-shoe vortices are compressed, velocities within the arms increase and scour depths tend to increase (see Figure 2.5).

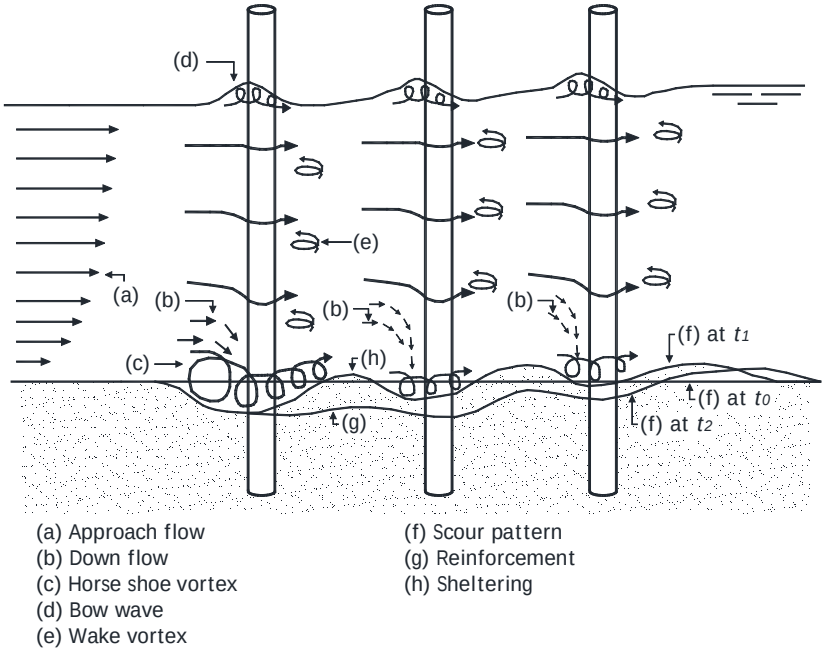

Figure 2.4 – Flow and scour patterns at a pier alignment for α = 0º

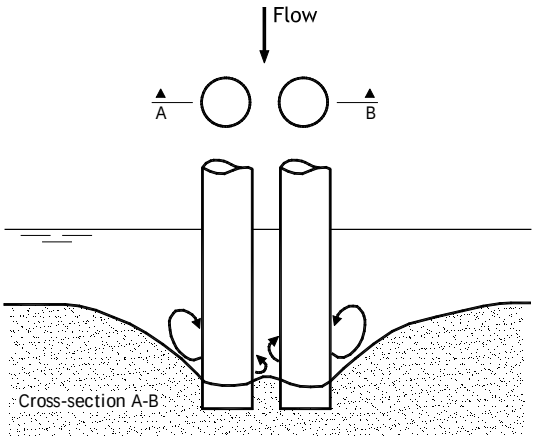

Figure 2.5 – Horse-shoe vortex compressed arms between two piers transverse to the approach flow

Zhao and Sheppard (1999) carried out tests at pile groups, using cylindrical and square piles of 3 parallel alignments – or columns – of 8 piles each. Tests lasted 26 hours, after which the authors claim that 90% of the equilibrium value was attained. The spacing was constant and equal to $3D_p$. For groups of cylindrical piles, the following observations were made about the scour development: *i*) scour initiated near the front piles of the group, individual scour holes formed around each pile and soon overlapped to form a large scour hole; *ii*) from the observation of the scour patterns, the existence of small horse-shoe vortices around each individual pile was evident; *iii*) 75% of the equilibrium scour depth was achieved in 3 to 5 hours; *iv*) during the tests, the formation of a dune immediately downstream of the pile group was observed. This dune is lower than that observed for a single pier with similar overall dimensions. From the dune shape, Zhao and Sheppard (1999) concluded that the wake vortex system at pile groups is different from that for a single pier, since the wake vortices from the front piles interact with the rear piles and there is more energy in the wake region, which leads to less deposition than for a single pier with the same overall dimensions. Turbulence behind a pile group is more homogeneous than for a single pier, resulting in a more uniform and flatter bed in the wake region.

2.4 Scour variables and parameters

The scouring process at single piers may be described by the following set of independent variables (*c.f.* Fael 2007):

i) Undisturbed flow variables: flow depth, d; slope of the energy line, S_f; gravity acceleration, g.

ii) Fluid variables: mass density, ρ; kinematic viscosity, ν.

iii) Bed sediment variables: median size, D_{50}; gradation coefficient, σ_D; mass density, ρ_s.

iv) Variables describing the pier: pier width, D_p; pier skew-angle factor, K_α; pier shape factor, K_s.

v) Variables describing the channel geometry: cross-section width, B; bottom slope, S_0; cross-section shape factor, K_g.

vi) Time, t.

In other words, the scour depth, d_s, at a given instant, t, is given by,

$$d_s = \varphi\left[\begin{matrix}\text{flow}(d, S_f, g), \text{fluid}(\rho, \nu), \text{bed sediment}(D_{50}, \sigma_D, \rho_s), \text{pier}(D_p, K_\alpha, K_s), \\ \text{channel}(B, S_0, K_g), \text{time}(t)\end{matrix}\right] \tag{2.1}$$

where φ stands for function, σ_D is defined as $0.5(D_{84.1}/D_{50} + D_{50}/D_{15.9})$ and D_x is the diameter for which x% by weight of a sediment mixture is smaller than a given mesh size of the mechanical sieve. The shape factor, K_s, is defined as the ratio of the equilibrium scour depth observed at a pier with a specific shape to the equilibrium scour depth observed at a cylindrical pier. The skew-angle factor K_α is defined as the ratio of the equilibrium scour depth observed at a pier

with a given skew-angle to the approach flow, α, to the equilibrium scour depth observed at the same pier for $\alpha = 0^o$. The cross-section shape factor, K_g, is defined as the ratio of the equilibrium scour depth observed at a pier inserted in a channel with a specific cross-section shape to the equilibrium scour depth observed at the same pier inserted in a channel with rectangular cross-section.

It should be noted here that, unlike in other studies, the average critical velocity for sediment entrainment, U_c, is not included in Equation 2.1 as independent variable since it is fully defined by g, d, S_f, ρ, ν, D_{50} and ρ_s for a given σ_D. For uniform flow, $S_0 = S_f$ and the friction velocity comes $u_* = (gRS_f)^{1/2} = (gRS_0)^{1/2}$, where $R = \varphi(B, d, K_g)$ is the cross-section hydraulic radius. Under these assumptions Equation 2.1 can be written as,

$$d_s = \left[d, u_*, g, \rho, \nu, D_{50}, \sigma_D, \Delta, D_p, K_\alpha, K_s, B, K_g, t\right] \tag{2.2}$$

where Δ = submerged density of the bed material = $(\rho_s - \rho)/\rho$. Choosing u_*, ρ and D_p for basic variables, Equation 2.2 reads,

$$\frac{d_s}{D_p} = \varphi\left(\frac{d}{D_p}, \frac{u_*^2}{gD_p}, \frac{u_* D_p}{\nu}, \frac{D_p}{D_{50}}, \sigma_D, \Delta, K_\alpha, K_s, \frac{B}{D_p}, K_g, \frac{u_* t}{D_p}\right) \tag{2.3}$$

Any non-dimensional parameter of Equation 2.3 may be replaced by any combination of that parameter with others as soon as the resulting set remains independent. Consequently Equation 2.3 can be replaced by any of the following equations,

$$\frac{d_s}{D_p} = \varphi\left(\frac{d}{D_p}, \frac{u_*^2}{\Delta g D_{50}}, \frac{u_* D_{50}}{\nu}, \frac{D_p}{D_{50}}, \sigma_D, \Delta, K_\alpha, K_s, \frac{B}{D_p}, K_g, \frac{u_* t}{D_p}\right) \tag{2.4}$$

$$\frac{d_s}{D_p} = \varphi\left(\frac{d}{D_p}, \frac{\tau_0}{\Delta\gamma D_{50}}, \frac{u_* D_{50}}{\nu}, \frac{D_p}{D_{50}}, \sigma_D, \Delta, K_\alpha, K_s, \frac{B}{D_p}, K_g, \frac{u_* t}{D_p}\right) \tag{2.5}$$

$$\frac{d_s}{D_p} = \varphi\left(\frac{d}{D_p}, \frac{\tau_0}{\tau_c}\frac{\tau_c}{\Delta\gamma D_{50}}, \frac{u_* D_{50}}{\nu}, \frac{D_p}{D_{50}}, \sigma_D, \Delta, K_\alpha, K_s, \frac{B}{D_p}, K_g, \frac{u_* t}{D_p}\right) \tag{2.6}$$

where $\tau_0 = \rho u_*^2$ is the average total bed shear stress, τ_c is the average critical bed shear stress of initiation of sediment motion and $\gamma = \rho g$ is the specific weight of the fluid (water).

According to the Shields diagram, $\tau_c/(\Delta\gamma D_{50}) = \varphi(u_* D_{50}/\nu)$ and Equation 2.6 may read:

$$\frac{d_s}{D_p} = \varphi\left(\frac{d}{D_p}, \frac{\tau_0}{\tau_c}\varphi'\left(\frac{u_* D_{50}}{\nu}\right), \frac{u_* D_{50}}{\nu}, \frac{D_p}{D_{50}}, \sigma_D, \Delta, K_\alpha, K_s, \frac{B}{D_p}, K_g, \frac{u_* t}{D_p}\right) \tag{2.7}$$

Equation 2.6 can also be written as

$$\frac{d_s}{D_p} = \varphi\left(\frac{d}{D_p}, \frac{\tau_0}{\tau_c}, \frac{u_* D_{50}}{\nu}, \frac{D_p}{D_{50}}, \sigma_D, \Delta, K_\alpha, K_s, \frac{B}{D_p}, K_g, \frac{u_* t}{D_p}\right) \tag{2.8}$$

Now, since $\tau_0/\tau_c = \rho u_*^2 / \rho u_{*c}^2$, where u_{*c} = critical shear velocity of initiation of sediment motion, Equation 2.8 comes

$$\frac{d_s}{D_p} = \varphi\left(\frac{d}{D_p}, \frac{u_*}{u_{*c}}, \frac{u_* D_{50}}{\nu}, \frac{D_p}{D_{50}}, \sigma_D, \Delta, K_\alpha, K_s, \frac{B}{D_p}, K_g, \frac{u_* t}{D_p}\right) \tag{2.9}$$

or

$$\frac{d_s}{D_p} = \varphi\left(\frac{d}{D_p}, \frac{u_*}{u_{*c}}, \frac{u_* D_p}{\nu}, \frac{D_p}{D_{50}}, \sigma_D, \Delta, K_\alpha, K_s, \frac{B}{D_p}, K_g, \frac{u_* t}{D_p}\right) \tag{2.10}$$

The non-dimensional parameter u_*/u_{*c} is frequently replaced by U/U_c for practical reasons. In this case, U = average approach flow velocity, *i.e.* average flow velocity in the channel reach upstream of the pier and U_c = critical average approach flow velocity of beginning of sediment motion. This replacement is practically exact in the particular case of fully developed flow on rough flat bed, where the equation

$$\frac{U}{u_*} = 5.75 \log\left(\frac{R}{k}\right) + B' \tag{2.11}$$

is known to apply. In this equation, k = height of grain roughness and B' = constant of integration of the logarithm law of the wall. For the condition of initiation of sediment motion, $U = U_c$ and Equation 2.11 remains valid, *i.e.*,

$$\frac{U_c}{u_{*c}} = 5.75 \log\left(\frac{R}{k}\right) + B' \tag{2.12}$$

This implies that, for rough flat bed, the identity $u_*/u_{*c} = U/U_c$ is unconditionally valid. The same result can be derived for hydraulically smooth or transition flat bed. Consequently, Equation (2.9) becomes

$$\frac{d_s}{D_p} = \varphi\left(\frac{d}{D_p}, \frac{U}{U_c}, \frac{u_* D_{50}}{\nu}, \frac{D_p}{D_{50}}, \sigma_D, \Delta, K_\alpha, K_s, \frac{B}{D_p}, K_g, \frac{u_* t}{D_p}\right) \tag{2.13}$$

and Equation (2.10) reads

$$\frac{d_s}{D_p} = \varphi\left(\frac{d}{D_p}, \frac{U}{U_c}, \frac{u_* D_p}{\nu}, \frac{D_p}{D_{50}}, \sigma_D, \Delta, K_\alpha, K_s, \frac{B}{D_p}, K_g, \frac{u_* t}{D_p}\right) \tag{2.14}$$

where, d/D_p = relative flow depth or flow shallowness; U/U_c = flow intensity, which represents the sediment transport capacity of the approach flow; u_*D_p/ν = shear velocity pier Reynolds number and u_*D_{50}/ν = shear Reynolds number, both conveying the effect of viscosity; D_p/D_{50} = relative sediment size or sediment coarseness, expressing the effect of the sediment size; σ_D = sediment gradation coefficient, accounting for the sediment non-uniformity; Δ = submerged density of the bed material; K_α = factor accounting for the effect of the pier skew-angle; K_s = pier shape coefficient; B/D_p = flow contraction ratio due to the presence of the pier; K_g = cross-section shape coefficient; u_*t/D_p = non-dimensional time.

In wide rectangular channels, K_g and B/D_p do not influence scour. In this context, wide channels are those where the effect of the flow contraction due to the presence of the pier as well as of the proximity of lateral walls are negligible. If the bed material is composed of sand, $\rho_s \approx 2650$ kgm^{-3}, and Δ can be eliminated from the derivation. Under the above assumptions, Equation 2.13 reads,

$$\frac{d_s}{D_p} = \varphi\left(\frac{d}{D_p}, \frac{U}{U_c}, \frac{u_* D_{50}}{\nu}, \frac{D_p}{D_{50}}, \sigma_D, K_\alpha, K_s, \frac{u_* t}{D_p}\right) \tag{2.15}$$

and Equation 2.14 is written as,

$$\frac{d_s}{D_p} = \varphi\left(\frac{d}{D_p}, \frac{U}{U_c}, \frac{u_* D_p}{\nu}, \frac{D_p}{D_{50}}, \sigma_D, K_\alpha, K_s, \frac{u_* t}{D_p}\right) \tag{2.16}$$

Assuming Equations 2.11 and 2.12 to hold, u_* may be replaced by U and Equations 2.15 and 2.16 can also read, respectively

$$\frac{d_s}{D_p} = \varphi\left(\frac{d}{D_p}, \frac{U}{U_c}, \frac{U D_{50}}{\nu}, \frac{D_p}{D_{50}}, \sigma_D, K_\alpha, K_s, \frac{U t}{D_p}\right) \tag{2.17}$$

and

$$\frac{d_s}{D_p} = \varphi\left(\frac{d}{D_p}, \frac{U}{U_c}, \frac{U D_p}{\nu}, \frac{D_p}{D_{50}}, \sigma_D, K_\alpha, K_s, \frac{U t}{D_p}\right) \tag{2.18}$$

In these equations, UD_{50}/ν, is the approach velocity sediment Reynolds number, UD_p/ν is the pier Reynolds number and Ut/D_p is a form of non-dimensional time.

Assuming that the flow within the scour hole is fully rough irrespective of the approach flow, the effects of viscosity can be neglected and both UD_{50}/ν or UD_p/ν may be eliminated from the previous equations. This assumption has been widely accepted in the last two-to-three decades but it deserves to be revisited.

Local scour depth at groups of piles, d_{sg}, depends on all the variables and parameters affecting scouring at single piers plus those describing the pile group. These are the pile spacing, s, the number of columns (parallel alignments), n, the number of rows (number of piles in each column), m, and the skew-angle of the columns, α, as defined in Figure 2.2.

Assuming the definition of additional variables and considering that the shape of the pile group is a function of the number of columns, n, number of rows, m, pile spacing, s/D_p, and pile group skew-angle, α, Equation 2.17 and 2.18 can be generalized for pile groups as,

$$\frac{d_{sg}}{D_p} = \varphi\left(\frac{d}{D_p}, \frac{U}{U_c}, \frac{UD_{50}}{\nu}, \frac{D_p}{D_{50}}, \sigma_D, K_\alpha, K_s, \frac{Ut}{D_p}, \frac{s}{D_p}, \alpha, m, n\right) \tag{2.19}$$

In Equation 2.19, the effect of viscosity may also be considered through UD_p/ν, u_*D_{50}/ν or u_*D_p/ν.

Under equilibrium conditions, where the scour depth no longer depends on time – assertion to be discussed in paragraph 2.5.1 –, Equation 2.18, for instance, and Equation 2.19 become, respectively

$$\frac{d_{se}}{D_p} = \varphi\left(\frac{d}{D_p}, \frac{U}{U_c}, \frac{UD_p}{\nu}, \frac{D_p}{D_{50}}, \sigma_D, K_\alpha, K_s\right) \tag{2.20}$$

and

$$\frac{d_{sge}}{D_p} = \varphi\left(\frac{d}{D_p}, \frac{U}{U_c}, \frac{UD_{50}}{\nu}, \frac{D_p}{D_{50}}, \sigma_D, K_\alpha, K_s, \frac{s}{D_p}, \alpha, m, n\right) \tag{2.21}$$

where d_{se} = equilibrium scour depth at a single pier and d_{sge} = equilibrium scour depth at a pile group. Equations 2.18 to 2.21 constitute the framework for the subsequent analysis, where the effects of the characteristic variables and non-dimensional parameters that affect scouring at single cylindrical piers and pile groups are discussed and characterized.

2.5 Effect of specific parameters on local scour depth at single piers

2.5.1 Effect of time

Local scour may occur for two distinct sediment transport conditions: *i) Clear-water scour*, which occurs when the bed sediment particles are not entrained by the undisturbed approach flow and consequently the sediment material removed from the scour hole is not refilled by the approach flow; *ii*) *Live-bed scour*, occurring when the approach flow has the capacity to entrain the upstream bed material and the scour hole is continuously supplied with sediment from upstream.

Figure 2.6 illustrates the typical scour depth time evolution of those distinct situations (clear-water and the live-bed). Clear-water equilibrium scour depth is reached when the flow becomes unable to remove particles from the scour hole. Equilibrium scour depth in live-bed conditions is attained when the average amount of sediment leaving the scour hole equals the average amount coming in; it is reached much faster than in clear-water flow conditions and it fluctuates around a average value reflecting the passage of bed forms.

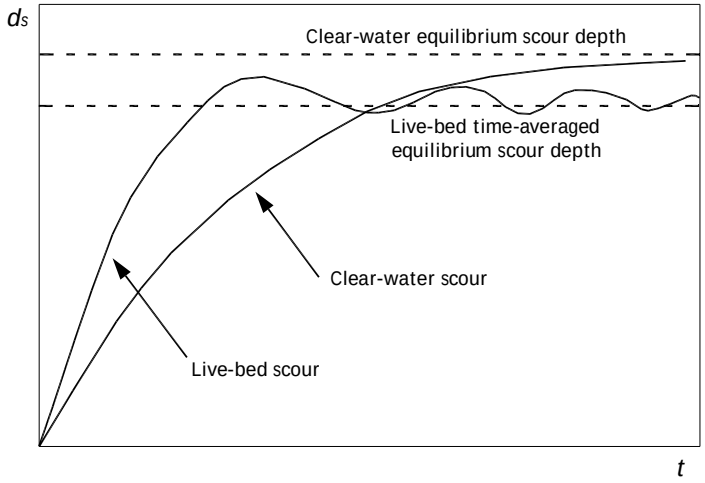

Figure 2.6 – Scour depth time development for clear-water and live-bed scour conditions, after Raudkivi and Ettema (1983)

For clear-water flow conditions, the concept of equilibrium is difficult to materialize in practice. Chabert and Engeldinger (1956) assumed that equilibrium occurs when the scour depth does not change "appreciably" in time. Ettema (1980) reported that there are three distinct phases of the scour process. He named them as the initial phase, principal phase and equilibrium phase. These phases are as follows:

i) the initial phase is characterized by the rapid scouring due to the down flow at the pier upstream face; the horse-shoe vortex does not play an important role and the sediment transport starts at the sides of the pier;

ii) the principal phase is dominated by the horse-shoe vortex action; during this phase, scour occurs in a narrow strip around the pier. As the scour hole develops, the strength of the horse-shoe vortex and the down flow gradually become unable to remove sediment from the entrainment zone;

iii) the equilibrium phase is reached when no further "significant" development in the scour hole exists.

Franzetti *et al.* (1982) described equilibrium as the state of scour development where no further change occurs with time and stressed that this condition may take an infinite time to occur. Olivetto and Hager (2002, 2005) argued that equilibrium cannot be achieved in finite time and that the scour hole never stops to develop; they have stated that end scour as the equilibrium state between vortical agents and the resistance of sediment to be scoured does not normally exist.

In opposition, other authors assume that equilibrium can be observed in finite time. Several methods can be found in the literature for the identification of the onset of the equilibrium phase. Ettema (1980) defined the time to equilibrium, t_e, as the time after which less than 1 mm of incremental scour depth is achieved in a 4 hours period. Cardoso and Bettess (1999) suggested that the equilibrium phase is achieved when the slope of plots of the scour depth *versus* the logarithmic of time changes and tends to zero. However, Radice *et al.* (2002) pointed out that this approach may also fail since scouring can be triggered again, after the observation of a long lasting quasi-horizontal plateaux. Melville and Chiew (1999) assumed that equilibrium is practically achieved when the increment of scour depth is less than 5% of the pier diameter in 24 hour. Coleman *et al.* (2003) pointed out that the equilibrium scour hole may continue to deepen at a relatively slow rate long after equilibrium conditions were thought to exist; they have extended the criterion of Melville and Chiew (1999) and defined the equilibrium time as the time at which the scour rate reduces to 5% of the smaller of the foundation length (pier diameter or abutment length) in a 24 hour period. Grimaldi (2005) suggested a more restrictive criterion: according to this author, equilibrium is reached when scour rate is less than $0.05D_p/3$ in 24 hour.

Assuming that equilibrium scour depth is attained asymptotically (at infinite time), Bertoldi and Jones (1998), suggested that the equilibrium scour depth of a given laboratory experiment can be calculated by adjusting a 4-parameter polynomial function to the finite time evolution of the scour depth. The polynomial function reads,

$$d_s = p_1\left(1-\frac{1}{1+p_1p_2t}\right)+p_3\left(1-\frac{1}{1+p_3p_4t}\right) \tag{2.22}$$

where p_1, p_2, p_3 and p_4 are parameters obtained by regression analysis applied to a given scour depth time record. The equilibrium scour depth, d_{se}, is obtained for $t = \infty$, which leads to $d_{se} = p_1 + p_3$.

Irrespective of the controversial issue of the equilibrium phase and its onset, several attempts have been made in the past to describe the temporal development of clear-water scour at single cylindrical piers. Those of Franzetti *et al.* (1982), Melville and Chiew (1999), Barkdoll (2000) and Oliveto and Hager (2002, 2005) are summarized next. Franzetti *et al.* (1982) have suggested the following scour depth evolution model.

$$\frac{d_s}{d_{se}} = 1 - \exp\left[-a_1 \left(\frac{Ut}{D_p} \right)^{a_2} \right] \tag{2.23}$$

and fixed constants a_1 and a_2 to be 0.028 and 1/3, respectively, based on a small number of tests where $0.6 \leq U/U_c \leq 1.0$. It should be noted here that the above model requires an independent predictor of the equilibrium scour depth, d_{se}. Franzetti *et al.* (1994) suggested that equilibrium scour at piers is achieved in practice when,

$$\frac{Ut}{D_p} > 2 \cdot 10^6 \tag{2.24}$$

Melville and Chiew (1999) have reported the results of a large number of experiments in which the depth of scour was monitored along time. They combined their data with data from other researchers and developed the following predictor of scour depth time evolution:

$$\frac{d_s}{d_{se}} = \exp\left\{ -0.03 \left| \frac{U_c}{U} \ln\left(\frac{t}{t_e} \right) \right|^{1.6} \right\} \tag{2.25}$$

The use of this model requires the independent prediction of d_{se} as well as of time to equilibrium, t_e. On this regard, Melville and Chiew (1999) proposed the following predictor valid for uniform sediments:

$$t_e = 48.26 \frac{D_p}{U} \left(\frac{U}{U_c} - 0.4 \right) \qquad \text{for} \qquad \frac{d}{D_p} > 6 \tag{2.26}$$

$$t_e = 30.89 \frac{D_p}{U} \left(\frac{U}{U_c} - 0.4 \right) \left(\frac{d}{D_p} \right)^{0.25} \qquad \text{for} \qquad \frac{d}{D_p} \leq 6 \tag{2.27}$$

Barkdoll (2000) carried out experiments and checked his data with the predictions of Melville and Chiew (1999); he has pointed out that the model proposed by Melville and Chiew (1999) over-predicts the scour depth at a given time. He also developed experiments with non-circular piers and observed that there is no significant difference in the normalized scour development with time (*i.e.* d_s/d_{se} *vs.* t/t_e). Based on a curve fitting to his experimental data, Barkdoll (2000)

presented a modified form of the equation proposed by Melville and Chiew (1999). The resulting predictor is,

$$\frac{d_s}{d_{se}} = \exp\left\{-0.154\left|\frac{U_c}{U}\ln\left(\frac{t}{t_e}\right)\right|\right\} \tag{2.28}$$

Oliveto and Hager (2002, 2005) and Kothyari *et al.* (2007) used the results from their experiments and suggested the following predictor of scour depth time evolution:

$$\frac{d_s}{D_p^{2/3} d^{1/3}} = 0.068 N \sigma_D^{-0.5} Fr_d^{1.5} \log\left(\frac{\sqrt{g' D_{50}}}{D_p^{2/3} d^{1/3}} t\right) \tag{2.29}$$

where N = pier shape factor = 1 for circular and 1.25 for rectangular piers, Fr_d = densimetric Froude number = $U/(g'D_{50})^{1/2}$, g' = submerged specific weight = $[(\rho_s-\rho)/\rho)]g$. This model renders infinite equilibrium scour depth for $t = \infty$. To face this difficulty, Kothyari *et al.* (2007) reported that equilibrium is archived at a finite time given by,

$$\log T_e = 4.8 Fr_d^{1/5} \qquad \text{for} \qquad Fr_d > Fr_{d\beta} \tag{2.30}$$

where $T_e = t_e/t_r$ = non-dimensional time at which equilibrium is attained, $Fr_{d\beta}$ = densimetric particle Froude number of scour entrainment = $z_R = (d\, D_p^2)^{1/3}$ and $t_r = z_R/[\sigma_D^{1/3}(g' D_{50})^{1/2}]$.

2.5.2 Effect of the approach flow velocity and size of the bed material

Hancu (1971) and Ettema (1980) pointed out that, for uniform non-ripple forming sediment (σ_g < ~1.5 and D_{50} > ~0.6 – 0.7 mm), the local scour depth at cylindrical piers increases almost linearly with U/U_c in the velocity range $0.5 \le U/U_c \le 1.0$. Later on, Melville and Chiew (1999) stressed that scour is triggered for $U/U_c \approx 0.4$.

According to Breusers *et al.* (1977), for $U/U_c \ge 1$ the equilibrium scour depth does not increase further with velocity. In the range $U/U_c \ge 1.0$, ripples or dunes start to develop. These bed forms supply the scour hole with successive waves of sediment that the horse-show vortex and the wake vortices continue to remove, but with reduced capacity to erode the original bed material (Chee 1982). This process tends to cause the decrease of d_{se} as U increases in the range $U_c < U <$ ~$2U_c$. For ~$2U_c < U <$ ~$4U_c$, the length of the dunes increases and their upstream slope reduces as flow velocity increases. Consequently, d_{se} increases again with the approach flow velocity and a new peak is reached for $U \approx 4U_c$. This peak is approximately equal to the one that occurs for $U = U_c$, but now in the upper-regime flat bed. For $U >$ ~$4U_c$, anti-dunes develop and the scour depth decreases again.

For fine sand, D_{50} < ~0.6 mm, the lower-regime flat bed practically does not exist. When U approaches U_c, the finer fraction of the sediment mixture is entrained by the flow (for U slightly smaller than U_c) and ripples appear in the sand bed. Ripples influence the scour development and reduce the equilibrium scour depth. This effect is illustrated in Figure 2.7 where tests results obtained for D_{50} < ~0.6 mm are compared with others obtained for $D_{50} \geq$ ~0.6 mm.

The described behaviour reflects one of the effects of sediment non-uniformity. Another one may be observed when, in the absence of ripples, D_{50} > ~0.6 mm, the selective sediment movement of finer particles may be initiated for flow velocities clearly smaller than U_c (as associated with D_{50}), leading to the formation of a superficial armour layer composed of the courser grains. This layer may drastically reduce the scour depth. Figure 2.8 represents the factor for the effect of sediment gradation (non-uniformity), $K\sigma_D$, as function of σ_D, for non-ripple forming sediment, D_{50} > ~0.6 mm. Under clear-water scour condition, for σ_D < 1.5, scour depth is practically unaffected; for σ_D = 3, for instance, the equilibrium scour depth may be reduced by a factor of ≈ 4.

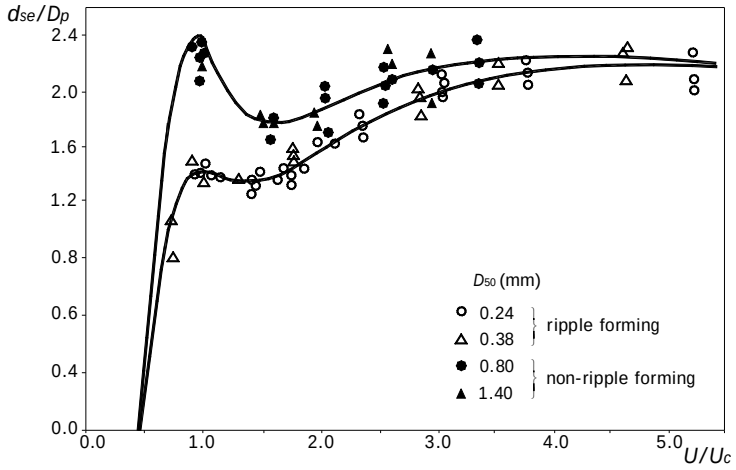

Figure 2.7 – Scour depth in uniform sediment at a cylindrical pier as a function of flow intensity in a deep flow relative to pier diameter, adapted from Raudkivi (1998)

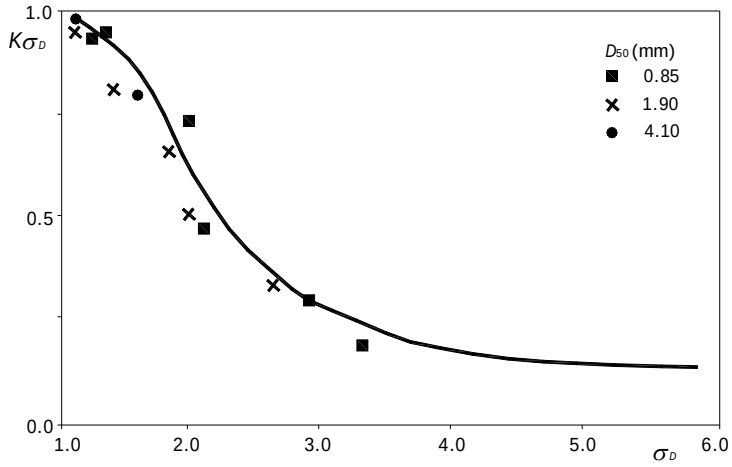

Figure 2.8 – Coefficient $K\sigma_D$ as function of σ_D, adapted from Raudkivi (1998)

2.5.3 Effect of the relative flow depth

The relative flow depth, d/D_p, is one of the major parameters controlling the scouring phenomenon (see Equations 2.17 to 2.21). According to Melville and Coleman (2000), the horse-shoe vortex interacts with the surface roller (bow wave) for comparatively shallow flow. As shown before, these two vortices display opposite rotating directions (see Figure 2.9).

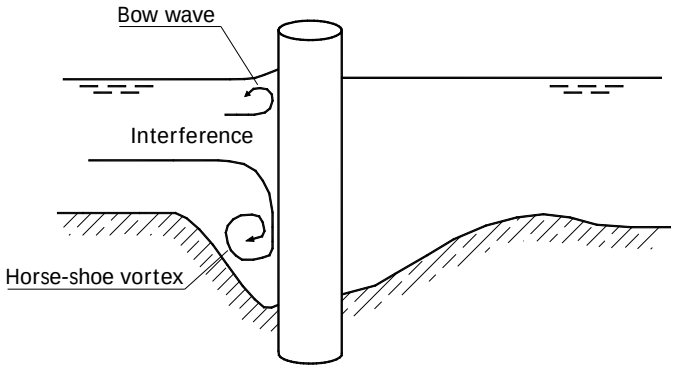

Figure 2.9 – Local scour depth variations with flow shallowness, adapted from Melville and Coleman (2000)

For comparatively deep flows, the scour depth increases with pier size and it is practically independent of the flow depth. For small values of d/D_p, associated with both shallow flows or wide piers, the surface roller interferes with the horse-shoe vortex and the scour depth increases with flow depth, d. For intermediate relative flow depths, the local scour depth is dependent from both d and D_p. Within this context, Breusers *et al.* (1977) suggested that the influence of flow depth on local scouring can be neglected when $d/D_p > 3$. Later on, Jones and Sheppard (2000) studied large piers and concluded that this threshold should be ≈ 2 while Melville and Coleman (2000) suggested that d_{se} is independent from d/D_p for $d/D_p > 10/7$.

Kandasamy (1989) studied the dependence of the equilibrium scour depth, d_{se}, from the flow depth, d, and pier diameter, D_p (or the abutment length), assuming that *i*) the flow intensity, U/U_c, is 1, to consider the most adverse scour depth situation, *ii*) viscous effects are negligible, *iii*) the flow cross-section is rectangular, *iv*) the flow contraction effects are negligible, *v*) the bed material is uniform, $\sigma_g < \sim 1.5$, and not susceptible to ripple formation, $D_{50} > \sim 0.6$ mm, *vi*) the relative sediment size D_p/D_{50} maximizes the scour depth ($D_p/D_{50} \approx 50$) and the obstacles are standard ($K_s = K_\alpha = 1$). Under these assumptions, it may be shown that Equation 2.20 reduces to

$$\frac{d_{se}}{D_p} = \varphi\left(\frac{d}{D_p}\right) \tag{2.31}$$

Kandasamy (1989) suggested the conceptual dependence of d_{se} from flow depth, d, and pier diameter, D_p, shown in Figure 2.10. The proposal of Kandasamy (1989) covered both bridge piers and bridge abutments.

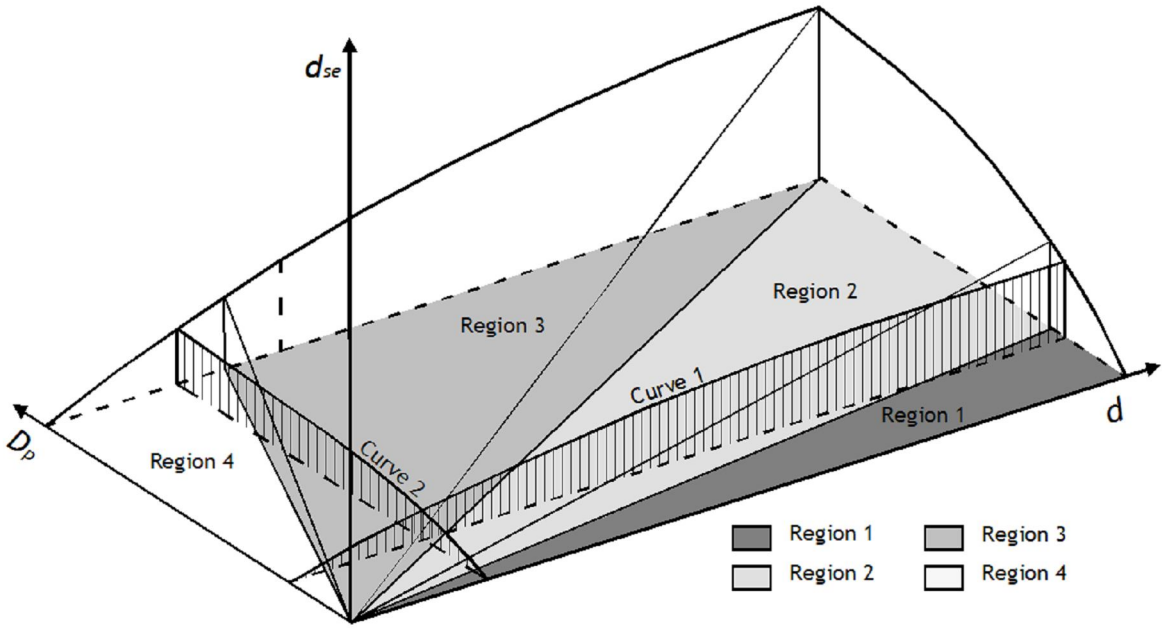

Figure 2.10 – Functional dependence $d_{se} = \varphi\ (d, D_p)$, after Kandasamy (1989)

According to Figure 2.10, the functional relation, $d_{se} = \varphi(d, D_p)$ is different in each of the four regions identified. In Region 1, the scour depth is independent from the flow depth. In Region 4 the scour depth is independent from the pier diameter. In Regions 2 and 3 the scour depth becomes increasingly more dependent from d and less dependent from D_p when moving from the boundary of Region 1 to the boundary of Region 4. Regions 1 and 2 refer essentially to pier data, while Regions 3 and 4 apply mostly to bridge abutments. Along Curve 1 (see Figure 2.10), d_{se} increases with d and, reaching Region 1, it becomes $d_{se} \approx 2.3D_p$, according to Kandasamy (1989). Along Curve 2, d_{se} increases with D_p and, when the curve reaches Region 4, $d_{se} = 10d$ (for abutments).

Figure 2.11 includes the data collected by Kandasamy (1989) from several sources. For $d/D_p > 6$, $d_{se} \approx 2.3D_p$, which shows that, according to this author, the flow depth would still impact on the scour depth for values of d/D_p as high as 6. Figure 2.11 also includes the scour predictor suggested by Cunha (1972); it can be concluded that this predictor presents the same trend as most of the data. However, for $d/D_p > 6$, d_{se}/D_p continues to increase, with no upper finite bound, which is unrealistic.

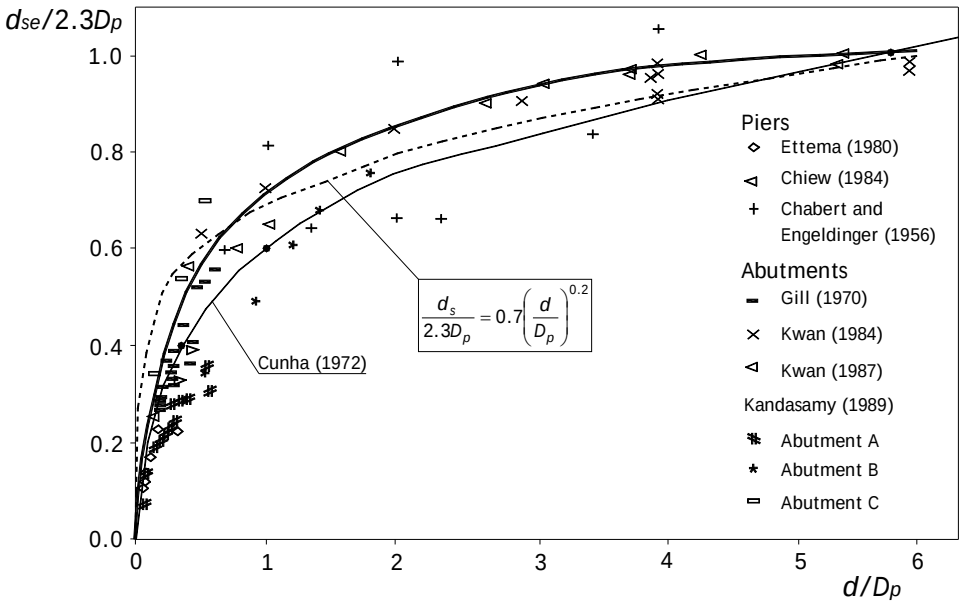

Figure 2.11 – Variation of relative scour depth with d/D_p, adapted from Kandasamy (1989)

Trying to summarize the mentioned contributions, whenever $D_p < d/b_1$, the equilibrium scour depth is given by,

$$\frac{d_{se}}{D_p} = C_1 \tag{2.32}$$

while for $D_p > d/b_2$, the equilibrium scour depth is given by,

$$\frac{d_{se}}{d} = C_2 \tag{2.33}$$

The values of b_1, b_2, C_1 and C_2 vary from one author to another. For cylindrical piers, Melville and Coleman (2000) suggested $b_1 = 1/0.7$, $b_2 = 1/5$, $C_1 = 2.4$ and $C_2 = 4.5$. In the last few decades several other authors proposed different values for C_1. For instance, Sheppard *et al.* (2004) proposed $C_1 = 2.5$.

Within the middle range, where the equilibrium scour depth depends from both d and D_p, Melville and Coleman (2000) suggested that,

$$\frac{d_{se}}{D_p} = C_3\left(\frac{D_p}{d}\right)^{\xi} \tag{2.34}$$

and proposed $C_3 = 2$ and $\xi = 0.5$, while Kandasamy (1989) suggested $C_3 = 1.61$ and $\xi = 0.2$.

2.5.4 Effect of relative sediment size

Most researchers claim that, for $D_p/D_{50} < \approx 8$, individual sediment particles are so large relative to the pier that scour develops mainly at the sides of the pier and the equilibrium scour depth is rather small. For $\approx 8 < D_p/D_{50} < \approx 50$, the sediment size is large relative to the dimension of the scour hole and erosion is impeded because the porous bed dissipates the horse-shoe vortex strength. For several decades it has been assumed that as $D_p/D_{50} > \approx 50$ scour depth would be unaffected by the relative sediment size (*e.g.* Ettema 1980; Raudkivi 1986; Breusers and Raudkivi 1991; Melville and Chiew 1999; Melville and Coleman 2000). These statements are based on experimental data obtained for a narrow range of D_p/D_{50} that tends not to cover conditions in nature. Recently, it has been pointed out that the relative sediment size can significantly affect the scour depth even for $D_p/D_{50} > \approx 50$.

Sheppard *et al.* (1995) carried out experiments for values of D_p/D_{50} of up to 1260 and reported that D_p/D_{50} acts as a scour reduction parameter for values beyond ≈ 50. Due to the differences in D_p/D_{50} between laboratory and field, this reduction can significantly impact on scour depth predictions at prototype scale whenever predictors are based on small scale laboratory data.

Jones and Sheppard (2000) carried out laboratory experiments with large piers in fine sand and also reported that local scour depth predictors based on laboratory tests tend to over-predict field values due to inappropriate scaling of D_p/D_{50}. Sheppard *et al.* (2004) carried out new local scour experiments for values of D_p/D_{50} of up to 4168 and reported the same trend. Figure 2.12 plots the relative scour depth, d_{se}/D_p as function of D_p/D_{50}, based on laboratory and field data with $U/U_c = 1$ and $d/D_p > 2$. It includes the data used to derive the Richardson and Davis (2001) pier scour equation, ($96 \leq D_p/D_{50} \leq 633$), 384 field measurements collected by Landers and Mueller (1996), ($8.5 \leq D_p/D_{50} \leq 19763$), and data from experiments carried out by Jones and Sheppard (2000), ($D_p/D_{50} \leq 4136$).

So, the relative sediment size, D_p/D_{50}, is possibly implicated in the deviation between field pier scour data and predictions based on empirical formulas derived from laboratory experiments. The reason why d_{se}/D_p decreases for large values of D_p/D_{50} is not well understood (Sheppard *et al.* 2004).

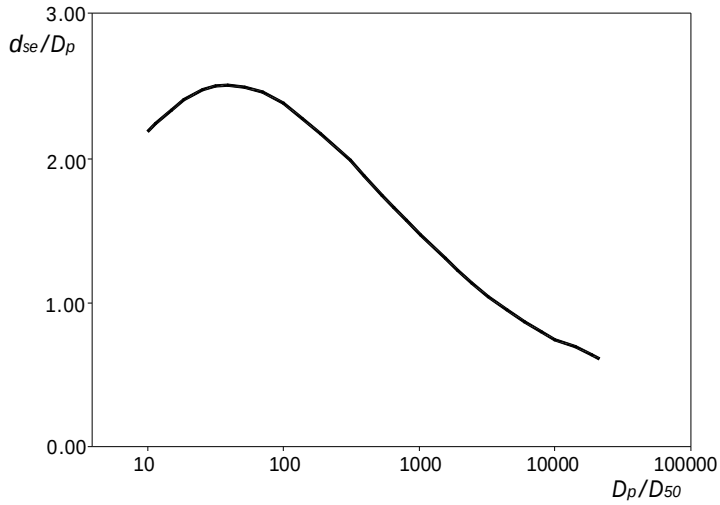

Figure 2.12 – Dependence of normalized scour depth on D_p/D_{50} for a circular pier, adapted from Jones and Sheppard (2000)

Sheppard *et al.* (2004) suggested that the equilibrium scour depth is mostly a function of the relative flow depth, flow intensity and relative sediment size. According to these authors,

$$\frac{d_{se}}{D_p} = 2.5\varphi_1\left(\frac{d}{D_p}\right)\varphi_2\left(\frac{U}{U_c}\right)\varphi_3\left(\frac{D_p}{D_{50}}\right) \tag{2.35}$$

where the effect of D_p/D_{50} on d_{se}/D_p is given by

$$\varphi_3 = \frac{D_p/D_{50}}{0.4(D_p/D_{50})^{1.2} + 10.6\left(D_p/D_{50}\right)^{-0.13}} \tag{2.36}$$

Lee and Sturm (2009) used data from Ettema (1980), Ting *et al.* (2001), Sheppard (2003), Sheppard and Miller (2006) as well as their own data and applied correction factors proposed by Melville and Sutherland (1988) in order to isolate the effect of D_p/D_{50}. They divided the experiments in two groups ($D_p/D_{50} > 25$ and $D_p/D_{50} < 25$), and obtained the following regression equations:

$$\frac{d_{se}}{D_p} = 5.0\log\left(\frac{D_p}{D_{50}}\right) - 4.0 \qquad \text{for} \qquad 6 \le \frac{D_p}{D_{50}} \le 25 \tag{2.37}$$

$$\frac{d_{se}}{D_p} = \frac{1.8}{\left(\frac{0.02D_p}{D_{50}} - 0.2\right)^2 + 1} + 1.3 \qquad \text{for} \qquad 25 \le \frac{D_p}{D_{50}} \le 10^4 \tag{2.38}$$

Lee and Sturm (2009) also examined the fitting of Equations 2.37 and 2.38 to field data from Landers and Mueller (1996) and Mueller and Wagner (2005), filtered to respect the conditions: *i*)

$U/U_c \leq 1$; *ii*) Froude number, $Fr < 0.4$; *iii*) scour not affected by debris accumulation; *iv*) $D_{50} > 0.1$ mm; *v*) measurements over time in the same bridge pier. The result is reproduced in Figure 2.13. However it should be noted here that the measured field values have a high degree of uncertainty and it is not exactly known if equilibrium scour depth had been reached or not.

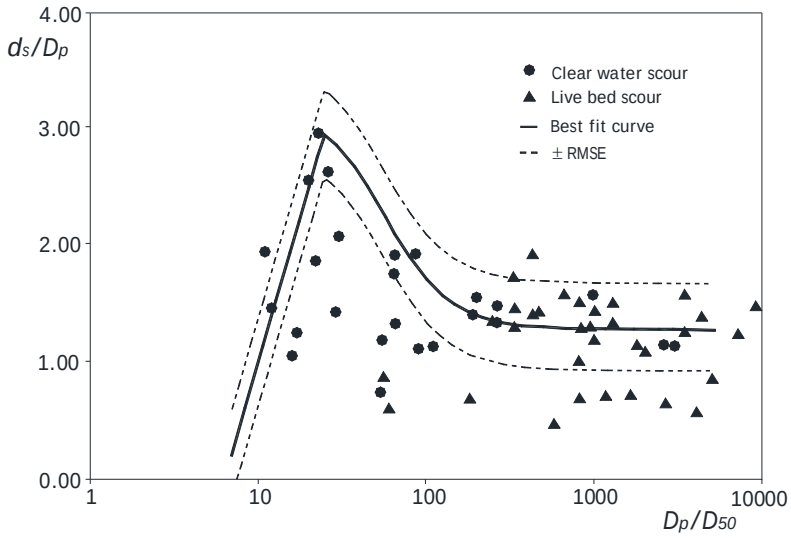

Figure 2.13 – Relative scour depth, d_{se}/D_p, as function of D_p/D_{50} for clear-water field data from Mueller and Wagner (2005), after Lee and Sturm (2009)

Lee and Sturm (2009) explained that with the increase of D_p/D_{50}, sediment grains continue to be lifted and swept inside the scour hole by the horse-shoe vortex, but the probability of being carried out of the scour hole reduces.

In spite of the clear evidence on the effect of D_p/D_{50} on d_{se}/D_p, recent engineering manuals (*e.g.* Breusers and Raudkivi 1991; Melville and Coleman 2000) ignore this fact. This is possibly due to the comparatively modest number of scour studies devoted to large piers, which may also be interpreted as a need for further studies on the effect of D_p/D_{50} on the equilibrium scour depth.

2.5.5 Effect of viscosity

The early studies of Shen *et al.* (1966) and Nicollet and Ramette (1971) indicate that viscosity may affect the scouring phenomenon at bridge piers. Naturally, any non-dimensional parameter conveying the effect of viscosity will lead to some form of Reynolds number. In this document the following forms of Reynolds number were already mentioned:

i) pier Reynolds number, UD_p/ν;

ii) approach velocity sediment Reynolds number, UD_{50}/ν;

iii) shear velocity pier Reynolds number, u_*D_p/ν;

iv) shear Reynolds number, u_*D_{50}/ν.

Some others define the sediment Reynolds number as $u_* k/\nu$, where k = Cte.D_{50} = height of the sediment grain rugosity.

According to Shen *et al.* (1969), since the horse-shoe vortex is the principal agent of scouring and its size is related with the pier Reynolds number, the equilibrium scour depth must depend from $Re_p = UD_p/\nu$. These authors collected data from several authors, added their own data related the equilibrium scour depth with Re_p (see Figure 2.14). They have suggested the equation

$$d_{se} = 0.000223\left(\frac{UD_p}{\nu}\right)^{0.619} \tag{2.39}$$

where d_{se} is given in m.

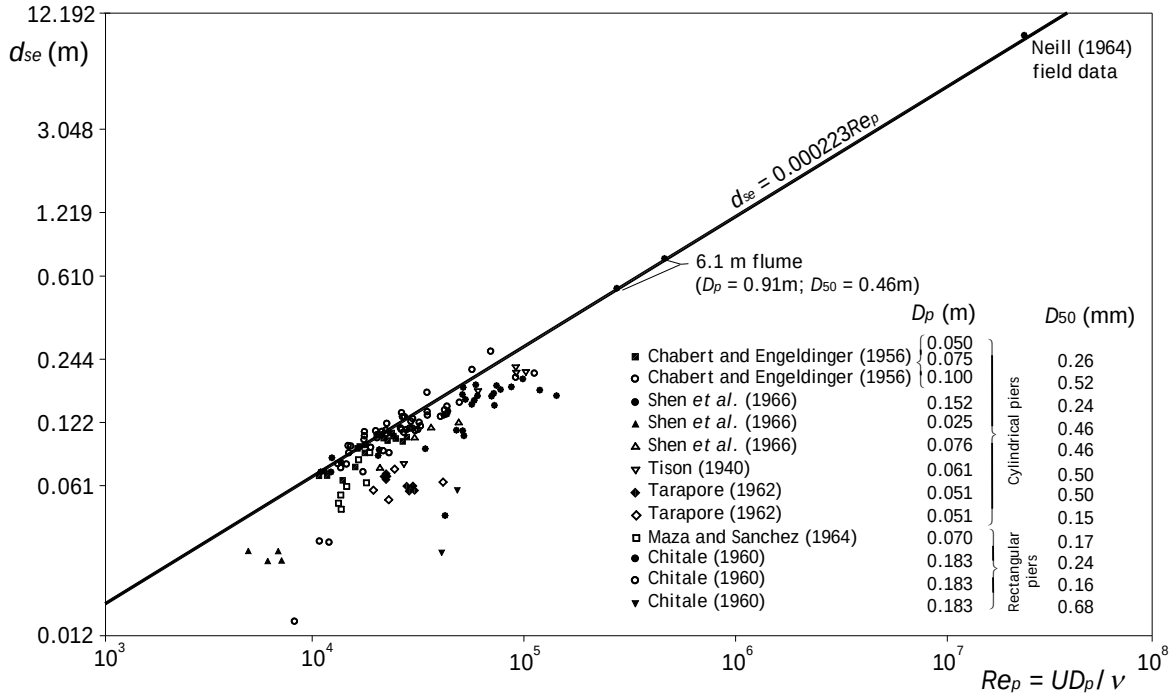

Figure 2.14 – Equilibrium scour depth *vs.* pier Reynolds number, adapted from Shen *et al.* (1969)

In the same line, Nicollet and Ramette (1971) proposed the relationship between d_{se}/D_p and both D_p/D_{50} and UD_{50}/ν presented in Figure 2.15. According to this figure, for approach velocity sediment Reynolds number, $Re_U = UD_{50}/\nu$, in the range $Re_U > \approx 10^3 - 10^4$ and sufficiently high values of D_p/D_{50} ($D_p/D_{50} > \approx 200$), d_{se} no longer depends on UD_{50}/ν. It is important to notice here that these authors covered values of D_p/D_{50} in the range $17 \leq D_p/D_{50} \leq 384$ and concluded that d_{se} diminishes as D_p/D_{50} increases, somehow anticipating the recent findings reported by Shepard *et al.* (2004) or Lee and Sturm (2009).

Coleman (1971) investigated the effect of viscosity on local scouring and concluded that the scour depth is free of viscous effects as soon as the pier Reynolds number, Re_p, is such that $Re_p > 10^4$. Approximately two decades later, Monti (1994) concluded the same for $Re_p > 7000$.

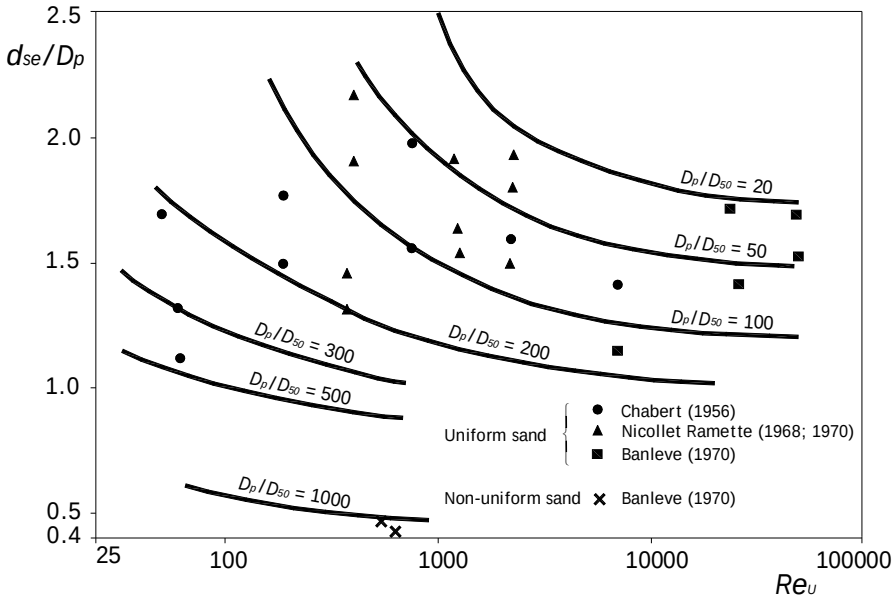

Figure 2.15 – Equilibrium scour depth, $d_{se} = \varphi(D_p/D_{50}; Re_U)$, after Nicollet and Ramette (1971)

Ignoring the mentioned results, the vast majority of the authors (*e.g.* Jain and Fisher 1980; Ettema *et al.* 1998; Melville and Coleman 2000; Oliveto and Hager 2002; Sheppard *et al.* 2004; Cardoso and Fael 2010; Sheppard and Renna 2010) overlooked any viscous effects on scouring. The reasoning behind this assumption is that, irrespective of the approach flow, the flow inside the scour hole must be fully rough due to the presence of flow structures such as the horse-shoe vortex or the wake vortices.

According to the Shields diagram, fully rough flow occurs in movable bed whenever $u_* D_{50}/\nu > 70 - 400$. Fixing the limit in 200, Oliveto and Hager (2002) argued, after some manipulations, that the flow is fully rough as soon as two conditions are satisfied: *i*) $k/d > \approx 0.002$; *ii*) $D_{50} > 0.40 - 0.80$ mm. These criteria seem controversial and may be discarding viscous effects of laboratory studies. For this reason it is important to further investigate the effect of viscosity on the scouring process.

2.5.6 Effect of pier shape

It is widely recognized that the pier shape impacts the adjacent flow streamlines. If the interference is small, the scour depth is also small as compared with the scour depth at obstacles that significantly modify the streamlines. The shape coefficient, K_s, is defined as the ratio between the equilibrium scour depth close to a pier of a given shape and the equilibrium scour depth at a single cylindrical pier.

A large number of shape factors have been suggested by different researchers on the basis of experimental data. Diab (2011) collected shape factors, K_s, included in some of the most quoted bibliography. The results are presented in Table 2.1.

Table 2.1 – Shape factors for bridge piers, Diab (2011)

Reference	Pier shape factor, K_s					
	Cylinder	Rectangular	Round nose	Stream-lined nose	Sharp nose	Elliptic
Tison (1940)	1.00	1.40	–	0.41 – 0.67	–	–
Chabert and Engeldinger (1956)	1.00	1.11	–	0.73	–	–
Breusers *et al.* (1977)	1.00	1.30	–	0.75	–	–
Mostafa (1994)	1.00	1.29	1.07	–	–	–
Melville (1997)	1.00	1.00	1.00	–	0.90	–
Hoffmans and Verheij (1997)	1.00	1.00 – 1.20	0.90	0.70 – 0.80	0.65 – 0.76	0.60 – 0.80
Richardson and Davis (2001)	1.00	1.10	1.00	–	0.90	–
Olivetto and Hager (2002)	1.00	1.20	–	–	–	–

The shape factors defined in Table 2.1 refer to the common pier shapes schematically shown in Figure 2.16. The values of K_s tend to increase for rectangular piers and to decrease for elliptical and stream-lined shapes.

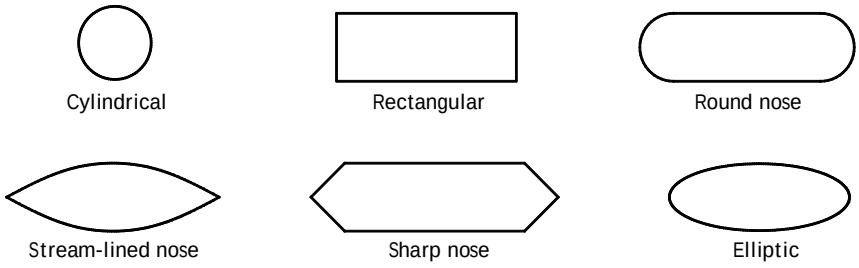

Figure 2.16 – Common pier shapes

2.5.7 Effect of pier skew-angle

The pier skew-angle factor, K_α, reflects the effect of the pier alignment towards the approach flow and it is an important factor affecting local scour around bridge piers. It was initially studied by Schneible (1951), followed by Laursen and Toch (1956), Chabert and Engeldinger (1956) and Mostafa (1994).

Figure 2.17, proposed by Laursen and Toch (1956), reflects the fact that the maximum scour depth at skewed piers with small values of L/D_p occurs at skew-angles slightly less than 90º, where the pier projected width is maximal (here, L = pier length).

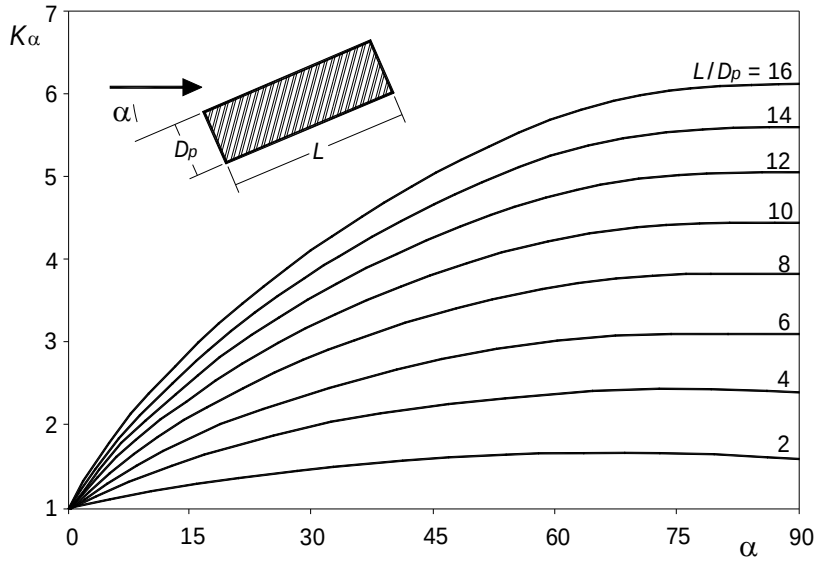

Figure 2.17 – Local scour depth variation with pier skew, *in* Melville and Coleman (2000)

To consider the effect of the skew-angle, Richardson and Davis (2001) recommend multiplying the scour depth predicted for α = 0º by the K_α, defined as,

$$K_\alpha = \left[\cos(\alpha) + \frac{L}{D_p}\sin(\alpha)\right]^{0.65} \tag{2.40}$$

2.6 Effects of specific parameters affecting local scour at pile groups

2.6.1 Introduction

Few studies about partly submerged pile groups were performed in the past as compared with the number of local scour studies at single cylindrical piers. Among them, those of Hannah (1978), Elliott and Baker (1985), Salim and Jones (1996), Zhao and Sheppard (1999), Smith (1999), Sumer and Fredsøe (2002), Ataie-Ashtiani and Beheshti (2006) may be mentioned. Amini *et al.* (2012) studied both submerged and partly submerged pile groups.

The effects of pile spacing, pile group skew-angle, number of aligned rows and shape of the pile group will be discussed next (see Equation 2.21).

2.6.2 Effect of pile group spacing

Spacing, *s*, between piles is one of the most important factors in characterizing local scour around pile groups. Figure 2.18 plots the scour depth at a group of two piers[(1)], d_{sge}, aligned with

[(1)] two or more piles aligned in a single line will be termed as pier group in this work.

the flow (α = 0º) normalized by the scour depth observed at an individual pier, d_{se1}, in the same bed and approach flow conditions, d_{sge}/d_{se1}, as function of the relative spacing, s/D_p. It derives from the experimental study carried out by Hannah (1978), where the time duration of the experiments was t_d = 7 hours. For s/D_p = 1, the piers touch each other and the scour depth at the font pier would be practically equal to the one obtained at a single pier, but, as the distance increases, reinforcing occurs at the front pier and the maximum scour is obtained for $s/D_p \approx 2.5$. Then, the interaction between piers reduces gradually until s/D_p = 11. For s/D_p > 11, the scour depth in the front pier would be again the same as at an isolated pier.

According to Hannah (1978), for s/D_p < 2, the pier group would behave as a single solid pier, originating only one horse-shoe vortex. Increasing the pier spacing within this range (s/D_p < 2), the scour depth also increases due to the increase in the pier group effective diameter. For $s/D_p \geq 2$, each pier creates its own horse-shoe vortex and the compression with the adjacent piers creates higher scour potential. By further increasing the pier spacing, the horse-shoe vortex compression decreases and the scouring potential diminishes.

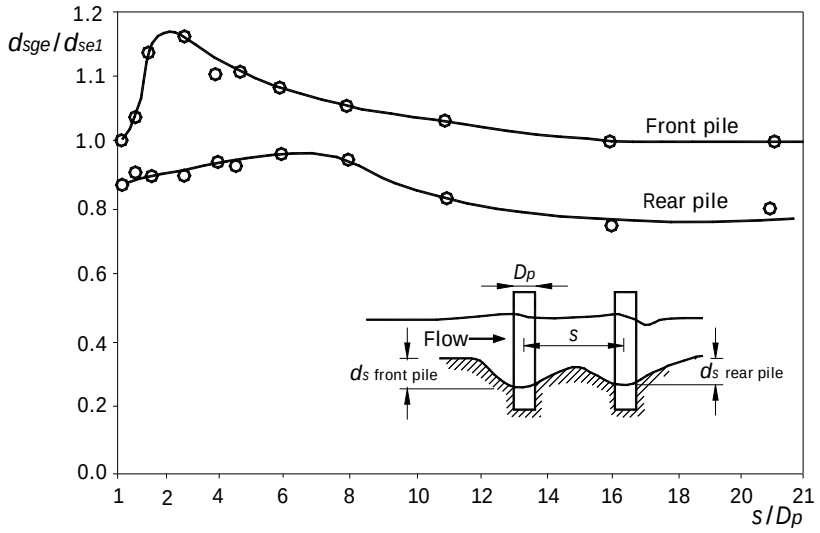

Figure 2.18 – Scour depth at two piers in line with the flow, after Raudkivi (1998)

Figure 2.19 reproduces the results for a group of two cylindrical piers aligned with α = [45º, 90º]. For α = 90º, the measured scour depth was equal in the two piers and the results are represented by a single curve; for s/D_p = 1, the observed scour depth is 1.93d_{se1} and gradually diminishes with the increase of pier spacing; for s/D_p = 11, the scour holes are completely separate and the bed level between them remains unchanged. For α = 45º, the observed scour depth in the front pier is similar to the one registered for α = 90º, while the scour depth observed at the rear pier exceeded that at the front pier for all the tested pier spacings. This is caused by the combined action of the wake vortices originated by the interaction of the approach flow with the front pier and the compression of the horse-shoe vortices between the two piers.

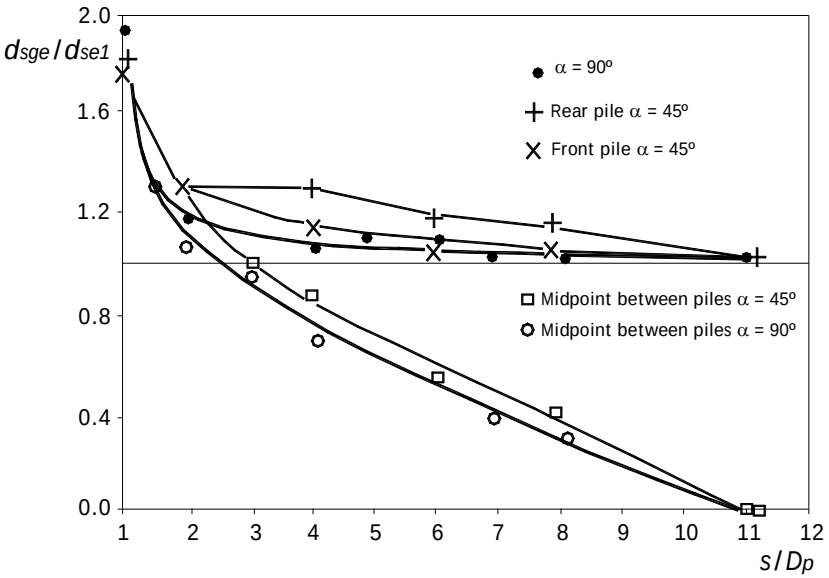

Figure 2.19 – Scour depth at two piers at α = [90º, 45º], as a function of pier spacing, after Raudkivi (1998)

Salim and Jones (1996) carried out scour tests at groups of square piles with n = [3, 4], m = [3, 5], α = 0º and $1.5 \leq s/D_p \leq 10$. The duration of the tests was t_d = 4 hours with some calibration runs of 24 hours. Salim and Jones (1996) suggested that, for s/D_p = 1, the scour depth is equal to the one obtained at a rectangular pier whose dimensions are equal to the sum of those of the individual piles. They also concluded that the scour depth increases as s/D_p increases from 1 to ≈3 and then decreases with the further increase of s/D_p to ≈10, where d_{sge} was the same as for single piers. Salim and Jones (1996) used their data to determine empirically the pile group spacing factor, defined as,

$$K_{sp} = \beta\left(1 - e^{1-s/D_p}\right) + e^{0.5\left(1-s/D_p\right)} \tag{2.41}$$

where β = 0.47 to best fit the data and β = 0.57 to envelope the data.

Ataie-Ashtiani and Beheshti (2006) investigated scour around pile groups with {n = [1, 2]; α = [0º, 90º]}, and evaluated the accuracy of some of the commonly used formulas for the prediction of the scour depth at pile groups. Most of their experiments lasted approximately 7 hours.

Figure 2.20, adapted from Ataie-Ashtiani and Beheshti (2006), shows that the scour depth increases with increasing s/D_p, to a maximum value at $s/D_p \approx 3$, and then decreases gradually with further increase of s/D_p to $s/D_p \approx 8$, where the observed scour depth at the pile group and at an individual pier are equal. It also shows that for piles aligned with the approach flow (Figure 2.20a), α = 0º, the scour depth at the rear pile is always smaller than at a single pier. Ataie-Ashtiani and Beheshti (2006) pointed out that the rear piles create a weaker horse-shoe vortex and experience live bed conditions, as it is supplied with the material removed from the front piles scour hole.

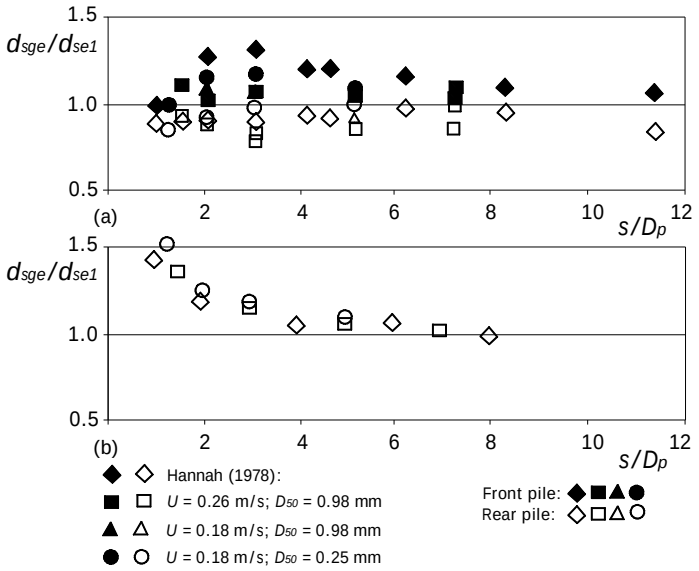

Figure 2.20 – Equilibrium scour depth plotted against pier spacing (a) twin pile group with α = 0º; (b) twin pile group with α = 90º, adapted from Ataie-Ashtiani and Beheshti (2006)

Amini *et al.* (2012) studied groups of circular piles aligned with the approach flow for $t_d \approx 8$ hours, $1 \leq s/D_p \leq 6$, $n = 2$, $m = [2, 4, 5]$, $U/U_c = 0.95$ and suggest that, for $s/D_p = 1$, the pile group produces one single horse-shoe vortex and the scour pattern is similar to the one produced by a single pier. For $s/D_p \leq 3.5$, the pile group still produces one single scour hole; for $s/D_p > 3.5$, the interference between adjacent piles diminishes and incipient individual scour holes are observed. With further increase of s/D_p, the individual scour holes tend to separate and, for $s/D_p > 5$, each pile creates one clearly individualized scour hole; consequently the maximum scour depth of the pile group becomes independent from s/D_p for $s/D_p > 5$.

Richardson and Davis (2001) and Sheppard and Renna (2005, 2010) define the pile group spacing factor, K_{sp}, for calculating the pile group equivalent diameter as

$$K_{sp} = 1 - \frac{4}{3}\left(1 - \frac{1}{W_g / D_p}\right)\left[1 - \left(\frac{s}{D_p}\right)^{-0.6}\right] \tag{2.42}$$

The pile group spacing factor decreases with the increase of s/D_p and this trend is more pronounced for higher values of the ratio W_g/D_p. It should be reminded here that W_g is the sum of the non-overlapping individual piles widths projected on a plane normal to the approach flow (see Figure 2.2).

From the discussion, it is important to notice that for pile groups aligned with the approach flow (α = 0º), $d_{sge} \approx d_{se1}$ for $s/D_p = 1$, that d_{sge}/d_{se1} is maximal for $s/D_p \approx [2, 3]$ and that further increasing s/D_p gradually decreases d_{sge} until $s/D_p > \approx 8 - 11$, where $d_{sge} \approx d_{se1}$.

2.6.3 The effect of pile group skew-angle

The pile group skew-angle to the approach flow, α (see Figure 2.2), is one of the key variables that affect the equilibrium scour depth. In spite of this, comparatively few works on the effect of α are reported in the literature.

Hannah (1978) was the first author to systematically run experiments on the effect of skew-angle. He has covered α values in the range, $0^o < \alpha < 90^o$, for groups of two cylindrical piers with centerline spacing of $5D_p$. His data are plotted in Figure 2.21. It can be concluded that the maximum scour depth occurs at the front pier for small skew-angles, while, for $\alpha > \sim 40^o$, the maximum scour depth shifts to the rear pier.

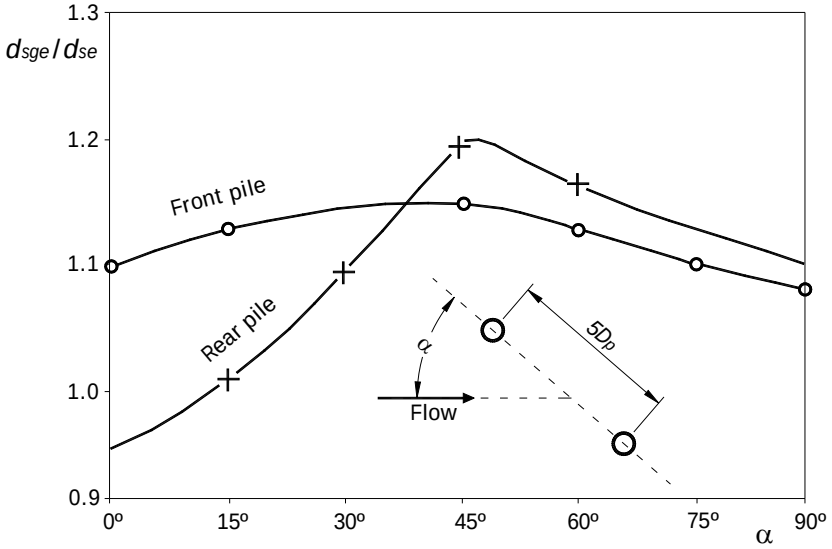

Figure 2.21 – Effect of skew-angle, α, on scour depths at two piers spaced five pier diameters apart, after Raudkivi (1998)

Salim and Jones (1996) carried out experiments with two groups of square piles at various skew-angles, to determine a skew-angle factor. One group was a matrical array with $n = 3$ and $m = [3, 5]$, while the other one was staggered, $m = 5$ piles alternating between 3 and 4 piles in each row. Spacing between the piles varied in the range $1 \leq s/D_p \leq 12$. The results have show that the skew-angle factor for a group of square piles is reasonably close to that for a solid pier with the same overall width-to-length ratio. Salim and Jones (1996) defined $K_{g\alpha}$ as,

$$K_{g\alpha} = \frac{d_{sge} / K_{sp}}{d_{se(\text{overall})}} \tag{2.43}$$

where d_{sge} = scour depth at the skewed pile group, K_{sp} = pile spacing factor, $d_{se(\text{overall})}$ = equilibrium scour depth of a solid equivalent pier, with the group overall dimensions, set at the same skew-angle.

Zhao and Sheppard (1999) carried out two sets of six experiments in order to assess the effect of the skew-angle at pile groups: *i*) first set for a group of cylindrical piles with n = 3, m = 8, D_p = 31.8 mm; $d \approx$ 215 mm, $0.60 \leq U/U_c \leq 0.65$, $s = 3D_p$, α = [0º, 15º, 25º, 35º, 45º, 90º], $t_d \approx$ 26 hour; *ii*) second set with that same configuration but square piles, $L = D_p$ = 31.8 mm; $d \approx$ 215 mm, $s = 3D_p$, α = [0º, 15º, 25º, 35º, 45º, 60º]. Zhao and Sheppard (1999) concluded that *i*) there are two major scour mechanisms – the horse-shoe vortex and the interaction of wake vortices with downstream piles, *ii*) at small skew-angles, $\alpha <$ ~20º, the horse-shoe vortex is the principal agent on the scour development and the maximum scour depth is observed at the front pile, *iii*) for $\alpha >$ ~20º, the scour process is dominated by the interaction of the wake vortices from upstream piles on downstream piles and the point of maximum scour depth moves along the upstream side of the pile group, exposed to the approach flow, *iv*) the maximum scour depth is observed for $\alpha \approx$ 25º and *v*) the predictor suggested by Richardson and Davis (2001) is conservative for local scour at pile groups, especially for groups of circular piles. Zhao and Sheppard (1999) applied Laursen and Toch (1956) skew-angle factor for rectangular piers, with L and D_p defined by the pile group outside dimensions and pointed out that this approach over predicts scour depths for skew-angles greater than 25º. Regarding the pile group with square piles, Zhao and Sheppard (1999) concluded that *i*) the maximum scour depth is observed for $\alpha \approx$ 60º *ii*) for the same pier diameter, group configuration and α = 0º, square piers produce greater scour depth than groups of circular piers; *iii*) the Laursen and Toch (1956) skew-angle factor for rectangular piers, with L and D_p defined by the pile group outside dimensions provide a reliable prediction of K_α.

The methods suggested by Richardson and Davis (2001) and Sheppard and Renna (2010) do not make use of K_α. According to these authors, this effect is implicitly included in the determination of the sum of the non-overlapping projected widths of the piles onto a plane normal to the approach flow, W_g. The pile group shape factor, K_{sg}, would also partly account for the effect of the skew-angle in the predictor of Sheppard and Renna (2010).

2.6.4 Effect of the number of aligned rows

The predictors for scour depth at pile groups suggested by Richardson and Davis (2001) and Sheppard and Renna (2010) define a factor that accounts for the effect of the number of aligned rows. According to Richardson and Davis (2001), this factor, K_m, reads

$$K_m = 0.9 + 0.1m - 0.0714(m-1)\left(2.4 - 1.1\frac{s}{D_p} + 0.1\left(\frac{s}{D_p}\right)^2\right) \tag{2.44}$$

The factor for the number of aligned rows, K_m, only applies for pile groups with $\alpha \approx$ [0º, 90º]. K_m increases with the increase of the number of aligned piles or rows, m, to a maximum that is attained for m = 6. For $m >$ 6 the factor K_m is calculated with m = 6.

Sheppard and Renna (2010) also suggest a coefficient for the number of aligned rows:

$$K_m = 0.056m - 0.056m\frac{s}{D_p} + 0.0056m + 0.95 \tag{2.45}$$

Again the factor K_m only applies for $\alpha \approx [0º, 90º]$, with a tolerance of $\pm$ 5º, and $s/D_p \leq 10$. The factor K_m increases with the increase of m for m $\leq$ 5. For $m > 5$ the factor K_m is calculated with m = 5.

2.6.5 Effect of shape pier group

The shape of a matrical pile group is fully defined by the pile spacing, s/D_p, number of aligned rows, m, and number of columns, n, and most of the predictors reported in literature do not include the pile group shape factor, K_{gs}.

One exception is the predictor suggested by Sheppard and Renna (2010), where a pile group shape factor, K_{gs}, is included for the determination of the pile group equivalent diameter. This factor depends on the pile group skew-angle, the pile spacing and also the shape of the individual piles.

$$K_{gs} = \frac{K_s - K_{gs}}{9}\left(\frac{s}{D_p}\right) + K_s - \frac{10}{9}\left(K_s - K_{gs}\right) \tag{2.46}$$

where $K_{s\ (pile)}$ = 1 for circular piles and $K_{gs\ (pile\ group)}$ = 1 for pile groups with $s/D_p > 3$ or n = 1. For pile groups with $s/D_p \leq 3$ and $n > 1$,

$$K_{gs} = 0.86 + 0.97\left|\alpha\frac{\pi}{180º} - \frac{\pi}{4}\right|^4 \tag{2.47}$$

2.7 Local scour prediction at single cylindrical piers

For engineering purposes, the first objective of local scour research is to obtain accurate equilibrium scour depth predictors. At present, the most quoted methods for local scour prediction at single piers are those of Melville and Coleman (2000), Richardson and Davis (2001) and Sheppard and Renna (2005, 2010).

The method proposed by Melville and Coleman (2000), reads as follows

$$d_s = K_d K_I K_{D50} K_s K_\alpha K_g K_t \tag{2.48}$$

where K_d = relative flow depth factor, K_I = flow intensity factor, K_{D50} = relative sediment size factor, K_s = pier shape factor, K_α = pier skew-angle factor, K_g = channel geometry factor and K_t =

time factor. For equilibrium scour depth at cylindrical bridge piers in uniform sediment with $D_p/D_{50} > \approx 25$, $U/U_c = 1.0$, and neglecting contraction and cross-section shape effects, Equation 2.48 reduces to

$$d_{se} = K_{dDp} \tag{2.49}$$

where,

$$K_{dDp} = \begin{cases} 2.4D_p & \text{for} \quad d/D_p > 10/7 \\ 2\sqrt{dD_p} & \text{for} \quad 1/5 < d/D_p < 10/7 \\ 4.5d & \text{for} \quad d/D_p < 1/5 \end{cases} \tag{2.50}$$

Richardson and Davis (2001) suggested a predictor based on the Colorado State University (CSU) equation,

$$\frac{d_{se}}{D_p} = 2.0 K_s K_\alpha K_3 K_4 \left(\frac{d}{D_p}\right)^{0.35} F_r^{\,0.43} \tag{2.51}$$

where K_s = pier shape factor, K_α = correction factor for pier skew, K_3 = correction factor for bed condition, K_4 = correction factor for armoring and $Fr = U/(gd)^{0.5}$ = approach flow Froude number.

For clear-water scour at single cylindrical piers in uniform sand, Equation 2.51 reduces to,

$$\frac{d_{se}}{D_p} = 2 \times 1.1 \left(\frac{d}{D_p}\right)^{0.35} Fr^{0.43} \tag{2.52}$$

Recently, Sheppard and Renna (2005, 2010) suggested a scour depth predictor for clear-water scour ($0.47 < U/U_c < 1.0$) at single cylindrical piers that reads,

$$\frac{d_{se}}{D_p} = 2.5 \tanh\left[\left(\frac{d}{D_p}\right)^{0.4}\right]\left\{1 - 1.2\left[\ln\left(\frac{U}{U_c}\right)\right]^2\right\}\left[\frac{D_p/D_{50}}{0.4\left(D_p/D_{50}\right)^{1.2} + 10.6\left(D_p/D_{50}\right)^{-0.13}}\right] \tag{2.53}$$

It is important to notice that, for clear-water scour at single cylindrical piers, flow intensity $U/U_c = 1$ and $D_p/D_{50} > \approx 25$, the contribution of Melville and Coleman (2000) includes the effect of d/D_p only, the contribution of Richardson and Davis (2001) considers d/D_p and Fr, while the contribution of Sheppard and Renna (2005, 2010) includes the effects of d/D_p, and D_p/D_{50}.

Recently, Arneson *et al.* (2012) recommend both the Richardson and Davis (2001) and the Sheppard and Renna (2010) methods for the prediction of the equilibrium scour depth at single

piers. They have also pointed out that the predictor proposed by Sheppard and Renna (2010) suites the best for wide piers in shallow flows on fine bed material.

2.8 Local scour prediction at pile groups

The predictors reported in this section were derived for complex piers composed by column, pile cap and pile group. In this context, Melville and Coleman (2000) multiply the result of the scour depth at an elemental pile by the product of two factors accounting for effects of spacing and skew-angle, $K_{sp}K_{\alpha}$. These aggregated factors are specified for pile groups of one and two columns, n = [1, 2] in Table 2.2. According to Melville and Coleman (2000) the scour depth at pile groups is not dependent from the number, m, of rows in the group.

Table 2.2 – Aggregated shape and skew-angle factors, $K_{sp}K_{\alpha}$, for pile groups, according to Melville and Coleman (2000)

Number of columns	$K_{sp}K_{\alpha}$			
	s/D_p	$\alpha < 5^o$	$5^o \leq \alpha \leq 45^o$	$\alpha = 90^o$
$n = 1$	2	1.12	1.40	1.20
	4	1.12	1.20	1.10
	6	1.07	1.16	1.08
	8	1.04	1.12	1.02
	10	1.00	1.00	1.00
$n = 2$	2	1.50	1.80	–
	4	1.35	1.50	–

Both Richardson and Davis (2001) and Sheppard and Renna (2005, 2010) propose the use of a pile group effective diameter, D_{pg}, that can be used into the predictors suggested for single piers. It is assumed that the local scour at a pile group is equal to the local scour that would occur for a single cylindrical pier with an equivalent diameter, D_{pg}, subjected to the same approach flow and bed conditions. According to Richardson and Davis (2001), the equivalent, D_{pg}, is the product of the sum of the non-overlapping individual pile widths projected on a plane normal to the approach flow, W_g, by the pile spacing factor, K_{sp}, and the factor for the number of rows, K_m, *i.e.*

$$D_{pg} = W_g K_{sp} K_m \tag{2.54}$$

As mentioned before, for the calculation of W_g, Richardson and Davis (2001) suggested to exclude piles other than those of the two rows and one column closest to the plane of projection, as illustrated in Figure 2.2. This procedure attempts to adjust the impact of each pile, according to the corresponding distance to the projection plane at the group front, were the scour depth is expected to be maximal.

Sheppard and Renna (2005, 2010) make use of the same definition of W_g. The pile group effective diameter defined by Sheppard and Renna (2005, 2010) is the product of W_g by the pile group submergence ratio factor, K_{dpg}, pile group spacing factor, K_{sp}, the factor for the number of aligned rows, K_m, and the pile group shape factor, K_{gs}.

$$D_{pg} = K_{dpg} K_{sp} K_m K_{gs} W_g \tag{2.55}$$

For groups composed of non-submerged piles, $K_{dpg} = 1$.

Later, Ataie-Ashtiani and Beheshti (2006), compared the predictions issued by the methods suggested by Melville and Coleman (2000) and Richardson and Davis (2001) against the data from Hannah (1978), Zhao and Sheppard (1999), as well as their own data, and defined two correction coefficients. According to Ataie-Ashtiani and Beheshti (2006), predictions given by the method suggested by Melville and Coleman (2000), should be multiplied by

$$K_{smn} = 1.118 \frac{m^{0.0895}}{n^{0.8949} \left(G / D_p\right)^{0.1195}} \tag{2.56}$$

where $G = s - D_p$ = free space between piles. Regarding the method suggested by Richardson and Davis (2001), Ataie-Ashtiani and Beheshti (2006) suggested the following correction factor.

$$K_{smn} = 1.11 \frac{m^{0.0396}}{n^{0.5225} \left(G / D_p\right)^{0.1153}} \tag{2.57}$$

3. EXPERIMENTAL SETUP, MEASURING EQUIPMENT AND PROCEDURE

3.1 Introduction

In the sequence of a short characterization of the experimental campaign carried out in the study, this chapter focus first in the description of two flumes used in the experimental campaign. These flumes were those of the Universidade da Beira Interior (UBI) and the Faculdade de Engenharia da Universidade do Porto (FEUP). Then, the measuring equipment and the experimental procedures are described and documented.

As mentioned in the introduction, data obtained in a third flume were used in this dissertation. Since the experiments were performed before the formal initiation of the dissertation and the amount of data is rather limited, this flume will only be shortly described in chapter 4.

3.2 Experimental campaign

Two main groups of experiments were made in the two described flumes. The first group refers to scouring at single cylindrical piers. These experiments were designed in order to cover the range of relative flow depth (or flow shallowness) values of d/D_p = [0.5, 1.0, 1.5, 2.0, 2.5, 3.0, 4.0, 5.0] and relative sediment size (or sediment coarseness) values of D_p/D_{50} = [58.1, 87.2, 127.9, 186.0, 232.6, 290.7, 366.3, 407.0, 465.1]. Table 3.1 summarizes the values of d/D_p and D_p/D_{50} of the 38 tests performed: 21 at UBI; the remaining 17 at FEUP. The choice of a given flume was decided so as to guarantee values of $B/d > 5$ and $B/D_p > 5$, this way avoiding serious wall and contraction effects, respectively.

Table 3.1 – Definition of the characteristic variables for the tests at single cylindrical piers

	D_p (mm)								
	50	75	110	160	200	250	315	350	400
d/D_p	D_p/D_{50}								
0.5			128	186	233	291	366	407	465
1.0	58	87							
1.5					233				
2.0			128	186					
2.5									
3.0							Tests run at UBI		
4.0		87					Tests run at FEUP		
5.0	58								

The second main group of experiments covered scouring at pile groups. These experiments were designed in order to characterize the effects of the pile spacing, s, skew-angle, α, and number of pile alignments (or columns) in the group, n (see Figure 2.2); the pile groups were defined for m = 4. 75 combinations of n = [1, 2, 3], s/D_p = [1, 2, 3, 4.5, 6] and α = [0º, 15º, 30º 45º, 90º] were covered. The 15 tests defined by {n = 1, α = [0º, 15º]} and [n = 2, α = 0º], for s/D_p = [1, 2, 3, 4.5, 6] were run at FEUP while the remaining 60 tests were run at UBI. Again, this distribution of tests per flume was made so as to mitigate wall and contraction effects.

Five special tests were finally run at UBI flume with the purpose of characterizing the effect of viscosity. The tests were designed to vary the approach flow Reynolds number, $R_e = Ud/\nu$ (and others forms of the non-dimensional viscosity presented in Chapter 2) while all the other non-dimensional parameters were kept constant.

During the study, the approach flow depth, the flow-discharge and the scour depth were measured according to the experimental procedure to be presented in the section 3.5. In a few cases the water temperature was also measured.

3.3 Description of the UBI flume, sand and piers

Figure 3.1 presents the plan view and the longitudinal central section of the UBI flume. It includes supply reservoir [1], channel [2], supply hydraulic circuits [4, 5, 6], electromagnetic flow-meters [9], double honey-comb diffusers [7], drainage circuit [8], acceleration ramp [10], hopper [11], downstream gate [12] and diffuser pipe [13].

The dimensions of the supply reservoir are 4.50 m x 10.00 m x 2.40 m (width x length x height). The channel is 28.00 m long, 4.00 m wide and 1.00 m high; it is made of concrete and it has 10 glass windows in the right wall. In the channel bottom, there is one recess box [3] that starts at 13.9 m from the flume entrance; its dimension are 4.00 m x 3.00 m x 0.60 m (width x length x depth). The channel and the recess box width may be reduced by using a set of stainless steel panels.

During the experimental campaign, the useful width of the channel assumed different values so as to attain sufficiently high approach flow depth and average velocities with the existing flow-discharge capacity whenever needed. For the tests on single cylindrical piers, only half of the flume width was used (B = 2.00 m). For the tests on pile groups, the approach flow depth was kept constant in all the tests (d = 0.20 m), allowing the run of two simultaneously tests. In this case, a thin vertical smooth wall made of plywood board was placed along the channel central axis, which made it possible to place two different pile groups within the channel recess box and run the corresponding experiments. In practice, the flume width was B = 2.00 m for each test. Finally, for the tests designed to isolate the effect of viscosity, the flume width was reduced to B = [1.50, 2.00] m, depending on the experiment.

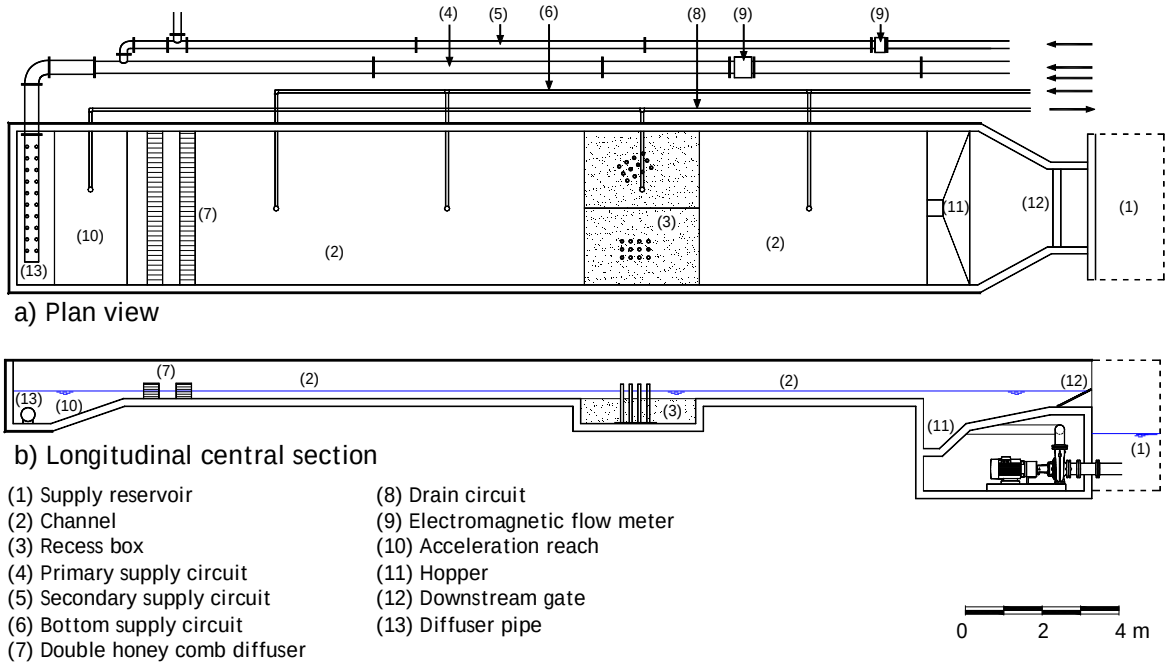

Figure 3.1 – Draft of the UBI flume: a) plan view; b) longitudinal central section

At the flume entrance, an ascending ramp [10] of ≈14º guarantees the transition from the diffuser pipe to the channel. This feature imposes the flow acceleration in a short reach, which promotes the flow distribution though the flume width. The two honey-comb diffusers [7] placed immediately downstream of the ramp are made of perforated bricks and 25 mm PVC pipes, respectively, both aligned with the main channel direction. They further improve the flow uniformity at the channel entrance.

The capacity of the hopper [11] is 2.3 m^3. It may collect the entrained sediments when they reach the far end of the flume. The downstream gate is 2.00 m wide [12] and allows for the water level regulation inside the flume (see Figure 3.2).

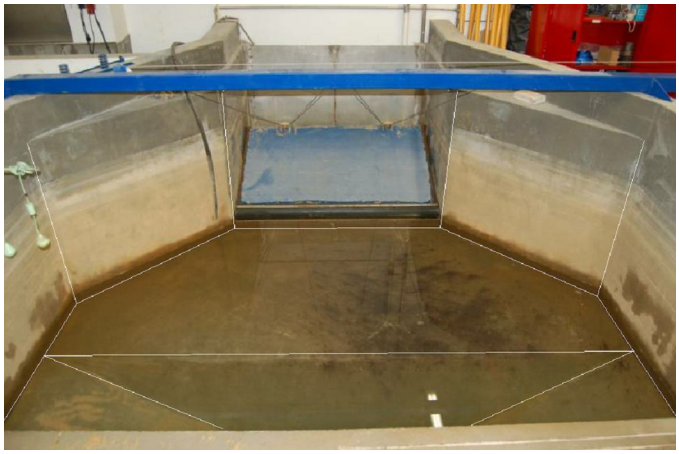

Figure 3.2 – Hopper and downstream flow gate

The main and secondary hydraulic circuits, [4] and [5], connect the supply reservoir to the diffuser pipe [13] and convey flow-discharges ranging from 0 ls^{-1} to 270 ls^{-1}. They are composed of ductile cast iron pipes, and include two variable speed centrifugal pumps, one per circuit (see Figure 3.3), valves and electromagnetic flow-meters [9]. The electric engines of the centrifugal pumps are connected through frequency converters that adjust the rotation speed so as to impose the pre-defined flow-discharge. The diffuser [13] is a perforated stainless steel pipe that promotes the uniform flow distribution trough the whole flume width.

Figure 3.3 – Centrifugal pumps

Figure 3.4 shows the brick and PVC honey-comb diffusers and Figure 3.5 shows the stainless steel diffuser pipe.

Figure 3.4 – Brick and PVC honeycomb diffusers

Figure 3.5 – Diffuser pipe

The flume also includes one secondary supply circuit [5] ending in three flume bottom nozzles. This circuit is used for filling purposes, conveying a flow-discharge of up to 5.0 ls^{-1}.

The flume is equipped with one motorized carriage (see Figure 3.6.a) and one light weight manual bridge (Figure 3.6b). Both move along the longitudinal axis of the channel on two precisely levelled rails. They are used to access the test area and the measuring equipment. A moving aluminium bar is used to support some measuring equipment; it also moves on the two rails.

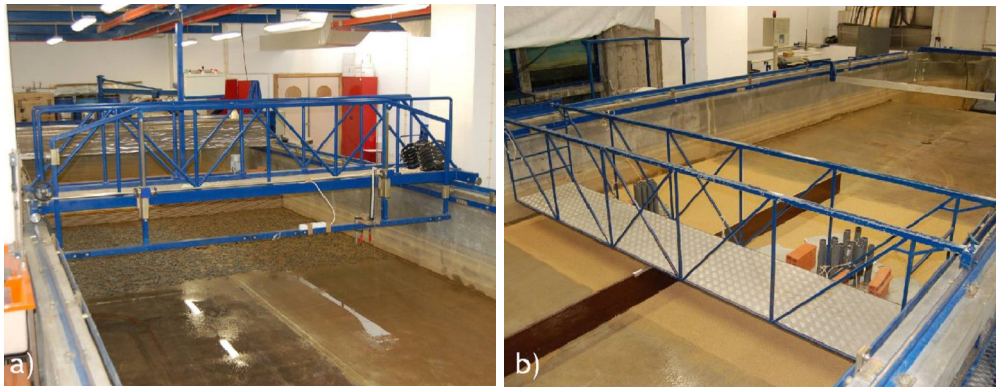

Figure 3.6 – a) Motorized movable bridge: b) manual light bridge

The flume recess box was filled with quartz sand creating the conditions for the scour holes to develop. The grain size distribution of the used sands was obtained by mechanical sieving, according to the Portuguese Specification LNEC E245 (1971). The results are shown in Figure 3.7. From the grain size distribution, the following characteristic diameters were obtained. For sand 1, $D_{84.1}$ = 1.15 mm; D_{50} = 0.86 mm; $D_{15.9}$ = 0.62 mm; for sand 2, $D_{84.1}$ = 1.94 mm; D_{50} = 1.28 mm; $D_{15.9}$ = 0.86 mm; for sand 3, $D_{84.1}$ = 3.9 mm; D_{50} = 3.00 mm; $D_{15.9}$ = 2.12 mm. The sediment gradation coefficient was calculated as $\sigma_D = 0.5(D_{84.1}/D_{50} + D_{50}/D_{15.9})$ and equals to 1.36, 1.50 and 1.36 for sands 1, 2 and 3, respectively. The values of σ_D are under ≈1.5, which indicates that the three sands may be considered uniform.

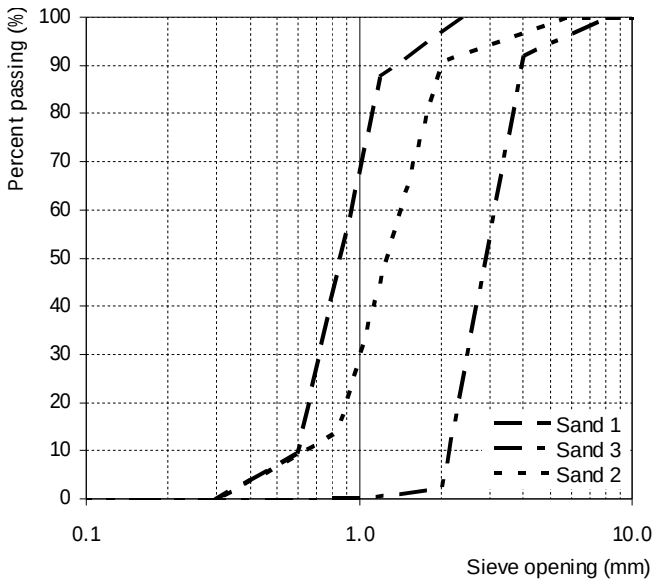

Figure 3.7 – Grain size distribution curve

The sand density, ρ_s, was obtained with the help of a helium pycnometer, according to the NP-83 (1965). The result was $\rho_s = 2660$ kgm^{-3}.

The average approach flow velocity for the threshold condition of initiation of motion of the sand was calculated through the equation of Neil (1967):

$$\frac{U_c^{\,2}}{\Delta g D_{50}} = 2.5\left(\frac{d}{D_{50}}\right)^{0.2} \tag{3.7}$$

For, d = 0.20 m, for instance, U_c is equal to 0.32 ms^{-1}, 0.38 ms^{-1} and 0.53 ms^{-1} for sand 1, 2 and 3, respectively.

The piers used in the groups of experiments on scouring at single cylindrical piers were simulated by PVC pipes with outside diameters D_p = [50, 75, 110, 160, 200, 250, 315, 350, 400] mm, placed on the bottom of the bed recess box at ≈1.0 m from the upstream boundary of the box. For pile groups, the individual cylindrical piles were simulated by PVC pipes with diameter D_p = 50 mm.

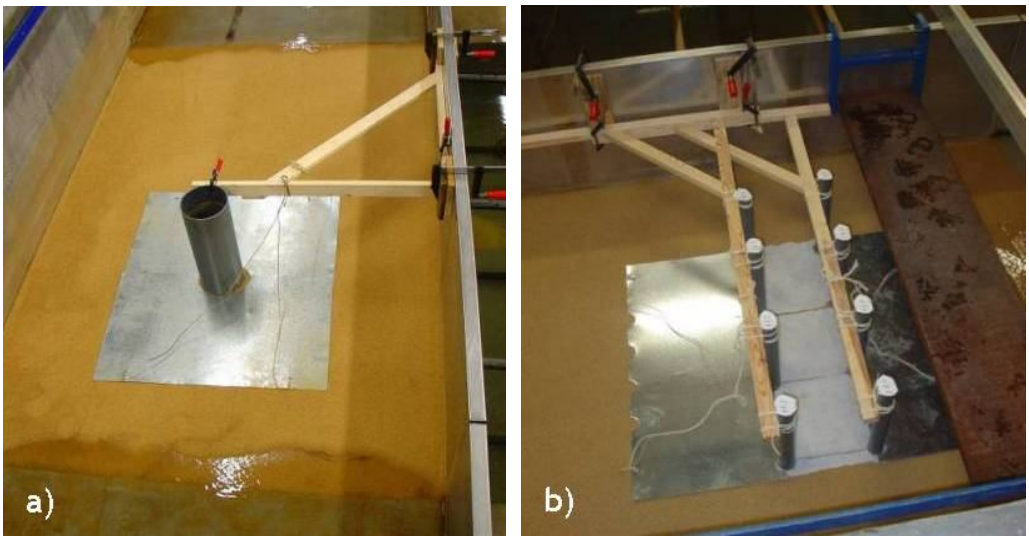

Figure 3.8 – Experiments preparation, before flume fill up: a) single pier; b) pile group

3.4 Description of the FEUP flume, sand and piers

Figure 3.9 presents the plan view and the longitudinal central section of the FEUP flume. It includes settling chamber [1], channel [2], bed recess box [3], hopper [4], downstream gate [5], constant head reservoir [6], electromagnetic flow-meters [7], false floor [8], inlet pipe [9], outlet to the return circuit [10].

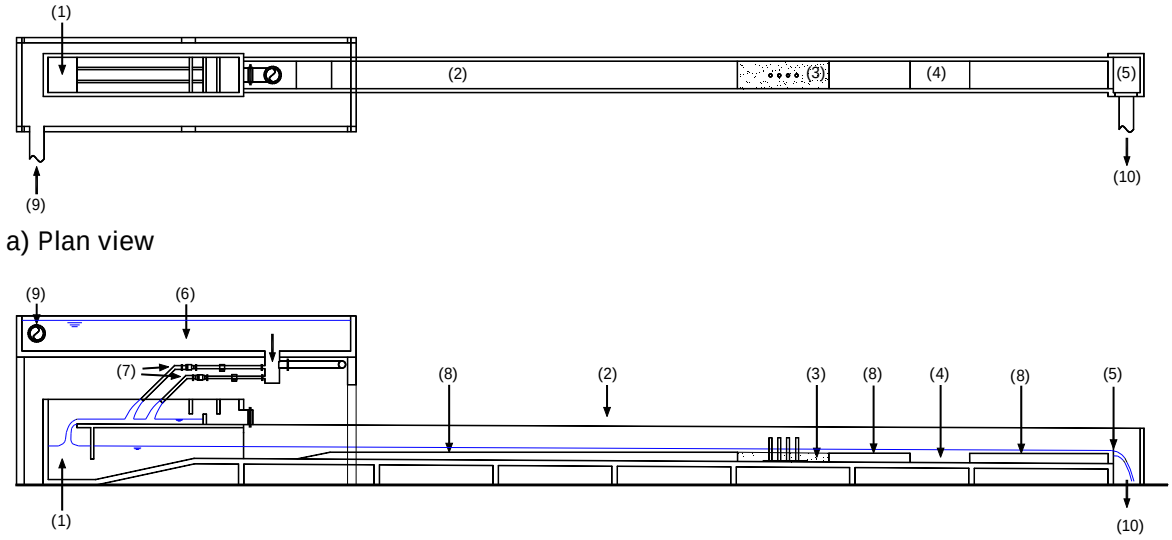

Figure 3.9 – Draft of the FEUP flume: a) plan view; b) longitudinal central section

The FEUP flume is 33.15 m long, 1.00 m wide and 1.0 m deep. The central bed recess box starts at 16.00 m from the entrance; the length of the box is 3.20 m and its depth is 0.35 m. The maximum flow discharge is 90 ls^{-1}. The main difference between FEUP flume and UBI flume is its smaller width, which determined the set of the experiments performed at FEUP.

The transition from the constant head reservoir [6] to the channel false floor [8] is made by a free fall and an ascending ramp. This ramp promotes the uniform flow distribution. As in UBI flume, the hopper [4] collects the entrained sediments and the downstream gate [5] allows the water level regulation inside the channel (see Figure 3.10); the flow discharge is measured by two electromagnetic flow-meters [7] installed at pipes situated between the constant head reservoir and the settling chamber [1].

Figure 3.10 – Downstream gate

The channel is equipped with a moving platform supported in its lateral walls. The platform, located over the recess box was used to fix a point gauge.

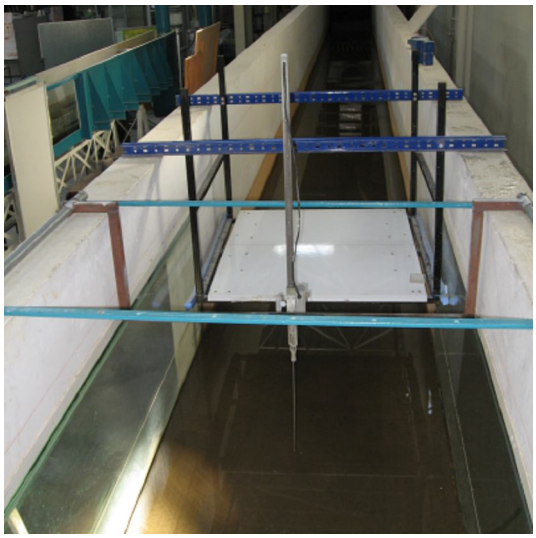

Figure 3.11 – Platform use do to fix the measuring equipment

The FEUP flume was used to run tests at single cylindrical piers and pile groups as specified in section 3.2. The piers and piles were simulated by PVC pipes and fixed to the floor of the recess box in the same way as in the UBI's experiments. The maximum diameter of single piers was D_p = 200 mm; the maximum number of columns was n = 2; the maximum skew-angle was 15º. The sand used to fill up the recess box in the FEUP flume was always sand 1 since the flume was not used to run tests on the effect of viscosity on scouring.

3.5 Measuring equipment

As stated before, the measured variables included the flow depth, the flow discharge, the scour depth and, in a few cases, the water temperature. The flow depth was measured by using point gauges. In UBI flume, one point gauge was fixed to the motorized bridge and used to measure the approach flow depth. In FEUP flume, the point gauge was fixed to the platform (see Figure 3.11). The point gauges were equipped with vernier scales (*nonius*) to the accuracy of ± 0.1 mm but the measurements were made with ± 1 mm error margin due to small water surface instabilities.

The flow discharge was measured by electromagnetic flow-meters, one per pipe of the water circuits. The principle of operation of the electromagnetic flow-meters is the Faraday law of induction, which states that a voltage is generated in a conductor when it moves through a magnetic field. This measurement principle is applied to a conductive fluid which flows in a pipe in which a magnetic field is generated perpendicular to the flow direction. The voltage induced in the fluid is measured by two electrodes located diametrically opposite to each other. The signal voltage is proportional to the magnetic induction and, as the magnetic induction,

electrode spacing and cross-section area are constant, the signal voltage is proportional to the average flow velocity, *U*. Figure 3.12 shows one of the electromagnetic flow-meters of the UBI's flume.

Figure 3.12 – Electromagnetic flow-meter

Scour depth measurements were made by using *adapted* point gauges, fixed to the moving aluminium bar in UBI and to the platform in FEUP. To ease the measurements, the tip of the gauges was painted in red on the extreme 20 mm. As this device lowers, the bed level reading is made when the red tip can no longer be seen out of the sand bed. Errors of the order of ± 1mm may be allocated to the measurements which were made with the aid of one acrylic pipe with one closed transparent end, slightly dipped into the flow. Figure 3.13 shows the point gauge mounted on the aluminium bar in the UBI flume. One exception to this procedure was the scour depth measurements at pile groups performed in FEUP. In these tests, a metric tape was glued to each pile face (see Figure 3.14) and the readings were performed through visualization with the aid of the acrylic pipe.

Figure 3.13 – Point gauge mounted in the aluminium bar

Figure 3.14 – Metric tape glued at each individual pile (FEUP only)

The water temperature in the UBI flume was measured with a mercury thermometer with ± 0.1ºC precision during the tests designed to assess the effects of viscosity on scouring.

3.6 Experimental procedure

Each test required the placement of piers or pile groups, the sand bed preparation, placement of protective metal sheets and filter fabric, flume fill up, flow depth and flow rate stabilization, removal of the protective metal sheets and filter fabric, measurement of the scour depth along time, flume depletion and photographic surveys of the scour hole. One test preparation included six stages:

i) Piers preparation and fixation – The procedures were exactly the same in both flumes. A plywood board was placed and fixed to the recess box floor. The piers larger than 50 mm were fixed to the board by four metal corners. For the 50 mm piles, 70 mm height nylon cylinders whose diameters were equal to the inside pile diameter, were used. To guarantee the verticality of piers and pile groups, the PVC pipes were also fixed to wood supports, at UBI, and steel supports, at FEUP, at their tops.

ii) Recess box fill up with quartz sand – During this action, the quartz sand was completely saturated with water and drained at least once to guarantee the adequate compaction.

iii) Sand bed levelling – Sand bed was precisely levelled with the help of long aluminium rulers to fit the sand level to the adjacent flume bed.

iv) Placement of the protection metal sheets and filter fabric – Before the tests, the area located around the pier or piles was covered with thin metallic plates. In the tests with pile groups, filter fabric was also used to cover the area between piles. This procedure was important to avoid unwanted scour while flow-rate and flow depth gradually attained the values established for each test.

v) Flume fill up – Before the start of the pumps, the UBI flume was gradually filled up through the bottom supply circuit [6]. In FEUP, the flume was filled up by using a public water supply system. This procedure was important to avoid the low depth and high flow velocity that would occur otherwise at the early stages of the flow-discharge and flow depth stabilization.

vi) Flow-discharge and flow-depth stabilization – In UBI flume, the experiment flow-discharge was chosen in the hydraulic circuit automaton and the centrifugal pump or pumps gradually archived the required flow-rate, while in FEUP the flow-discharge was controlled by adjusting a valve in the hydraulic circuit. In the meantime, the flow depth was manually adjusted by operating the downstream gate. When both flow rate and flow depth attained the desired values, the protective metal sheets were removed, the scour hole started to develop and the measurement sequence was initiated.

The scour depth time evolution was monitored by measuring the scour depth with the point gauge (or metric scale for the pile groups at FEUP), several times during the first hour. Afterwards, the interval between measurements increased and, after the first day, few measurements were carried out per day. The experiments were run at least 7 days.

The scour depth measurements were made at the location where the maximum scour depth is observed, *i.e.* immediately upstream of the piers. In the case of pile groups experiments, the measurements were performed at all piles in the group.

Once a given experiment was stopped, the flume was slowly drained. After that, the scour hole pattern was photographed. Figure 3.15 shows the recess box and piers and at the end of the tests, after the flume depletion, for a single pier and a pile group. The measuring locations are marked with a white dot.

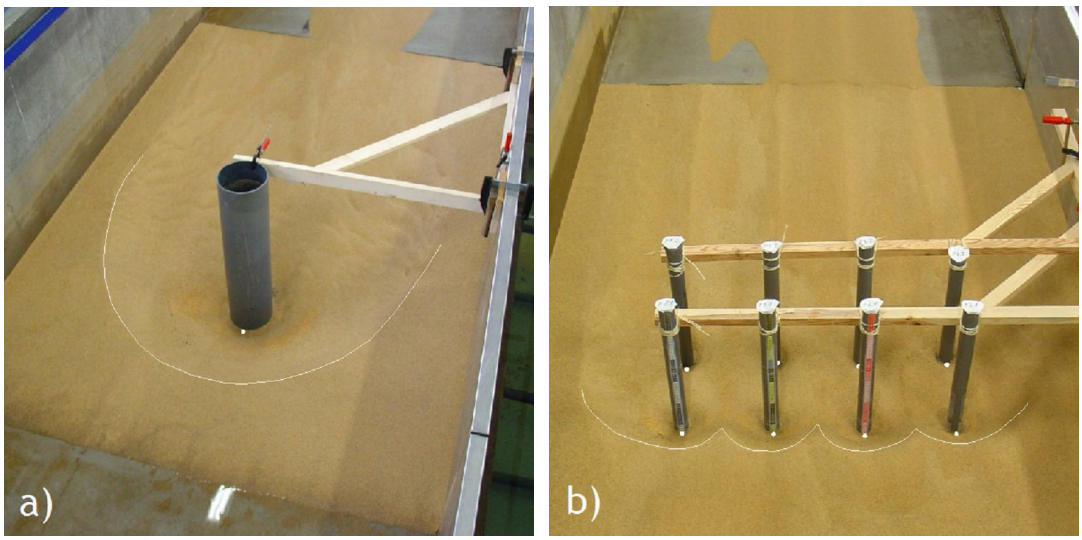

Figure 3.15 – Typical scour patterns at experiment end: a) single pier; b) pile group

It should be stressed at this stage that the approach reach located upstream of the piers stayed undisturbed along the entire duration of the experiments; this long term stability ensured that scour holes did not add with the effect of upstream bed degradation that could occur otherwise.

4. ASSESSING EQUILIBRIUM CLEAR-WATER SCOUR AROUND SINGLE CYLINDRICAL PIERS

4.1 Introduction

Since the nineteen fifties, many researchers have performed experimental studies to understand the scour process at bridge piers and abutments as well as to derive scour depth predictors. The pioneer works of Chabert and Engeldinger (1956) and Laursen (1963) deserve a special mention. Until two decades ago, many studies on this topic reported experiments that might have lasted not long enough to reach equilibrium.

In the last decade, the research on the time evolution of the scour depth was intensified; the works of Cardoso and Bettess (1999), Melville and Chiew (1999), Oliveto and Hager (2002, 2005), Radice *et al.* (2002), Coleman *et al.* (2003) or Kothyari *et al.* (2007) can be mentioned, among others. Some of these studies were based on long-lasting clear-water experiments assumed to have reached equilibrium.

In this context, it should be noted that Ettema (1980) identified three phases of the scour process, irrespective of the state of movement of the sediment bed upstream (clear-water or live-bed) and the type of obstacle (pier or abutment): the initial phase, characterized by the fast scour rate produced by the down-flow at the pier face; the principal phase, which begins when the horse-shoe vortex starts to dominate the scouring process; the equilibrium phase, where the scour depth "practically" does not increase anymore. Hoffmans and Verheij (1997) refer to four phases: initial phase; development phase; stabilization phase and equilibrium phase. Other authors introduce nuances to the classification of the scour phases or name them differently but the basic concepts remain.

In clear-water scour, the principal phase lasts for very long and the equilibrium scour depth is approached asymptotically (Chabert and Engeldinger 1956). This phase is assumed to occur when the scour depth does not change "appreciably" with time.

From above, it can be anticipated that the equilibrium concept is rather subjective since each author has a different interpretation of the meaning of words like "practically" or "appreciably". This subjectivity has important implications on the time required to materialize equilibrium in the laboratory. Franzetti *et al.* (1994) suggested that equilibrium scour at piers is achieved when

$Ut/D_p > 2 \cdot 10^6$ (U = approach flow velocity; t = time; D_p = pier diameter). Melville and Chiew (1999) defined time to equilibrium as the time when the rate of scour reduces to 5% of the pier diameter in a 24-hour period. Coleman *et al.* (2003) defined the equilibrium time as the time at which the rate of scour reduces to 5% of the smaller of the foundation length (pier diameter or abutment length) or the flow depth in the succeeding 24-hour period. In the same line, Grimaldi (2005) suggested a more restrictive criterion, namely, the reduction of scour rate to less than $0.05D_p/3$ in 24 hours. The value of 5% (or 0.05), though pragmatic, is obviously arbitrary; if the variation is reduced to, say, 2% – which is arbitrary as well – the time needed to reach equilibrium may be significantly longer. Adopting a suggestion by Ettema (1980), Cardoso and Bettess (1999) assessed the onset of the equilibrium phase as the time where the slope of plots of the scour depth versus the logarithm of time changes and tends to zero, in an attempt to mitigate arbitrariness. Radice *et al.* (2002) claim that this approach may also fail since scouring can be triggered again, after the observation of a long-lasting quasi-horizontal plateau.

A few predictors of (finite) time to equilibrium were derived in the last decade, including, for piers, the predictors of Melville and Chiew (1999) and Kothyari *et al.* (2007), and, for abutments, those of Coleman *et al.* (2003) and Fael *et al.* (2006).

Quoting Coleman *et al.* (2003), an apparently equilibrium scour hole may continue to deepen at a relatively slow rate long after equilibrium conditions were thought to exist. Some investigators argue that the equilibrium cannot be achieved in finite time and that the scour hole never stops to develop. Among these authors, Franzetti *et al.* (1982) and Oliveto and Hager (2002, 2005) can be pointed out. Oliveto and Hager (2005), for instance, state that "end scour as the equilibrium state between the vortical agents and the resistance of sediments to be scoured does not normally exist". However, in an apparent contradiction, these authors also state that the concept of equilibrium scour is an essential feature that needs to be accounted for in models for scour predictions.

The definition of time to equilibrium plays an important role in the design of scour experiments searching for accurate equilibrium scour predictors. How long should experiments be until the scouring rate becomes "insignificant" or "practically" null? In an attempt to overcome this practical difficulty, Bertoldi and Jones (1998) suggested the extrapolation – to infinite time – of a 4-parameters polynomial function fitted to the time records of the scour depth, measured in experiments of comparatively short duration.

The objective of this research is to assess the pertinence of the suggestion by Bertoldi and Jones (1998) as well as of a similar approach, based on a 6-parameters polynomial function. The results of these approaches are compared, in terms of the equilibrium scour depth, with those associated to the criteria of Melville and Chiew (1999), Cardoso and Bettess (1999) or Grimaldi (2005). Predictors of time to equilibrium suggested by Franzetti *et al.* (1994), Melville and Chiew (1994) and Kothyari *et al.* (2007) will equally be assessed.

4.2 The polynomial functions

According to Bertoldi and Jones (1998), equilibrium is reached at infinite time and the equilibrium scour depth of a given experiment can be calculated by adjusting the polynomial function

$$d_s = p_1\left(1-\frac{1}{1+p_1p_2t}\right)+p_3\left(1-\frac{1}{1+p_3p_4t}\right) \tag{4.1}$$

to the recorded time evolution of the scour depth; in Equation 4.1, d_s is the scour depth at instant t and p_1, p_2, p_3 and p_4 are parameters obtained by regression analysis. The equilibrium scour depth, d_{se}, is obtained for $t = \infty$, *i.e.*, $d_{se} = p_1 + p_3$.

In the present study, the following generalization of the previous polynomial function

$$d_s = p_1\left(1-\frac{1}{1+p_1p_2t}\right)+p_3\left(1-\frac{1}{1+p_3p_4t}\right)+p_5\left(1-\frac{1}{1+p_5p_6t}\right) \tag{4.2}$$

is assessed too. Here, p_5 and p_6 are extra polynomial parameters; the equilibrium scour depth, d_{se}, comes as $d_{se} = p_1 + p_3 + p_5$.

4.3 Experiments

Five experiments were carefully run on purpose to collect data to check the pertinence of assessing the equilibrium scour, in laboratory conditions, through the approaches referred in the Introduction.

Experiments were carried out in a 12.7 m long, 0.83 m wide, and 1.0 m deep concrete glass-walled flume. The central reach of the flume, starting at 5.0 m from the entrance, includes a 3.1 m long and 0.35 m deep recess in the bed. The experimental set-up includes a closed hydraulic circuit where the discharge can be varied from 0.0 ls^{-1} to 90 ls^{-1}. The flow discharge is measured with an electromagnetic flow meter installed in the circuit. At the entrance of the flume, one honeycomb diffuser aligned with the flow direction regularizes the flow trajectories and guarantees the (lateral) uniform flow distribution. Immediately downstream this device, a short ascending gravel ramp makes the transition to the sand bed. At the downstream end of the flume, a tailgate allows the regulation of the water level. The water falls into a 100 m^3 reservoir, where the hydraulic circuits start.

Depending on the experiment, the bed recess was filed with two different uniform quartz sands: sand 1 (ρ_s = 2660 kgm^{-3}; D_{50} = 0.86 mm; σ_D = 1.36) and sand 2 (ρ_s = 2660 kgm^{-3}; D_{50} = 1.28 mm; σ_D = 1.50). Here, D_{50} = median size of the sand size distribution; σ_D = geometric standard deviation

of the sand size distribution; ρ_s = sand density. Single vertical cylindrical piers were simulated by PVC pipes with diameters D_p = 0.063 m, 0.075 m and 0.080 m, placed at ≈1.5 m from the upstream border of the bed recess. Then the flume bed was covered with a 0.1 m thick layer of the same sands, this way allowing for up to 0.45 m deep scour holes at the piers.

Prior to each test, the sand bed was levelled. The area located around the pier was covered with a thin metallic plate to avoid uncontrolled scour at the beginning of the experiment. The flume was filled gradually from the downstream end through a small hydraulic circuit, imposing high water depth and low flow velocity. The discharge corresponding to the chosen approach flow velocity was passed through the flume. The flow depth was regulated by adjusting the downstream tailgate. Once the flow depth was established, the metallic plate was removed and the experiment started. Scour was immediately initiated and the depth of scour hole was measured, to the accuracy of ± 1 mm, with an adapted point gauge, every ≈ 5 minutes during the first hour. Afterwards, the interval between measurements increased and, after the first day, few measurements were carried out per day. The approach reach located upstream the piers stayed undisturbed along the entire duration of the experiments; this long term stability is important to ensure that scour holes do not add with the effect of upstream bed degradation that could occur otherwise.

4.4 Results and discussion

The values of the most important independent variables characterizing the experiments are summarized in Table 4.1. The study was made for reasonably high flow depth, d = 0.13 m, 0.15 m and 0.16 m. The approach flow velocity, U, was selected to be 80% or 86% (*cf.* Table 4.1) of the sand entrainment velocity (beginning of motion), U_c. This variable was calculated through the equation suggested by Neil ($U_c^2/(\Delta g D_{50}) = 2.5(d/D_{50})^{0.2}$); $\Delta = \rho_s/\rho - 1$; ρ = water density; g = acceleration of gravity. For Test 1 (for example), where d = 0.16 m and D_{50} = 0.86 mm, U_c, U and the flow discharge, Q, were, respectively, 0.314 ms^{-1}, 0.252 ms^{-1} and 34 ls^{-1}. The aspect ratio was such that $B/d \geq 5.2$ (B = flume width) and the contraction ratio was $B/D_p \geq 10.4$. These values indicate that wall effect and contraction effect are negligible. Since $D_{50} > 0.8$ mm and ρ_s = 2660 kgm^{-3} viscous effects can be expected to be small, according to Kothyari *et al.* (2007). Tests lasted 24.9 days ≤ t_d ≤ 45.6 days (t_d = test duration), *i.e.*, much longer than common experiments. The relative flow depth, d/D_p was kept reasonably constant and ≈2, rendering the effect of this parameter on the equilibrium scour depth negligibly small; relative sediment size, D_p/D_{50}, varied in the range $49.2 \leq D_p/D_{50} \leq 93.0$, which maximizes the scour depth.

Table 4.1 – Characteristic variables of the experiments

Test	d (m)	D_p (mm)	D_{50} (mm)	t_d (day)	U/U_c (-)	d/D_p (-)	D_p/D_{50} (-)
1	0.16	75	0.86	34.9	0.80	2.13	87.2
2	0.16	80	0.86	45.6	0.86	2.00	93.0
3	0.16	80	1.28	29.7	0.80	2.00	62.5
4	0.15	75	1.28	24.9	0.80	2.00	58.6
5	0.13	63	1.28	29.0	0.80	2.06	49.2

The time records of the scour depth are available at http://w3.ualg.pt/~rlanca/riverflow2010.htm; they are also plotted in Figure 4.1 as d_s *v.s.* t (log scale); they are also given in Figure 4.2 by exploiting the coordinates suggested by Oliveto and Hager (2002; 2005), *i.e.*

$$Z = \frac{d_s}{z_R} \quad \therefore \quad z_R = \left(dD_p{}^2\right)^{1/3} \tag{4.3}$$

and

$$T = \frac{t}{t_R} \quad \therefore \quad t_R = \frac{z_R}{\sigma_D{}^{1/3}\left(\Delta g D_{50}\right)^{1/2}} \tag{4.4}$$

Figure 4.2 also includes the predictor of time evolution of scour depth proposed by Oliveto and Hager (2005):

$$Z = 0.068 N \sigma_D{}^{-1/2} Fr_d{}^{3/2} \log T \tag{4.5}$$

where $Fr_d = U/(\Delta g D_{50})^{1/2}$ is the densimetric Froude number and $N = 1$ is a shape factor. Fr_d was practically equal for the experiments with a given sand and was taken as the corresponding sand average for purposes of plotting Equation 4.5.

The inspection of Figure 4.1 indicates that equilibrium was never clearly reached. This is more evident for Test 1 and Test 2, run for the finer sand. In the case of Test 1, two dotted horizontal segments are included, corresponding to horizontal plateaux where equilibrium could, a priori, be claimed to have been reached, according to Cardoso and Bettess (1999). Similar plateaux appear in the other experiments, rendering it clear that the criticism of Radice *et al.* (2002) is pertinent.

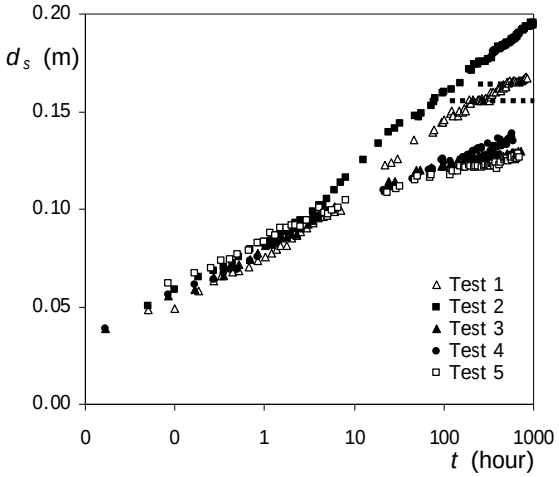

Figure 4.1 – Time evolution of the scour depth

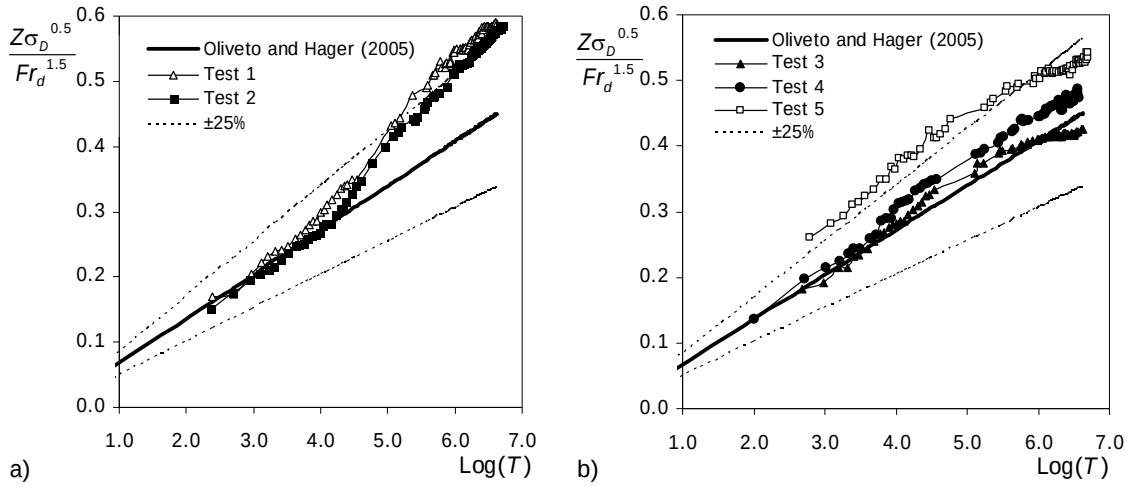

Figure 4.2 – Time evolution of the scour depth written in the coordinates of Oliveto and Hager (2005)

The analysis of Figure 4.2 reveals that, with the exception of Test 5, *i*) the predictor of Oliveto and Hager (2005) fits the data perfectly, for $T < 10^4$, *ii*) the slope of the observed scour depth evolution is steeper than the slope of the predictor for the finer sand when $T > 10^4$, *iii*) a tendency to equilibrium is identifiable in the case of the coarser sand (see Test 3 and Test 5); *iv*) the 25% band around the predictor does not really accommodate measurements of Test 1 (for $T > 10^5$) and Test 5.

The time records of scour depth were finally exploited within the framework of Kothyari´s *et al.* (2007) predictor of scour depth time evolution. It was concluded that this predictor does not perform better than the predictor of Oliveto and Hager (2005) since most of the experimental data fall outside the 25% band; the predictor of Kothyari *et al.* (2007) largely under predicts scour depth in four of the five cases.

Although equilibrium was not unambiguously reached, it seems reasonable to postulate that equilibrium must exist since, in nature, there are abutment-like structures where the flow kept running since ever while the scour depth did not increase to infinite. Yet, one has to recognize that *i*) the probability of occurrence of a sufficiently strong turbulent event capable of entraining bed grains will never be null; *ii*) this probability decreases as scour progresses, tending asymptotically to zero. Consequently, *i*) the scour depth will tend to equilibrium but *ii*) the time required for equilibrium may be rather large, idealized as infinite. This is the concept behind Equation 4.1 suggested by Bertoldi and Jones (1998) to be fitted to finite-time records of scour and derive the equilibrium (end) scour depth, for $t = \infty$.

Thus, Equation 4.1 was fitted to the five data sets. Figure 4.3.a) shows the result of this procedure as applied to Test 2. Two extents of the record were used in the fitting process: 25 days and the full record. It becomes clear that *i*) the fitted curves do not perfectly adhere to the scour data, particularly for large values of t; *ii*) deviations are more pronounced when the fitting process is applied to the shorter duration.

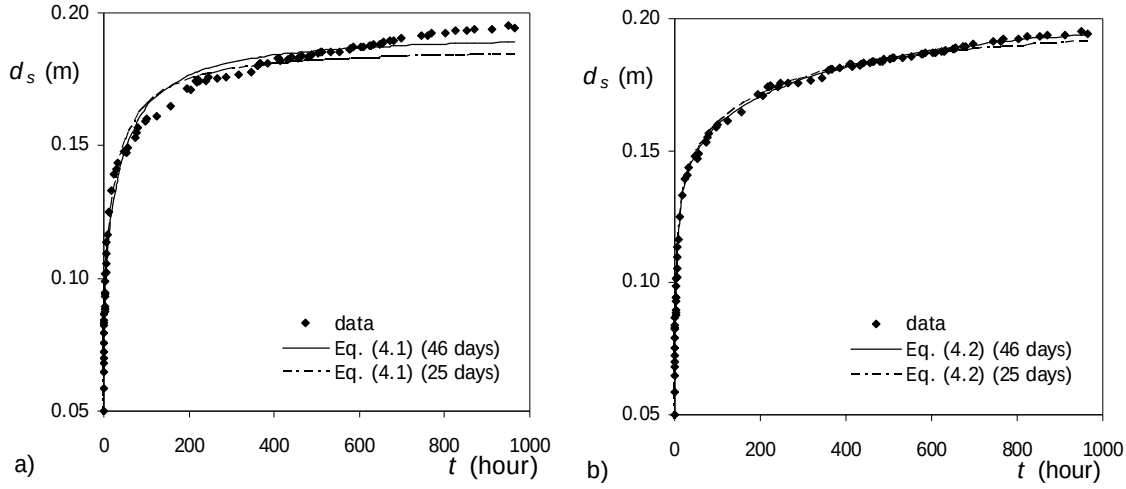

Figure 4.3 – a) Data of Test 2 adjusted by Equation 4.1; b) idem for Equation 4.2

The trend shown in Figure 4.3.a) was also observed for the other four experiments although it was less pronounced, particularly for experiments corresponding to the coarser sand. The identification of such trend led to the consideration of Equation 4.2 in the analysis. From Figure 4.3.b) it is obvious that this equation fits the data much closer. For this reason, Equation 4.2 was used to derive the end scour of each experiment. It must be stressed that *i*) the calculations inherently carry unknown errors, *ii*) the errors decrease as the lengths of the scour records used in the fitting procedure increase.

Since Test 2 was the longer one, it was used to check the order of magnitude of deviations of end scour depth calculated from different length experiments. For this purpose, the time record was truncated at three different durations, $t_r < t_d$. Equation 4.2 was applied to the four issued

records and the deviations were evaluated assuming that the true end scour is obtained from the extrapolation of the entire record (≈46 days) to infinite. The output deviations were –4.2% for t_r = 25 days, –2.5% for t_r = 30 days and –1.2% for t_r = 35 days. It can be assumed that, for the remaining (shorter) experiments, deviations associated to the extrapolation of Equation 4.2 to $t = \infty$ will be of the same order of magnitude or smaller. Smaller deviations are expectable, namely, for Tests 3, 4 and 5, which seem to have attained scour depths closer to equilibrium (*cf.* Figure 4.2.b).

The end scour values, d_{se}, calculated by fitting Equation 4.2 to the complete scour depth records are given in Table 4.2. It should be retained here that the determination coefficients of the fitting process were always higher than 0.99. These values of d_{se} are compared with those obtained by applying the procedures of Melville and Chiew (1999), Cardoso and Bettess (1999) and Grimaldi (2005) to assess equilibrium in laboratory conditions.

Table 4.2 – Comparison of time to equilibrium and end scour depth obtained from scour measurements through different approaches

Test	d_{se} (m)	M&C (1999)			C&B (1999)			G (2005)		
	Eq. (4.2)	t_M (day)	d_{se} (m)	Δd_{se} (%)	t_C (day)	d_{se} (m)	Δd_{se} (%)	t_G (day)	d_{se} (m)	Δd_{se} (%)
1	0.173	3.1	0.139	-19	12.4	0.159	-8	6.1	0.150	-13
2	0.210	5.1	0.161	-23	19.4	0.182	-13	10.0	0.174	-17
3	0.130	3.1	0.121	-7	4.5	0.127	-2	3.1	0.121	-7
4	0.140	4.2	0.124	-11	8.2	0.132	-6	6.9	0.126	-10
5	0.128	3.1	0.118	-8	6.3	0.124	-3	5.0	0.118	-8

M&C (1999) = Melville and Chiew (1999); C&B (1999) = Cardoso and Bettess (1999); G (2005) = Grimaldi (2005).

According to the criterion of Melville and Chiew (1999) – which coincides with the criterion of Coleman *et al.* (2003) in the present situation –, equilibrium should have been obtained at time t_M (*cf.* Table 4.2). The criterion of Cardoso and Bettess (1999), illustrated in Figure 4.4, for Test 3, leads to the values of time to equilibrium, t_C, included in the same table; the equilibrium time associated with the criterion of Grimaldi (2005) is t_G. The criterion of Cardoso and Bettess (1999) was applied to the last plateau of each scour record.

The inspection of Table 4.2 leads to conclude that: *i*) in general, $t_C > t_G \geq t_M$; *ii*) the three methods lead to the experimental under estimation of the equilibrium scour depth; *iii*) as expectable from the values of t_C, the smaller deviations on d_{se} are those issued by the method of Cardoso and Bettess (1999); *iv*) the stronger deviations occurred for the finer sand (Test 1 and 2) irrespective of the method; *v*) deviations range from –2% (for t_C, Test 3) to –23% (for t_M, Test 2).

Conclusion *iv*) might derive from the fact that, since the sand is finer, the intensity of the vortical system – which can be expected to be similar in the five experiments as D_p, d and U did

not change much – remains strong enough to entrain the bed sediment for longer time, leading to higher durations before equilibrium is reached.

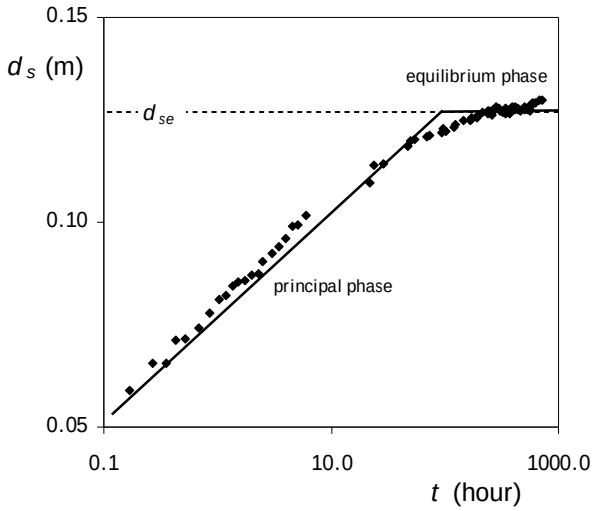

Figure 4.4 – Definition of time to equilibrium and end-scour depth according to Cardoso and Bettess (1999)

The values of Table 4.2 should still be added with those of the deviations inherent to the use of the 6-parameters polynomial function, Equation 4.2. These deviations where seen to be –1% to –4%. In practice, this means that the use of common methods to estimate pier end-scour depth from laboratory tests can lead to under estimations of up to ≈30%, depending on the method. In contrast, the methods of Cardoso and Bettess (1999) and Bertoldi and Jones (1998) were verified to be practically equivalent for assessing equilibrium scour at abutments by Fael *et al.* (2006).

The literature on local scour includes some predictors of time to equilibrium. The predictor of Franzetti *et al.* (1994) was already presented in Section 2.5.1, while for $d/D_p \approx 2.0$ the predictor of Melville and Chiew (1999) reads

$$t_M = 30.89 \frac{D_p}{U} \left(\frac{U}{U_c} - 0.4 \right) \left(\frac{d}{D_p} \right)^{0.25} \tag{4.6}$$

with t_M expressed in days; the predictor of time to equilibrium suggested by Kothyari *et al.* (2007) is

$$\log T = 4.8 Fr_d^{1/5} \tag{4.7}$$

where T and Fr_d keep the same meaning as in Equations 4.4 and 4.5.

The values of time to equilibrium issued from these three predictors are presented in Table 4.3, where the subscript F. stands for Franzetti *et al.* (1994) and the subscript K. stands for Kothyari *et al.* (2007). The table also includes the equilibrium scour depths observed at time to

equilibrium and the percent deviations towards the equilibrium scour depth calculated through Equation 4.2 as extrapolated to $t = \infty$. The values of t_M are, with no surprise, similar to those presented in Table 4.2; $t_F > t_M \approx t_K$ in all cases. The values of percent deviation on the estimated equilibrium scour depth are significant and vary between –4% and –24%.

The previous discussion profusely shows that common methods used in practice to decide on whether a given scour experiment has reached the equilibrium phase or not may be erroneous. It also shows that known predictors of time to equilibrium may imply significantly wrong predictions of equilibrium depth.

Table 4.3 – Comparison of time to equilibrium and end scour depth obtained from existing predictors

Test	d_{se} (m)	F (1994)			M&C (1999)			K (2007)		
	(Eq. 4.2)	t_F (day)	d_{se} (m)	Δd_{se} (%)	t_M (day)	d_{se} (m)	Δd_{se} (%)	t_K (day)	d_{se} (m)	Δd_{se} (%)
1	0.173	6.3	0.150	-13	4.1	0.145	-16	4.0	0.145	-16
2	0.210	6.2	0.161	-23	4.5	0.160	-24	5.2	0.165	-22
3	0.130	5.4	0.124	-4	3.4	0.121	-7	3.6	0.122	-6
4	0.140	5.1	0.125	-11	3.2	0.121	-14	3.4	0.125	-11
5	0.128	4.3	0.118	-8	2.8	0.117	-9	2.8	0.116	-9

F (1994) = Franzetti *et al.* (1994); M&C (1999) = Melville and Chiew (1999); K (2007) = Kothyari *et al.* (2007).

So, the following question is raised: how long should last experiments on local scour at single cylindrical piers to assure sufficiently precise predictions of equilibrium depth? Assuming equilibrium to occur at $t = \infty$, Equation 4.2 was systematically applied to three partitions of each scour record defined at t_r = 4, 7 and 15 days. It is worth to note that the determination coefficient was in all cases > 0.99. The outputs of this procedure are compared in Table 4.4 with those obtained from the entire records.

Table 4.4 – Equilibrium scour depth obtained by adjusting and extrapolating Equation 4.2 to scour records of different durations.

Test	d_{se} (m); Δd_{se} (%)						
	Entire record	4 days	Δd_{se} (%)	7 days	Δd_{se} (%)	15 days	Δd_{se} (%)
1	0.173	0.157	-9	0.161	-7	0.165	-5
2	0.210	0.166	-21	0.220	5	0.201	-4
3	0.130	0.128	-1	0.128	-1	0.130	0
4	0.140	0.157	12	0.140	0	0.137	-2
5	0.128	0.127	-1	0.125	-2	0.125	-3

Table 4.4 indicates that *i*) the 6-parameters polynomial extrapolations on the basis of 4 days-long experiments are not satisfactory; *ii*) reasonable extrapolations are expectable from ≈ 7

days-long records; *iii*) only marginal improvements may be expected from experiments lasting longer than 7 days.

4.5 Conclusions

From the previous discussion, the following important conclusions can be drawn:

i) Scour experiments at single cylindrical piers, run for up to ≈46 days, did not unambiguously reach equilibrium, with special emphasis in the tests with the finer sand.

ii) Common methods used in practice to decide on the initiation of the equilibrium phase may be rather erroneous.

iii) Known predictors of time to equilibrium may lead to significantly wrong predictions of equilibrium scour depth.

iv) Typically 7 days long scour-depth records adjusted trough Equation 4.2 and extrapolated to infinite time seem to render robust vales of the equilibrium scour depth at single cylindrical piers.

5. CLEAR-WATER SCOUR AT LARGE CYLINDRICAL PIERS

5.1 Introduction

It is widely recognized that local scour at bridge foundations is a common cause of bridges failure. In spite of the research efforts on this topic during the last five or six decades, the time evolution of scour depth and its ultimate "equilibrium" value remains a subject of concern for hydraulic engineers and researchers.

Research has been made mostly through experimentation. Early contributions of Chabert and Engeldinger (1956), Laursen and Toch (1956), Laursen (1958, 1962, 1963) or Shen *et al.* (1966, 1969) may be mentioned. In the last two decades, several comprehensive summaries of up-to-date knowledge on local scour at bridge foundations have been published, including, for example, by Breusers and Raudkivi (1991) and Melville and Coleman (2000).

A significant number of existing studies reported experiments whose duration may have been too short to reach equilibrium or to sufficiently approach this stage. Most of them are for small sediment coarseness ratios, D_p/D_{50} (D_p = pier diameter; D_{50} = median grain size). These time and coarseness limitations of experimental studies may be among the causes of reported discrepancies between field observations and predictions obtained through formulations derived from experimentation.

Time plays an important role in scour. It is well established that, under live-bed conditions, scour depth tends to equilibrium very quickly, while under clear-water conditions scour takes place much more slowly. Many researchers attempted to develop equations to predict local scour time evolution. Pioneers in this work include Ahmad (1953), Liu *et al.* (1961), Sarma (1967) or Breusers *et al.* (1977).

Ettema (1980) identified three phases of the scouring process: the initial phase, characterized by the fast scour development produced by the down-flow at the upstream face of obstacles; the principal phase, which begins when the horse-shoe vortex starts to dominate the process; the equilibrium phase, when the scour depth practically does not increase anymore. In clear-water scour, the principal phase lasts for a long time and the equilibrium scour depth is approached asymptotically.

Ettema (1980) suggested a logarithmic formula to predict scour evolution which applies to the principal phase. Wong (1982) exploited Ettema's formulation for abutments. These contributions involve the fluid viscosity but this variable is possibly discardable as the flow structures within the scour hole tend to be characteristic of a rough turbulent regime. For the same purpose, Franzetti *et al.* (1982) proposed an exponential function that involves the equilibrium scour depth, d_{se}, and two coefficients, a_1 and a_2. Melville and Chiew (1999) introduced a time factor in their scour predictor that includes the time needed to attain equilibrium, hereafter termed "time to equilibrium", and flow intensity, U/U_c (U = average approach flow velocity; U_c = critical average velocity for the beginning of sediment motion). Oliveto and Hager (2002, 2005) developed a predictor in which the densimetric Froude number is a major parameter; according to this predictor, scour depth tends to infinity with time. More recently, Kothyari *et al.* (2007) kept the structure of Oliveto and Hager's model, but included a criterion for an ultimate scour depth which occurs at the time to equilibrium.

The equilibrium concept is rather subjective; different authors present different approaches to cope with it. Some argue that equilibrium is reached in a finite time. In this line, Melville and Chiew (1999) presented a predictor of time to equilibrium for cylindrical piers and Cardoso and Fael (2010) have suggested another one for abutments. Others state that equilibrium scour cannot be achieved in a finite time (Franzetti *et al.* 1982) or implicitly suggest that scour is not upper bounded. The reported subjectivity has important implications in many respects, including in the design of scour experiments.

Assuming that equilibrium scour is only achieved in infinite time, the question of how long should experiments last to sufficiently approach equilibrium was recently addressed by Lança *et al.* (2010) and Simarro *et al.* (2011). According to Lança *et al.* (2010), the extrapolation to infinite time of seven days-long scour depth records adjusted by a 6-parameters polynomial function – that keeps the structure of the 4-parameters polynomial function suggested by Bertoldi and Jones (1998) – renders robust values of the equilibrium scour-depth at single cylindrical piers. Simarro *et al.* (2011) performed a comparative study of different contributions and corroborated that the 6-parameters polynomial function provides the minimum root mean square errors and the most reliable d_{se} values obtained through extrapolation to $t = \infty$ of recorded scour depths. Simarro *et al.* (2011) also concluded that the exponential function of Franzetti *et al.* (1982) describes scour-depth time evolution with a similar precision, with the advantage of using only two coefficients (a_1 and a_2) and the equilibrium scour depth, d_{se}. Coefficients a_1 and a_2, as well as d_{se}, can be postulated to depend on the parameters that control scouring.

The practical use of the exponential function as a scour predictor requires a priori knowledge of the equilibrium scour depth (Franzetti *et al.* 1982). Important studies on scouring (*e.g.* Ettema 1980, Melville and Chiew 1999) have successively assumed that the equilibrium scour depth does not depend on sediment coarseness, D_p/D_{50}, for $D_p/D_{50} > \sim 50$. This view has been recently

disputed by, *e.g.*, Sheppard *et al.* (1995, 1999, 2004) and Lee and Sturm (2009). Sheppard *et al.* (1995, 1999) carried out experiments covering values of the sediment coarseness ratio up to 1260 while Sheppard *et al.* (2004) extended the range up to 4155 and concluded that sediment coarseness does influence the equilibrium scour depth. According to these studies, d_{se} decreases with increasing sediment coarseness ratio for $D_p/D_{50} > \sim 50$.

Despite of the contributions of Sheppard *et al.* (1995, 1999, 2004) and Lee and Sturm (2009), there is still a lack of information on scouring for comparatively high sediment coarseness ratios, D_p/D_{50}. The widespread idea according to which D_p/D_{50} does not influence scour for $D_p/D_{50} > \sim 50$ still is taken to be valid. For clear water scour, close to the condition of initiation of motion, bed sediment must be such that $D_{50} > \sim 0.6$ mm to avoid ripples. Consequently, large sediment coarseness ratios require large values of the pier diameter, D_p, and of the approach flow depth, d, in order to satisfy the simultaneous need to simulate realistic values of flow shallowness, d/D_p. Avoiding wall and contraction effects – for large pier diameter and flow depth – implies the need for wide facilities and flow discharges that do not exist in most laboratories.

The availability of two comparatively large flumes rendered it possible to generate, in this study, additional scour data for values of sediment coarseness ratio in the range $58 \leq D_p/D_{50} \leq 465$, while covering flow shallowness values, d/D_p, in the range $0.5 \leq d/D_p \leq 5.0$, for flow intensity, U/U_c, close to the condition of initiation of motion ($U/U_c \approx 1$). Thirty eight tests lasting between 7 and 14 days were run for this purpose.

The new data were obtained with the specific objectives of *i*) revisiting the influence of sediment coarseness on the equilibrium scour depth and *ii*) improving scour depth time evolution modelling by making use of the exponential function suggested by Franzetti *et al.* (1982).

5.2 Framework for analysis

Pier scour depth at a given instant, t, can be described by the following set of independent variables:

$$d_s = \varphi\left[\begin{matrix}\text{flow}(d, S_f, g), \text{fluid}(\rho, \nu), \text{bed material}(D_{50}, \sigma_D, \rho_s), \\ \text{pier}(D_p, K_\alpha, K_s), \text{channel}(B, S_0, K_g), \text{time}(t)\end{matrix}\right] \tag{5.1}$$

where, apart from those variables already defined, d_s = scour depth at instant t, S_f = slope of the energy line; g = acceleration of gravity; ρ and ν = fluid density and kinematic viscosity, respectively; σ_D = gradation coefficient of the bed material; ρ_s = sediment density; K_α and K_s = coefficients describing the alignment and the shape of the pier, respectively; B = channel width; S_0 = channel bed slope; K_g = coefficient describing the geometry of the channel cross-section. It should be noted here that the average critical velocity for sediment entrainment, U_c, is not included as an independent variable since it is fully defined by g, d, S_f, ρ, ν, D_{50} and ρ_s.

For uniform flows in wide rectangular channels, $R \approx d$, $S_f = S_0$, $K_g = 1$ and B does not influence scour. In this context, wide channels are those where the effects of flow contraction due to the presence of piers as well as wall effects are negligible. For clear-water flat bed flows, S_f can be replaced by both the friction velocity, $u_* = (gdS_f)^{0.5}$, or the average approach flow velocity, U. If the bed material is composed of uniform, non-ripple-forming sand, which implies $D_{50} > \sim 0.6$ mm, $\sigma_D < 1.5$ and $\rho_s \approx$ constant, then σ_D and ρ_s can be eliminated from Equation 5.1. For cylindrical piers, $K_s = 1$ and $K_\alpha = 1$. In the case of fully developed flow on a flat bed, where it can be shown that $u_* / u_{*c} = U/U_c$ (u_{*c} = critical bed shear velocity for sediment entrainment), keeping in mind Shields' diagram and assuming that within the scour hole the flow is fully rough irrespective of the approach flow regime, the kinematic viscosity, ν, no longer influences the scouring process.

Under the above assumptions, *i.e.*, cylindrical piers inserted in uniform, fully-developed turbulent flows, in wide rectangular channels with a flat bed composed of uniform, non-ripple-forming sand, Equation 5.1 can be transformed into (Fael 2007):

$$\frac{d_s}{D_p} = \varphi\left(\frac{d}{D_p}, \frac{U}{U_c}, \frac{D_p}{D_{50}}, \frac{Ut}{D_p}\right) \tag{5.2}$$

For U/U_c = constant (usually $U/U_c \approx 1.0$ in laboratory conditions so as to maximize the scour depth), non-dimensional equilibrium scour depth reads:

$$\frac{d_{se}}{D_p} = \varphi_1\left(\frac{d}{D_p}, \frac{D_p}{D_{50}}\right) \tag{5.3}$$

since t no longer interferes.

The first objective of this study seeks, in practice, a sound characterization of Equation 5.3. The second objective consists of further specifying the model suggested by Franzetti *et al.* (1982), in the sequence of the findings of Simarro *et al.* (2011). The model reads:

$$\frac{d_s}{d_{se}} = 1 - \exp\left[-a_1\left(\frac{Ut}{D_p}\right)^{a_2}\right] \tag{5.4}$$

According to the original reference, a_2 should be constant ($a_2 \approx 1/3$), while a_1 is rather small and seems to vary in the range $0.021 < a_1 < 0.042$. By comparing Equation 5.2 and Equation 5.4, it becomes obvious that the model suggested by Franzetti *et al.* (1982) may be completed by relating a_1 and a_2 with the parameters that do not explicitly appear in Equation 5.4, *i.e.*, the flow shallowness, d/D_p, and the sediment coarseness, D_p/D_{50}. For U/U_c = constant, it seems reasonable to assume, *a priori*, that:

$$a_1 = \varphi_2\left(\frac{d}{D_p}, \frac{D_p}{D_{50}}\right) \tag{5.5}$$

$$a_2 = \varphi_3\left(\frac{d}{D_p}, \frac{D_p}{D_{50}}\right) \tag{5.6}$$

The experiments reported herein were designed so as to contribute to the definition of the functional relations φ_1, φ_2 and φ_3 of Equations 5.3, 5.5 and 5.6, respectively.

5.3 Experimental setup and procedure

Two flumes were used in the experimental study. One is 28.00 m long, 2.00 m wide and 1.00 m deep. This flume includes a closed hydraulic circuit whose maximum flow discharge is 270 ls^{-1}. Discharge was measured by an electromagnetic flow meter installed in the circuit to an accuracy of ± 0.5% of full scale. At the entrance of the flume, two honeycomb diffusers aligned with the flow direction smoothed the flow trajectories and guaranteed a uniform transversal flow distribution. The entrance uniform distribution was confirmed through velocity profile measurements. Immediately downstream from the diffusers, a 5.00 m long bed reach was covered with small gravel to provide proper roughness and guarantee fully developed flow. The central reach of the flume, starting at 13.90 m from the entrance, includes a 3.00 m long, 2.00 m wide and 0.60 m deep recess box in the bed. At the downstream end of the flume, a tailgate allows the regulation of the water depth. At the end of the flume the water falls into a 100 m^3 reservoir, where the hydraulic circuit starts.

Single vertical cylindrical piers were simulated by PVC pipes with diameters D_p = {50, 75, 110, 160, 200, 250, 315, 350, 400 mm}, placed at ~1.0 m from the upstream boundary of the bed recess box.

The second flume is 33.15 m long, 1.00 m wide and 1.0 m deep; its central reach starts at 16.00 m from the entrance; the maximum flow discharge is 90 ls^{-1}. Similar provisions to the ones described above for the 2.0 m wide larger flume (namely honeycomb and floor roughness at the entrance of the channel) were provided to guarantee similar working conditions for the flow recirculation circuit on this flume. The recess box is 3.20 m long, 1.0 m wide and 0.35 m deep. The maximum pier diameter was 200 mm, so as to avoid contraction effects.

A uniform quartz sand (ρ_s = 2660 kgm^{-3}; D_{50} = 0.86 mm; σ_D = 1.36) was used to fill each of the recess boxes of the two channels.

Prior to each experiment, the sand bed was perfectly leveled. The area located around the pier was covered with a thin metallic plate to avoid uncontrolled scour at the beginning of each experiment. The flumes were filled gradually through small hydraulic circuits, imposing a high

water depth and low flow velocity. The discharge corresponding to the chosen approach flow velocity was then passed through the flumes. The flow depth was regulated by adjusting the downstream tailgates. Once the discharge and flow depth were established, the metallic plates were removed and the experiments started.

Scour immediately initiated and the depth of scour hole was measured, to an accuracy of ± 1 mm, with adapted point gauges, approximately every 5 minutes during the first hour. Afterwards, the interval between measurements increased and, after the first day, a few measurements were carried out per day. When the scour rate was less than approximately 2 mm ($\approx 2D_{50}$) in 24 hours and at least 7 days had passed, the experiments were stopped. The sand bed approach reach located upstream of the piers stayed undisturbed through the entire duration of the experiments; this long term stability ensured that the scour depth was not supplemented by upstream bed degradation.

5.4 Results and discussion

5.4.1 Data characterization

The values of the most important control variables and non-dimensional parameters characterizing the experiments are summarized in Table 5.1. It can be concluded that a reasonably high flow depth ($0.050 \text{ m} \leq d \leq 0.400 \text{ m}$) was always guaranteed. The average flow velocity, U, was $0.93 \leq U/U_c \leq 1.04$, U_c being calculated using the predictor of Neil (1967). The aspect ratio B/d was guaranteed to be greater than 5.0, this way avoiding significant wall effects on the flow field. The ratio of channel width to pier diameter, B/D_p, was at least 5.0 and was observed to guarantee that scour holes never reached the lateral walls of the flumes. Since $D_{50} > 0.8$ mm, viscous effects, if any, were expected to be negligible, according to Oliveto and Hager (2002). Since the duration of the experiments, t_d, was greater than 7 days, one can reliably extrapolate scour records to infinite time (Simarro *et al.* 2011). On average, the duration of the experiments was 2.3 times longer than the time to equilibrium given by the criterion suggested by Melville and Coleman (2000) ($\Delta d_s < 0.05 D_p$ in 24 hours; Δd_s = increment of scour depth). The approach flow depth values were adjusted in accordance with the different pier diameters tested in order to achieve the range of flow shallowness values, $d/D_p \approx \{0.5, 1.0, 1.5, 2.0, 2.5, 3.0, 4.0, 5.0\}$. Sediment coarseness, D_p/D_{50}, took nine values in the range $58.1 \leq D_p/D_{50} \leq 465.1$, covering comparatively high values of this parameter, which enables an enhanced characterization of the sediment coarseness effect on the scour depth.

Table 5.1 – Characteristic control variables and non-dimensional parameters of the experiments

Test	d (m)	D_p (m)	U/U_c	d/D_p	D_p/D_{50}	t_d (hour)	d_{se} (m)	d_{se}/D_p
1	0.055	0.110	0.97	0.5	127.9	170	0.180	1.64
2	0.080	0.160	0.97	0.5	186.0	168	0.226	1.41
3	0.100	0.200	0.97	0.5	232.6	170	0.263	1.32
4	0.125	0.250	0.97	0.5	290.7	168	0.282	1.13
5	0.158	0.315	0.93	0.5	366.3	223	0.348	1.10
6	0.175	0.350	1.04	0.5	407.0	306	0.337	0.96
7	0.200	0.400	0.96	0.5	465.1	288	0.409	1.02
8	0.050	0.050	0.97	1.0	58.1	168	0.116	2.31
9	0.075	0.075	0.97	1.0	87.2	168	0.164	2.18
10	0.110	0.110	0.97	1.0	127.9	168	0.199	1.81
11	0.160	0.160	0.95	1.0	186.0	285	0.231	1.44
12	0.200	0.200	0.96	1.0	232.6	261	0.297	1.48
13	0.250	0.250	0.98	1.0	290.7	263	0.365	1.46
14	0.315	0.315	0.98	1.0	366.3	186	0.388	1.23
15	0.350	0.350	0.97	1.0	407.0	291	0.409	1.17
16	0.400	0.400	0.95	1.0	465.1	224	0.448	1.12
17	0.075	0.050	0.97	1.5	58.1	168	0.119	2.38
18	0.113	0.075	0.97	1.5	87.2	168	0.176	2.34
19	0.165	0.110	0.96	1.5	127.9	241	0.225	2.04
20	0.225	0.160	1.01	1.4	186.0	267	0.306	1.91
21	0.300	0.200	0.98	1.5	232.6	262	0.361	1.80
22	0.375	0.250	0.96	1.5	290.7	221	0.374	1.50
23	0.100	0.050	0.97	2.0	58.1	170	0.127	2.54
24	0.150	0.075	0.97	2.0	87.2	169	0.163	2.17
25	0.220	0.110	1.01	2.0	127.9	216	0.209	1.90
26	0.300	0.160	0.98	1.9	186.0	330	0.267	1.67
27	0.400	0.200	0.95	2.0	232.6	219	0.329	1.65
28	0.125	0.050	0.97	2.5	58.1	168	0.111	2.22
29	0.188	0.075	0.96	2.5	87.2	191	0.147	1.96
30	0.275	0.110	0.98	2.5	127.9	184	0.234	2.13
31	0.375	0.160	0.96	2.3	186.0	313	0.279	1.74
32	0.150	0.050	0.96	3.0	58.1	173	0.110	2.19
33	0.225	0.075	1.01	3.0	87.2	197	0.171	2.27
34	0.330	0.110	0.96	3.0	127.9	169	0.223	2.02
35	0.200	0.050	0.96	4.0	58.1	170	0.134	2.67
36	0.300	0.075	0.98	4.0	87.2	314	0.198	2.63
37	0.250	0.050	1.00	5.0	58.1	237	0.117	2.33
38	0.375	0.075	0.96	5.0	87.2	315	0.184	2.46

Time records of the scour depths are available at http://w3.ualg.pt/~rlanca/largepiers.pdf; The tests 1 to 7, for d/D_p = 0.5, are plotted in Figure 5.1 in the coordinates suggested by Oliveto and Hager (2002; 2005), *i.e.*,

$$\frac{Z\sigma_D^{0.5}}{Fr_d^{1.5}} \qquad \text{and} \qquad T = \frac{t}{t_R} \tag{5.7}$$

where

$$Z = \frac{d_s}{z_R} \qquad z_R = \left(D_p{}^2 d\right)^{1/3} \qquad Fr_d = \frac{U}{\left(\Delta g D_{50}\right)^{1/2}} \qquad t_R = \frac{z_R}{\sigma_D{}^{1/3}\left(\Delta g D_{50}\right)^{1/2}} \tag{5.8}$$

Above, the gradation coefficient is defined as $\sigma_D = (D_{84.1}/D_{15.9})^{0.5}$ and $\Delta = (\rho_s - \rho)/\rho$. Figure 5.1 also plots the predictor of Oliveto and Hager (2005), as a solid line, by assuming a shape factor of 1, corresponding to cylindrical piers, as well as the ±25% band around the predictor. Similar plots were produced for the other seven d/D_p groups; they do not substantially differ from Figure 5.1. The inspection of this figure reveals that the predictor proposed by Oliveto and Hager (2005) does not match the data. The plots do not either display any horizontal plateau denoting an equilibrium phase as proposed by Cardoso and Bettess (1999) for vertical wall abutments.

The applicability of the time-factor model suggested by Melville and Coleman (2000) was also not supported by the data.

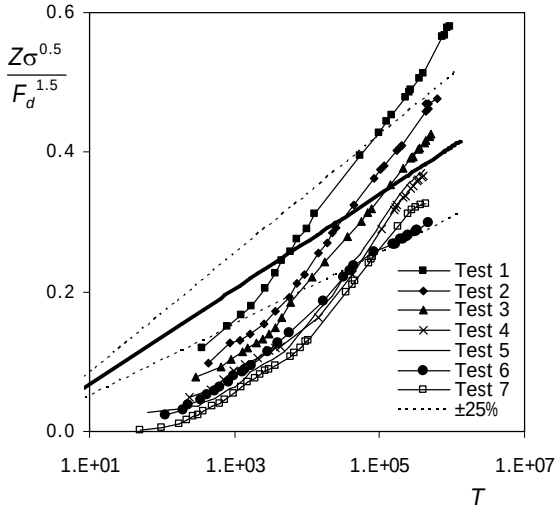

Figure 5.1 – Time evolution of scour depth presented in the coordinates of Oliveto and Hager (2005) for $d/D_p = 0.5$

Although equilibrium scour does not seem to have been unambiguously reached in any experiment, it seems reasonable to postulate that equilibrium must exist since, in nature, there are structures where scour depth developed for geologic eras and did not increase to infinity. Yet, it is recognized that the probability of occurrence of a sufficiently strong turbulent event capable of entraining sediment grains from the scour hole will never be null; however, this probability decreases as scour develops, tending asymptotically to zero. Thus, it is assumed here that an equilibrium scour depth exists although time taken to achieve this equilibrium may be rather large, conceptually infinite. For this reason, scour depth records were fitted using regression with the following polynomial function,

$$d_s = p_1\left(1 - \frac{1}{1 + p_1 p_2 t}\right) + p_3\left(1 - \frac{1}{1 + p_3 p_4 t}\right) + p_5\left(1 - \frac{1}{1 + p_5 p_6 t}\right) \tag{5.9}$$

so as to obtain the equilibrium scour depth, d_{se}, as suggested by Lança *et al.* (2010). In the above polynomial equations, parameters p_1, p_2, …, p_6 have no physical meaning; however, it is obvious that, for $t = \infty$, $d_s = d_{se} = p_1 + p_3 + p_5$. The equilibrium scour depths obtained through the fitting procedure are included in Table 5.1. It should be noted here that the equilibrium scour depths obtained in this way are, on average, 10% higher than those measured on the seventh day of the experiments.

5.4.2 Equilibrium scour depth

The experimental values of d_{se}/D_p are plotted against D_p/D_{50} in Figure 5.2. The data are organized in four classes of d/D_p. Due to experimental limitations, there are few measurements corresponding to $d/D_p > 3.0$. Figure 5.2.a) also plots the regression lines associated with the three smaller flow shallowness classes, d/D_p = {[0.5 – 1.0], [1.5 – 2.0], [2.5 – 3.0]; Figure 5.2.b) includes the predictions of Shepard and Renna (2010) for d/D_p = 0.5, 3.0 and 5.0.

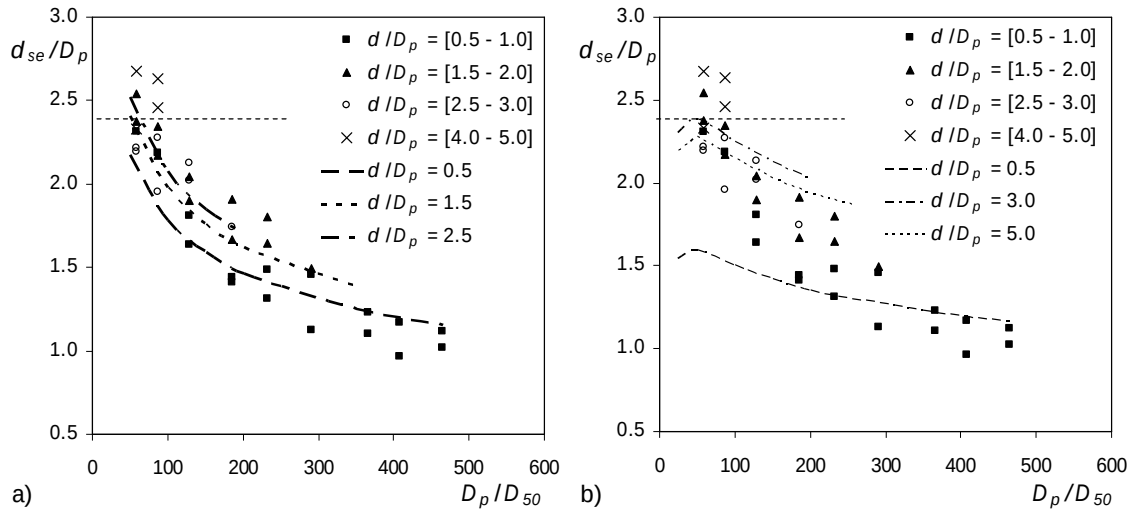

Figure 5.2 – Functional dependence of d_{se}/D_p on D_p/D_{50}: a) Independent fit; b) Sheppard and Renna (2010)

Inspection of Figure 5.2, reveals that the parameter D_p/D_{50} clearly influences d_{se}/D_p in the experimental range, leading to decreasing scour depth as D_p/D_{50} increases. This conclusion qualitatively corroborates the findings of Sheppard *et al.* (1995, 1999, 2004) and Lee and Sturm (2009). Yet, the decrease seems to be more marked than that predicted by the model of Sheppard and Renna (2010).

Within the experimental range ($0.5 \leq d/D_p \leq 5.0$), d/D_p also influences d_{se}/D_p, as expected. Figure 5.3 shows the data organized in four classes of D_p/D_{50}. It is clear that d_{se}/D_p increases with d/D_p. It is to be noted from both Figure 5.2 and Figure 5.3 that the classical upper bound defined by $d_{se}/D_p \approx 2.4$ was exceeded for the higher values of d/D_p in the sediment coarseness class D_p/D_{50} = [58.1 – 87.2]. This result is in line with the findings of Sheppard *et al.* (2004), where, for the extrapolation of scour depth records to $t = \infty$, the 4-parameter polynomial equation of

Bertoldi and Jones (1998) was adopted. Sheppard *et al.* (2004) suggested the upper bound of d_{se}/D_p to be 2.5. Somehow, this increase of the upper bound seems to reflect the assessment of the equilibrium scour depth as occurring at $t = \infty$.

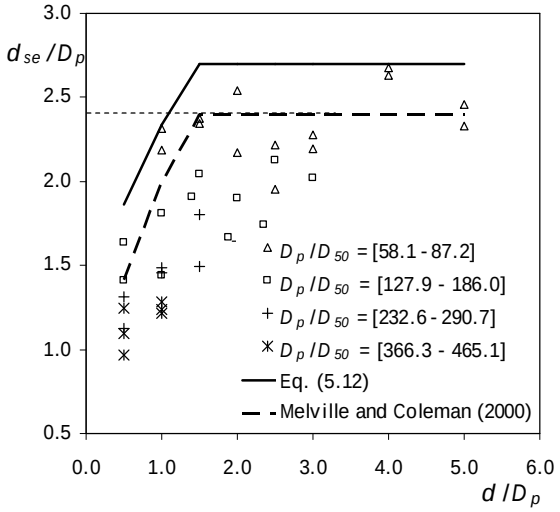

Figure 5.3 – Envelope curve for the functional dependence of d_{se}/D_p on d/D_p

The double dependence of d_{se}/D_p on flow shallowness, d/D_p, and sediment coarseness, D_p/D_{50}, is captured by the following regression equation (determination coefficient $r^2 = 0.83$),

$$\frac{d_{se}}{D_p} = 7.0\left(\frac{D_p}{D_{50}}\right)^{-0.283}\left(\frac{d}{D_p}\right)^{0.093} \tag{5.10}$$

for $58.1 \le D_p/D_{50} \le 465.1$ and $0.5 \le d/D_p \le 5.0$.

For practical engineering application, the following predictor is suggested:

$$\frac{d_{se}}{D_p} = K_d K_{D_{50}} \tag{5.11}$$

where

$$K_d = \begin{cases} 2.35\left(\dfrac{d}{D_p}\right)^{0.34} & \text{for } 0.5 \le \dfrac{d}{D_p} \le 1.5 \\ 2.7 & \text{for } \dfrac{d}{D_p} > 1.5 \end{cases} \tag{5.12}$$

and

$$K_{D_{50}} = \begin{cases} 5.8\left(\dfrac{D_p}{D_{50}}\right)^{-0.381} & \text{for } 100 < \dfrac{D_p}{D_{50}} < 465 \\ 1.0 & \text{for } 58 < \dfrac{D_p}{D_{50}} < 100 \end{cases} \tag{5.13}$$

Equation 5.12 constitutes the envelope to the data plotted in Figure 5.3; it is structurally similar to the curves of Melville and Coleman (2000) though leading to higher values. Equation 5.13 constitutes the envelope curve of the K_{D50} data plotted in Figure 5.4. The values of K_{D50} were back calculated from the values of d_{se}/D_p reported in Table 5.1 by assuming K_d to be given by Equation 5.12. Equation 5.13 is significantly different from the proposal of Melville and Coleman (2000) for $D_p/D_{50} > 100$. For the particular case where $d/D_p > 1.5$, the present proposal renders equilibrium scour depths smaller than those predicted through the model of Melville and Coleman (2000) for values of $D_p/D_{50} > 137.4$. Equations 5.11, 5.12 and 5.13 are recommended for the prediction of safe values of scour depth. In practice, their use still requires the adoption of appropriate factors to take into account the effects of flow intensity, pier shape, pier alignment, gradation coefficient and density of bed the material, contraction scour, cross-section shape and time. The remainder of this work concentrates on the effect of time on scour depth.

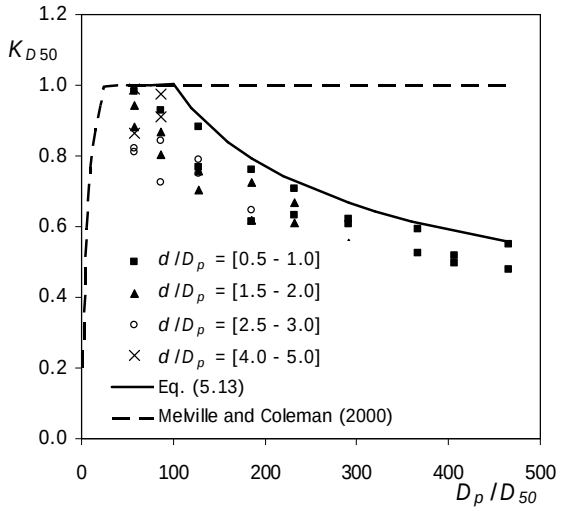

Figure 5.4 – Functional dependence of K_{D50} on D_p/D_{50}

5.4.3 Time evolution of the scour depth

Since the value of d_{se} is known for each experiment, Equation 5.4 could be fitted to each scour depth time record and the output of the fitting process were the values of a_1 and a_2. The associated determination coefficients, r^2, were always higher than 0.97. The values of a_1 and a_2 are included in Table 5.2 and plotted against D_p/D_{50} in Figure 5.5.

Table 5.2 – Values obtained for a_1 and a_2

Test	a_1	a_2	Test	a_1	a_2
1	0.037	0.275	20	0.018	0.328
2	0.024	0.319	21	0.025	0.301
3	0.020	0.334	22	0.011	0.388
4	0.012	0.381	23	0.064	0.233
5	0.006	0.438	24	0.034	0.297
6	0.013	0.410	25	0.029	0.310
7	0.005	0.458	26	0.020	0.329
8	0.070	0.232	27	0.015	0.352
9	0.046	0.249	28	0.041	0.314
10	0.034	0.292	29	0.042	0.281
11	0.019	0.360	30	0.037	0.277
12	0.017	0.356	31	0.017	0.321
13	0.019	0.340	32	0.070	0.224
14	0.017	0.366	33	0.041	0.268
15	0.018	0.358	34	0.031	0.282
16	0.015	0.374	35	0.057	0.229
17	0.080	0.212	36	0.027	0.275
18	0.053	0.249	37	0.025	0.277
19	0.036	0.257	38	0.032	0.266

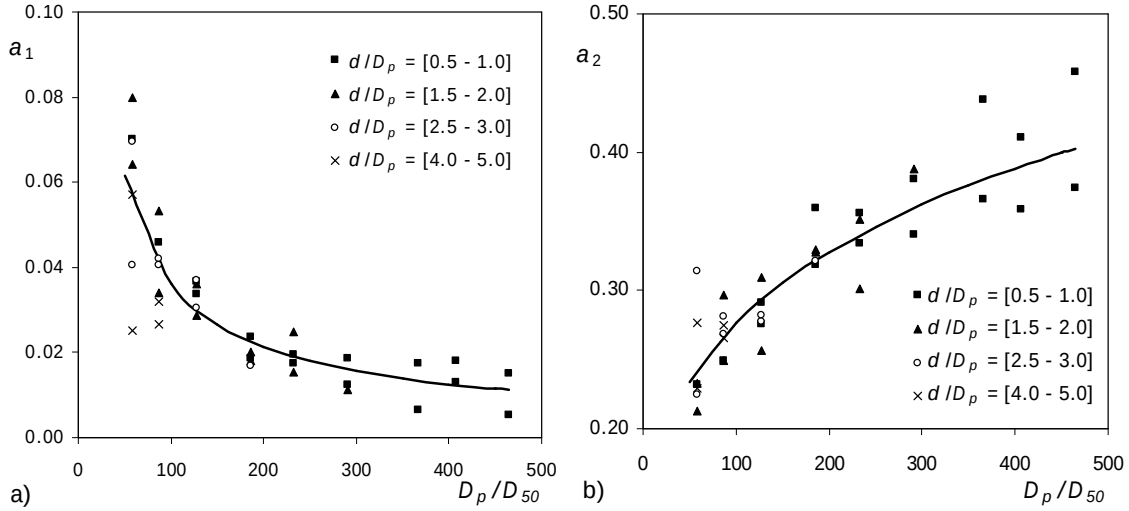

Figure 5.5 – Functional dependence of a) a_1 on D_p/D_{50}; b) a_2 on D_p/D_{50}

From Table 5.2, it can be concluded that a_1 varies in the range $0.005 \leq a_1 \leq 0.080$, with an average value of 0.031, while a_2 varies within the range $0.212 \leq a_2 \leq 0.458$, with an average value of 0.311. These intervals of a_1 and a_2 contain the proposals of Franzetti *et al.* (1982), *i.e.*, $a_1 = 0.028$ and $a_2 = 1/3$. From Figure 5.5, it is clear that a_1 displays a strong dependence on the sediment coarseness, D_p/D_{50}. The dependence of a_2 on the same parameter is also clear. No obvious variation of a_1 or a_2 with d/D_p was identified. The coefficients a_1 and a_2 relate with D_p/D_{50} as follows:

$$a_1 = 1.22\left(\frac{D_p}{D_{50}}\right)^{-0.764} \tag{5.14}$$

$$a_2 = 0.09\left(\frac{D_p}{D_{50}}\right)^{0.244} \tag{5.15}$$

The determination coefficients are r^2 = 0.76 and 0.77, respectively. From the above, the use of the model of Franzetti *et al.* (1982) for the prediction of scour depth time evolution, Equation 5.4, is suggested, a new contribution of this study being the specification of coefficients a_1 and a_2 through Equation 5.14 and Equation 5.15. It is worth stressing that this contribution only applies to cylindrical piers inserted in uniform, fully-developed turbulent flows, in wide rectangular channels with a flat bed composed of uniform, non-ripple-forming sand, close to the condition of beginning of sediment motion ($U/U_c \approx 1.0$).

5.4.4 Validation of the time evolution scour depth model

Simarro *et al.* (2011) have published five long-duration experiments on scouring at cylindrical piers that, apart from U/U_c being slightly smaller than 1.0 ($0.88 \leq U/U_c \leq 0.94$), respect the restrictions mentioned above. Time records of the scour depths are represented in Appendix A. The data from these experiments, as well as from seven additional tests carried out in this study, were used for validation of the above model. The duration of the seven additional experiments was 7 days in all cases; the corresponding characteristic control variables are summarized in Table 5.3, which also includes the values of d_{se}, a_1 and a_2 calculated through Equation 5.10, Equation 5.14 and Equation 5.15, respectively.

Table 5.3 – Characteristic variables and non-dimensional parameters of the validation experiments

Test	d (m)	D_p (m)	d/D_p	D_p/D_{50}	Predicted		
					d_{se} (m)	a_1	a_2
R1	0.050	0.110	0.46	127.9	0.181	0.030	0.294
R2	0.080	0.075	1.07	87.2	0.149	0.040	0.268
R3	0.110	0.075	1.47	87.2	0.154	0.040	0.268
R4	0.113	0.250	0.45	290.7	0.326	0.016	0.359
R5	0.075	0.160	0.47	186.0	0.238	0.023	0.322
R6	0.200	0.100	2.00	116.3	0.194	0.032	0.287
R7	0.200	0.150	1.33	174.4	0.250	0.024	0.317

Equation 5.4 was used to predict the scour depth time evolution. The outputs are compared with measurements in Figure 5.6, where the experiments of Simarro *et al.* (2011) are used in Figure 5.6.a) while the tests made in this study are included in Figure 5.6.b).

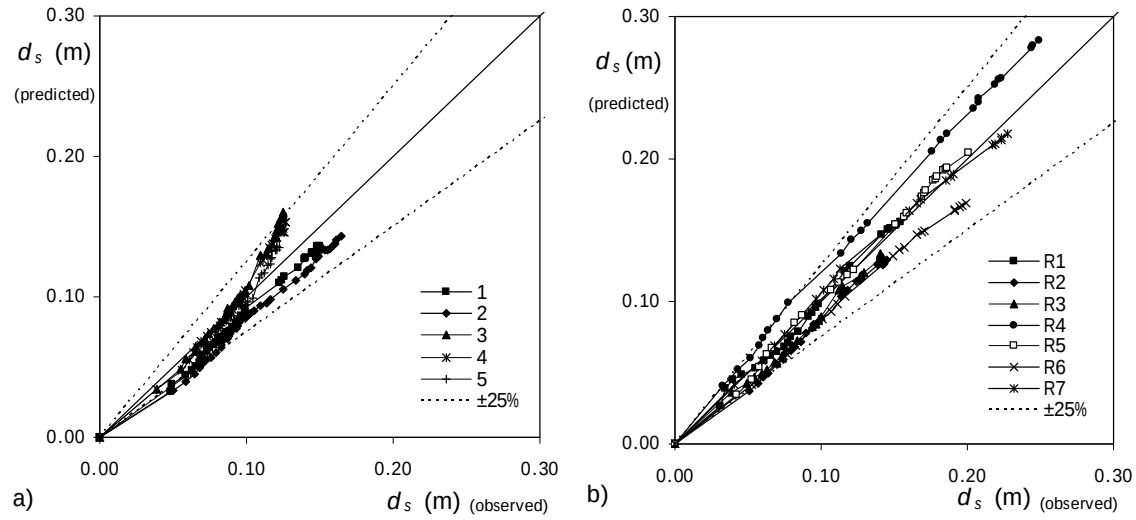

Figure 5.6 – Predictions versus observed scour depth time evolution: a) Simarro *et al.* (2011); b) present study

The inspection of Figure 5.6 reveals that the suggested predictor describes the scour depth time evolution for independent data sets within deviations of ±25% around the line of perfect agreement.

5.5 Conclusions

The most important conclusions of this study are as follows:

i) The equilibrium scour depth decreases with D_p/D_{50}, for D_p/D_{50} > ~100, corroborating the findings of Sheppard *et al.* (1995, 1999, 2004) and Lee and Sturm (2009), which implies refuting the classical assumption according to which the equilibrium scour depth would not depend on D_p/D_{50} for D_p/D_{50} > ~25. The sediment size factor, K_{D50}, may be obtained through Equation 5.13.

ii) Safe predictions of the equilibrium scour depth may be obtained through Equation 5.11, valid for cylindrical piers inserted in uniform, fully-developed turbulent flows in wide rectangular channels with flat bed composed of uniform, non-ripple sand, flow intensity $U/U_c \approx 1.0$, $58 \leq D_p/D_{50} \leq 465$ and $0.50 \leq d/D_p \leq 5.0$.

iii) Under the same restrictions, the exponential model of Franzetti *et al.* (1982), Equation 5.4, properly describes the time evolution of scour depth as soon as its coefficients a_1 and a_2 are specified through Equation 5.14 and Equation 5.15, respectively.

6. EFFECT OF SPACING AND SKEW-ANGLE ON CLEAR-WATER SCOUR AT PIER ALIGNMENTS

6.1 Introduction

Bridge decks are often supported by single-row pier groups, termed here as pier alignments. It is well known that piers located at alluvial river beds may induce the development of scour holes that, in extreme conditions, lead to structural bridge failures. The prediction of equilibrium scour depth is a key issue of bridge design, and this may be more difficult at pier alignments than at single piers due to the interaction of vortices and the concomitant interdependence of scour holes.

Many studies on local scouring at single piers have been carried out since the nineteen fifties; the corresponding results are widely published in the literature, including some engineering manuals (*e.g.* Breusers and Raudkivi 1991, Melville and Coleman 2000, Richardson and Davis 2001 or Sheppard and Renna 2010).

Scouring at pier alignments requires and deserves additional research work since, by comparison with local scour studies at single cylindrical piers, few studies are reported in the literature. Those few that exist, authored by Hannah (1978), Elliott and Baker (1985), Salim and Jones (1996), Zhao and Sheppard (1999), Sumer and Fredsøe (2002), Ataie-Ashtiani and Beheshti (2006), were indeed made in the context of, mostly, short-duration scour studies at pile groups of complex piers. Since the methods available for the prediction of scour depth at complex piers – supposedly valid for pier alignments too – are based on a relatively small number of short duration experiments, the obtained results inherently carry a considerable degree of uncertainty.

This study is focused in further characterizing the effect of pier spacing and alignment skew-angle on the maximum clear-water scour depth at pier alignments consisting of four cylindrical piers. The accuracy of two methods used in engineering practice to predict scour depth at pier alignments is also assessed.

6.2 Framework for analysis

According to Fael (2007), clear-water scour at single cylindrical piers inserted in wide rectangular channels, whose bed is composed of uniform non-ripple forming sand, can be demonstrated to be dependent on the following set of non-dimensional parameters

$$\frac{d_s}{D_p} = \varphi\left(\frac{d}{D_p}, \frac{U}{U_c}, \frac{D_p}{D_{50}}, \frac{Ut}{D_p}\right) \tag{6.1}$$

as soon as the approach flow is fully developed and uniform and the flow inside the scour hole is rough turbulent (free of viscous effects). In Equation 6.1, d_s = scour depth; D_p = pier diameter; d = approach flow depth; U = approach flow velocity; U_c = approach flow velocity for the threshold condition of sediment entrainment; D_{50} = median sediment size; t = time; d/D_p = flow shallowness or relative approach flow depth; U/U_c = flow intensity; D_p/D_{50} = sediment coarseness or relative sediment size; Ut/D_p = non-dimensional time.

It should be noted here that *i*) by fully developed flow, it is meant that the boundary layer covers the entire flow depth; *ii*) it is assumed that wall effects are negligible and the velocity field is bi-dimensional at the central zone of the channel where the pier alignment is placed as soon as $B/d > 5$, B = channel width; *iii*) sand is considered uniform if $\sigma_D < 1.5$ (σ_D = sediment gradation coefficient); *iv*) and ripples do not occur if $D_{50} > 0.6$ mm.

Assuming the definition of additional variables included in Figure 6.1, Equation 6.1 can be generalized for pier alignments as

$$\frac{d_s}{D_p} = \varphi\left(\frac{d}{D_p}, \frac{U}{U_c}, \frac{D_p}{D_{50}}, \frac{Ut}{D_p}, \frac{s}{D_p}, \alpha, K_s, m\right) \tag{6.2}$$

where s = pier spacing; α = alignment skew-angle; K_s = pier shape coefficient; m = number of piers in the alignment.

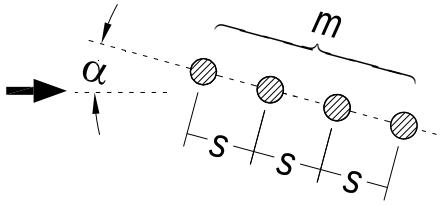

Figure 6.1 – Characteristic variables of a pier alignment

It is worth to note that n parallel alignments form pile groups commonly integrated in complex piers. In the case of pile groups supporting un-submerged pile caps, Equation 6.2 can still be generalized as follows:

$$\frac{d_s}{D_p} = \varphi\left(\frac{d}{D_p}, \frac{U}{U_c}, \frac{D_p}{D_{50}}, \frac{Ut}{D_p}, \frac{s}{D_p}, \alpha, K_s, m, n\right) \tag{6.3}$$

For *i*) $d/D_p \geq \sim 4$, where scour depth is maximized and does no longer depend much on the approach flow depth; *ii*) cylindrical piers ($K_s = 1$) and *iii*) at the equilibrium stage, characterized by the fact that d_s is independent from t (denoted as d_{se}), Equation 6.3 is written as:

$$\frac{d_{se}}{D_p} = \varphi\left(\frac{U}{U_c}, \frac{D_p}{D_{50}}, \frac{s}{D_p}, \alpha, m, n\right) \tag{6.4}$$

For $U/U_c = 1$, where d_{se} is known to be maximal, and assuming D_p/D_{50} to be restricted to a narrow range of values, Equation 6.4 becomes:

$$\frac{d_{se}}{D_p} = \varphi\left(\frac{s}{D_p}, \alpha, m, n\right) \tag{6.5}$$

The parameters of Equations 6.4 and 6.5 constitute the framework of analysis of the studies previously mentioned in the Introduction (see Table 6.1).

Table 6.1 – Control variables and non-dimensional parameters of studies known to date

Author	α(º)	s/D_p	n	m	U/U_c	t_d (h)	Shape[1]
H	0 – 90	1 – 21	1	2	0.7	≈ 7	Circular
E&B	0	1.6 – 13.2	1	3	0.5 –1.0	NS	RC
S&J	0 – 50	1 – 10	3	3	1.0	4	Square
Z&S	0 – 90	3	3	8	0.65	26	C+S
A&B	0	1 – 11	1; 2; 3	1; 2; 3	0.7 – 0.9	≈ 8	Circular
A[2]	0	1 – 6	2; 3	2; 4; 5	0.95	≈ 8	Circular

H = Hannah (1978); E&B = Elliott and Baker (1985); S&J = Salim and Jones (1996); Z&S = Zhao and Sheppard (1999); A&B = Ataie-Ashtiani and Beheshti (2006); A = Amini *et al.* (2012); C+S = circular and square; RC = round nose rectangular; NS = non-specified. [1] shape of the pier cross-section; [2] experiments on uniform spacing and un-submerged pile groups.

From Table 6.1, it is clear that the typical duration, t_d, of the experiments reported in the literature is rather short as compared to the time needed to approach the equilibrium phase. Yet, it should be noted here that some of the authors have made one or two longer validation experiments. According to Simarro *et al.* (2011), the duration of the experiments should be, at least, 7 days, to allow for the adequate prediction of equilibrium scour at single cylindrical piers. This minimum duration is possibly optimistic for pier alignments since the scouring process can be anticipated to be more complex and slower. Consequently, conclusions issued from the mentioned studies do not seem to guarantee accurate predictions of the equilibrium scour depth at pile groups and pier alignments.

In the studies characterized in Table 6.1, the sand was always uniform; with the exception Hannah (1978), Amini *et al.* (2012) and, in some cases, Ataie-Ashtiani and Beheshti (2006), the remaining authors have used fine sand, prone to lead to the formation of ripples in the approach flow reach. In the study of Salim and Jones (1996), ripples have certainly shown up since $U/U_c \approx 1.0$.

In general, the quoted authors concluded that the maximum scour depth decreases with the increase of the spacing between the piles. Exceptionally, Ataie-Ashtiani and Beheshti (2006) reported that for two piles aligned with the approach flow, *i.e.*, $\alpha = 0^o$, the maximum scour depth is observed for $s/D_p = 3$; the same authors also report that, for $\alpha = 90^o$, the maximum scour depth occurs for $s/D_p = 1$.

For the scour depth prediction at pile groups defined by $\alpha = 0^o$, Salim and Jones (1996) – who worked on square cross-section piles – suggested that the scour depth is equal to the one obtained at a rectangular pier whose dimensions are equal to the sum of the individual piles sides. These authors also concluded that *i*) the effect of the skew-angle on the scour depth at the pile group and at the equivalent solid pier can be considered the same and ii) the skew-angle that maximizes scour depth is $\alpha = 30^o$. According to Zhao and Sheppard (1999), the maximum scour depth is observed for $\alpha = 25^o$ in the case of pile groups made of cylindrical piles.

Amini *et al.* (2012) – who focused their study on pile groups with $\alpha = 0^o$ – suggested that, for $s/D_p = 1$, the pile group produces one single horse-shoe vortex and the scour pattern is similar to the one produced by a single pier. For $s/D_p \leq 3.5$, the pile group still produces one single scour hole; when $s/D_p > 3.5$, the interference between adjacent piles diminishes and incipient individual scour holes can be observed. With further increases of s/D_p, the individual scour holes tend to separate and, for $s/D_p > 5$, each pile has one clearly individualized scour hole; consequently the maximum scour depth of the pile group becomes independent from s/D_p for $s/D_p > 5$.

Some of the predictors used in engineering practice to calculate the equilibrium scour depth at pile groups are based on methods initially developed for single cylindrical piers. In the cases of Richardson and Davis (2001) and Sheppard and Renna (2010), the concept of equivalent diameter emerges. The equivalent diameter is defined as the diameter of a single cylindrical pier that leads to the same equilibrium depth as the pile group. In the case of non-submerged cylindrical pile groups, the equivalent diameter depends on the non-overlapping individual pile widths, projected in a plane normal to the approach flow, W_g, as well as on coefficients that account for *i*) the pile spacing, K_{sp}, and *ii*) the number of rows aligned with the approach flow, K_m, if $\alpha < 5^o$.

The objective of this study is to contribute to the improved characterization of the equilibrium scour depth at pier alignments on the basis of systematic experimentation. The most important

difference of this study as compared with those carried out in the past consists in the long duration of the experiments.

6.3 Experimental set-up

Two flumes were used in the experimental study. One of them is 28.00 m long, 2.00 m wide and 1.00 m deep and it includes a closed hydraulic circuit whose maximum flow discharge is 135 ls^{-1}. Discharge is measured with an electromagnetic flow meter installed in the circuit. At the entrance of the flume, two honeycomb diffusers aligned with the flow direction smooth the flow trajectories and guarantee the lateral uniform flow distribution. Immediately downstream from the diffusers, a 5.00 m long bed reach is covered with fine gravel, to provide proper roughness and guarantee fully developed flow. The central reach of the flume, starting at 13.90 m from the entrance, includes a 3.00 m long, 2.00 m wide and 0.60 m deep recess box in the bed. At the downstream end of the flume, a tailgate allows for the regulation of the water depth. The water falls into a 100 m^3 reservoir, where the hydraulic circuit starts.

The bed recess box was filed with uniform quartz sand (ρ_s = 2660 kgm^{-3}; D_{50} = 0.86 mm; σ_D = 1.36).

The experiments were carried out with a constant approach flow depth, d = 0.20 m, and average velocity, U, approximately equal to the critical velocity for sediment entrainment, $U_c \approx 0.33$ ms^{-1}. For this velocity, the scour depth can be expected to be maximal as soon as the remaining parameters of Equation 6.3 are kept constant.

Individual cylindrical piers were simulated by PVC pipes with diameter D_p = 50 mm. Alignments of four piers were placed approximately at the center of the bed recess box; both the pier spacing and the alignment skew-angle were systematically varied: $s/D_p = \{1, 2, 3, 4.5, 6\}$; $\alpha = \{0º, 15º, 30º, 45º, 90º\}$. The choice of four piers per alignment was made assuming that a bigger number of piers would not impact the conclusions.

The second flume differs from the previously described one in its dimensions. It is 33.15 m long, 1.00 m wide and 1.0 m deep; its central reach starts at 16.00 m from the entrance; the maximum flow discharge is 90 ls^{-1}; the depth of the recess box is 0.35 m. The sand used in this flume as well as control variables such as flow depth and velocity, diameter of individual piers, m and spacing were the same as in the first flume. Due to width restrictions, it was used to run experiments with small skew-angles to avoid wall and contraction effects.

Prior to each experiment, the sand bed was levelled with the adjacent concrete bed. The area located around the pier alignment was covered with a thin metallic plate to avoid uncontrolled scour at the beginning of each experiment. Flumes were filled gradually through independent small-discharge hydraulic circuits, imposing high water depth and low flow velocity. The

discharge corresponding to the chosen approach flow velocity was then passed through each flume. The flow depth was regulated by adjusting the downstream tailgates. Once the discharge and flow depth were established, the metallic plates were removed and the experiments started.

Scour immediately initiated and the depth of scour hole was measured at each individual pier, to the accuracy of ±1 mm, with adapted point gauges, with a high frequency during the first day. Afterwards, the interval between measurements increased and three or four measurements were carried out per day. When the scour rate was less than ~2 mm (~ $2D_{50}$) in 24 hour and at least ~7 days had passed, the experiments were stopped. The sand bed approach reach located upstream the piers was verified to stay undisturbed along the entire duration of the experiments; this long term stability ensured that scour depth did not add with upstream bed degradation.

6.4 Results and discussion

Twenty six experiments were carried out. One of them was run for a single cylindrical pier (D_p = 50 mm). Table 6.2 records the main variables and non-dimensional parameters of the twenty five experiments run for pier alignments; it includes the alignment skew-angle, α, pier spacing, s, the normalized pier spacing, s/D_p, the sum of the non-overlapping individual pier widths projected on a plane normal to the approach flow, W_g, and the experiment duration, t_d.

Table 6.2 – Control variables of the experiments and equilibrium scour depths

Exp.	α (º)	s (m)	s/D_p	W_g (m)	t_d (day)	d_{sge} (m)	d_{sge}/d_{se1}
1		0.050	1.0	0.050	11.0	0.153	1.13
2		0.100	2.0	0.050	16.0	0.160	1.18
3	0	0.150	3.0	0.050	13.7	0.152	1.12
4		0.225	4.5	0.050	16.2	0.184	1.36
5		0.300	6.0	0.050	11.2	0.136	1.00
6		0.050	1.0	0.089	11.2	0.157	1.15
7		0.100	2.0	0.128	13.2	0.152	1.12
8	15	0.150	3.0	0.167	15.4	0.162	1.19
9		0.225	4.5	0.200	8.9	0.183	1.35
10		0.300	6.0	0.200	11.2	0.170	1.25
11		0.050	1.0	0.125	6.9	0.246	1.81
12		0.100	2.0	0.200	6.9	0.242	1.78
13	30	0.150	3.0	0.200	7.7	0.212	1.56
14		0.225	4.5	0.200	7.2	0.198	1.46
15		0.300	6.0	0.200	7.7	0.177	1.30
16		0.050	1.0	0.156	7.9	0.316	2.33
17		0.100	2.0	0.200	6.9	0.174	1.28
18	45	0.150	3.0	0.200	9.9	0.149	1.09
19		0.225	4.5	0.200	8.2	0.158	1.16
20		0.300	6.0	0.200	7.9	0.144	1.06
21		0.050	1.0	0.200	10.3	0.354	2.61
22		0.100	2.0	0.200	9.6	0.190	1.40
23	90	0.150	3.0	0.200	9.4	0.175	1.29
24		0.225	4.5	0.200	7.2	0.159	1.17
25		0.300	6.0	0.200	7.8	0.127	0.94

The flow shallowness, d/D_p = 4.00, flow intensity, $U/U_c \approx 1.00$, and sediment coarseness, $D_p/D_{50} \approx 60$, were chosen so as to maximize the alignment scour depth, d_{sge} (Sheppard *et al.* 2004). The ratio B/d = {5, 10} guarantees the absence of wall effects. The ratio B/W_g was typically bigger than 10 as a precaution to avoid contraction scour. In a few cases, for α = 15º, the ratio went down to 5, as the experiments on this skew-angle were made in the 1.0 m wide flume. In no case contraction scour was observed, since the borders of the scour holes never reached the walls of the flumes.

It is postulated here that equilibrium is attained asymptotically. Consequently, the time records of scour depth were extrapolated to $t = \infty$ through the 6-parameter polynomial technique suggested by Lança *et al.* (2010) as a means to estimate the equilibrium scour depth associated to each pier. The corresponding maxima, d_{sge}, as well as their ratios to the reference equilibrium scour depth produced at the single cylindrical pier, d_{sge}/d_{se1}, are also included in Table 6.2. The location of the deepest scour hole changed from experiment to experiment and d_{sge} attends to this fact. The reference scour depth was d_{se1} = 0.136 m, leading to d_{se1}/D_p = 2.72. This value compares with d_{se}/D_p = 2.4, as suggested by authors such as Melville and Coleman (2000), and the increase is possibly ascribable to the long duration of the test as well as to the extrapolation of the scour records to infinite time.

It should be noticed that pier alignments defined by s/D_p = 1 can be assumed to behave as one equivalent single pier whose shape is that of a round-nose rectangular pier, as sketched in Figure 6.2 (dashed perimeter). The associated ratio of pier length to pier width is, in this study, L/D_p = 4.

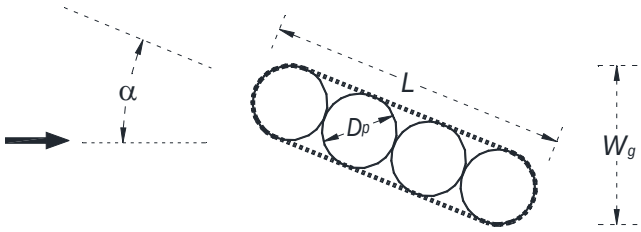

Figure 6.2 – Equivalent single pier defined for s/D_p = 1

Assuming that the above conceptualization is right, the following equation should hold:

$$d_{sge}\big|_{\alpha} = K_{\alpha} K_s (d_{sge}\big|_{\alpha=0}) \tag{6.6}$$

where K_α = skew-angle factor and K_s = pier shape factor, while the remaining symbols are self explanatory.

Figure 6.3 presents the time records of the scour depth at the pier alignments by exploiting two key control variables of the experiments, *i.e.*, the skew-angle, α, and the normalized pier

spacing, s/D_p. The longer records are truncated at t = 200 h and the scale of d_s is the same for all experiments. The reference equilibrium scour depth, d_{se1}, is also represented. The pier P1 is the pier located the most upstream and the pier P4 is the most downstream, with the exception of the experiments defined by α = 90º, where the concepts of upstream and downstream no longer apply.

From Figure 6.3 and Table 6.2, the following important conclusions can be drawn:

i) For α = 0º, the deepest scour hole is always ob-served at the pier P1. The fact that scour holes are shallower at the remaining piers in the alignment is possibly induced by the effect of "shadow", *i.e.*, to the decrease of the approach flow velocity – since mass is diverted by the piers located upstream – as well as by the deposition of sand originated at upstream scours holes. The maximum scour depth, recorded at the pier P1, is approximately 15% higher than the reference scour depth, d_{se1} (see Table 6.2), for s/D_p = {1, 2, 3}; this increase more than doubles for s/D_p = 4.5 and vanishes for s/D_p = 6. For small values of s/D_p, the scour depth increase can be explained by the interaction of the horse-shoe vortices at individual piers; on top of that, the wake vortices originated at the sides of piers P2 to P4 provide extra siphoning strength and capacity to transport sand downstream, as compared with the situation observed at single cylindrical piers, this way contributing to increase the maximum scour depth at the pier group; the combination of these two effects seems to be maximal for s/D_p = 4.5 and then vanish for s/D_p = 6. This result is not much different from the suggestion of Ashtiani and Beheshti (2006) who reported the maximum scour depth for s/D_p = 3, as α = 0º.

ii) When α = 15º, the scour depth time evolution is approximately the same at the four piers in the alignment, except for s/D_p = 4.5 where the deepest scour hole is observed at P4. On top of that, the values of d_{sge}/d_{se1} are not significantly different from those observed for α = 0º, conflicting with intuition and some findings reported in the literature (*e.g.* Zhao and Sheppard 1999).

iii) For α = {30º; 45º; 90º}, scour depth systematically decreases with s/D_p.

iv) For s/D_p = 6, scour depth shows a weak dependence on α. Yet, ≈ 25% – 30% scour increase is observed for α = {15º, 30º}, as compared with the isolated cylindrical pier.

v) With the exception of s/D_p = 1, the deepest scour holes are observed for α = 30º and s/D_p = {2; 3}. In these cases, piers downstream of P1 are located in the path of highly energetic wake vortices originated upstream (see Figure 6.4), and the maximum scour depth is observed at P3 or P4 for all s values except s/D_p = 6 (where it occurs at P2). The ratio d_{sge}/d_{se1} is ≈ 1.7 and it slightly decreases until 1.3 for s/D_p = 6.

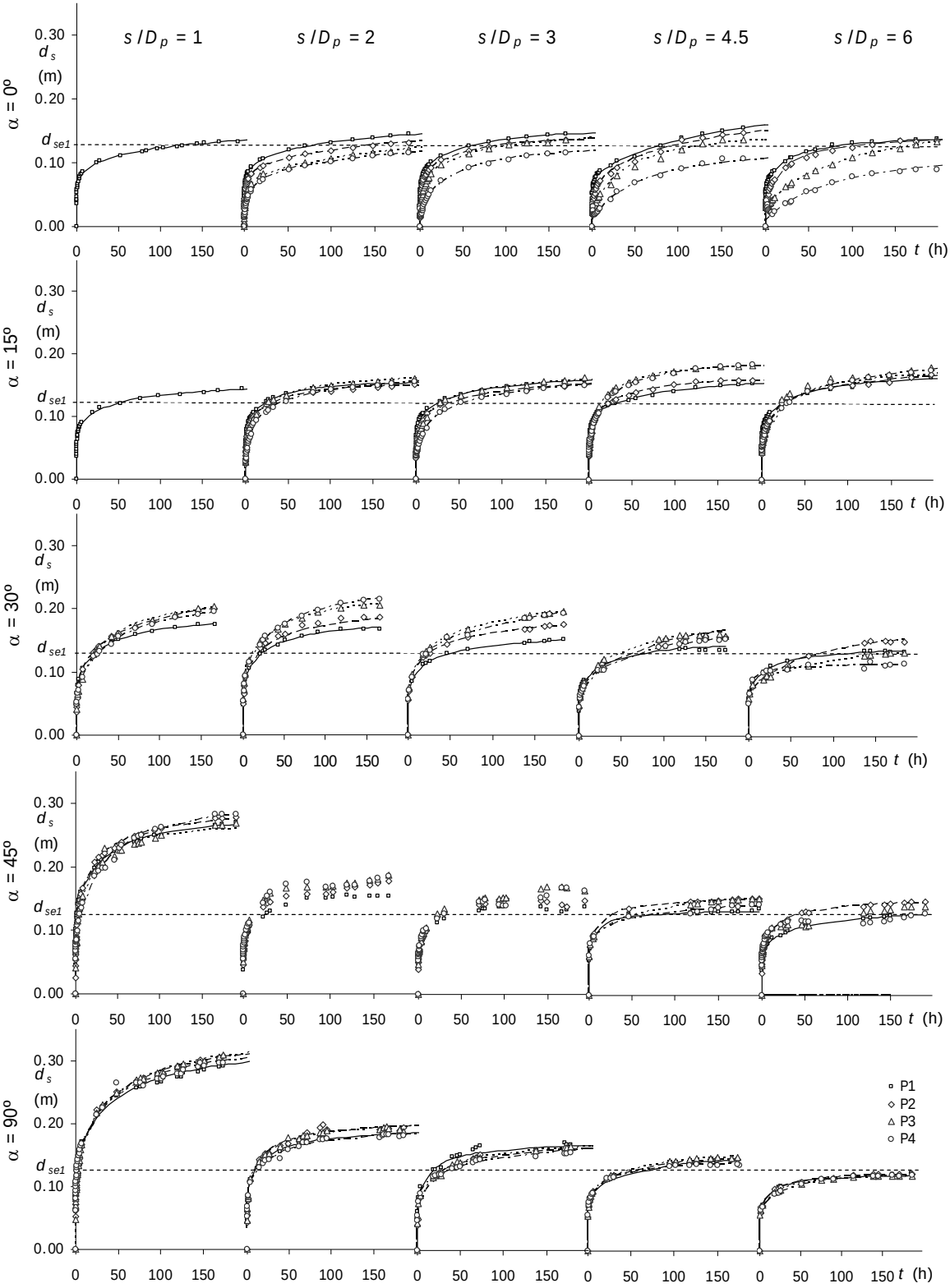

Figure 6.3 – Scour depth time evolution at pier alignments for α = [0º; 15º; 30º; 45º; 90º] and s/D_p = [1.0; 2.0; 3.0; 4.5; 6.0]

vi) For α = 45º, small oscillations are observed in the scour depth time evolution, especially for s/D_p = {2; 3} (see Figure 6.3). It can be speculated that these oscillations occur due to the interaction of horse-shoe vortices arms with wake vortices separated from the upstream pier. This explanation requires experimental confirmation. The ratio d_{sge}/d_{se1} is ≈ 2.3 for s/D_p = 1 and clearly decreases with s/D_p; d_{sge}/d_{se1} ≈ 1.3 when s/D_p = 2.

vii) When α = 90º, the scour depth time evolution presents minor differences at different piers; it seems though that the thalweg is located at P2 or P3. For s/D_p = 1, the pier acts as a single pier with one single horse-show vortex. The scour depth is the biggest. For s/D_p = 2, different horse-show vortices are believed to be present, the corresponding arms being compressed by the flow acceleration in the spacing between piers. With the increase of s/D_p, this group effect tends to vanish and each pier in the alignment tends to behave as a single one. The ratio d_{sge}/d_{se1} is ≈ 2.6 for s/D_p = 1, d_{sge}/d_{se1} ≈ 1.35 for s/D_p = {2; 3} and d_{sge}/d_{se1} ≈ 1 for s/D_p = 6.

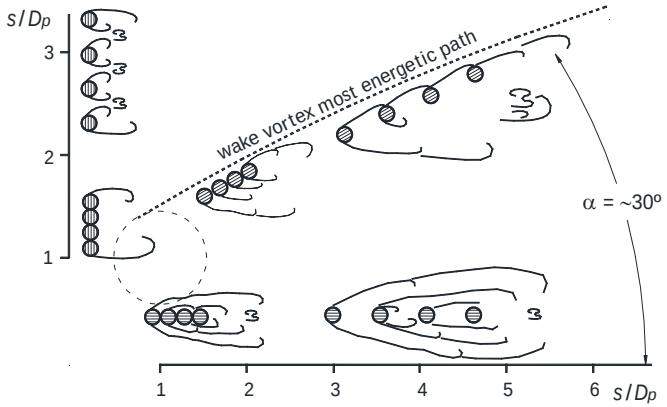

Figure 6.4 – System of wake vortices at pier alignments

Most of the previous conclusions are translated in Figure 6.5 where the ratio d_{sge}/d_{se1} is plotted against s/D_p and α.

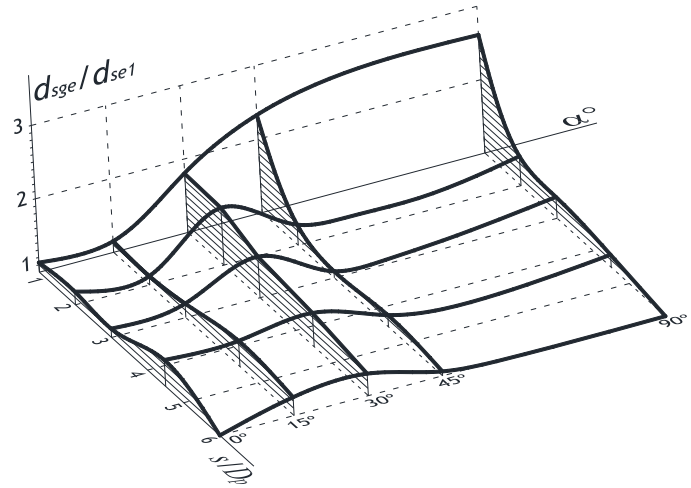

Figure 6.5 – Variation of d_{sge}/d_{se1} with s/D_p and α

Keeping in mind the pier conceptualization of Figure 6.2, it is possible to reproduce, within an error margin of 10%, the equilibrium scour depths measured for $s/D_p = 1$ by assuming $K_s = 1$ (valid for round-nose rectangular piers) and $K_\alpha = \{2.0; 2.3; 2.5\}$ for, respectively, $\alpha = \{30º; 45º; 90º\}$, as suggested by Richardson and Davis (2001).

For the most common s/D_p values used in engineering practice, *i.e.*, $s/D_p > \approx 3$, the equilibrium scour depth increases {15%; 30%; 30%; 10%; 10%} for, respectively, $\alpha = \{0º; 15º; 30º; 45º; 90º\}$ as compared with the expected value at a single cylindrical pier with the same diameter, D_p, as the individual piers. This shows that, for $s/D_p > 3$, the worst skew-angles tend to be in the range of $15º \leq \alpha \leq 30º$.

The data set obtained in this study constitutes an independent basis for the assessment of existing predictors of scour depth at pile groups and pier alignments. For this reason, the predictions issued by the methods of Richardson and Davis (2001) and Sheppard and Renna (2010) were compared with measurements. Figure 6.6 displays the values of d_{sge}/d_{se1} predicted by both methods against the corresponding measured values. Deviation bands of 25 and 40% towards perfect agreement are also included; d_{se1} stands, in both axes, for the measured value.

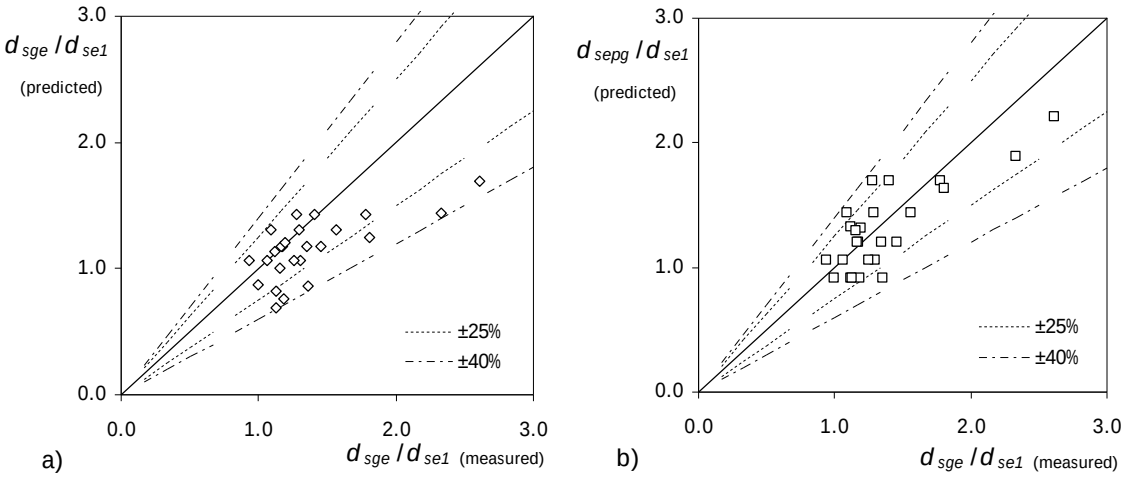

Figure 6.6 – Measured d_{sge}/d_{se1} *v.s.* corresponding predictions, according to a) Richardson and Davis (2001) and b) Sheppard and Renna (2010)

From the inspection of Figure 6.6, it can be concluded that an important number of measurements exceed the corresponding predictions. This is more evident for the method of Richardson and Davis (2001). It is also worth of notice that some measurements exceed the predictions by approximately 40%, which is rather significant.

6.4 Conclusions

From the previous discussion, the following summary of conclusions can be drawn:

i) When $\alpha = \{0º; 15º\}$, $d_{sge}/d_{se1} < 1.35$ and the maxima scour depths occur for $s/D_p \approx 4.5$.

ii) For α = {30º; 45º; 90º}, the scour depth systematically decreases with s/D_p.

iii) When s/D_p = 6, d_{sge}/d_{se1} < 1.25 – 1.30 for α = {15º; 30º}, while $d_{sge}/d_{se1} \approx 1$ for the remaining skew-angles.

iv) When s/D_p = 1, the pier alignment can be treated as a single round-nose rectangular pier whose cross-section is defined as the envelope of the adjacent piers.

v) Excluding s/D_p = 1 the maximum scour depth occurs for α = 30º and s/D_p = {2; 3}, where $d_{sge}/d_{se1} \approx 1.7$.

vi) Common methods applied in engineering practice to predict scour depth at pier alignments may provide under-predictions of the order of up to 40%.

7. CLEAR-WATER SCOUR AT PILE GROUPS

7.1 Introduction

For major river crossings, there is increasing use of bridge foundations that consist of a number of piles supporting a pile cap. Piers composed of a column, pile cap and pile group are often known as complex piers. The foundations of the piles are often deep but if the piles rely on skin friction, rather than end-loading, to support the weight of the bridge, the foundations can be vulnerable to scour. There have been a number of recent bridge failures caused by scour at such pile groups.

This study focuses on local scour at pile groups in which the level of the pile cap is above the water level. Pile groups may be composed of one or more alignments – or columns – of piles. Pile groups composed of only one such column of piles are frequently used, without pile cap, to directly support bridge decks. For this reason, this particular group configuration is also referred to as a pier alignment herein.

Local scour at pile groups is more complex and difficult to predict than that at single piers. The increased complexity is due to the interaction of vortices generated at individual piles and to the concomitant interdependence of scour holes around each pile.

Local scouring at submerged and partly submerged pile groups has already been addressed in the past. However, further research efforts seem to be needed as, by comparison with local scour studies at single piers, the number of studies reported in the literature on scouring at pile groups is small. They include those of Hannah (1978), Elliott and Baker (1985), Salim and Jones (1996), Zhao and Sheppard (1999), Smith (1999), Sumer and Fredsøe (2002), Ataie-Ashtiani and Beheshti (2006) and Amini *et al.* (2012), which mostly report on short duration scour experiments. Due to this short duration, their results may be postulated to inherently carry important uncertainties.

Lança *et al.* (2012) have shown that clear-water scour depth at pile groups inserted in wide rectangular channels whose bed is composed of uniform non-ripple forming sand (D_{50} > 0.6 mm; σ_D < 1.5; D_{50} = median sand size; σ_D = sand gradation coefficient) is given by (see Figure 7.1)

$$\frac{d_{sg}}{D_p} = \varphi\left(\frac{d}{D_p}, \frac{U}{U_c}, \frac{D_p}{D_{50}}, \frac{Ut}{D_p}, \frac{s}{D_p}, \alpha, K_s, m, n\right) \tag{7.1}$$

where φ stands for function, d_{sg} = maximum scour depth at the pile group at instant t; D_p = individual pile width; d = approach flow depth; U = approach flow velocity; U_c = approach flow velocity for the threshold condition of sediment entrainment; t = time; d/D_p = flow shallowness or relative approach flow depth; U/U_c = flow intensity; D_p/D_{50} = sediment coarseness or relative sediment size; Ut/D_p = non-dimensional time; s = pile spacing; α = pile group skew-angle; K_s = shape factor of individual piles; m = number of rows in the group; n = number of columns in the group and s/D_p = normalized pile spacing.

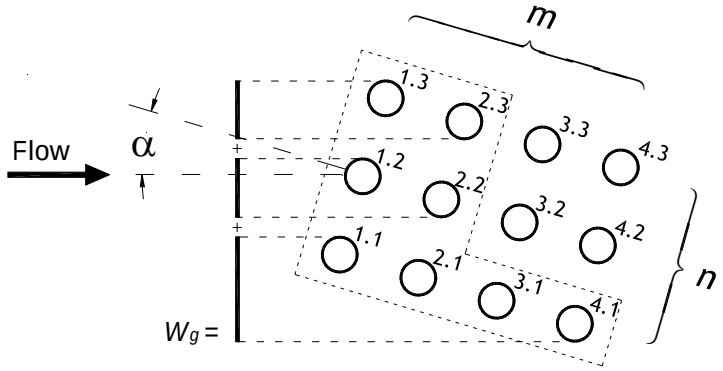

Figure 7.1 – Characteristic variables of a pile group

Equation 7.1 is valid if the approach flow is fully developed and uniform, the flow structure inside the scour hole is free of viscous effects, the wall effects are negligible and the velocity field is two-dimensional at the central section of the channel (which is guaranteed for $B/d > 5$, B = channel width). For sufficiently large values of d/D_p, where the scour depth no longer significantly depends on the approach flow depth, Equation 7.1 becomes:

$$\frac{d_{sg}}{D_p} = \varphi\left(\frac{U}{U_c}, \frac{D_p}{D_{50}}, \frac{Ut}{D_p}, \frac{s}{D_p}, \alpha, m, n\right) \tag{7.2}$$

if the individual piles are cylindrical (K_s = 1). At the equilibrium stage, the maximum scour depth, d_{sg}, practically does not depend on time and here is denoted by d_{sge}. For U/U_c = 1 and $D_p/D_{50} \approx 50$, the equilibrium scour depth is widely recognized to be a maximum. Under these conditions, Equation 7.2 becomes:

$$\frac{d_{sge}}{D_p} = \varphi\left(\frac{s}{D_p}, \alpha, m, n\right) \tag{7.3}$$

which may be replaced by

$$K_{pg} = \frac{d_{sge}}{d_{se1}} = \varphi\left(\frac{s}{D_p}, \alpha, m, n\right) \tag{7.4}$$

In Equation 7.4 d_{se1} is the equilibrium scour depth at an isolated pile or pier subjected to the same hydrodynamic conditions as those in Equation (7.3) – where d_{se1}/D_p would be constant – and K_{pg} is an aggregated pile group factor that accounts for spacing, skew-angle, the number of columns and the number of rows.

Equation 7.2 to Equation 7.4 constitute the framework for the analysis of the results of the present experimental study as well as of the studies performed to date. Table 7.1 summarizes the values α, s/D_p, n, m and U/U_c covered by previous studies. It also includes the duration of the reported tests, t_d, and describes the shape of the elemental piles cross-section.

Table 7.1 – Control variables and non-dimensional parameters of studies known to date

Author	α (º)	s/D_p	n	m	U/U_c	t_d (h)	Shape[1]
H	0 – 90	1 – 21	1	2	0.72	≈ 7	circular
E&B	0	1.6 – 13.2	1	3	0.5 – 1	NS	RC
S&J	0 – 50	1 – 10	3	8	1.00	4	square
Z&S	0 – 90	3	3	8	0.65	26	C + S
S [2]	0 – 70	3; 6	2; 3	4; 8	0.89 – 0.96	65 – 137	square
A&B	0	1 – 11	1; 2; 3	1; 2; 3	0.66 – 0.88	≈ 8	circular
A [2]	0	1 – 6	2; 3	2; 4; 5	0.95	≈ 8	circular

H = Hannah (1978); E&B = Elliott and Baker (1985); S&J = Salim and Jones (1996); Z&S = Zhao and Sheppard (1999); S = Smith (1999); A&B = Ataie-Ashtiani and Beheshti (2006); A = Amini *et al*. (2012); C+S = circular and square; RC = round nose rectangular; NS = non-specified. [1] shape of the pile cross-section; [2] refers to the experiments on uniform spacing and un-submerged pile groups.

It is also important to report that, apart from Hannah (1978), Amini *et al.* (2012) and, in some cases, Ataie-Ashtiani and Beheshti (2006), the remaining authors have used fine sand (D_{50} < 0.6 mm), which is prone to the formation of ripples in the approach flow reach. In the study of Salim and Jones (1996), ripples most likely occurred since $U/U_c \approx 1.0$. This is potentially an extra source of uncertainty for these results.

Also, according to Simarro *et al.* (2011), the duration of scour tests should be, at least, 7 days to allow for the adequate prediction of equilibrium scour at single cylindrical piers. This duration is possibly short for pile groups since the scouring process can be expected to be more complex and slower. It is clear that, excepting the four tests of Smith (1999), the typical duration of the tests reported in the literature on pile groups is rather short as compared to the time needed to sufficiently approach the equilibrium phase. Consequently, conclusions drawn from the above earlier studies on scouring at pile groups (including some integrated in current predictors) do not seem to guarantee accurate predictions of the equilibrium scour depth.

The present study focus on the effect of pile spacing, s/D_p, skew-angle, α, as well as number of columns of the pile group, n, on the maximum scour depth at pier groups, and pays special attention to the effect of time. The specific question under investigation in this regard is

whether the pile group factor, K_{pg}, remains unchanged or not as the scour process evolves through time. For these purposes, a systematic experimental campaign was carried out by performing 75 long-duration ($t_d \geq \approx 7$ days) experiments. These experiments correspond to all the combinations of the following group properties: n = [1, 2, 3], α = [0º, 15º, 30º, 45º, 90º] and s/D_p = [1, 2, 3, 4.5, 6], by keeping m = 4.

7.2 Experimental setup and procedure

Two flumes were used in the study. One was 28.0 m long, 2.00 m wide and 1.00 m deep. It included a closed hydraulic circuit whose maximum flow discharge was 135 ls^{-1}. Discharge was measured by an electromagnetic flow meter installed in the circuit. At the entrance of the flume, two honeycomb diffusers aligned with the flow direction smoothed the flow trajectories and guaranteed a uniform transversal flow distribution. Immediately downstream from the diffusers, a 5.00 m long bed reach was covered with small gravel to provide proper roughness and guarantee fully developed flow. The central reach of the flume, starting at 13.90 m from the entrance, contained a 3.00 m long, 2.00 m wide and 0.60 m deep recess box in the bed. At the downstream end of the flume, a tailgate allowed the regulation of the water depth. The water fell into a 100 m^3 reservoir, where the hydraulic circuit started.

For this case, the tests were carried out with constant approach flow depth, d = 0.20 m, and average velocity, U, approximately equal to the critical velocity for sediment entrainment, $U_c \approx$ 0.32 ms^{-1}. For this velocity, the scour depth can be expected to be maximal provided that the remaining parameters of Equation 7.2 are kept constant.

Individual cylindrical piles were simulated by PVC pipes with diameter D_p = 50 mm. Pile groups defined by m = 4 were placed at the center of the bed recess box for 60 of a total of 75 different combinations of pile spacing, number of columns and skew-angle. The bed recess box was filled with uniform quartz sand (density, ρ_s = 2660 kgm^{-3}; D_{50} = 0.86 mm; σ_D = 1.36).

The second flume was 33.2 m long, 1.00 m wide and 1.00 m deep; its central reach started at 16.0 m from the entrance; the depth of the bed recess box was 0.35 m. The maximum flow discharge was 90 ls^{-1}. The sand used in this flume as well as the imposed flow depth and velocity, diameter of elemental piles, number of rows (m = 4) and spacing, s/D_p = [1, 2, 3, 4.5, 6], were the same as in the first flume. Due to width restrictions, this flume was used for only 15 of the total number of tests defined by {n = [1], α = [0º, 15º]} and {n = [2], α = [0º]}, for s/D_p = [1, 2, 3, 4.5, 6].

Prior to each test, the sand of the corresponding recess box was leveled with the adjacent bed. The area located around the piles was covered with thin metallic plates combined with filter fabric to avoid uncontrolled scour at the beginning of each test. The flumes were filled gradually through independent small-discharge hydraulic circuits, imposing high water depth and low flow

velocity. The discharge corresponding to the chosen approach flow velocity (0.31 ms^{-1}) was then passed through each flume. The flow depth was regulated by adjusting the downstream tailgates. Once the discharge and flow depth were established, the metallic plates and filter were carefully removed and the tests started.

Scour was immediately initiated and the depth of scour hole was measured immediately upstream of each elemental pile, to an accuracy of ±1 mm, with adapted point gauges, at high frequency (up to five per hour) during the first day. Afterwards, the interval between measurements increased and, from the first day, three or four measurements were made per day. The minimum duration of each experiment was 7 days. The sand bed approach reach located upstream of the piles stayed undisturbed through the entire duration of the tests; this long term stability ensured that scour depth was not supplemented by upstream bed degradation.

Five reference experiments for single cylindrical piles defined by D_p = [50, 100, 150, 200, 400] mm were also run for $t_d \approx 7$ days, keeping all the other variables unchanged.

7.3 Results and discussion

7.3.1 Data presentation and characterization

Table 7.2 records the characteristic variables and non-dimensional parameters of the 75 experiments. It includes the skew-angle, α, the normalized pile spacing, s/D_p, the sum of the non-overlapping elemental pile widths projected on a plane normal to the approach flow direction, W_g, as defined in Figure 7.1 (in accordance to Richardson and Davis 2001; Sheppard and Renna 2010), the channel width, B, normalized by W_g, and the test duration, t_d.

The flow shallowness, $d/D_p = 4$, flow intensity, $U/U_c \approx 0.97$, and sediment coarseness, $D_p/D_{50} = 58$, are expected to practically maximize the equilibrium scour depth, d_{sge}. Indeed, not only *i*) in accordance to Melville and Coleman (2000) – for instance – the scour depth does no longer increase with the flow depth for $d/D_p > 10/7$, as *ii*) it is widely accepted that the maximum scour depth occurs for $U/U_c \approx 1.0$ as soon as the bed is composed of uniform non-ripple forming sand and also *iii*) the scour depth reaches its maximum for $D_p/D_{50} \approx 50$, as shown in recent studies by Sheppard *et al.* (1995, 1999, 2004). It may also be expected that the ratio B/d = [5, 10], depending on the flume, guarantees the absence of serious wall effects. The ratio B/W_g, being always ≥ 5, ensures that contraction scour is not significant, while in no case did the edge of the scour hole reach the lateral walls of the flumes.

Table 7.2 – Control variables of the tests and equilibrium scour depths

		n = 1					n = 2					n = 3				
α (º)	s/D_p	Test	W_g (m)	B/W_g	t_d (day)	d_{sge} (m)	Test	W_g (m)	B/W_g	t_d (day)	d_{sge} (m)	Test	W_g (m)	B/W_g	t_d (day)	d_{sge} (m)
0	1.0	1	0.050	20.0	11.0	0.153	26	0.100	10.0	13.2	0.261	51	0.150	13.3	8.10	0.327
	2.0	2	0.050	20.0	16.0	0.160	27	0.100	10.0	15.2	0.185	52	0.150	13.3	7.00	0.211
	3.0	3	0.050	20.0	13.7	0.152	28	0.100	10.0	14.1	0.183	53	0.150	13.3	7.20	0.208
	4.5	4	0.050	20.0	16.2	0.149	29	0.100	10.0	9.1	0.146	54	0.150	13.3	8.20	0.218
	6.0	5	0.050	20.0	11.2	0.136	30	0.100	10.0	7.1	0.156	55	0.150	13.3	8.50	0.139
15	1.0	6	0.089	11.2	11.2	0.157	31	0.137	14.6	7.0	0.299	56	0.185	10.8	8.20	0.334
	2.0	7	0.128	7.8	13.2	0.152	32	0.204	9.8	7.0	0.240	57	0.279	7.2	8.20	0.305
	3.0	8	0.167	6.0	15.4	0.162	33	0.255	7.8	7.0	0.183	58	0.342	5.8	7.80	0.250
	4.5	9	0.200	5.0	8.9	0.183	34	0.300	6.7	7.2	0.205	59	0.400	5.0	8.50	0.208
	6.0	10	0.200	5.0	11.2	0.170	35	0.300	6.7	8.9	0.204	60	0.400	5.0	7.80	0.170
30	1.0	11	0.125	16.0	6.9	0.246	36	0.168	11.9	6.8	0.316	61	0.212	9.4	7.00	0.347
	2.0	12	0.200	10.0	6.9	0.242	37	0.287	7.0	6.8	0.331	62	0.373	5.4	8.00	0.378
	3.0	13	0.200	10.0	7.7	0.212	38	0.300	6.7	7.8	0.278	63	0.400	5.0	8.30	0.280
	4.5	14	0.200	10.0	7.2	0.198	39	0.300	6.7	6.9	0.217	64	0.400	5.0	7.20	0.237
	6.0	15	0.200	10.0	7.7	0.177	40	0.300	6.7	7.7	0.200	65	0.400	5.0	7.90	0.228
45	1.0	16	0.156	12.8	7.9	0.316	41	0.191	10.5	12.0	0.335	66	0.227	8.8	8.90	0.359
	2.0	17	0.200	10.0	7.0	0.175	42	0.250	8.0	9.0	0.257	67	0.300	6.7	12.00	0.329
	3.0	18	0.200	10.0	9.9	0.156	43	0.250	8.0	9.0	0.244	68	0.300	6.7	8.90	0.279
	4.5	19	0.250	8.0	8.2	0.158	44	0.250	8.0	8.1	0.189	69	0.300	6.7	7.20	0.182
	6.0	20	0.200	10.0	8.0	0.144	45	0.250	8.0	8.9	0.177	70	0.300	6.7	11.60	0.160
90	1.0	21	0.200	10.0	10.3	0.354	46	0.200	10.0	8.8	0.369	71	0.200	10.0	7.40	0.328
	2.0	22	0.200	10.0	9.6	0.190	47	0.200	10.0	12.1	0.212	72	0.200	10.0	7.80	0.255
	3.0	23	0.200	10.0	9.4	0.175	48	0.200	10.0	8.3	0.189	73	0.200	10.0	7.30	0.187
	4.5	24	0.200	10.0	7.2	0.159	49	0.200	10.0	6.9	0.178	74	0.200	10.0	7.20	0.151
	6.0	25	0.200	10.0	7.8	0.127	50	0.200	10.0	7.7	0.141	75	0.200	10.0	7.00	0.145

It is assumed herein that equilibrium is attained asymptotically. The time records of scour depth were extrapolated to $t = \infty$ through the 6-parameter polynomial technique suggested by Lança *et al.* (2010) as a means to estimate the equilibrium scour depth, d_{sge}, associated to each individual pile in the group. The d_{sge} values included in Table 7.2 are the groups' maxima, irrespective of the location of the pile at which it occurred.

Figures 7.2 and 7.3 present the time records of the scour depths at individual piles directly exposed to the approach flow (piles 1.1, 2.1, 3.1, 4.1 1.2, 1.3, *cf.* Figure 7.1), for α = [0º, 30º], respectively. Data are organized according to the number of columns of the pile group, n, and the normalized pile spacing, s/D_p. The longer records were truncated at t = 200 h and the scale of the scour depth is the same in both figures to aid comparison. The reference equilibrium scour depth obtained at the single pier with D_p = 50 mm, d_{se1}, is also plotted (horizontal dashed lines). The complete time records of the scour depth are available at http://w3.ualg.pt/~rlanca/pilegroups.pdf, where figures similar to Figures 7.2 and 7.3 are also included for α = [15º, 45º, 90º].

7.3.2 Flow structure and scour mechanisms

It is widely recognized that the main features of the flow structure around single piers comprise: down-flow, horse-shoe vortex, wake vortices and the bow wave. At pile groups, the flow structure and its interaction with the mobile bed are rather more complex. According to Hannah (1978), depending on the values of α and s/D_p, the flow structure may comprise sheltering, interaction of wake vortices and systems of compressed horse-shoe vortices. The flatter bed topography induced by the rear piles may facilitate the mobility of bed grains, thus reinforcing the scour depth at the most upstream piles, as compared with the scour depth at an isolated equal diameter pier. Scour *reinforcement* is quite evident in Figure 7.2, particularly for n = [2, 3]. This effect tends to attenuate as the pile spacing increases.

Whenever present, *sheltering* leads to the reduction of the approach velocity at downstream piles, weakening the strength of the associated horse-shoe vortices and reducing the scour depth. This was observed in many experiments, but it is not evident in Figures 7.2 and 7.3 since the plotted data refer to piles directly exposed to the approach flow (where the scour depth tends to be maximal).

The vortices from the upstream piles are convected downstream and may interact with the rear piles. In this case, the *interaction of wake vortices* may lead to a downstream increase in sediment entrainment capacity. The scour increase potentially caused by this phenomenon depends on the convection speed of the vortices and the distance between their path and the piles. From Table 7.2, it can be concluded that, for a given combination of n and s/D_p except s/D_p = 1, the scour depth is maximal for α = 30º; from Figure 7.3, it can also be seen that maximum scour occurs at the rear piles of the first column (piles 3.1 and 4.1, see Figure 7.1) when α = 30º. This may be interpreted as an indication that such piles are located in the path of the most energetic wake vortices generated upstream.

For the case of piles transverse to the flow, *i.e.* α = [0º, 90º], the effect of *compression of the inner arms* of the horse-shoe vortices can be observed as soon as $s/D_p > 1$. The compressed arms lead to an increase of the local velocity, impacting on the scour depth. This effect increases as the pile spacing decreases. In the limit, for s/D_p = 1, the pile group acts as a single pier, with no inner horse-shoe arms. It is important to point out that for $s/D_p \leq 3.0$ a single scour hole was observed. For s/D_p = 4.5 the scour holes of the individual piles tend to separate and, for s/D_p = 6.0, only weak interaction between scour at each pile was observed (see Figure 7.4.b). These findings are in agreement with those of Amini *et al.* (2012).

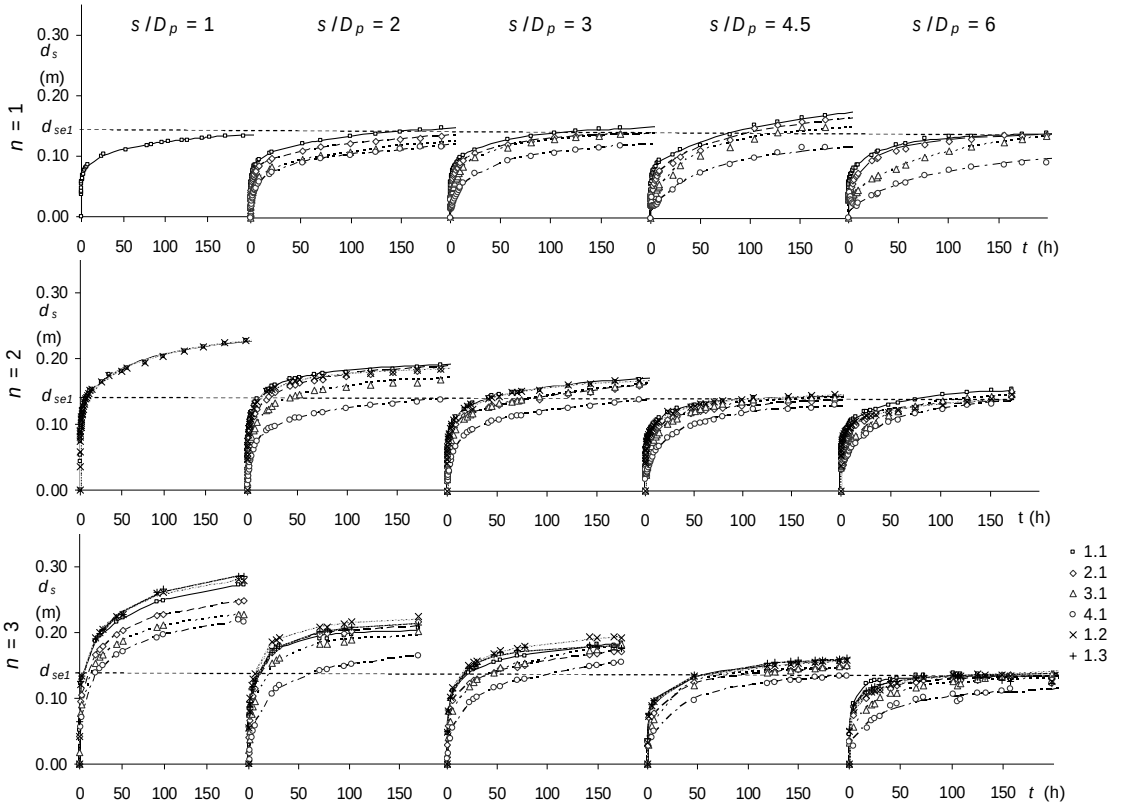

Figure 7.2 – Scour depth time evolution at pile groups for α = 0º

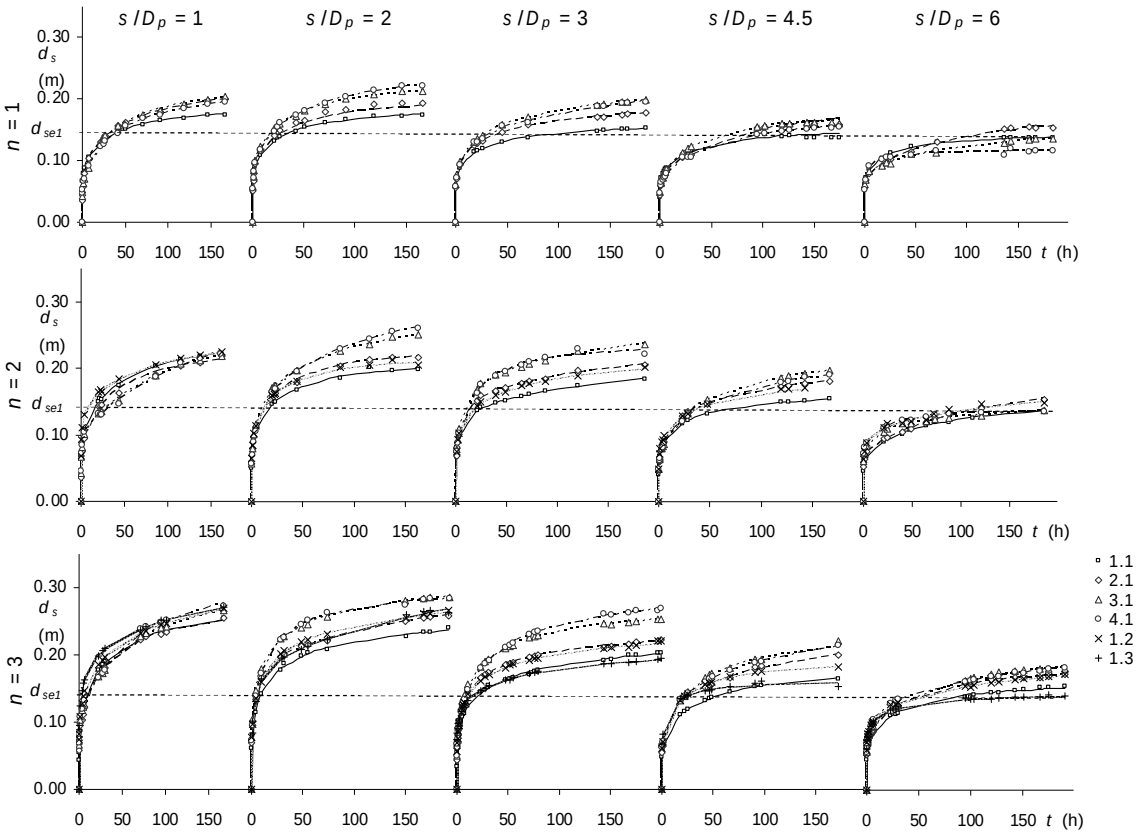

Figure 7.3 – Scour depth time evolution at pile groups for α = 30º

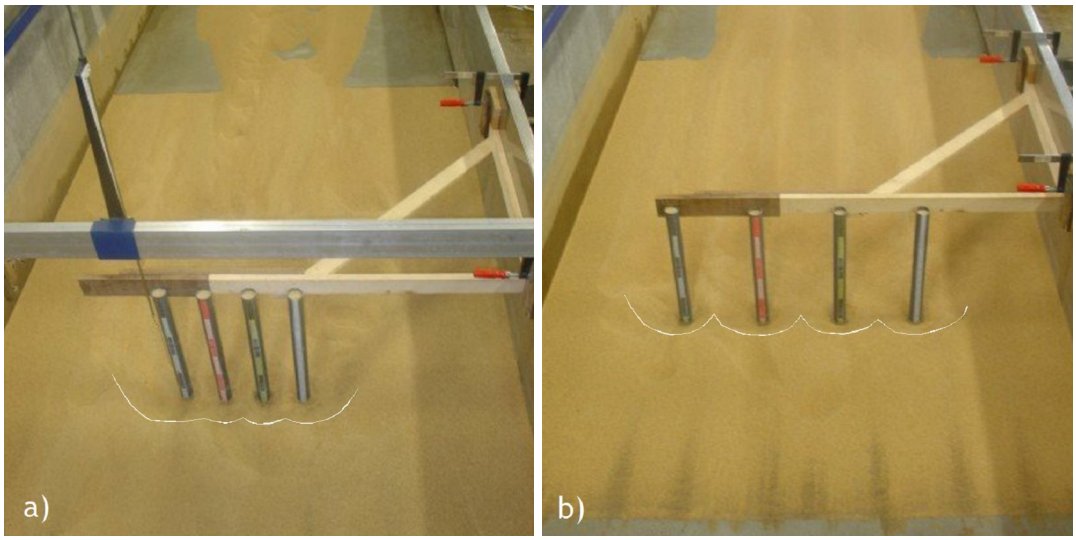

Figure 7.4 – Scour patterns: a) test 22 [n = 1, α = 90º, s/D_p = 2.0]; b) test 25 [n = 1, α = 90º, s/D_p = 6.0]

7.3.3 Effect of time on the scour process

The motivation for the present study derived from the fact that most of the tests reported in the literature so far were carried out for rather short durations. Table 7.3 summarizes the values of the maxima scour depths measured at t = [8, 24, 168 (≡ 7 days)] hours normalized by the equilibrium scour depths, d_{sge}. At t = 8 hours, the maxima scour depth is only (54 ± 6) % of the corresponding equilibrium value. The similar statistics for t = [24, 168] hours are (65 ± 7) % and (87 ±6) %, respectively, which corroborates that the scour experiments at pile groups lasting less than 7 days may implicitly contain important uncertainties in the equilibrium scour depth.

Table 7.3 – Ratio of the maxima scour depths measured at t = [8, 24, 168] hours and the maxima equilibrium scour depths

n	s/D_p	α = 0º			α = 15º			α = 30º			α = 45º			α = 90º		
		t (h)			t (h)			t (h)			t (h)			t (h)		
		8	24	168	8	24	168	8	24	168	8	24	168	8	24	168
1	1.0	0.56	0.65	0.86	0.60	0.70	0.90	0.44	0.56	0.82	0.52	0.65	0.88	0.48	0.60	0.86
	2.0	0.55	0.63	0.83	0.63	0.76	0.97	0.48	0.60	0.85	0.64	0.80	0.96	0.61	0.75	0.94
	3.0	0.58	0.69	0.90	0.60	0.70	0.90	0.48	0.60	0.85	0.63	0.78	0.95	0.58	0.71	0.88
	4.5	0.53	0.50	0.91	0.54	0.70	0.92	0.43	0.54	0.78	0.61	0.73	0.89	0.58	0.68	0.88
	6.0	0.58	0.72	0.93	0.57	0.67	0.94	0.50	0.58	0.80	0.62	0.76	0.94	0.66	0.79	0.93
2	1.0	0.53	0.62	0.85	0.45	0.54	0.76	0.45	0.53	0.72	0.47	0.60	0.87	0.48	0.59	0.84
	2.0	0.66	0.78	0.94	0.46	0.58	0.83	0.40	0.50	0.75	0.53	0.67	0.90	0.57	0.72	0.92
	3.0	0.57	0.66	0.85	0.60	0.76	0.99	0.46	0.58	0.77	0.48	0.59	0.80	0.57	0.70	0.88
	4.5	0.64	0.77	0.93	0.44	0.60	0.85	0.48	0.60	0.85	0.51	0.61	0.84	0.57	0.68	0.86
	6.0	0.60	0.70	0.91	0.49	0.60	0.82	0.46	0.52	0.75	0.62	0.69	0.91	0.67	0.78	0.94
3	1.0	0.50	0.61	0.86	0.45	0.55	0.84	0.50	0.58	0.80	0.45	0.58	0.85	0.54	0.70	0.92
	2.0	0.64	0.80	0.96	0.42	0.54	0.77	0.43	0.53	0.69	0.46	0.58	0.84	0.54	0.65	0.80
	3.0	0.55	0.67	0.86	0.51	0.67	0.83	0.48	0.61	0.87	0.44	0.57	0.86	0.62	0.76	0.94
	4.5	0.43	0.52	0.69	0.47	0.62	0.82	0.46	0.57	0.77	0.54	0.64	0.86	0.67	0.80	1.00
	6.0	0.73	0.84	0.95	0.56	0.70	0.92	0.44	0.53	0.75	0.71	0.79	0.98	0.68	0.79	0.97

From Table 7.3 it becomes clear that for α = 30º, the scour process evolved at a rate that is slower than for the other angles since the corresponding average ratios are [0.46, 0.56, 0.79] for t = [8, 24, 168] hours, respectively. This reveals that, though the deepest scour holes are observed for α = 30º (*cf.* Table 7.2), they take a considerable longer time to stabilize than for other configurations.

One specific question investigated in this study is whether the pile group factor, K_{pg}, defined by Equation 7.4 remains unchanged or not as scour evolves in time. The inspection of Table 7.4 reveals that the values of ΔK_{pg} given by

$$\Delta K_{pg} = 100 \frac{\left(K_{pg}\right)_{t=\infty} - \left(K_{pg}\right)_{t}}{\left(K_{pg}\right)_{t=\infty}} \tag{7.5}$$

do not change appreciably in time. In Equation 7.5 $(K_{pg})_{t=\infty}$ = pile group factor at equilibrium and $(K_{pg})_t$ = pile group factor at instant t. Excluding the values corresponding to α = 30º, the average absolute values of ΔK_{pg} are [11%, 11%, 8%] for t = [8, 24, 168] hours, respectively, while the maximum and the minimum values are 27% and –29%, both for t = 8 h. These results indicate that the scour depth at pile groups and at the isolated elemental pier evolve through time at reasonably similar rates, the scour holes remaining essentially self-similar with time. A larger difference is observed for α = 30º, where average ΔK_{pg} = [19%, 14%, 9%] arise for t = [8, 24, 168] hours, respectively. This means that, despite the short durations of the previous studies and the inherently strong deviations from the equilibrium stage, with marked under-evaluation of both d_{sge} and d_{se1}, there is no direct experimental reason for coefficients such as the pile spacing coefficient, K_{sp}, or the coefficient for the number of aligned rows, K_m, integrated in current scour predictors (*e.g.*, Richardson and Davis (2001) or Sheppard and Renna (2010)) to be unreliable.

Table 7.4 – Values of ΔK_{pg} at t = [8, 24, 168] hours

n	s/D_p	α = 0º			α = 15º			α = 30º			α = 45º			α = 90º		
		t (h)			t (h)			t (h)			t (h)			t (h)		
		8	24	168	8	24	168	8	24	168	8	24	168	8	24	168
1	1.0	1	0	1	–5	–7	–4	23	14	5	8	0	–2	15	7	0
	2.0	4	3	4	–12	–17	–12	15	8	1	–14	–23	–11	–7	–15	–9
	3.0	–2	–6	–4	–6	–7	–4	15	8	2	–11	–20	–10	–3	–10	–1
	4.5	7	22	–6	5	–8	–7	24	17	10	–8	–13	–3	–2	–5	–2
	6.0	–2	–10	–7	0	–4	–8	12	11	7	–9	–17	–9	–16	–22	–8
2	1.0	6	4	1	20	16	13	20	19	17	18	8	0	16	9	2
	2.0	–17	–20	–9	20	10	4	30	23	14	6	–3	–4	–1	–11	–6
	3.0	0	–1	2	–5	–17	–14	18	11	11	15	9	8	–1	–7	–1
	4.5	–13	–18	–8	22	8	2	16	7	2	9	6	3	0	–4	1
	6.0	–6	–8	–5	13	8	5	19	20	14	–9	–7	–5	–18	–20	–9
3	1.0	13	6	0	21	16	3	13	11	7	21	10	2	5	–7	–6
	2.0	–13	–24	–11	27	16	11	25	19	20	19	11	3	4	1	7
	3.0	3	–3	1	10	–3	4	16	6	–1	23	13	1	–10	–17	–9
	4.5	25	20	20	16	5	5	18	12	11	5	2	0	–18	–23	–16
	6.0	–29	–29	–10	1	–7	–6	23	19	13	–26	–22	–13	–20	–21	–12

7.3.4 Dependence of the pier group factor from the pile spacing and the skew-angle

Table 7.5 summarizes the values of K_{pg} defined at equilibrium ($t = \infty$) for $m = 4$. It should be reiterated here that, in the context of the present study, K_{pg} accounts for several effects, namely, spacing, skew-angle and number of columns, n. In Figure 7.5, the values of K_{pg} are plotted against α and spacing, s/D_p, for the three adopted n values.

Table 7.5 – Pile group factors, K_{pg}

n	s/D_p	$\alpha = 0^o$	$\alpha = 15^o$	$\alpha = 30^o$	$\alpha = 45^o$	$\alpha = 90^o$
	1.0	1.13	1.15	1.81	2.33	2.61
	2.0	1.18	1.12	1.78	1.29	1.40
1	3.0	1.12	1.19	1.56	1.15	1.29
	4.5	1.10	1.35	1.46	1.16	1.17
	6.0	1.00	1.25	1.30	1.06	0.94
	1.0	1.92	2.20	2.33	2.47	2.71
	2.0	1.36	1.76	2.44	1.90	1.56
2	3.0	1.35	1.35	2.04	1.80	1.39
	4.5	1.08	1.51	1.60	1.39	1.31
	6.0	1.15	1.51	1.47	1.30	1.04
	1.0	2.41	2.46	2.55	2.65	2.42
	2.0	1.56	2.25	2.78	2.42	1.87
3	3.0	1.53	1.84	2.06	2.05	1.37
	4.5	1.60	1.53	1.75	1.34	1.11
	6.0	1.03	1.26	1.68	1.18	1.07

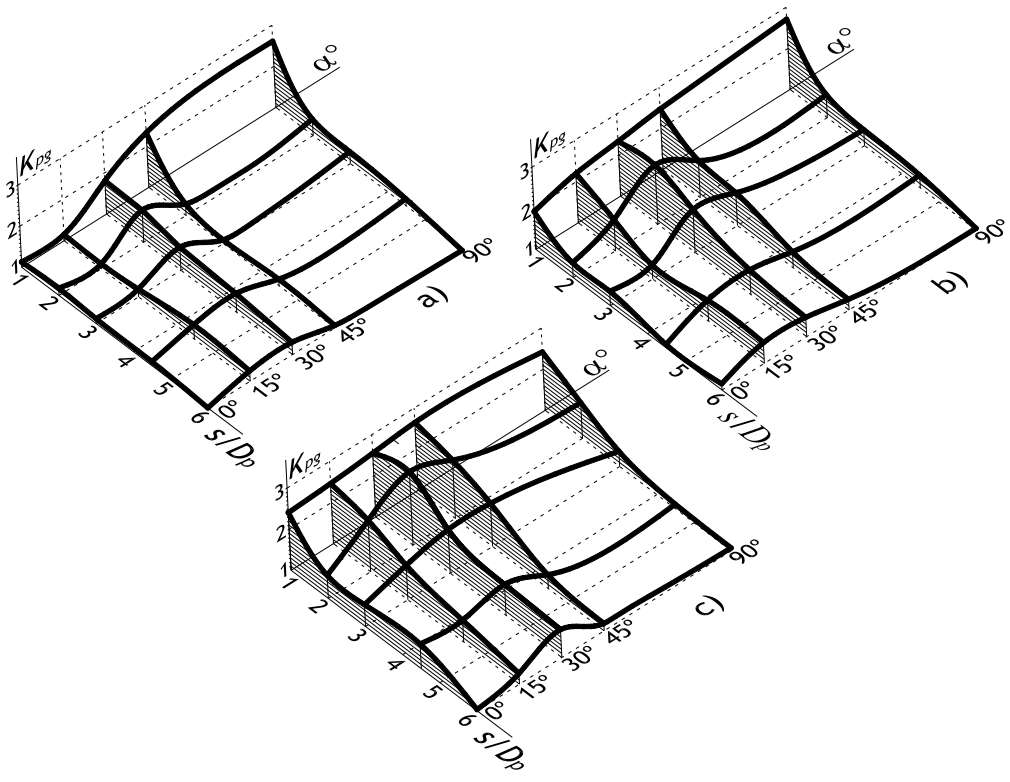

Figure 7.5 – Variation of K_{pg} with s/D_p and α for a) $n = 1$; b) $n = 2$; c) $n = 3$

Referring to n = 1 (pier alignment), the joint observation of Figure 7.2, Table 7.5 and Figure 7.5.a, shows that, for α = 0º, the deepest scour hole is always observed at the pier 1.1 (see Figure 7.2). The maximum scour depth leads to $K_{pg} \approx 1.15$ (see Table 7.5) for s/D_p = [1, 2, 3, 4.5], possibly due to the phenomenon of scour reinforcement; the pile group factor decreases to 1.0 for s/D_p = 6. For the same case (n = 1), α = 15º, the values of K_{pg} are not significantly different from those observed for α = 0º, conflicting with intuition and some findings reported in the literature (*e.g.* Zhao and Sheppard 1999). For the other skew-angles, α = [30º, 45º, 90º], still for n = 1, scour depth systematically decreases with s/D_p. Nevertheless, for s/D_p = 6, n = 1, scour depth shows a weak dependence on α; yet, K_{pg} values of the order of 1.25 ~ 1.30 were observed for α = [15º, 30º]. With the exception of s/D_p = 1, the deepest scour holes observed for n = 1 occur for {α = 30º, s/D_p = [2, 3]}; in these cases, $K_{pg} \approx 1.7$, while it slightly decreases to 1.3 for s/D_p = 6. For [α = 45º, n = 1], $K_{pg} \approx 2.3$ as s/D_p = 1 and clearly decreases with s/D_p, becoming $K_{pg} \approx 1.3$ for s/D_p = 2. For α = 90º, n = 1, and s/D_p = 1, the alignment acts as a single pier with one single horse-shoe vortex; the scour depth is the greatest; for s/D_p = 2, different horse-shoe vortices are believed to be present, the corresponding arms being compressed by the flow acceleration in the space between the piers. With the increase of s/D_p, this group effect tends to vanish and each pier in the alignment α = 90º tends to behave as a single one: the values of K_{pg} for α = 90º are $K_{pg} \approx$ [2.6, 1.4, 1.3, 1,0] for s/D_p = [1, 2, 3, 6], respectively.

Qualitatively, the overall variation of K_{pg} with α and s/D_p for n = [2, 3] does not significantly differ from the variation described for n = 1. However, the detailed analysis of Table 7.5 and Figures 7.5.b and 7.5.c, shows that, with one single exception [α = 0º, s/D_p = 4.5], the values of K_{pg} are systematically higher for n = 2 than for n = 1. This increase is confirmed for n = 3 (as compared with n = 2) for s/D_p = [2, 3], while a decreasing trend is identified for s/D_p = 6 (excluding α = 30º). Except for {α = 30º, s/D_p = 2, n = [2, 3]}, the maximum scour depth is observed for s/D_p = 1 as soon as α > 15º, irrespective of n. The scour depth and the pile group factor K_{pg} significantly increase for small spacing and α = [0º, 15º] as n increases. It can also be remarked that, for n = 3, K_{pg} is clearly higher if α = 0º and $s/D_p \leq 4.5$ than it is for n = [1, 2].

In view of the experimental evidence described above, the following equation was derived for practical engineering applications:

$$K_{pg} = \beta \left(\frac{s}{D_p} \right)^{\gamma} n^{\delta} \Bigg|_{\alpha = \text{const.}} \tag{7.6}$$

the values of β, γ and δ being those obtained through regression analysis for each α value. They are included in Table 7.6, together with the determination coefficient, r^2.

Table 7.6 – Coefficients β, γ and δ for different skew-angles

angle α	0º	15º	30º	45º	90º
β	1.412	1.509	1.994	2.083	2.460
γ	-0.295	-0.234	-0.234	-0.407	-0.538
δ	0.389	0.425	0.292	0.284	0.041
r^2	0.81	0.77	0.81	0.90	0.94

Assuming that, instead of d_{se1}, the scaling length that best accounts for the scouring process at pile groups is the equilibrium scour depth, d_{sew}, at an isolated cylindrical pier of diameter W_g, Equation 7.4 reads:

$$K_{pgw} = \frac{d_{sge}}{d_{sew}} = \varphi\left(\frac{s}{D_p}; \alpha; m; n\right) \tag{7.7}$$

where K_{pgw} is the pile group factor associated with W_g. In this study, it was possible to obtain the empirical values of d_{sew} from the equilibrium scour depth measured at the reference cylindrical piers, D_p = [50, 100, 150, 200, 400] mm. The variation of K_{pgw} with s/D_p, α and n, for m = 4, may be described by an equation structurally similar to Equation 7.6, where the coefficients β_w, γ_w and δ_w are those included in Table 7.7.

Table 7.7 – Coefficients β_w, γ_w and δ_w for different skew-angles

angle α	0º	15º	30º	45º	90º
β	1.302	0.967	1.099	1.069	1.110
γ	-0.231	-0.449	-0.390	-0.514	-0.538
δ	-0.161	0.155	0.043	0.100	0.042
r^2	0.67	0.85	0.96	0.91	0.94

From the values of the determination coefficient, r^2, a slightly improved representation of the scour data through the formulation behind Equation 7.7 seems to be achieved as compared with Equation 7.6, the only exception corresponding to α = 0º. Though based on a large and robust data set and established for the most unfavorable scour conditions, it should be stressed that Equations 7.6 and 7.7 are strictly limited to the case where m = 4; they may be used, alternatively, to extend the scope of precise predictors of scour depth at single piers to the prediction of scour at pile groups.

7.3.5 Further discussion

Irrespective of the number of columns in the group, collapsed pile groups defined by s/D_p = 1 may be assumed to behave as single rectangular piers with rounded-corners as sketched in Figure 7.6 (dashed perimeter). The associated ratios of the equivalent pier length, L, to width, a, are, L/a = [4, 2, 4/3], for n = [1, 2, 3], respectively, as soon as $\alpha \leq$ 45º. For α = 90º, L and a may be

interchanged, the ratio L/a becoming L/a = [1/4, 1/2, 3/4], which corresponds to assume m = 3, n = 4 and α = 0º (see Figure 7.1).

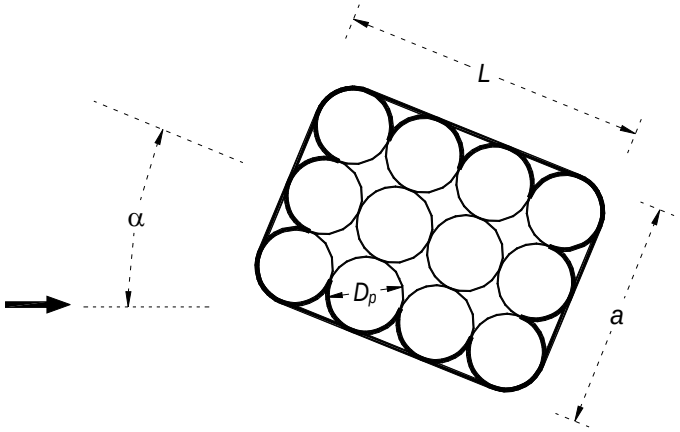

Figure 7.6 – Pile group idealized as a pier for s/D_p = 1

The idea behind Figure 7.6 was first suggested by Salim and Jones (1996). According to these authors, the scour depth at pile groups composed of square piles is equal to the scour depth at single rectangular solid piers whose dimensions are the sum of the dimensions of the individual piles. According to this idea, the following equation may be assumed to hold:

$$d_{sge} = K_\alpha K_s d_{se} \tag{7.8}$$

where K_α = skew-angle coefficient, K_s = shape coefficient of the idealized pier and d_{se} = equilibrium scour depth at the reference cylindrical pier defined by $D_p = a$, for α = 0º and $D_p = L$ for α = 90º.

For n = [1, 2, 3] and $\alpha \leq$ 45º, pier dimensions are L = 0.20 m and a = [0.050, 0.100, 0.150] m, respectively; for α = 90º, a = 0.200 m and L = [0.05, 0.100, 0.150] as n = [1, 2, 3]. The equilibrium scour depth measured at the reference cylindrical piers, D_p = [50, 100, 150, 200] mm was d_{se} = [0.136, 0.218, 0.252, 0.297] m, leading to d_{se}/D_p = [2.72, 2.18, 1.68, 1.48]. The value of the normalized scour depth for D_p = 50 mm exceeds 2.4, the classical value suggested by authors such as Melville and Coleman (2000). This is possibly imputable to the long duration of the present tests as well as to the improved assessment of the equilibrium scour depth resulting from the extrapolation of the scour records to $t = \infty$. The decreasing ratios of d_{se}/D_p are certainly due to the decrease of d/D_p (since d was kept equal to 0.20 m) but may also be associated with the increase of D_p/D_{50}.

The ratios of the equilibrium scour depth at pile groups defined by s/D_p = 1 and α = [0º, 90º] to those of isolated equal-width piers led to the K_s values included in Table 7.8. They are of the same order of magnitude as those suggested, for instance, by Melville and Coleman (2000) (K_s =

1.1), though slightly higher. This small increase is ascribable to the lateral recesses of the collapsed "pier" that influence the detachment of erosive wake vortices.

Table 7.8 – Shape coeficients of the idealized single piers defined for $s/D_p = 1$

α (º)	a (m)	L (m)	K_s
0	0.050	0.200	1.13
0	0.100	0.200	1.20
0	0.150	0.200	1.30
90	0.200	0.050	1.19
90	0.200	0.100	1.24
90	0.200	0.150	1.10

The K_α values plotted against α for each n in Figure 7.7 where obtained by dividing the equilibrium scour depth at the pile groups defined by $\alpha \neq [0º, 90º]$ by the values of K_s included in Table 7.8 and, then, by the values of d_{se} at the equal width cylindrical pier. Figure 7.7 shows that K_α depends on the number of columns, n, *i.e*, on the ratio L/a. For $\alpha > 15º$, K_α decreases as n increases, reflecting the tendency for the pile group to approach the cylindrical shape, this way becoming less dependent on the orientation relative to the flow direction.

Compared with the values of K_α suggested by, *e.g.*, Melville and Coleman (2000) or Richardson and Davis (2001) for solid rectangular piers, those plotted in Figure 7.7 are slightly smaller for $L/a = 4$, particularly for $\alpha = 15º$, but they are practically the same for $L/a = 2$. The deviations are within common experimental scatter.

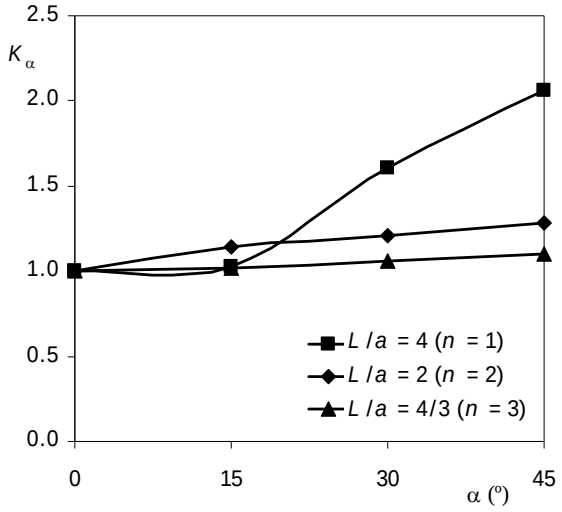

Figure 7.7 – Variation of angle factor, K_α, with α and n.

In view of the quality of the present data set, the applicability of two current engineering methods used to calculate the scour depth at pile groups – those of Richardson and Davis (2001) and Sheppard and Renna (2010) – was assessed. Their predictions are compared with the measurements in Figure 7.8. The most obvious conclusion is that both methods may

underestimate the scour depth. The predictions of Sheppard and Renna (2010) are scattered around the line of perfect agreement within a band defined by – 20% and + 40%. Increasing the scour predictions by a factor of 1.2 seems enough to reproduce the lower bound of the scour depths measured in this study.

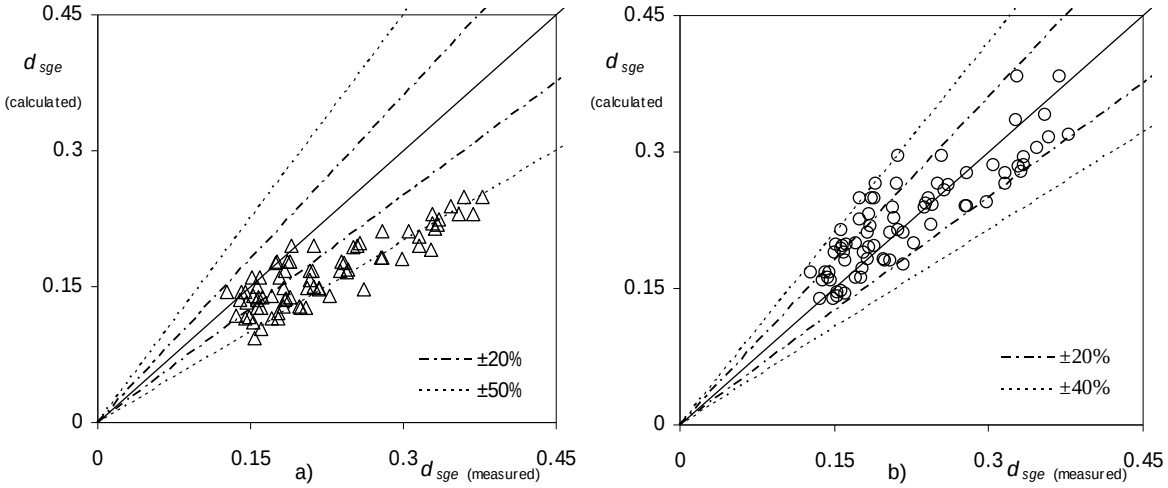

Figure 7.8 – Measured *vs.* calculated scour depths: a) through the method of Richardson and Davis (2001); b) through the method of Sheppard and Renna (2010)

On the contrary, the predictions of Richardson and Davis (2001) almost systematically underestimate the scour depth; in many cases, the underestimation is more than 50%. The possible sources for this discrepancy are discussed next. For partly submerged pile groups built of cylindrical piles inserted in uniform sand in the absence of bed-forms, the predictor of Richardson and Davis (2001) reads:

$$\frac{d_{sge}}{d} = 2 \times 1.1 \left(\frac{D_{pg}}{d} \right)^{0.65} F_r^{0.43} \tag{7.9}$$

where D_{pg} = effective diameter of the equivalent solid pier and $F_r = U/(gd)^{0.5}$ = approach flow Froude number. According to Richardson and Davis (2001), the effective diameter, D_{pg}, is in turn given by

$$D_{pg} = K_{sp} K_m W_g \tag{7.10}$$

with K_{sp} = coefficient for pile spacing and K_m = coefficient for the number of aligned rows. Those authors offer predictors for K_{sp} and K_m.

The inversion of Equation 7.9 allowed a back calculation of the values of D_{pg} corresponding to the observed d_{sge}. For α = 0º and n = 1, the method predicts K_{sp} = 1 and D_{pg} becomes $D_{pg} = K_m D_p$ (since $W_g = D_p$). The values of K_m back calculated from tests 1 to 6 using this method are 1.44 to

2.51 times those directly calculated through the predictor suggested by Richardson and Davis (2001). From the entire data set, it was also concluded that the ratio between the product $K_{sp}K_m$ back calculated from the measured scour depths is 1.85 ± 0.42 times those directly calculated through the predictors; this ratio varies between 1.04 and 2.85. This fact raises the question whether the discrepancies are the result of inappropriate predictors of K_{sp} and K_m or the result of a wrong scour predictor itself (Equation 7.9) or both. The application of Equation 7.9 to the prediction of maximum scour depth at the five single cylindrical piers tested in the present work, produced d_{se} = [0.093, 0.147, 0.191, 0.230, 0.361] m for D_p = [50, 100, 150, 200, 400] mm, respectively, while the observed scour values where [0.136, 0.218, 0.252, 0.297, 0.402] m, *i.e.*, [1.46, 1.48, 1.32, 1.29, 1.11] times deeper. These values show that on top of the discrepancies due to K_m, part of the under-prediction is ascribable to the basic scour equation while there is no direct evidence on the performance of the predictor K_{sp}. Yet, since this is the same in both assessed methods and the method of Sheppard and Renna (2010) reasonably reproduces the measurements, this may be interpreted as an indication that K_{sp} is properly predicted.

7.4 CONCLUSIONS

The present study focus on the effect of pile spacing, skew-angle and number of columns of the pile group on the maximum scour depth at pile groups composed of cylindrical piles inserted in uniform, fully-developed turbulent flows in wide rectangular channels with flat bed composed of uniform, non-ripple forming sand. The effect of time on scouring at pile groups is also investigated. It was shown that scour experiments at pile groups lasting less than 7 days may implicitly contain important uncertainties on the equilibrium scour depth. However, in spite of the short durations of the previous studies and the inherent deviations from equilibrium scour, it would seem that coefficients such as the pile spacing coefficient or the coefficient for the number of aligned rows may be reliable, since the scour depth at pile groups remain essentially self-similar in time.

With the exception of s/D_p = 1 (collapsed pile group), the maximum scour depth occurs for α = 30º. For this configuration (α = 30º) the maxima scour depths tend to occur at the rear piles of the first column, which may be interpreted as an indication that such piles are located in the path of the most energetic wake vortices generated upstream. Collapsed pile groups tend to behave as single piers whose dimensions are the sum of the dimensions of the individual piles, reiterating the suggestion of Salim and Jones (1996). Pier alignments, defined by n = 1, tend to behave as single piers for $s/D_p \geq 6$, except for α = [15º, 30º], where scour reinforcement is observed.

Safe predictions of the pile group factor, defined as the ratio between the maximum scour depth at a pile group and the maximum scour depth at an isolated elemental cylindrical pier under the same hydrodynamic conditions, can be obtained using Equation 7.6, which may be useful in practice if a precise predictor of scour at an isolated single pier is applied. Equation 7.7,

constitutes an alternative to Equation 7.6, in which case the scaling depth is the equilibrium scour depth at a cylindrical pier whose diameter is W_g, *i.e.*, the sum of the non-overlapping pier-widths projected in a plane normal to the approach flow.

The methods of Richardson and Davis (2001) and Sheppard and Renna (2010) may both under-predict the scour depth at pile groups. However, a multiplying factor of $\approx$1.2 applied to the predictions of Sheppard and Renna (2010) seems enough to reproduce the lower bound of measured scour depths. The deviations are much more serious in regard to the method of Richardson and Davis (2001), where a large number of measurements exceed predictions by more than 50%. This deviation seems induced by the predictor of scour depth at single piers as well as by the predictor of the coefficient for the number of aligned rows, K_m.

8. EFFECT OF VISCOSITY ON THE EQUILIBRIUM SCOUR DEPTH AT SINGLE CYLINDRICAL PIERS

8.1 Introduction

Equilibrium scour depth around cylindrical piers inserted in uniform, fully developed flows, in wide rectangular channels whose bed is composed of uniform, non-ripple-forming sand may be described by the equation (Fael 2007):

$$\frac{d_{se}}{D_p} = \varphi\left(\frac{d}{D_p}, \frac{U}{U_c}, \frac{u_* D_{50}}{\nu}, \frac{D_p}{D_{50}}\right) \tag{8.1}$$

where φ stands for function, d_{se} = equilibrium scour depth, D_p = pier diameter, d = depth of the undisturbed approach flow, U = average velocity of the undisturbed approach flow, U_c = approach flow velocity for the threshold condition of sediment entrainment, u_* = bed shear velocity, D_{50} = sediment size, ν = fluid kinematic viscosity. Herein, $u_* D_{50}/\nu = Re_s$ = shear Reynolds number. It should be noted that fully developed flows, necessarily self-similar along the main flow direction, are not necessarily fully rough; wide channels are those where wall effects as well as the effect of flow contraction due to the presence of piers are negligible; uniform, non-ripple-forming sand is defined by $\rho_s \approx 2660$ kgm^{-3}, $D_{50} > \approx 0.6$ mm and $\sigma_D < 1.5$. Here, ρ_s = sand density and σ_D = gradation coefficient of the sand.

For U/U_c = constant and d/D_p = constant, the non-dimensional equilibrium scour depth reads:

$$\frac{d_{se}}{D_p} = \varphi\left(\frac{u_* D_{50}}{\nu}, \frac{D_p}{D_{50}}\right) \tag{8.2}$$

Replacing u_* by U (which is valid for fully developed flow on flat bed), Equation (8.2) may assume the following equivalent forms:

$$\frac{d_{se}}{D_p} = \varphi\left(\frac{U D_{50}}{\nu}, \frac{D_p}{D_{50}}\right) \tag{8.3}$$

or

$$\frac{d_{se}}{D_p} = \varphi\left(\frac{UD_p}{\nu}, \frac{D_p}{D_{50}}\right) \tag{8.4}$$

where $UD_{50}/\nu = Re_U$ = approach velocity sediment Reynolds number and $UD_p/\nu = Re_p$ = pier Reynolds number. It is widely recognized that the condition $U/U_c \approx 1.0$ maximizes the equilibrium scour depth, d_{se}, and that, for $d/D_p > \approx 2.0$, d_{se} is also maximal and no longer significantly depends on d/D_p.

The pioneering research works of Shen *et al.* (1966) and Nicollet and Ramette (1971) indicate that viscosity may affect d_{se}, corroborating the pertinence of the previous equations. Indeed, according to Shen *et al.* (1969), d_{se} depends on the pier Reynolds number, $Re_p = UD_p/\nu$, since the horse-shoe vortex is the principal agent of the scouring process and the size of this vortical flow structure depends on Re_p. Nicollet and Ramette (1971) characterized Equation (8.3) on the basis of experimental evidence: they have concluded that the equilibrium scour depth depends on $Re_U = UD_{50}/\nu$ (see Equation (8.3)), for $Re_U < \sim 10^4$ if $D_p/D_{50} < \sim 200$, while for values of $D_p/D_{50} > \sim 200$, the above limit of Re_U increases. Coleman (1971) has reported that d_{se} is independent from Re_p for $Re_p > 10^4$ and while Monti (1994) suggested that the scouring process is free of viscous effects if Re_p is over 7000.

In spite of the mentioned contributions, important studies on scouring may have overlooked the effect of viscosity (*e.g.* Jain and Fisher 1980; Ettema *et al.* 1998; Melville and Coleman 2000; Oliveto and Hager 2002; Sheppard *et al.* 2004; Cardoso and Fael 2010; Sheppard and Renna 2010). The assumption seem to be that the flow is fully rough inside the scour hole, *i.e.*, free of viscous effects, due to the presence of highly turbulent flows structures such as down-flow, horse-shoe vortex and wake vortices irrespective of the approach flow regime.

In the attempt to define the conditions for fully rough approach flow and, consequently, to define the sufficient conditions for the scouring process to become free of viscous effects, Oliveto and Hager (2002) have suggested that the approach flow must be such that: *i*) $k/d > \approx 0.002$; *ii*) $D_{50} > 0.4 - 0.8$ mm. Here, k = equivalent sand roughness of Nikuradse, frequently accepted to be slightly higher than D_{50}. According to the Shields diagram, the second condition seems rather permissive since it renders values of $Re_s = u_* D_{50}/\nu \approx 15$ at the threshold condition of sediment entrainment for D_{50} = 0.8 mm; for such value of Re_s, the flow is clearly transitional, still conveying viscous effects.

This chapter reports the results of the experiments conceived to revisit the effect of viscosity on scouring. Bearing in mind that the Shields diagram defines fully rough flow for $Re_s = u_* D_{50}/\nu > 70 - 400$, a set of five experiments were performed by varying Re_s between ≈ 12.0 and ≈ 105.6. The lower value is clearly transitional flow while the upper value falls in the border between transitional and fully rough flow. Three experiments were performed for d/D_p = 1.00 and another

two for d/D_p = 1.5 by keeping constant the remaining non-dimensional parameters of Equation (8.1). The variation of Re_s was achieved by choosing different sands, which led to different values of U_c, U, D_p and d, *i.e*, to different values of any form of Reynolds number (Re_s, Re_p, Re_U or simply $Re = Ud/\nu$ = common approach flow Reynolds number). This set of experiments will be completed by running the third experiment for d/D_p = 1.5, another two for a new sand characterized by $D_{50} \approx$ 2.0 mm and, finally, two full scale experiments. At that stage, this (revised) chapter will be converted into a technical note to be submited to a prestigious international journal.

8.2 Experiments

Experiments were carried out in a 28.0 m long, 4.00 m wide and 1.00 m deep concrete flume. This flume included a closed hydraulic circuit whose maximum flow discharge was 270 ls^{-1}. Discharge was measured by an electromagnetic flow meter installed in the circuit to an accuracy of ± 0.5% of full scale. Depending on the experiment, the flume was narrowed to 2.00 m or 1.50 m in order to guarantee combinations of sufficiently high average approach flow velocity and flow depth. At the entrance of the flume, two honeycomb diffusers aligned with the main flow direction smoothed the flow trajectories and promoted a uniform transversal flow distribution. The central reach of the flume, starting at 13.90 m from the entrance, included a 3.00 m long, 2.00 m wide and 0.60 m deep recess box in the bed. At the downstream end of the flume, a tailgate allowed the regulation of the water depth. At the end of the flume the water fell into a 100 m^3 reservoir, where the hydraulic circuit started.

Single cylindrical piers were simulated by PVC pipes defined by D_p = [50, 75, 175] mm. The piers were placed at ~1.0 m from the upstream boundary of the bed recess box. Each couple of experiments, corresponding to the two adopted relative flow depths, d/D_p = [1.0, 1.5], was run with a different uniform quartz sand, ρ_s = 2660 kgm^{-3}, placed within the bed recess box: sand 1 (D_{50} = 0.86 mm; σ_D = 1.36) for D_p = 50 mm; sand 2 (D_{50} = 1.28 mm; σ_D = 1.50) for D_p = 75 mm; sand 3 (D_{50} = 3.00 mm; σ_D = 1.36) for D_p = 175 mm.

Prior to each experiment, the sand bed was perfectly leveled. The area located around the pier was covered with a thin metallic plate to avoid uncontrolled scour at the beginning of each experiment. The flume was filled gradually through a small hydraulic circuit, imposing a high water depth and low flow velocity. The discharge corresponding to the chosen approach flow velocity was then passed through the flume. The flow depth was regulated by adjusting the downstream tailgate. Once the discharge and flow depth were established, the metallic plate was removed and the experiment started.

Scour immediately initiated and the depth of scour hole was measured, to an accuracy of ±1 mm, with one adapted point gauge, approximately every 10 minutes during the first hour. Afterwards, the interval between measurements increased and, after the first day, a few

measurements were carried out per day. When the scour rate was less than approximately 2 mm ($\approx 2D_{50}$) in 24 hours and at least 7 days had passed, the experiments were stopped.

The sand bed approach reach located upstream of the piers stayed undisturbed through the entire duration of the experiments; this long term stability ensured that the scour depth was not supplemented by upstream bed degradation.

8.3 Results and discussion

The values of the most important control variables and non-dimensional parameters characterizing the experiments are summarized in Tables 8.1 and 8.2. Table 8.1 include the flume width, B, sediment size, D_{50}, pier diameter, D_p, flow depth, d, relative flow depth, d/D_p, relative sediment size, D_p/D_{50}, average approach flow velocity for the threshold condition of sediment entrainment, U_c, flow-discharge, Q, average approach flow velocity, U, the ratios B/d and B/D_p and the approach flow bed shear velocity, u_*.

The bed shear velocity, u_*, was obtained trough the equation

$$\frac{U}{u_*} = 5.75 \log\left(\frac{12.27 R \chi}{k}\right) \tag{8.5}$$

valid for transition and rough flows, where: χ = parameter function of k/δ', suggested by Einstein (1950), R = hydraulic radius and δ' = thickness of the viscous sub-layer.

Table 8.1 – Control variables and non-dimensional parameters of the tests

Test	B (m)	D_{50} (mm)	D_p (m)	d (m)	d/D_p	D_p/D_{50}	U_c (ms^{-1})	Q (ls^{-1})	U (ms^{-1})	B/d	B/D_p	u_* (ms^{-1})
1	2.00	0.86	0.050	0.050	1.0	58.1	0.281	27	0.272	40.0	40.0	0.0162
2	2.00	0.86	0.050	0.075	1.5	58.1	0.293	43	0.284	26.7	40.0	0.0159
3	4.00	1.28	0.075	0.075	1.0	58.6	0.343	100	0.333	53.3	53.3	0.0197
4	1.50	3.00	0.175	0.175	1.0	58.3	0.525	134	0.509	8.6	8.6	0.0325
5	1.50	3.00	0.175	0.263	1.5	58.3	0.547	209	0.530	5.7	8.6	0.0322

From Table 8.1, it can be concluded that reasonably high flow depth (0.050 m $\leq d \leq$ 0.263 m) was always guaranteed. The average flow velocity, U, was U/U_c = 0.97 in all cases, U_c being calculated through the predictor of Neil (1967). D_p/D_{50} was $\approx$ 58, practically maximizing the effect of the relative sediment size on d_{se}; σ_D was smaller than 1.5 in all cases. The aspect ratio was chosen to be $B/d \geq 5.7$, this way avoiding significant wall effects on the flow field. The ratio of channel width to pier diameter, B/D_p, was at least 8.6 and was observed to guarantee that scour holes never reached the lateral walls of the flume.

Table 8.2 includes the water temperature, T, water kinematic viscosity, ν, all forms of Reynolds number (Re_s, Re_U, Re_p, Re), equilibrium scour depth, d_{se}, and equilibrium scour depth normalized by the pier diameter, d_{se}/D_p. Since the experiments lasted more than 7 days, the equilibrium scour depth, d_{se}, was obtained by extrapolating the scour depth time records to $t = \infty$ through a six parameters polynomial function, as suggested by Lança *et al.* (2010).

The water temperature was not measured during experiments 1 and 2. Since these experiments were run during a period where the water temperature has statistically varied between 15º and 20º in the past, the kinematic viscosity of the water is assumed to vary accordingly. In these cases, the included values of Reynolds numbers refer to T = 17.5 ºC.

Table 8.2 – Temperature, equilibrium scour depth and derived non-dimensional parameters

Test	T (ºC)	ν (10^{-6}m^{2}s^{-1})	u_*D_{50}/ν	UD_{50}/ν	UD_p/ν	Ud/ν	d_{se} (m)	d_{se}/D_p
1	15 – 20	1.156 – 1.004	12.9	217	12615	12615	0.116	2.31
2	15 – 20	1.156 – 1.004	12.7	226	13137	19705	0.119	2.38
3	18	1.065	23.7	400	23437	23437	0.167	2.23
4	24	0.923	105.6	1655	96541	96541	0.296	1.69
5	24	0.923	104.7	1723	100536	150804	0.324	1.85

Assuming $k \approx D_{50}$, the ratio k/d was [0.011, 0.017] for d/D_p = [1.5, 1.0], respectively. Since these values are higher than 0.002, condition *i)* of Oliveto and Hager (2002) was fulfilled; the second condition was also fulfilled since D_{50} was always D_{50} > 8 mm. However, the shear Reynolds number, $Re_s = u_*D_{50}/\nu$, varied in the range $12.9 \le Re_s \le 105.6$, which is not sufficiently high to unquestionably guarantee fully rough approach flow. From this assessment, it seems reasonable to conclude that viscous effects cannot be excluded *a priori*, at least in experiments 1, 2 and 3. They seem indeed be present as, according to Figure 8.1, where d_{se}/D_p is plotted against a) Re_s, b) Re_U, c) Re_p and d) Re the non-dimensional scour depth does not remain constant as it should be if viscosity played no role in the scouring process.

It is also clear that the non-dimensional scour depth decreases with all forms of the Reynolds number, which may be interpreted as if usual laboratory experiments — where viscous effects may be expected — rendered excessive scour depths as compared to non-viscous natural situations. However, this conclusion needs to be confirmed after the two full scale experiments are run.

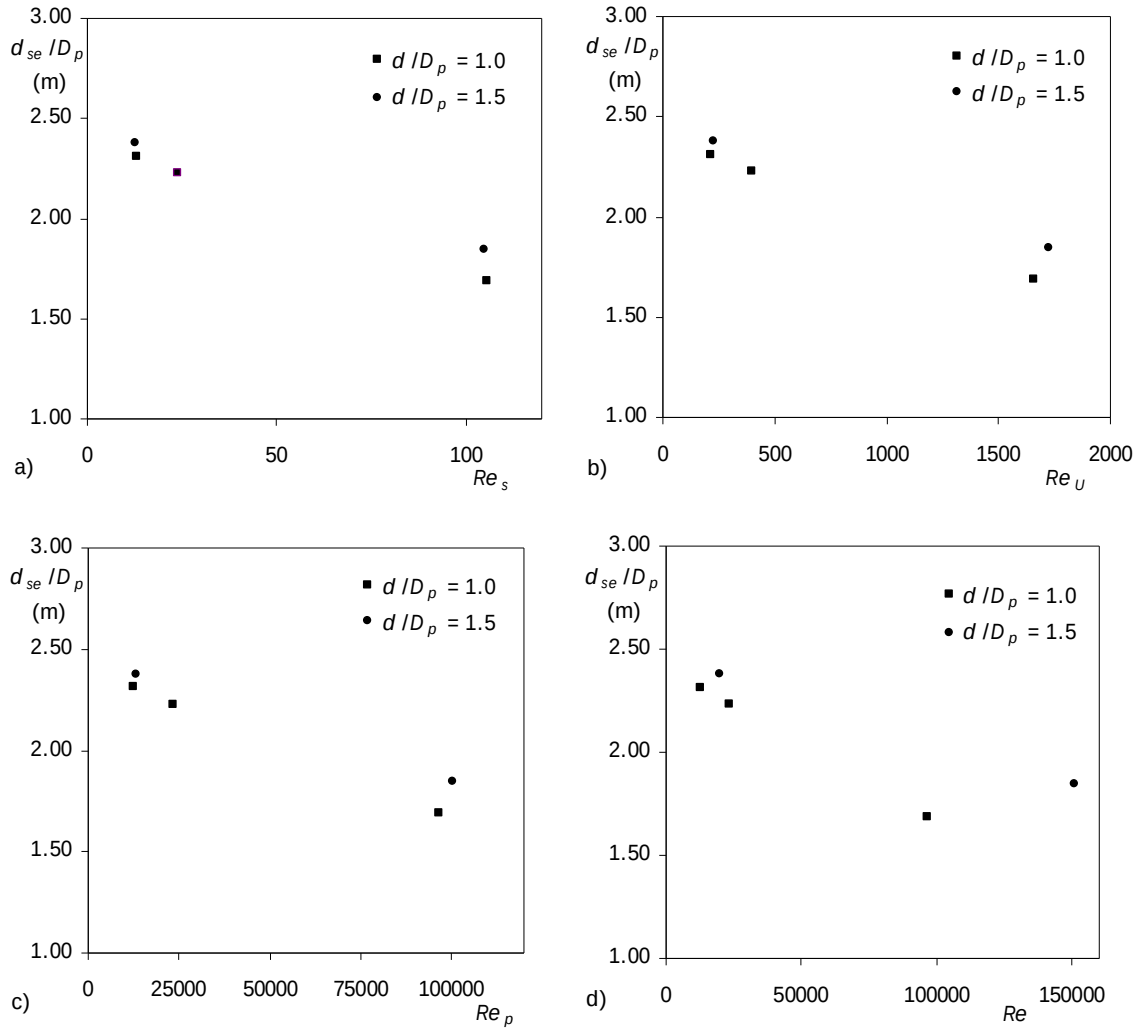

Figure 8.1 – Variation of d_{se}/D_p with a) Re_s; b) Re_U; c) Re_p; d) Re

8.4 Conclusions

From the previous discussion, the following conclusions can be drawn:

i) Viscosity affects the equilibrium scour depth for small values of Re.

ii) The equilibrium scour depth decreases as Re_s increases, corroborating the findings of Shen *et al.* (1969) and Nicollet and Ramette (1971).

iii) Comparatively small values of Re_s tend to maximize d_{se}/D_p, leading to safe (through un-economic) predictors of scour depth.

9. CONCLUSIONS AND FUTURE WORK

9.1 Conclusions

The contribution of this study to the understanding and characterization of scouring at single cylindrical piers and pile groups lies on the following achievements:

Concerning the pertinence of existing approaches to assess the onset of the equilibrium phase of scour at single cylindrical piers in experimental studies, it was concluded that:

i) Scour experiments at single cylindrical piers, run for up to ~46 days, did not unambiguously reach equilibrium, with special emphasis in the tests with the finer sand;

ii) Common methods used in practice to decide on the initiation of the equilibrium phase may be rather erroneous.

iii) Known predictors of time to equilibrium may lead to significantly wrong predictions of equilibrium scour depth.

iv) Typically 7 days long scour-depth records adjusted though Equation (4.2) and extrapolated to infinite time seem to render robust vales of the equilibrium scour depth at single cylindrical piers.

On the influence of the relative sediment size and flow shallowness on scouring at single cylindrical piers inserted in uniform, fully-developed turbulent flows in wide rectangular channels with flat bed composed of uniform, non-ripple sand, flow intensity $U/U_c \approx 1.0$, $58 \leq D_p/D_{50} \leq 465$ and $0.50 \leq d/D_p \leq 5.0$, it was concluded that:

i) The equilibrium scour depth decreases with the increase of D_p/D_{50}, for $D_p/D_{50} > \sim 100$, corroborating the findings of Sheppard *et al.* (1995, 1999, 2004) and Lee and Sturm (2009), which implies refuting the classical assumption according to which the equilibrium scour depth would not depend on D_p/D_{50} for $D_p/D_{50} > \sim 25$.

ii) A good predictor of the sediment size factor, K_{D50}, is given by Equation (5.13).

iii) Safe predictions of the equilibrium scour depth may be obtained through Equation (5.11), valid for cylindrical piers.

iv) The exponential model of Franzetti *et al.* (1982), Equation (5.4), properly describes the time evolution of scour depth as soon as its coefficients a_1 and a_2 are specified through Equation (5.14) and Equation (5.15), respectively.

Concerning the characterization of the effect of spacing, skew-angle and time on the maximum scour depth at alignments composed of four cylindrical piers, it was concluded that:

i) For α = [30º; 45º; 90º], the scour depth systematically decreases with s/D_p, while for α = [0º, 15º] the scour depth is approximately constant irrespective of the value of s/D_p.

ii) For s/D_p = 1, the pier alignment can be treated as a single round-nose rectangular pier whose cross-section is defined as the envelope of the adjacent piers.

iii) Excluding s/D_p = 1 the maximum scour depth occurs for α = 30º and s/D_p = [2; 3], where $d_{sepg}/d_{se1} \approx 1.7$.

iv) Common methods applied in engineering practice to predict scour depth at pier alignments may provide under predictions of the order of up to 40%.

On the characterization of the effect of pile spacing, skew-angle, time and number of pile group columns on the maximum scour depth at pile groups composed of four cylindrical pile rows, it was concluded that:

i) Scour experiments at pile groups lasting less than 7 days may implicitly contain important uncertainties on the equilibrium scour depth.

ii) In spite of the short durations of the previous studies and the inherent deviations from equilibrium scour, it would seem that coefficients such as the pile spacing coefficient or the coefficient for the number of aligned rows may be reliable, since the scour depth at pile groups remain essentially self-similar in time.

iii) With the exception of s/D_p = 1 (collapsed pile group), the maximum scour depth occurs for α = 30º. For this configuration (α = 30º) the maxima scour depths tend to occur at the rear piles of the first column, which may be interpreted as an indication that such piles are located in the path of the most energetic wake vortices generated upstream.

iv) Collapsed pile groups tend to behave as single piers whose dimensions are the sum of the dimensions of the individual piles, reiterating the suggestion of Salim and Jones (1996).

v) Safe predictions of the pile group factor, defined as the ratio between the maximum scour depth at a pile group and the maximum scour depth at an isolated elemental cylindrical pier under the same hydrodynamic conditions, can be obtained using Equation (7.6), which may be useful in practice if a precise predictor of scour at an isolated single pier is applied.

vi) Equation (7.7), constitutes an alternative to Equation (7.6), in which case the scaling depth is the equilibrium scour depth at a cylindrical pier whose diameter is W_g, *i.e.*, the sum of the non-overlapping pier-widths projected in a plane normal to the approach flow.

vii) The methods of Richardson and Davis (2001) and Sheppard and Renna (2010) may both under-predict the scour depth at pile groups. However, a multiplying factor of $\approx$1.2 applied to the predictions of Sheppard and Renna (2010) seems enough to reproduce the lower bound of measured scour depths.

viii) The method of Richardson and Davis (2001) under predicts the measurements by more than 50%. This deviation seems induced by the predictor of scour depth at single piers as well as by the predictor of the coefficient for the number of aligned rows, K_m.

On the assessment of the effect of viscosity on the scouring process, it was concluded that:

i) Viscosity affects the equilibrium scour depth for small values of Re.

ii) The equilibrium scour depth decreases as Re_s increases, corroborating the findings of Shen *et al.* (1969) and Nicollet and Ramette (1971).

iii) Comparatively small values of Re_s tend to maximize d_{se}/D_p, leading to safe (through un-economic) predictors of scour depth.

9.2 Future work

From the knowledge obtained during this study, several research topics are suggested for future work in the domain of scouring at single cylindrical piers, pier alignments, pile groups and complex piers:

i) The conclusions about the effect of viscosity on equilibrium scour depth were based on few tests. More laboratory tests are required to corroborate these findings and suggest a factor to consider the effect of viscosity on the equilibrium scour depth.

ii) Suggest a predictor for the pile group equivalent diameter, using the scour depth time evolution data at single cylindrical piers and pile groups.

iii) Suggest a scour depth predictor valid for complex piers, using the results obtained in the present study for single cylindrical piers, pier alignments and pier groups jointly with data from tests at submerged pile groups, and complex piers.

Most of the existing knowledge about local scour derives from laboratory tests run in steady flow conditions. However many bridge piers are constructed in rivers estuaries or in lagoon channels where tidal flows act continuously. The high cost of such structures justifies the accurate prediction of the equilibrium scour depth based on predictors developed for such conditions. For this reason it is suggested the experimental characterization of the local scour at single cylindrical piers, pier alignments, pile groups and also complex piers for tidal flow conditions.

REFERENCES

Amini, A., Melville, B.W., Ali, T. M. and Ghazali, A. H. (2012). "Clear-water local scour around pile groups in shallow-water flow." *Journal of Hydraulic Engineering*, 138(2), 177 – 185.

Arnerson, L. A., Zevenbergen, L. W., Lagasse, P. F. and Clopper, P. E. (2012). "Evaluating scour at bridges." National Highway Institute, Arlington, VA.

Ataie-Ashtiani, B. and Beheshti, A. A. (2006). "Experimental investigation of clear-water local scour at pile groups." *Journal of Hydraulic Engineering*, 132(10), 1100 – 1104.

Ahmad, M. (1953). "Experiments on design and behaviour of spur dikes." *Proceedings of the International Hydraulic Convention*, Minneapolis, MN, 145 – 159.

Barkdoll, B.B. (2000). "Time scale for local scour at bridge piers." *Journal of Hydraulic Engineering*, 126(10), 793 – 794.

Bertoldi, D.A. and Jones, J.S. (1998). "Time to scour experiments as an indirect measure of stream power around bridge piers." *Proceedings of the International Water Resource Engineering Conference*, Memphis, TN, 264 – 269.

Breusers, H. N. C. and Raudkivi, A. (1991). "Scouring." A. A. Balkema. Rotterdam, The Netherlands.

Breusers, H. N. C., Nicollet, G. and Shen, H. W. (1977). "Local scour around cylindrical piers." *Journal of Hydraulic Research*, 15(3), 211 – 252.

Cardoso, A. H. and Bettess, R. (1999). "Effects of time and channel geometry on scour at bridge abutments." *Journal of Hydraulic Engineering*, 125(4), 388 – 399.

Cardoso, A. H. (1998). "Hidráulica fluvial". Fundação Calouste Gulbenkian, Lisboa, Portugal.

Cardoso, A. H. and Fael, C. M. S. (2010). "Time to equilibrium at vertical-wall bridge abutments." *Proceedings of the ICE – Water Management*,163(10), 509 – 513.

Chabert, J. and Engeldinger, P. (1956). "Etude des affouillements autour des piles des ponts." Laboratoire National d'Hydraulique, Chatou, France.

Chee R.K.W. (1982), "Live-Bed Scour at Bridge Sites." *Report No. 216*, University of AuckLand, Auckland, New Zealand.

Chitale, S. V. (1960). Discussion of "Scour at bridge crossing." by Laursen, E. M. , *Journal of the Hydraulic Division*, ASCE, 86(HY9), 137 – 142.

Coleman, N. L. (1971). "Analyzing laboratory measurements of scour at cylindrical piers in sand beds." *Proceedings 14th Congress*, IAHR, Paris, France, 307 – 313.

Coleman, S.E., Lauchlan, C.S. and Melville, B.W. (2003). "Clear-water scour development at bridge abutments." *Journal of Hydraulic Research*, 41(5), 521 – 531.

Cunha, L.V. (1972). "Erosões localizadas junto de obstáculos salientes de margens." *Memória nº 428*, Laboratório Nacional de Engenharia Civil, Lisboa, Portugal.

Dargahi, B. (1987) "Flow field and local scouring around a cylinder." *Bulletin TITRA–VBI–137*, Royal Institute of Technology, Stockholm, Sweden.

Dey S., Bose S. K. and Sastry G. L. N. (1992). "Clear water scour at circular piers, part I: Flow model." *Proceedings of 8th Congress of Asia and Pacific Division*, IAHR, Pune, India, Vol.3, 69 – 80.

Dey, S. and Raikar, R. V. (2007). "Characteristics of horseshoe vortex in developing scour holes at piers." *Journal of Hydraulic Engineering*, 133(4), 399 – 413.

Diab, R. (2011). "Experimental Investigation on scouring around piers of different shape and alignment in gravel." *PhD Thesis*, TU Darmstadt, Darmstadt, Deutschland.

Einstein, H. A. (1950). "The bed load function of the sediment transport in open channels." *Technical Bulletin 1026*, Soil Conservation Service, U.S. Department of Agriculture.

Elliott, K. R. and Baker, C. J. (1985). "Effect of pier spacing on scour around bridge piers." *Journal of Hydraulic Engineering*, 111(7), 1105 – 1109.

Ettema, R. (1980). "Scour at bridge piers." *Report No. 216*, University of Auckland, Auckland, New Zealand.

Ettema, R., Melville, B. W. and Barkdoll, B. (1998). "Scale effect in pier-scour experiments." *Journal of Hydraulic Engineering*, ASCE, 124(6), 639 – 642.

Fael, C. M. S. (2007). "Erosões localizadas junto de encontros de pontes e respectivas medidas de protecção." *PhD Thesis*, University of Beira Interior, Covilhã, Portugal.

Fael, C.M.S., Simarro-Grande, G., Martín-Vide J.P. and Cardoso, A.H. (2006). "Local scour at vertical-wall abutments under clear-water flow conditions." *Water Resources Research*, 42(W10408), 1 – 12.

Franzetti, S., Larcan, E. and Mignosa, P. (1982). "Influence of tests duration on the evaluation of ultimate scour around circular piers." *Proceedings of the International Conference on the Hydraulic Modelling of Civil Engineering Structures*, Coventry, England, 381 – 396.

Franzetti, S., Malavasi, S. and Piccinin, C. (1994). "Sull'erosione alla base delle pile di ponte in acque chiare." *Proceedings of XXIV Convegno di Idraulica e Costruzioni Idrauliche*, Napoli, Italy, II(T4), 13 – 24.

Gill, M.A. (1970). "Bed erosion around obstructions in rivers." *PhD Thesis*, University of London, London, United Kingdom.

Grimaldi, C. (2005). "Non-conventional countermeasures against local scouring at bridge piers." *PhD Thesis*, University of Calabria, Cosenza, Italy.

Hancu, S. (1971). "Sur le calcul des affouillements locaux dans la zone des piles des ponts." *Proceedings of the 14th IAHR Congress*, Paris, France, 299 – 313.

Hannah, C. R. (1978). "Scour at pile groups." Report No. 78–3, *M.S. Thesis*, University of Canterbury, Christchurch, New Zealand.

Hjorth, P. (1975). "Studies on the nature of local scour." Bulletin *Series A No. 46*, Institutionen for teknisk vattenresurslara, Lund, Sweden.

Hoffmans, G.J.C.M. and Verheij, H.J. (1997). "Scour manual." A.A. Balkema, Rotterdam, The Netherlands.

Jain, S. C. and Fischer, E. E. (1980). "Scour around bridge piers at high flow velocities." *Journal of Hydraulic Division*, 106(11), 1827 – 1841.

Jones, J. S. and Sheppard, D. M., (2000). "Scour at wide bridge piers." *Proceedings of the World Water Conference*, ASCE, Minneapolis, MN.

Kandasamy, J. K. (1989). "Abutment scour." *Report Nº 458*, University of Auckland, Auckland, New Zealand.

Kothyari U. C., Hager W. H. and Oliveto G. (2007). "Generalized approach for clear-water scour at bridge foundation elements." *Journal of Hydraulic Engineering*, 133(11), 1229 – 1240.

Kwan, T.F. (1984). "Study of abutment scour." Report No. 328, *M.S. Thesis*, University of Auckland, New Zealand.

Kwan, T.F. (1987). "A study of abutment scour." *PhD Thesis*, University of Auckland, New Zealand.

Lança, R., Fael, C. and Cardoso, A. H. (2010). "Assessing equilibrium clear-water scour around single cylindrical piers." *River Flow 2010*, Dittrich *et al.* (editors), 1207 – 1213.

Lança, R., Fael, C., Maia, R., Pêgo, R. and Cardoso, A. H. (2012). "Effect of spacing and skew-angle on clear-water scour at pier alignments." *Proceedings of River Flow 2012*, Muñoz, R. (editor), 927 – 933.

Landers, M. N. and Mueller, D. S. (1996). "Channel scour at bridges in the United States." *FHWA–RD–95–184*, Federal Highway Administration, Washington, D.C.

Laursen, E. M. (1958). "Scour at bridge crossings." Iowa Highway Research Board, Ames, Iowa.

Laursen, E.M., (1962), "Scour at bridge crossings." *Transactions of the American Society of Civil Engineers*, 127(1), 166 – 209.

Laursen, E.M. (1963). "An analysis of relief bridge scour." *Journal of Hydraulics Division*, ASCE, 89(HY3), 93 – 118.

Laursen, E. M. and Toch, A. (1956). "Scour around bridge piers and abutments." *Bulletin No.4*, Iowa Highways Research Board, Ames, IA.

Lee, S. O. and Sturm, T. W. (2009). "Effect of sediment size scaling on physical modelling of bridge scour." *Journal of Hydraulic Engineering*, 135(10), 793 – 802.

Liu, H. K., Chang, F. M. and Skinner, M.M. (1961). "Effect of bridge construction on scour and backwater." *Report no. CER60 - HKL 22*, Colorado State University, CO.

Maza, A. and Sabchez, B. (1964). "Contribucion al estudio de solcavacion local en pilas de puente." Universidade Federal do Rio Grande do Sul, Brasil.

Melville, B. W. (1975). "Local scour at bridge sites." *Report No. 117*, University of Auckland, Auckland, New Zealand.

Melville, B. W. and Sutherland, A. J. (1988). "Design method for local scour at bridge piers." *Journal of Hydraulic Engineering*, 114(10), 1210 – 1226.

Melville, B. W. (1997), "Pier and abutment scour – an integrated approach." *Journal of Hydraulic Engineering*, 123(2), 125 – 136.

Melville, B. W. and Chiew, Y. M. (1999). "Time scale for local scour at bridge piers." *Journal of Hydraulic Engineering*, 125(1), 59 – 65.

Melville, B. W. and Coleman, S. E. (2000). "Bridge scour." *Water Resources publications*, LLC, CO.

Monti, R. (1994). "Indagine sperimentale delle caratteristiche fluidodinamiche del campo di moto intorno a una pila circolare." *PhD Thesis*, Polytechnic of Milan.

Mostafa, E. A. (1994). "Scour around skewed bridge piers." *PhD Thesis*, University of Alexandria, Alexandria, Egypt.

Mueller, D. S. and Wagner, C. R. (2005). "Field observations and evaluations of streambed scour at bridges." *Report No. FHWA-RD-03-052*, U.S. Department of Transportation, Federal Highway Administration, McLean, VA.

Neil, C. R. (1964). "River-bed scour." *Technical publication No. 623*, Canadian Good Roads Association, Ottawa, Canada.

Neil, C. R. (1967). "Mean velocity criterion for scour of coarse uniform bed-material." *Proceedings of the 12th IAHR Congress*, Forth Collins, CO, 3(C6), 1 – 9.

Nicollet, G. and Ramette (1971). "Deformation des lits alluvionnaires affouillements autour des piles de ponts cylindriques." Direction des Etudes et Recherches (EDF), France.

Oliveto, G. and Hager, W. H. (2002). "Temporal evolution of clear-water pier and abutment scour." *Journal of Hydraulic Engineering*, 128(9), 811 – 820.

Oliveto, G. and Hager, W. H. (2005). "Further results to time-dependent local scour at bridge elements." *Journal of Hydraulic Engineering*, 131(2), 97 – 105.

Radice, A., Franzetti, S. and Balio, F. (2002). "Local scour at bridge abutments." *River Flow 2002*, Bousmar and Zech (eds.), 1059 – 1068.

Raudkivi, A. J. (1986), "Functional trends of scour at bridge piers." *Journal of Hydraulic Engineering*, 112 (1), 1 – 13.

Raudkivi, A. J. (1998), "Loose boundary hydraulics." Pergamum Press, London, UK.

Raudkivi, A. J. and Ettema, R. (1983). "Clear-water scour at cylindrical piers." *Journal of Hydraulic Engineering*, 109 (3), 339 – 350.

Richardson, E. V. and Davis, S. R. (2001). "Evaluating scour at bridges." Federal Highway Administration, Forth Colins, CO.

Salim, M. and Jones, J. S. (1996). "Scour around exposed pile foundations." *Proceedings of the North American Water and Environment Congress*, ASCE, Anaheim, CA.

Sarma, K.V.N. (1967). "Study of scour phenomenon and its functional form." *PhD Thesis*, Indian Institute of Science, Bangalore, India.

Schneible, D. E. (1951). "An investigation of the effect of bridge-pier shape on the relative depth of scour." *PhD Thesis*, State University of Iowa, Iowa City, IA.

Shen, H.W., Schneider, V.R. and Karaki, S.S. (1966). "Mechanics of local scour." *Pub. No. CER 66-HWS-VRS-SK22*, Colorado State University, Fort Collins, CO.

Shen, H. W., Schneider, V. R. and Karaki, S. S. (1969). "Local scour around bridge piers." *Journal of the Hydraulic Division*, 95(HY6), 1919 – 1940.

Sheppard, D. M., Ontowirjo, B. and Zhao, G., (1999). "Local scour near single piles in steady currents." *Stream Stability and Scour at Highway Bridges, Compendium of papers, ASCE Water Resources Conferences 1991 – 1998*, E. V. Richardson and P. F. Lagasse, eds., 1809 – 1813.

Sheppard (2003). "Large scale and live bed local pier scour experiments – phase 1, large scale, Clearwater scour experiments." *FDOT Contract Number BB–473*, Tallahassee.

Sheppard, D. M. and Renna, R. (2005). "Florida Scour Manual." Florida Department of Transportation, Tallahassee, FL.

Sheppard, D. M. and Miller Jr., W. (2006) "Live-bed local pier scour experiments." *Journal of Hydraulic Engineering*, 132(7), 635 – 642.

Sheppard, D. M. and Renna, R. (2010). "Florida Bridge Scour Manual." Florida Department of Transportation, Tallahassee, FL.

Sheppard, D. M., Ontowirjo, B. and Zhao, G. (1995). "Local scour near single piles in steady currents." *Proceedings of the 1st Hydraulics Engineering Conference*, San Antonio, TX.

Sheppard, D. M., Odeh, M. and Glasser, T. (2004). "Large scale Clear-water local pier scour experiments." *Journal of Hydraulic Engineering*, 130(10), 957 – 963.

Simarro, G., Fael, C.M.S. and Cardoso, A. H. (2011). "Estimating equilibrium scour depth at cylindrical piers in experimental studies." *Journal of Hydraulic Engineering*, 137(9), 1089 – 1093.

Smith, W.L. (1999). "Local Structure-Induced Sediment Scour at Pile Groups." *M.S. Thesis*, University of Florida, Gainesville, FL.

Sumer, B. M. and Fredsøe, J. (2002). "The Mechanics of Scour in the Marine Environment." *Advanced Series on Ocean Engineering*. World Scientific Publishing Co. Pte. Ltd., Singapore.

Tarapore, Z. S. (1962). "A theoretical and experimental determination of the erosion pattern around obstructions placed in an alluvial channel with particular reference to vertical circular cylinders and piers." *PhD Thesis*, University of Minnesota, Minneapolis, MN.

Ting, F. C. K., Briaud, J.L., Chen, H. C., Gudavalli, R., Perugu, S. and Wei, G. (2001). "Flume tests for scour in clay at circular piers." *Journal of Hydraulic Engineering*, 127(11), 969 – 978.

Tison, L. J. (1940). “Erosion autour des piles de ponts en riviere.” *Annales des Travaux publics de Belgique*, 41 (6), 813 – 817.

Wong W. H. (1982). "Scour at bridge abutments." *Report Nº 275*, University of Auckland, New Zealand.

Zhao, G. and Sheppard, D. M. (1999). “The effect of flow skew angle on sediment scour near pile groups”. *Stream Stability and Scour at Highway Bridges, ASCE Compilation of Conference Papers*, 377 – 391.

APPENDIX A – TESTS AT SINGLE CYLINDRICAL PIERS

Test	d (mm)	D_p (mm)	U_c (m/s)	U (m/s)	U/U_c	d/D_p	D_p/D_{50}	t_d (hour)	d_{se} (mm)	d_{se}/D_p
1	55	110	0.28	0.28	0.97	0.5	127.9	170	180.1	1.64

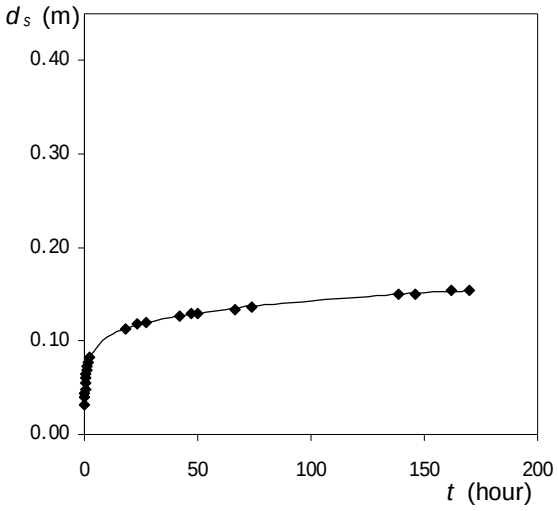

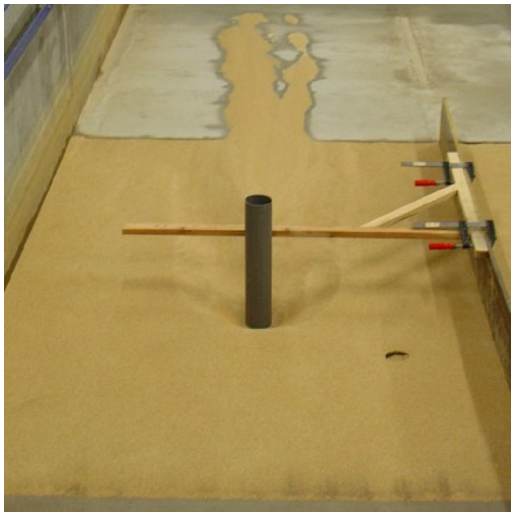

Test 1

t (hour)	d_s (m)	t (hour)	d_s (m)	t (hour)	d_s (m)
0.00	0.000	2.40	0.083	145.88	0.150
0.07	0.032	10.00	0.105	162.18	0.154
0.15	0.040	17.90	0.114	170.02	0.154
0.23	0.044	23.23	0.118		
0.32	0.048	27.30	0.120		
0.50	0.054	42.12	0.127		
0.67	0.060	47.08	0.129		
0.83	0.065	50.25	0.130		
1.08	0.068	66.58	0.134		
1.37	0.073	73.77	0.136		
1.85	0.077	138.42	0.150		

Test	d (mm)	D_p (mm)	U_c (m/s)	U (m/s)	U/U_c	d/D_p	D_p/D_{50}	t_d (hour)	d_{se} (mm)	d_{se}/D_p
2	80	160	0.29	0.29	0.97	0.5	186.0	168	226.2	1.41

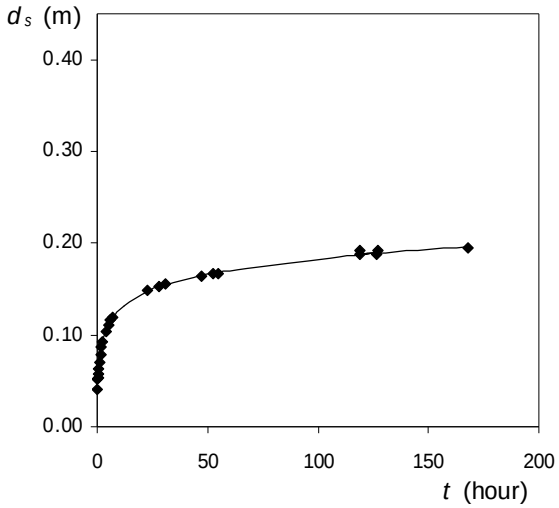

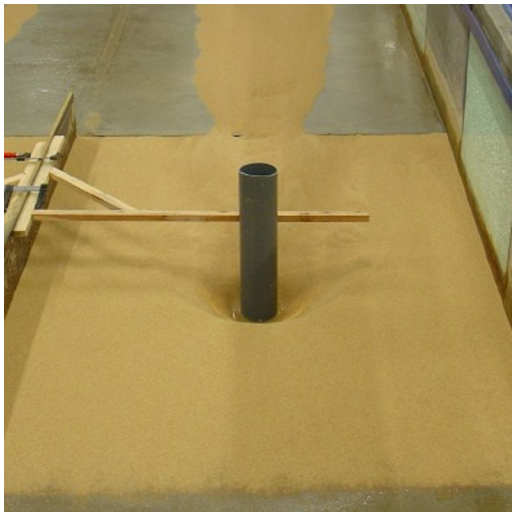

Test 2

t (hour)	d_s (m)	t (hour)	d_s (m)	t (hour)	d_s (m)
0.00	0.000	5.03	0.111	126.62	0.189
0.12	0.040	6.03	0.116	119.17	0.192
0.23	0.052	6.90	0.119	126.93	0.192
0.32	0.054	12.00	0.132	168.00	0.195
0.43	0.057	22.88	0.148		
0.68	0.063	28.17	0.154		
0.97	0.070	30.90	0.155		
1.55	0.078	47.40	0.164		
1.98	0.087	52.23	0.167		
2.45	0.092	54.67	0.167		
3.82	0.104	119.22	0.187		

Test	d (mm)	D_p (mm)	U_c (m/s)	U (m/s)	U/U_c	d/D_p	D_p/D_{50}	t_d (hour)	d_{se} (mm)	d_{se}/D_p
3	100	200	0.30	0.29	0.97	0.5	232.6	170	263.1	1.32

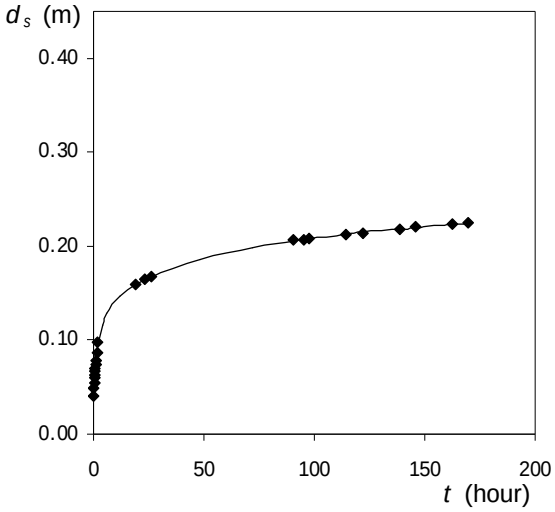

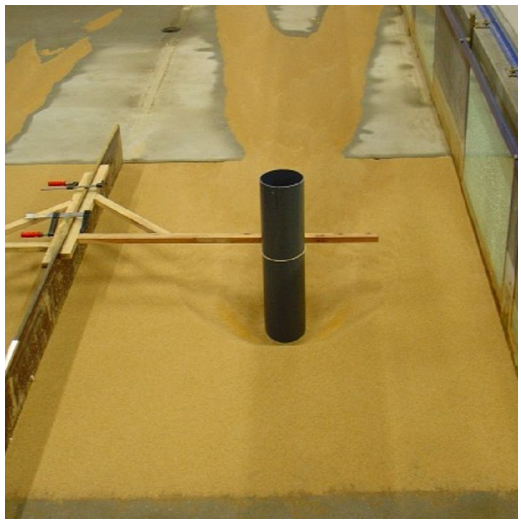

Test 3

t (hour)	d_s (m)	t (hour)	d_s (m)	t (hour)	d_s (m)
0.00	0.000	2.02	0.097	97.82	0.208
0.10	0.041	4.00	0.116	114.50	0.213
0.22	0.049	6.00	0.128	122.10	0.214
0.30	0.055	12.00	0.147	138.73	0.218
0.43	0.060	18.98	0.159	145.97	0.220
0.50	0.063	23.05	0.165	162.65	0.223
0.68	0.067	25.92	0.168	169.80	0.225
0.83	0.070	48.00	0.186		
1.02	0.074	72.00	0.199		
1.25	0.079	90.53	0.207		
1.50	0.086	95.38	0.208		

Test	d (mm)	D_p (mm)	U_c (m/s)	U (m/s)	U/U_c	d/D_p	D_p/D_{50}	t_d (hour)	d_{se} (mm)	d_{se}/D_p
4	125	250	0.31	0.30	0.97	0.5	290.7	168	282.1	1.13

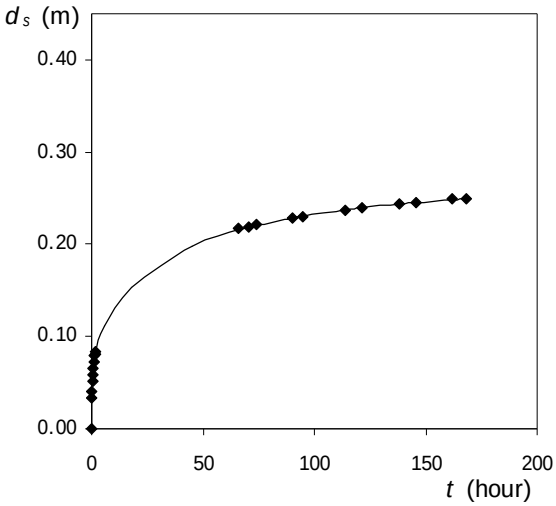

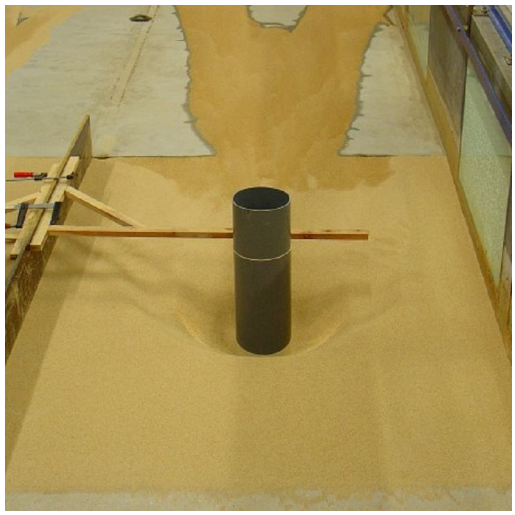

Test 4

t (hour)	d_s (m)	t (hour)	d_s (m)	t (hour)	d_s (m)
0.00	0.000	18.00	0.153	162.12	0.249
0.10	0.033	45.00	0.198	168.03	0.250
0.20	0.041	66.05	0.217		
0.30	0.051	70.50	0.219		
0.42	0.059	73.82	0.221		
0.58	0.065	90.00	0.229		
0.88	0.072	95.00	0.230		
1.25	0.079	113.67	0.237		
1.55	0.081	121.55	0.240		
1.82	0.083	137.92	0.244		
6.00	0.111	145.50	0.246		

Test	d (mm)	D_p (mm)	U_c (m/s)	U (m/s)	U/U_c	d/D_p	D_p/D_{50}	t_d (hour)	d_{se} (mm)	d_{se}/D_p
5	158	315	0.32	0.29	0.93	0.5	366.3	223	348.1	1.10

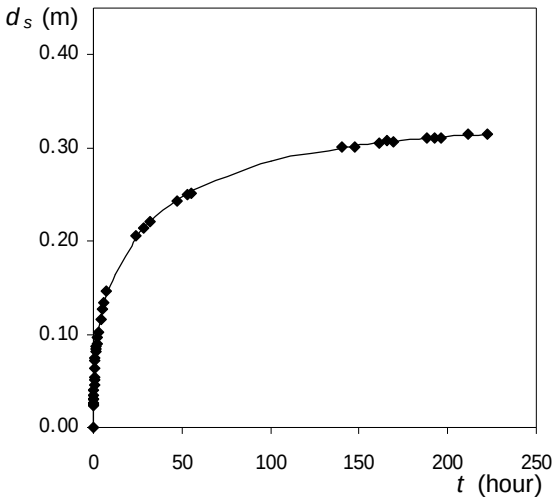

Test 5

t (hour)	d_s (m)	t (hour)	d_s (m)	t (hour)	d_s (m)	t (hour)	d_s (m)
0.00	0.000	0.73	0.064	6.03	0.134	147.37	0.302
0.03	0.024	0.88	0.071	7.62	0.146	161.53	0.306
0.07	0.025	1.03	0.075	12.00	0.164	165.37	0.307
0.10	0.027	1.28	0.081	23.78	0.205	169.18	0.307
0.13	0.030	1.53	0.084	28.45	0.214	188.43	0.311
0.17	0.031	1.78	0.087	31.70	0.222	192.65	0.310
0.20	0.035	2.03	0.090	47.37	0.243	196.32	0.310
0.28	0.040	2.53	0.096	52.70	0.249	211.77	0.314
0.37	0.046	3.03	0.103	55.45	0.251	222.73	0.315
0.45	0.052	4.07	0.116	100.00	0.285		
0.53	0.054	5.12	0.127	139.95	0.301		

Test	d (mm)	D_p (mm)	U_c (m/s)	U (m/s)	U/U_c	d/D_p	D_p/D_{50}	t_d (hour)	d_{se} (mm)	d_{se}/D_p
6	175	350	0.32	0.33	1.04	0.5	407.0	306	337.3	0.96

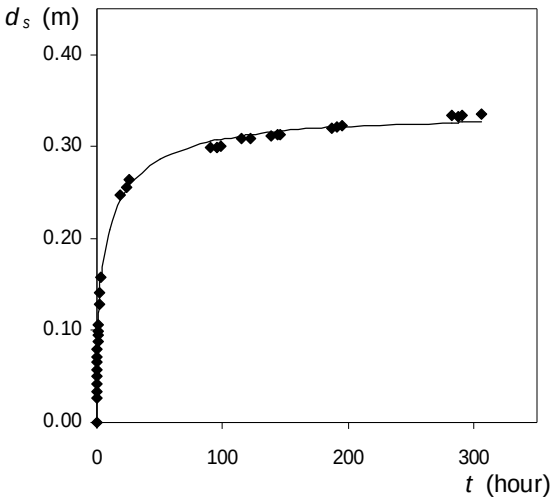

Test 6

t (hour)	d_s (m)	t (hour)	d_s (m)	t (hour)	d_s (m)	t (hour)	d_s (m)
0.00	0.000	0.83	0.099	95.17	0.299	287.33	0.333
0.07	0.027	1.00	0.106	98.33	0.300	290.33	0.334
0.12	0.034	1.70	0.128	114.50	0.308	306.08	0.335
0.13	0.042	2.35	0.141	122.33	0.308		
0.20	0.051	3.37	0.158	138.75	0.312		
0.25	0.058	10.00	0.209	143.42	0.313		
0.32	0.065	18.50	0.248	146.17	0.313		
0.37	0.071	23.25	0.256	187.00	0.319		
0.48	0.079	26.08	0.264	191.33	0.321		
0.58	0.088	50.00	0.287	195.00	0.322		
0.75	0.095	90.25	0.299	282.33	0.334		

Test	d (mm)	D_p (mm)	U_c (m/s)	U (m/s)	U/U_c	d/D_p	D_p/D_{50}	t_d (hour)	d_{se} (mm)	d_{se}/D_p
7	200	400	0.32	0.31	0.96	0.5	465.1	288	409.2	1.02

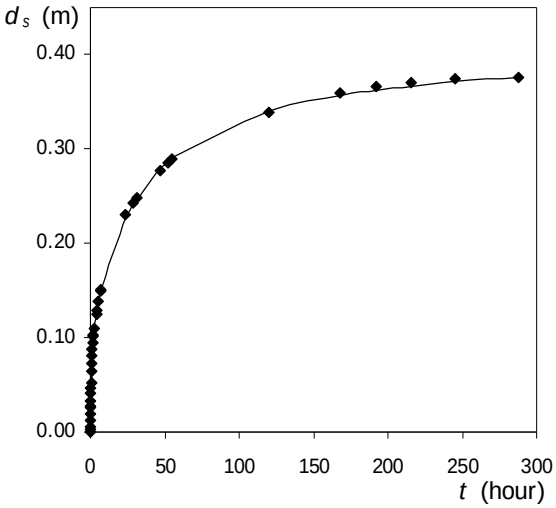

Test 7

t (hour)	d_s (m)	t (hour)	d_s (m)	t (hour)	d_s (m)	t (hour)	d_s (m)
0.00	0.000	0.67	0.064	6.58	0.149	215.67	0.371
0.03	0.002	0.83	0.073	7.08	0.152	245.58	0.375
0.07	0.006	1.00	0.081	23.33	0.230	287.58	0.377
0.12	0.012	1.28	0.088	28.58	0.243		
0.15	0.020	1.50	0.094	31.00	0.249		
0.18	0.025	1.80	0.101	47.33	0.277		
0.22	0.028	2.00	0.103	52.33	0.285		
0.25	0.033	2.50	0.110	55.08	0.289		
0.33	0.041	4.00	0.124	119.58	0.339		
0.42	0.047	4.50	0.129	167.42	0.360		
0.50	0.053	5.50	0.139	191.75	0.366		

Test	d (mm)	D_p (mm)	U_c (m/s)	U (m/s)	U/U_c	d/D_p	D_p/D_{50}	t_d (hour)	d_{se} (mm)	d_{se}/D_p
8	50	50	0.28	0.27	0.97	1.0	58.1	168	115.6	2.31

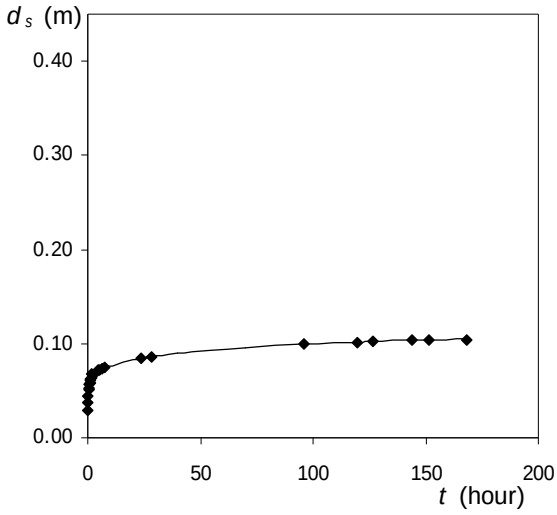

Test 8

t (hour)	d_s (m)	t (hour)	d_s (m)	t (hour)	d_s (m)
0.00	0.000	2.08	0.066	119.58	0.102
0.05	0.029	1.58	0.068	126.83	0.102
0.18	0.037	4.65	0.072	143.73	0.104
0.27	0.045	5.40	0.073	151.45	0.104
0.38	0.051	6.33	0.074	168.03	0.104
0.48	0.053	7.53	0.074		
0.73	0.057	23.93	0.084		
0.88	0.059	28.55	0.087		
1.10	0.061	40.00	0.090		
1.35	0.063	70.00	0.096		
1.58	0.064	96.08	0.099		

Test	d (mm)	D_p (mm)	U_c (m/s)	U (m/s)	U/U_c	d/D_p	D_p/D_{50}	t_d (hour)	d_{se} (mm)	d_{se}/D_p
9	75	75	0.29	0.28	0.97	1.0	87.2	168	163.9	2.18

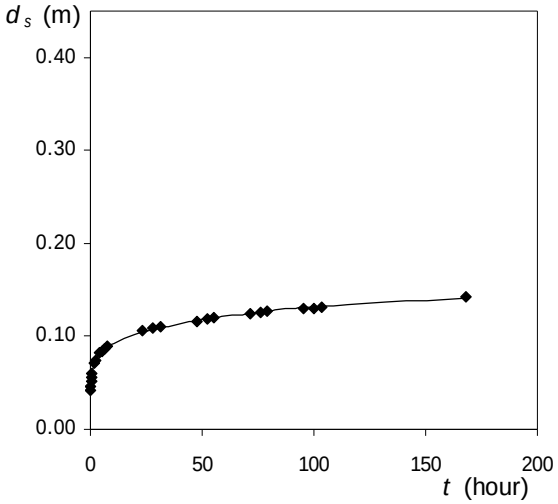

Test 9

t (hour)	d_s (m)	t (hour)	d_s (m)	t (hour)	d_s (m)
0.00	0.000	7.33	0.089	100.17	0.131
0.10	0.042	23.22	0.106	103.22	0.132
0.17	0.046	28.18	0.109	168.03	0.143
0.33	0.052	31.32	0.110		
0.52	0.056	47.52	0.117		
0.70	0.060	52.08	0.118		
1.65	0.072	55.22	0.120		
2.10	0.074	71.52	0.124		
4.25	0.082	76.20	0.126		
5.35	0.084	79.30	0.127		
6.43	0.087	95.57	0.130		

Test	d (mm)	D_p (mm)	U_c (m/s)	U (m/s)	U/U_c	d/D_p	D_p/D_{50}	t_d (hour)	d_{se} (mm)	d_{se}/D_p
10	110	110	0.30	0.29	0.97	1.0	127.9	168	198.9	1.81

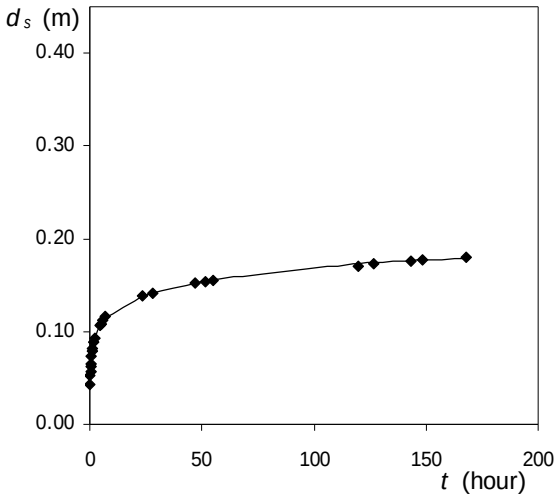

Test 10

t (hour)	d_s (m)	t (hour)	d_s (m)	t (hour)	d_s (m)
0.00	0.000	4.32	0.106	143.17	0.176
0.10	0.042	5.05	0.108	148.70	0.177
0.20	0.052	6.02	0.112	168.02	0.180
0.30	0.057	7.13	0.116		
0.38	0.062	23.27	0.139		
0.48	0.065	28.17	0.142		
0.77	0.074	47.25	0.152		
1.03	0.079	51.32	0.154		
1.25	0.081	55.03	0.155		
1.77	0.088	119.77	0.171		
2.27	0.093	126.50	0.174		

Test	d (mm)	D_p (mm)	U_c (m/s)	U (m/s)	U/U_c	d/D_p	D_p/D_{50}	t_d (hour)	d_{se} (mm)	d_{se}/D_p
11	160	160	0.32	0.30	0.95	1.0	186.0	285	231.1	1.44

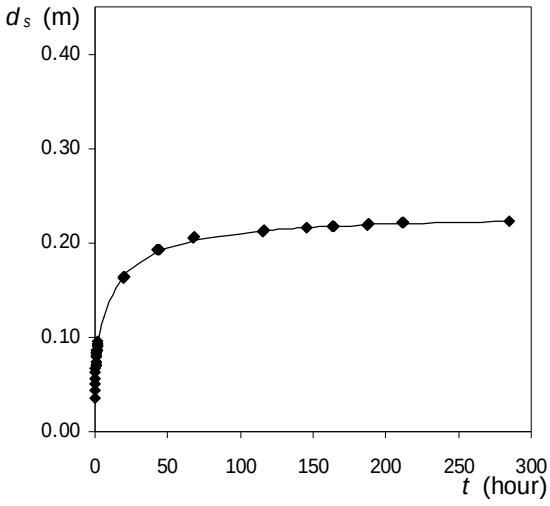

Test 11

t (hour)	d_s (m)	t (hour)	d_s (m)	t (hour)	d_s (m)	t (hour)	d_s (m)	t (hour)	d_s (m)
0.00	0.000	0.85	0.081	19.15	0.162	115.43	0.212	187.95	0.220
0.05	0.035	0.97	0.083	19.52	0.163	115.93	0.213	188.45	0.220
0.10	0.043	1.05	0.083	19.93	0.164	116.43	0.213	210.90	0.221
0.15	0.050	1.17	0.086	20.48	0.164	145.25	0.216	211.45	0.221
0.20	0.056	1.33	0.087	42.98	0.193	145.80	0.216	211.95	0.221
0.28	0.063	1.50	0.090	43.45	0.193	163.10	0.217	212.43	0.222
0.37	0.067	1.67	0.092	43.93	0.193	163.43	0.217	285.20	0.223
0.45	0.070	1.83	0.093	44.43	0.193	163.95	0.217		
0.53	0.072	2.00	0.096	67.28	0.205	164.50	0.217		
0.62	0.074	6.00	0.122	67.93	0.206	187.00	0.219		
0.73	0.079	14.00	0.152	115.08	0.212	187.45	0.219		

Test	d (mm)	D_p (mm)	U_c (m/s)	U (m/s)	U/U_c	d/D_p	D_p/D_{50}	t_d (hour)	d_{se} (mm)	d_{se}/D_p
12	200	200	0.32	0.31	0.96	1.0	232.6	261	296.5	1.48

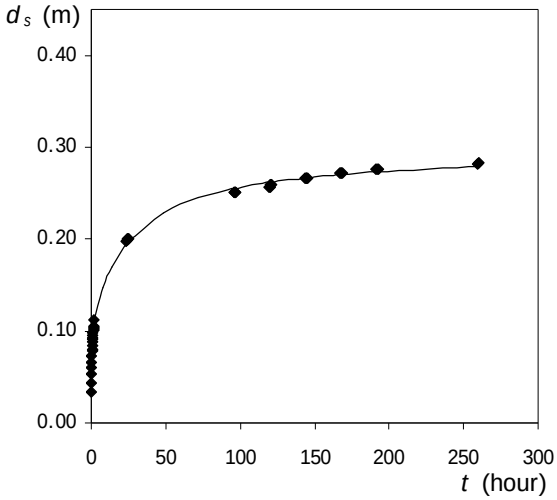

Test 12

t (hour)	d_s (m)	t (hour)	d_s (m)	t (hour)	d_s (m)	t (hour)	d_s (m)	t (hour)	d_s (m)
0.00	0.000	0.82	0.091	23.50	0.198	120.05	0.257	191.47	0.276
0.05	0.034	0.93	0.093	24.00	0.199	120.58	0.259	191.97	0.276
0.10	0.044	1.05	0.095	24.50	0.200	121.05	0.259	192.47	0.276
0.15	0.053	1.17	0.098	25.00	0.201	143.63	0.266	259.00	0.282
0.20	0.060	1.33	0.100	48.00	0.228	144.13	0.266	260.52	0.283
0.27	0.065	1.50	0.102	72.00	0.245	144.58	0.266	261.23	0.283
0.35	0.072	1.67	0.104	95.63	0.251	145.13	0.266		
0.43	0.078	1.83	0.105	96.13	0.251	167.10	0.272		
0.52	0.081	2.00	0.112	96.63	0.251	167.63	0.272		
0.60	0.084	8.00	0.148	97.18	0.251	168.13	0.272		
0.70	0.088	14.00	0.170	119.52	0.257	168.63	0.272		

Test	d (mm)	D_p (mm)	U_c (m/s)	U (m/s)	U/U_c	d/D_p	D_p/D_{50}	t_d (hour)	d_{se} (mm)	d_{se}/D_p
13	250	250	0.33	0.32	0.98	1.0	290.7	263	365.0	1.46

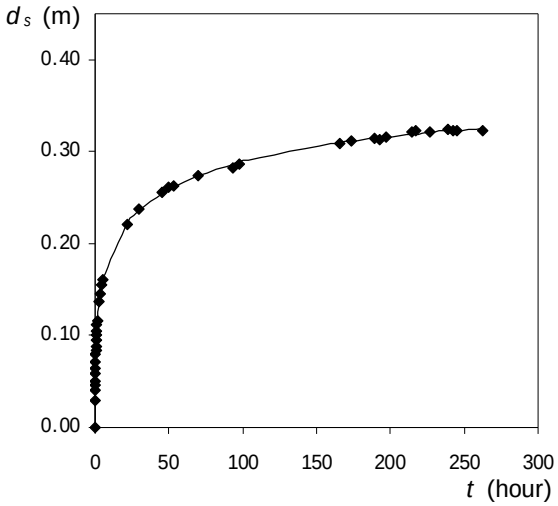

Test 13

t (hour)	d_s (m)	t (hour)	d_s (m)	t (hour)	d_s (m)	t (hour)	d_s (m)
0.00	0.000	0.72	0.095	45.05	0.256	214.85	0.322
0.03	0.029	0.88	0.101	49.88	0.262	216.73	0.323
0.07	0.041	1.05	0.106	53.38	0.263	226.75	0.322
0.10	0.046	1.30	0.112	69.47	0.274	238.95	0.324
0.13	0.051	1.55	0.117	93.47	0.283	242.82	0.323
0.17	0.059	2.80	0.137	97.88	0.286	245.22	0.322
0.22	0.064	3.55	0.145	165.88	0.310	262.88	0.322
0.30	0.072	4.55	0.155	173.30	0.312		
0.38	0.080	5.30	0.161	189.30	0.315		
0.47	0.083	21.47	0.221	192.48	0.313		
0.55	0.088	29.63	0.237	197.40	0.316		

Test	d (mm)	D_p (mm)	U_c (m/s)	U (m/s)	U/U_c	d/D_p	D_p/D_{50}	t_d (hour)	d_{se} (mm)	d_{se}/D_p
14	315	315	0.34	0.33	0.98	1.0	366.3	186	388.3	1.23

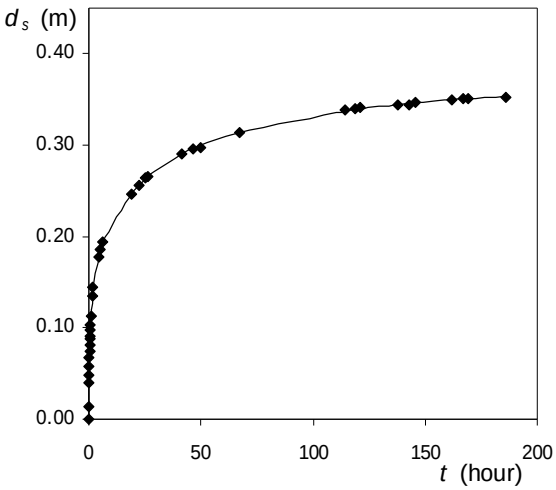

Test 14

t (hour)	d_s (m)	t (hour)	d_s (m)	t (hour)	d_s (m)	t (hour)	d_s (m)
0.00	0.000	0.63	0.103	41.72	0.291	166.80	0.351
0.03	0.014	1.02	0.113	46.47	0.295	169.25	0.351
0.10	0.040	1.45	0.135	49.80	0.297	185.80	0.352
0.13	0.048	1.83	0.145	66.97	0.314		
0.18	0.057	4.37	0.178	114.13	0.339		
0.23	0.068	5.23	0.185	118.55	0.340		
0.30	0.074	6.42	0.194	120.88	0.341		
0.35	0.082	19.05	0.247	137.72	0.345		
0.42	0.088	22.47	0.256	142.80	0.345		
0.47	0.091	25.47	0.264	145.88	0.346		
0.55	0.098	26.47	0.266	161.72	0.350		

Test	d (mm)	D_p (mm)	U_c (m/s)	U (m/s)	U/U_c	d/D_p	D_p/D_{50}	t_d (hour)	d_{se} (mm)	d_{se}/D_p
15	350	350	0.34	0.33	0.97	1.0	407.0	291	408.7	1.17

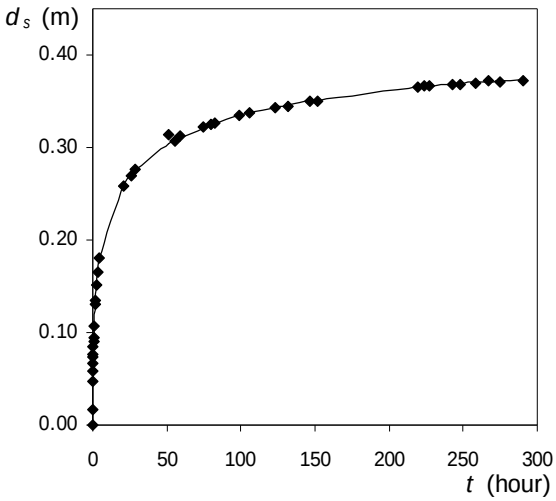

Test 15

t (hour)	d_s (m)	t (hour)	d_s (m)	t (hour)	d_s (m)	t (hour)	d_s (m)
0.00	0.000	1.40	0.129	74.45	0.322	226.78	0.366
0.03	0.017	1.62	0.135	79.45	0.325	242.78	0.368
0.12	0.045	2.28	0.149	82.53	0.326	248.12	0.369
0.18	0.058	3.33	0.167	98.53	0.334	258.70	0.370
0.23	0.066	4.45	0.181	106.03	0.337	266.78	0.371
0.30	0.075	20.95	0.260	122.78	0.344	274.62	0.372
0.33	0.078	25.78	0.270	131.37	0.346	290.78	0.374
0.38	0.083	28.20	0.275	146.95	0.351		
0.47	0.090	50.95	0.304	151.70	0.352		
0.53	0.094	55.53	0.308	218.95	0.365		
0.80	0.109	58.87	0.311	223.95	0.366		

Test	d (mm)	D_p (mm)	U_c (m/s)	U (m/s)	U/U_c	d/D_p	D_p/D_{50}	t_d (hour)	d_{se} (mm)	d_{se}/D_p
16	400	400	0.35	0.33	0.95	1.0	465.1	224	448.4	1.12

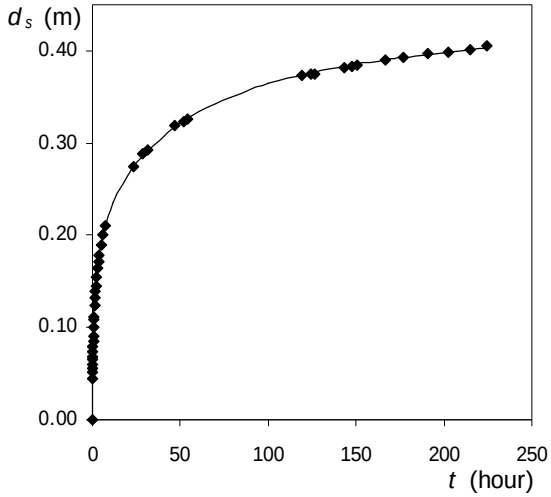

Test 16

t (hour)	d_s (m)	t (hour)	d_s (m)	t (hour)	d_s (m)	t (hour)	d_s (m)	t (hour)	d_s (m)
0.00	0.000	0.67	0.101	5.00	0.189	100.00	0.364	215.08	0.402
0.03	0.044	0.83	0.109	6.00	0.200	119.33	0.373	224.42	0.406
0.07	0.052	1.00	0.112	7.17	0.210	124.50	0.375		
0.10	0.056	1.25	0.124	12.00	0.236	126.50	0.375		
0.13	0.060	1.50	0.132	23.58	0.275	143.33	0.382		
0.17	0.065	1.75	0.139	28.25	0.288	148.00	0.383		
0.20	0.069	2.00	0.145	31.08	0.293	150.67	0.385		
0.25	0.073	2.50	0.155	46.50	0.319	166.83	0.390		
0.33	0.079	3.00	0.164	52.08	0.323	176.75	0.394		
0.42	0.085	3.50	0.171	53.75	0.327	191.08	0.397		
0.50	0.091	4.00	0.178	70.00	0.343	202.25	0.398		

Test	d (mm)	D_p (mm)	U_c (m/s)	U (m/s)	U/U_c	d/D_p	D_p/D_{50}	t_d (hour)	d_{se} (mm)	d_{se}/D_p
17	75	50	0.29	0.28	0.97	1.5	58.1	168	118.9	2.38

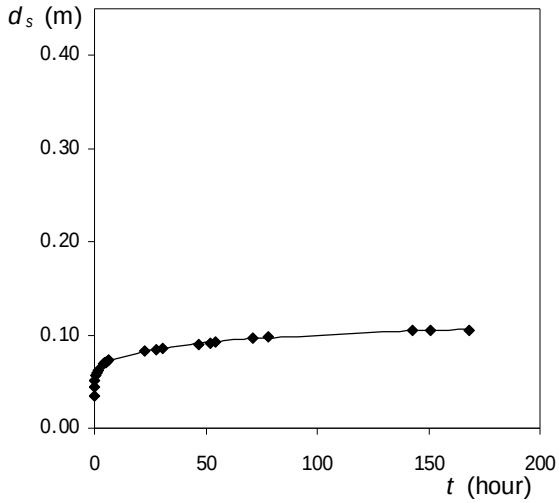

Test 17

t (hour)	d_s (m)	t (hour)	d_s (m)	t (hour)	d_s (m)
0.00	0.000	6.20	0.073	168.00	0.105
0.07	0.035	22.82	0.083		
0.20	0.044	27.50	0.084		
0.27	0.051	30.40	0.086		
0.67	0.056	46.90	0.090		
1.13	0.060	51.83	0.092		
1.45	0.062	54.53	0.092		
3.82	0.069	71.07	0.096		
4.58	0.071	77.85	0.098		
5.17	0.071	142.77	0.105		
5.82	0.072	150.67	0.105		

Test	d (mm)	D_p (mm)	U_c (m/s)	U (m/s)	U/U_c	d/D_p	D_p/D_{50}	t_d (hour)	d_{se} (mm)	d_{se}/D_p
18	113	75	0.30	0.30	0.97	1.5	87.2	168	175.8	2.34

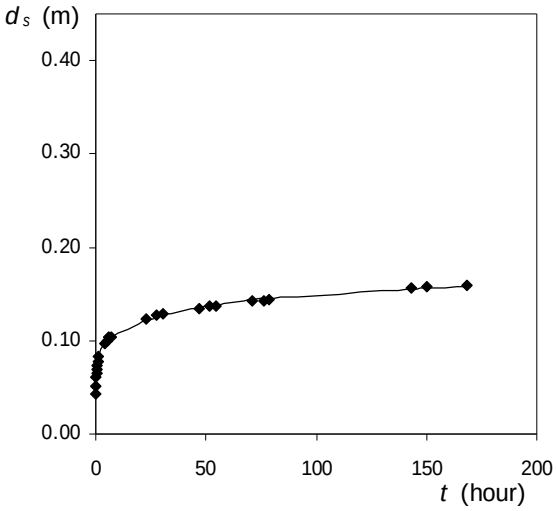

Test 18

t (hour)	d_s (m)	t (hour)	d_s (m)	t (hour)	d_s (m)
0.00	0.000	6.05	0.103	143.05	0.156
0.07	0.043	6.85	0.104	150.38	0.158
0.13	0.052	22.92	0.124	168.15	0.159
0.27	0.061	27.45	0.127		
0.38	0.066	30.48	0.129		
0.53	0.070	46.73	0.134		
0.63	0.073	51.80	0.137		
0.92	0.078	54.53	0.137		
1.35	0.083	70.95	0.142		
3.88	0.097	76.03	0.143		
5.02	0.100	78.72	0.144		

Test	d (mm)	D_p (mm)	U_c (m/s)	U (m/s)	U/U_c	d/D_p	D_p/D_{50}	t_d (hour)	d_{se} (mm)	d_{se}/D_p
19	165	110	0.32	0.30	0.96	1.5	127.9	241	224.6	2.04

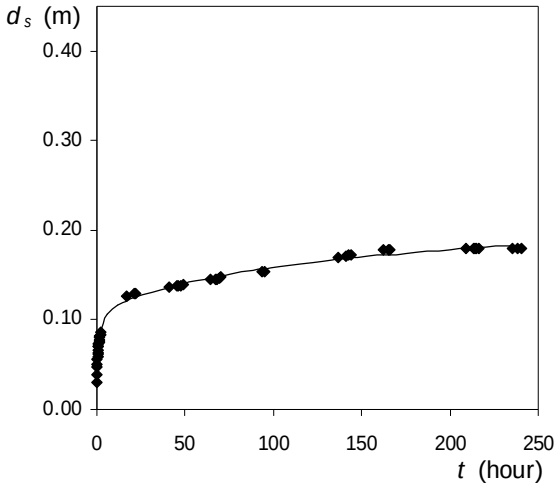

Test 19

t (hour)	d_s (m)	t (hour)	d_s (m)	t (hour)	d_s (m)	t (hour)	d_s (m)	t (hour)	d_s (m)
0.00	0.000	0.87	0.071	16.80	0.127	69.35	0.146	209.05	0.179
0.05	0.030	0.98	0.074	21.30	0.129	70.18	0.147	213.25	0.179
0.10	0.039	1.10	0.074	21.90	0.129	93.33	0.154	214.12	0.179
0.15	0.047	1.22	0.077	41.25	0.137	94.72	0.154	214.73	0.179
0.20	0.051	1.38	0.078	45.25	0.138	136.95	0.170	216.70	0.179
0.28	0.056	1.55	0.080	46.32	0.138	141.22	0.171	235.22	0.180
0.37	0.059	1.72	0.082	47.73	0.139	142.28	0.172	237.98	0.180
0.45	0.061	1.88	0.084	48.75	0.139	143.75	0.172	240.67	0.180
0.53	0.063	2.05	0.086	64.03	0.145	162.05	0.178		
0.62	0.067	6.00	0.106	67.27	0.146	165.37	0.179		
0.75	0.070	12.00	0.116	67.67	0.146	166.12	0.179		

Test	d (mm)	D_p (mm)	U_c (m/s)	U (m/s)	U/U_c	d/D_p	D_p/D_{50}	t_d (hour)	d_{se} (mm)	d_{se}/D_p
20	225	160	0.33	0.33	1.01	1.4	186.0	267	305.7	1.91

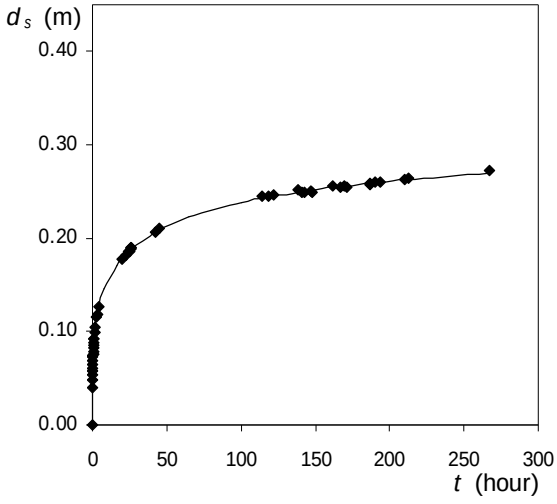

Test 20

t (hour)	d_s (m)	t (hour)	d_s (m)	t (hour)	d_s (m)	t (hour)	d_s (m)	t (hour)	d_s (m)
0.00	0.000	0.58	0.078	8.00	0.147	65.00	0.223	166.83	0.255
0.08	0.040	0.67	0.082	16.00	0.171	100.00	0.238	169.75	0.256
0.13	0.048	0.85	0.087	20.25	0.178	114.00	0.245	170.75	0.255
0.17	0.053	1.00	0.086	22.42	0.182	118.58	0.245	186.42	0.259
0.20	0.057	1.08	0.092	24.50	0.186	121.50	0.246	186.92	0.258
0.23	0.060	1.17	0.093	25.50	0.186	138.00	0.252	190.50	0.260
0.27	0.065	1.50	0.099	25.58	0.190	141.00	0.249	193.67	0.260
0.32	0.069	2.00	0.105	25.60	0.190	142.50	0.249	210.00	0.263
0.37	0.073	2.83	0.116	26.00	0.189	146.68	0.251	212.58	0.264
0.42	0.075	3.25	0.119	42.00	0.206	147.75	0.250	267.38	0.272
0.50	0.076	4.50	0.126	44.83	0.211	161.83	0.256		

Test	d (mm)	D_p (mm)	U_c (m/s)	U (m/s)	U/U_c	d/D_p	D_p/D_{50}	t_d (hour)	d_{se} (mm)	d_{se}/D_p
21	300	200	0.34	0.33	0.98	1.5	232.6	262	360.6	1.80

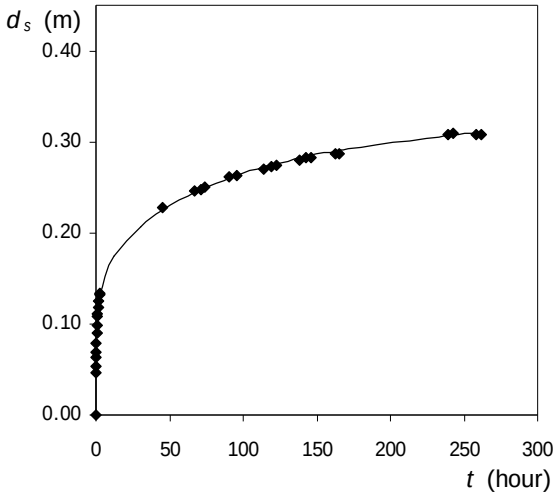

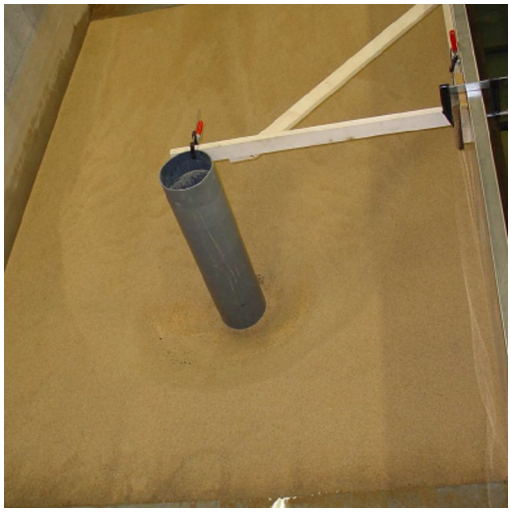

Test 21

t (hour)	d_s (m)	t (hour)	d_s (m)	t (hour)	d_s (m)	t (hour)	d_s (m)
0.00	0.000	2.02	0.126	114.25	0.270	261.50	0.308
0.05	0.046	2.52	0.132	119.17	0.273		
0.08	0.053	2.67	0.133	122.25	0.275		
0.17	0.063	12.00	0.174	138.50	0.279		
0.25	0.070	30.00	0.207	143.00	0.283		
0.33	0.079	45.25	0.228	146.17	0.282		
0.58	0.090	66.58	0.246	162.50	0.287		
0.75	0.099	71.25	0.248	165.33	0.286		
1.05	0.108	74.25	0.250	239.17	0.308		
1.25	0.112	90.25	0.262	242.58	0.309		
1.52	0.118	95.33	0.263	258.25	0.308		

Test	d (mm)	D_p (mm)	U_c (m/s)	U (m/s)	U/U_c	d/D_p	D_p/D_{50}	t_d (hour)	d_{se} (mm)	d_{se}/D_p
22	375	250	0.34	0.33	0.96	1.5	290.7	221	373.8	1.50

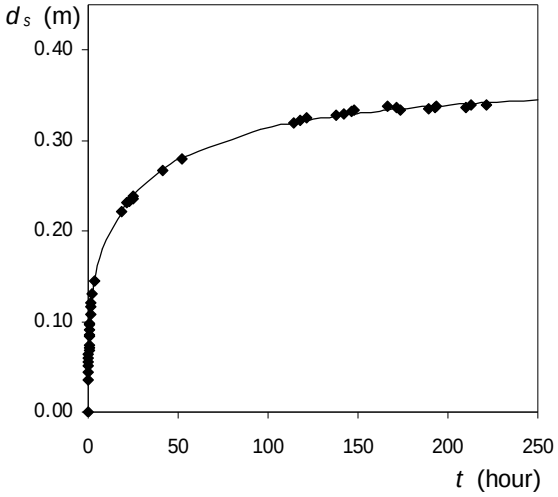

Test 22

t (hour)	d_s (m)	t (hour)	d_s (m)	t (hour)	d_s (m)	t (hour)	d_s (m)	t (hour)	d_s (m)
0.00	0.000	0.68	0.084	21.60	0.232	142.02	0.330	221.35	0.339
0.03	0.035	0.78	0.091	22.85	0.233	146.68	0.332		
0.10	0.043	0.85	0.096	25.02	0.236	147.77	0.333		
0.17	0.051	0.93	0.098	25.35	0.239	166.30	0.338		
0.22	0.055	1.18	0.108	41.27	0.267	171.52	0.337		
0.30	0.060	1.43	0.116	52.35	0.280	173.47	0.334		
0.33	0.064	1.68	0.121	96.00	0.312	189.22	0.335		
0.38	0.069	2.18	0.131	113.93	0.320	192.77	0.337		
0.45	0.071	3.52	0.144	118.18	0.323	193.60	0.338		
0.52	0.073	8.00	0.180	121.68	0.325	209.93	0.336		
0.60	0.085	18.68	0.222	137.68	0.328	212.68	0.339		

Test	d (mm)	D_p (mm)	U_c (m/s)	U (m/s)	U/U_c	d/D_p	D_p/D_{50}	t_d (hour)	d_{se} (mm)	d_{se}/D_p
23	100	50	0.30	0.29	0.97	2.0	58.1	170	127.1	2.54

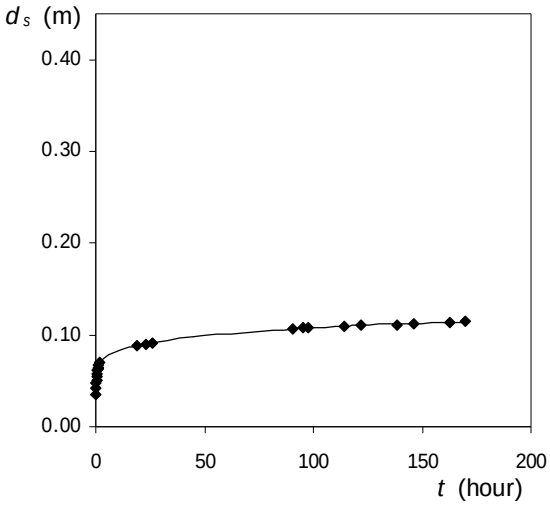

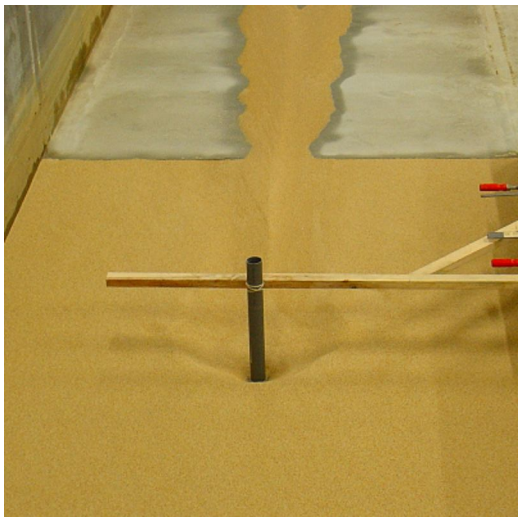

Test 23

t (hour)	d_s (m)	t (hour)	d_s (m)	t (hour)	d_s (m)
0.00	0.000	2.00	0.070	122.08	0.110
0.08	0.035	6.00	0.079	138.68	0.111
0.15	0.043	12.00	0.084	145.95	0.112
0.28	0.048	18.93	0.088	162.60	0.114
0.38	0.051	23.03	0.090	169.78	0.115
0.48	0.055	25.87	0.092		
0.63	0.057	45.00	0.098		
0.82	0.062	90.52	0.106		
0.97	0.064	95.33	0.108		
1.23	0.065	97.80	0.108		
1.45	0.067	114.45	0.110		

Test	d (mm)	D_p (mm)	U_c (m/s)	U (m/s)	U/U_c	d/D_p	D_p/D_{50}	t_d (hour)	d_{se} (mm)	d_{se}/D_p
24	150	75	0.31	0.30	0.97	2.0	87.2	169	162.7	2.17

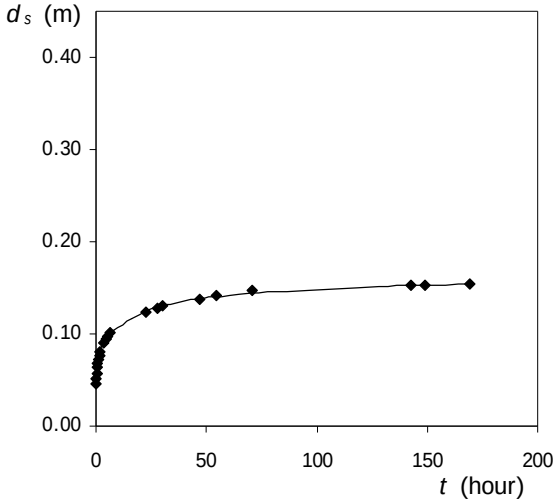

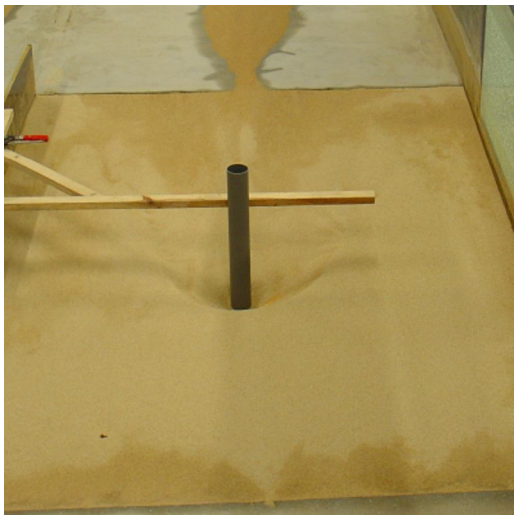

Test 24

t (hour)	d_s (m)	t (hour)	d_s (m)	t (hour)	d_s (m)
0.00	0.000	5.47	0.098	149.18	0.152
0.12	0.046	6.50	0.101	169.00	0.154
0.18	0.051	8.00	0.104		
0.33	0.058	16.00	0.117		
0.50	0.064	22.65	0.124		
0.72	0.069	27.68	0.128		
0.98	0.073	30.43	0.130		
1.47	0.077	46.82	0.138		
1.75	0.080	54.60	0.141		
3.65	0.091	70.57	0.147		
4.45	0.094	142.80	0.152		

Test	d (mm)	D_p (mm)	U_c (m/s)	U (m/s)	U/U_c	d/D_p	D_p/D_{50}	t_d (hour)	d_{se} (mm)	d_{se}/D_p
25	220	110	0.33	0.33	1.01	2.0	127.9	216	208.9	1.90

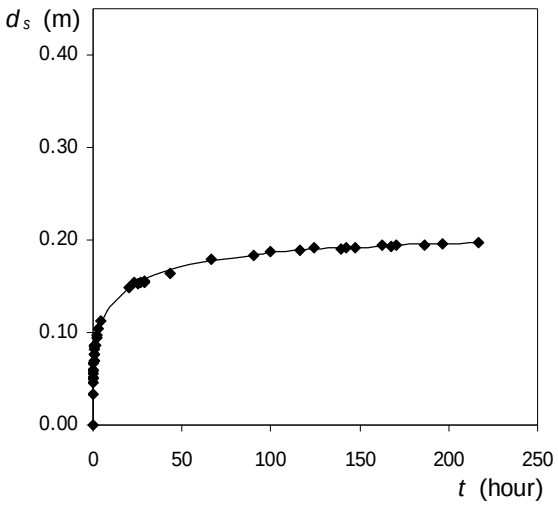

Test 25

t (hour)	d_s (m)	t (hour)	d_s (m)	t (hour)	d_s (m)	t (hour)	d_s (m)
0.00	0.000	0.57	0.076	16.00	0.140	116.60	0.189
0.03	0.034	0.65	0.077	20.25	0.149	124.03	0.192
0.07	0.046	0.73	0.082	23.00	0.154	139.50	0.191
0.10	0.050	0.92	0.084	25.33	0.153	142.37	0.192
0.13	0.051	1.08	0.086	26.58	0.154	147.68	0.191
0.17	0.055	1.25	0.086	28.55	0.154	162.75	0.194
0.20	0.058	1.83	0.095	29.25	0.156	167.75	0.193
0.23	0.060	2.25	0.097	43.63	0.164	170.75	0.194
0.32	0.066	3.25	0.104	66.25	0.179	186.75	0.195
0.40	0.070	4.25	0.112	90.08	0.183	196.33	0.196
0.48	0.070	8.00	0.123	99.92	0.187	216.42	0.198

Test	d (mm)	D_p (mm)	U_c (m/s)	U (m/s)	U/U_c	d/D_p	D_p/D_{50}	t_d (hour)	d_{se} (mm)	d_{se}/D_p
26	300	160	0.34	0.33	0.98	1.9	186.0	330	267.1	1.67

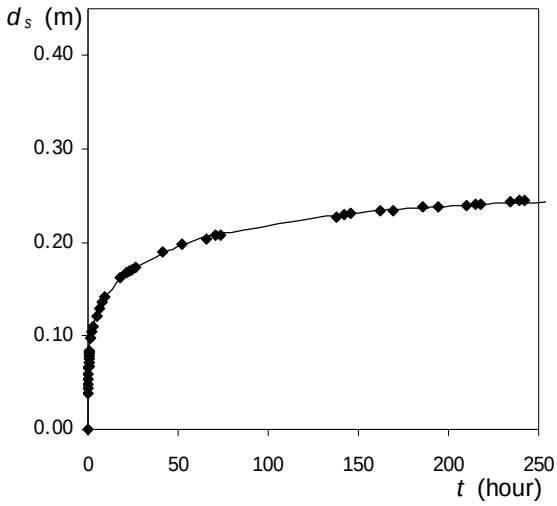

Test 26

t (hour)	d_s (m)	t (hour)	d_s (m)	t (hour)	d_s (m)	t (hour)	d_s (m)	t (hour)	d_s (m)
0.00	0.000	0.78	0.081	21.35	0.167	145.8	0.231	305.97	0.247
0.05	0.039	0.85	0.082	22.88	0.169	162.22	0.234	314.63	0.247
0.08	0.044	0.95	0.084	24.12	0.171	169.47	0.233	329.97	0.247
0.13	0.049	1.67	0.098	26.22	0.173	186.05	0.237		
0.18	0.053	2.37	0.105	41.38	0.190	194.22	0.238		
0.23	0.059	2.78	0.110	51.97	0.198	209.97	0.239		
0.32	0.066	4.92	0.122	65.72	0.204	214.8	0.241		
0.42	0.067	6.40	0.129	70.88	0.208	217.97	0.241		
0.47	0.071	7.53	0.137	73.72	0.208	234.05	0.244		
0.60	0.076	9.23	0.142	137.72	0.227	238.97	0.245		
0.68	0.078	18.05	0.163	142.47	0.230	242.05	0.245		

Test	d (mm)	D_p (mm)	U_c (m/s)	U (m/s)	U/U_c	d/D_p	D_p/D_{50}	t_d (hour)	d_{se} (mm)	d_{se}/D_p
27	400	200	0.35	0.33	0.95	2.0	232.6	219	329.4	1.65

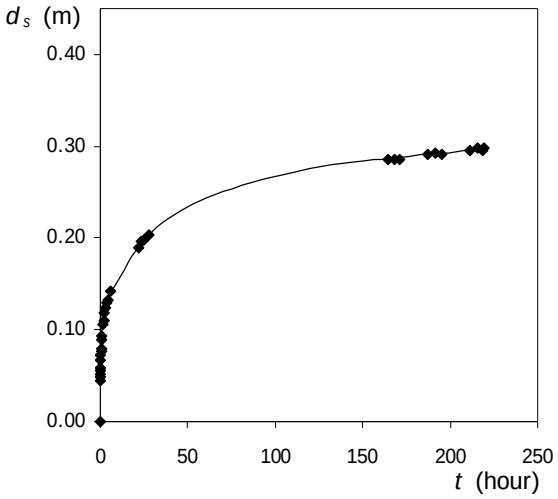

Test 27

t (hour)	d_s (m)	t (hour)	d_s (m)	t (hour)	d_s (m)	t (hour)	d_s (m)
0.00	0.000	0.88	0.093	27.68	0.203	215.35	0.299
0.03	0.045	1.38	0.105	40.00	0.222	218.38	0.296
0.07	0.048	1.87	0.110	70.00	0.251	219.02	0.298
0.10	0.052	2.52	0.118	120.00	0.275		
0.13	0.055	3.02	0.124	164.43	0.286		
0.17	0.059	3.70	0.130	168.18	0.286		
0.25	0.066	4.55	0.133	171.18	0.286		
0.33	0.072	5.75	0.142	187.27	0.291		
0.42	0.077	21.72	0.190	191.85	0.292		
0.50	0.080	23.68	0.197	195.02	0.291		
0.67	0.089	24.77	0.198	211.60	0.296		

Test	d (mm)	D_p (mm)	U_c (m/s)	U (m/s)	U/U_c	d/D_p	D_p/D_{50}	t_d (hour)	d_{se} (mm)	d_{se}/D_p
28	125	50	0.31	0.30	0.97	2.5	58.1	168	111.0	2.22

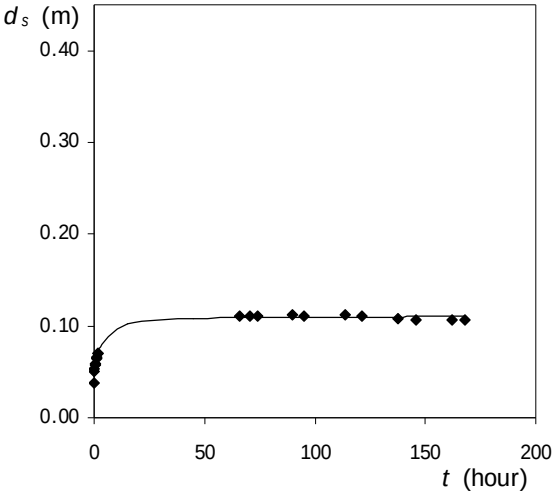

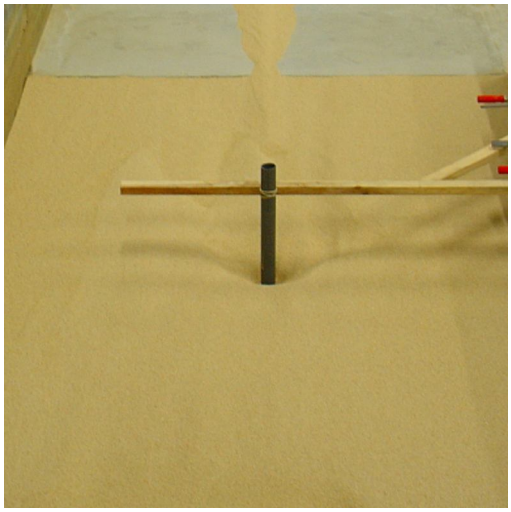

Test 28

t (hour)	d_s (m)	t (hour)	d_s (m)	t (hour)	d_s (m)
0.00	0.000	45.00	0.108	168.03	0.111
0.07	0.038	66.05	0.110		
0.20	0.051	70.47	0.111		
0.27	0.053	73.82	0.111		
0.42	0.057	89.97	0.112		
0.55	0.060	95.00	0.111		
0.88	0.065	113.63	0.112		
1.22	0.066	121.55	0.111		
1.55	0.070	137.88	0.111		
1.78	0.071	145.50	0.111		
15.00	0.103	162.08	0.111		

Test	d (mm)	D_p (mm)	U_c (m/s)	U (m/s)	U/U_c	d/D_p	D_p/D_{50}	t_d (hour)	d_{se} (mm)	d_{se}/D_p
29	188	75	0.32	0.31	0.96	2.5	87.2	191	146.7	1.96

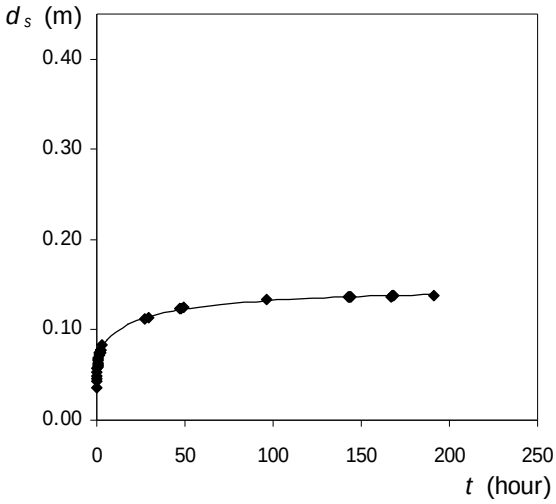

Test 29

t (hour)	d_s (m)	t (hour)	d_s (m)	t (hour)	d_s (m)	t (hour)	d_s (m)
0.00	0.000	0.85	0.066	3.08	0.083	143.73	0.137
0.05	0.036	0.97	0.068	6.00	0.089	144.22	0.137
0.10	0.043	1.10	0.069	18.00	0.106	166.82	0.137
0.15	0.046	1.22	0.071	27.13	0.112	167.28	0.138
0.20	0.050	1.38	0.073	29.70	0.113	167.75	0.138
0.28	0.054	1.55	0.074	46.82	0.124	168.25	0.138
0.37	0.057	1.72	0.075	47.53	0.124	190.93	0.138
0.45	0.059	1.90	0.075	49.18	0.125		
0.53	0.061	2.05	0.077	96.30	0.134		
0.62	0.062	2.22	0.078	142.80	0.136		
0.73	0.064	2.38	0.078	143.23	0.137		

Test	d (mm)	D_p (mm)	U_c (m/s)	U (m/s)	U/U_c	d/D_p	D_p/D_{50}	t_d (hour)	d_{se} (mm)	d_{se}/D_p
30	275	110	0.33	0.33	0.98	2.5	127.9	184	234.3	2.13

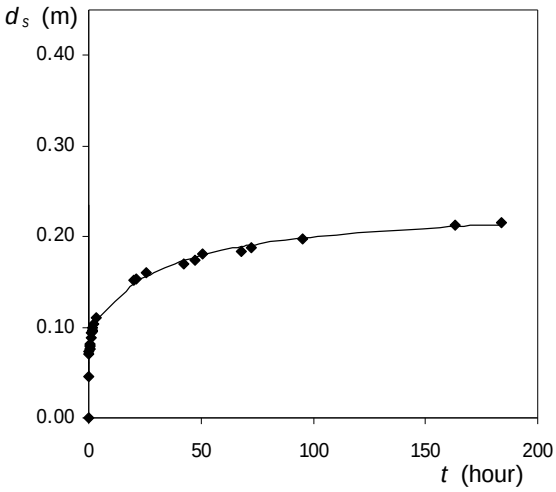

Test 30

t (hour)	d_s (m)	t (hour)	d_s (m)	t (hour)	d_s (m)
0.00	0.000	1.42	0.095	68.00	0.184
0.07	0.045	1.67	0.097	72.42	0.188
0.15	0.070	1.92	0.100	95.33	0.198
0.25	0.073	2.42	0.104	163.50	0.213
0.37	0.076	3.17	0.110	184.10	0.216
0.43	0.076	19.78	0.151		
0.50	0.079	20.92	0.153		
0.58	0.080	25.50	0.161		
0.67	0.081	42.13	0.170		
0.92	0.088	47.22	0.174		
1.17	0.094	50.50	0.181		

Test	d (mm)	D_p (mm)	U_c (m/s)	U (m/s)	U/U_c	d/D_p	D_p/D_{50}	t_d (hour)	d_{se} (mm)	d_{se}/D_p
31	375	160	0.34	0.33	0.96	2.3	186.0	313	278.8	1.74

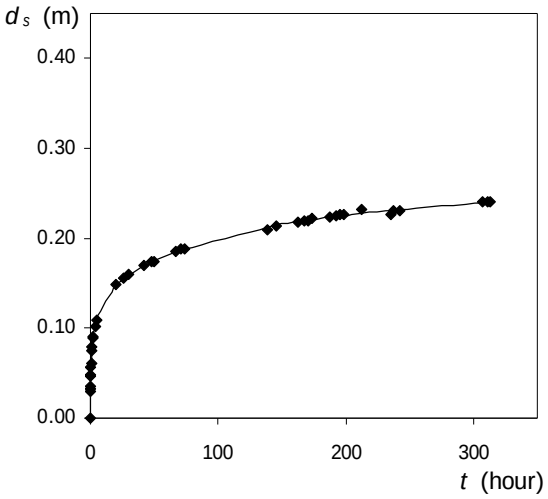

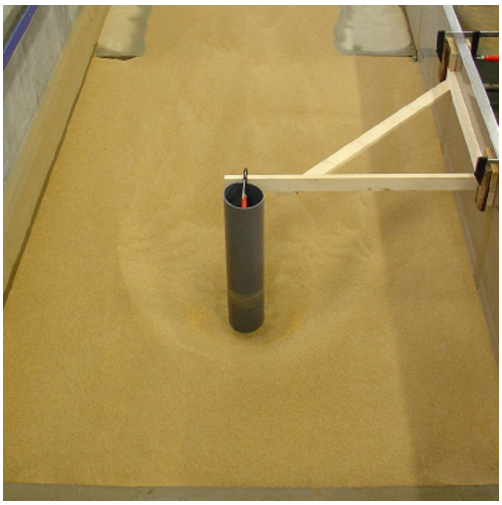

Test 31

t (hour)	d_s (m)	t (hour)	d_s (m)	t (hour)	d_s (m)	t (hour)	d_s (m)
0.00	0.000	2.33	0.090	73.40	0.188	212.72	0.232
0.03	0.029	3.97	0.102	138.32	0.210	235.15	0.227
0.07	0.033	4.95	0.109	146.07	0.213	237.15	0.230
0.10	0.036	19.93	0.148	162.40	0.218	241.90	0.230
0.15	0.047	26.30	0.155	167.40	0.220	306.73	0.241
0.23	0.048	29.48	0.160	170.32	0.219	311.15	0.240
0.42	0.057	42.17	0.169	174.00	0.222	312.90	0.240
0.52	0.061	47.50	0.174	187.32	0.224		
0.95	0.074	49.57	0.174	192.35	0.226		
1.27	0.079	66.73	0.185	195.38	0.226		
1.90	0.089	71.15	0.189	198.35	0.227		

Test	d (mm)	D_p (mm)	U_c (m/s)	U (m/s)	U/U_c	d/D_p	D_p/D_{50}	t_d (hour)	d_{se} (mm)	d_{se}/D_p
32	150	50	0.31	0.30	0.96	3.0	58.1	173	109.7	2.19

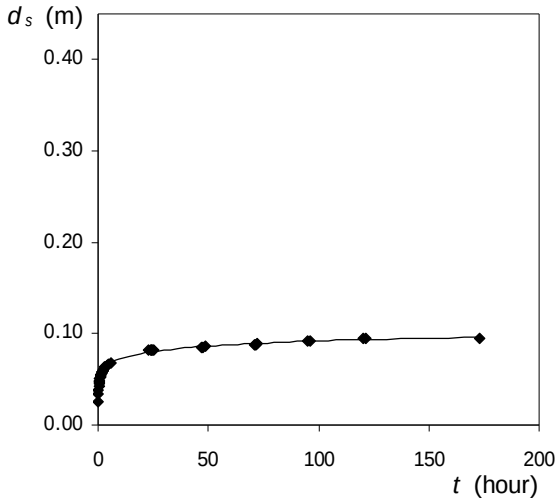

Test 32

t (hour)	d_s (m)	t (hour)	d_s (m)	t (hour)	d_s (m)	t (hour)	d_s (m)
0.00	0.000	1.05	0.054	4.15	0.065	70.92	0.088
0.07	0.025	1.22	0.054	4.92	0.066	71.35	0.088
0.13	0.034	1.38	0.056	6.07	0.068	72.18	0.089
0.22	0.038	1.55	0.056	23.08	0.082	95.27	0.092
0.30	0.042	1.72	0.058	23.80	0.082	96.28	0.092
0.38	0.045	1.88	0.059	24.20	0.082	120.30	0.095
0.47	0.046	2.10	0.059	24.80	0.082	121.40	0.095
0.55	0.048	2.22	0.060	25.25	0.082	173.17	0.095
0.63	0.048	2.38	0.061	46.88	0.086		
0.72	0.051	3.03	0.063	47.53	0.086		
0.88	0.052	3.52	0.063	48.72	0.086		

Test	d (mm)	D_p (mm)	U_c (m/s)	U (m/s)	U/U_c	d/D_p	D_p/D_{50}	t_d (hour)	d_{se} (mm)	d_{se}/D_p
33	225	75	0.33	0.33	1.01	3.0	87.2	197	170.6	2.27

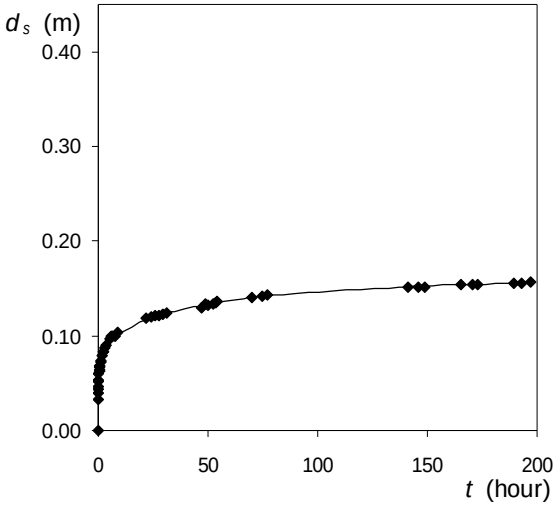

Test 33

t (hour)	d_s (m)	t (hour)	d_s (m)	t (hour)	d_s (m)	t (hour)	d_s (m)	t (hour)	d_s (m)
0.00	0.000	0.62	0.068	6.58	0.100	50.25	0.133	165.50	0.154
0.03	0.033	0.78	0.069	7.92	0.100	52.25	0.133	170.67	0.154
0.07	0.039	0.97	0.074	8.58	0.103	53.25	0.135	173.17	0.154
0.10	0.044	1.08	0.072	21.75	0.118	54.08	0.137	189.58	0.156
0.13	0.047	1.58	0.079	24.25	0.120	69.83	0.141	192.92	0.156
0.17	0.051	2.08	0.083	25.67	0.121	74.45	0.142	196.87	0.156
0.20	0.053	2.58	0.083	27.67	0.121	76.83	0.143		
0.28	0.060	3.08	0.088	29.58	0.123	96.00	0.146		
0.37	0.063	3.58	0.090	31.08	0.124	141.42	0.152		
0.45	0.064	5.08	0.097	47.00	0.130	146.08	0.152		
0.53	0.067	6.08	0.099	48.67	0.134	149.08	0.152		

Test	d (mm)	D_p (mm)	U_c (m/s)	U (m/s)	U/U_c	d/D_p	D_p/D_{50}	t_d (hour)	d_{se} (mm)	d_{se}/D_p
34	330	110	0.34	0.33	0.96	3.0	127.9	169	222.6	2.02

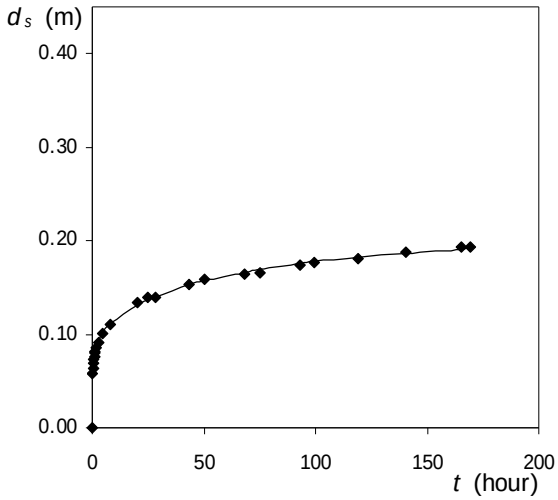

Test 34

t (hour)	d_s (m)	t (hour)	d_s (m)	t (hour)	d_s (m)
0.00	0.000	8.00	0.110	140.42	0.187
0.23	0.058	20.08	0.134	165.25	0.193
0.32	0.063	24.62	0.139	169.40	0.193
0.43	0.068	28.23	0.140		
0.70	0.074	43.50	0.153		
0.88	0.076	50.25	0.159		
1.07	0.080	68.20	0.164		
1.25	0.081	75.42	0.166		
1.77	0.085	93.08	0.174		
2.67	0.091	99.53	0.176		
4.72	0.101	119.05	0.181		

Test	d (mm)	D_p (mm)	U_c (m/s)	U (m/s)	U/U_c	d/D_p	D_p/D_{50}	t_d (hour)	d_{se} (mm)	d_{se}/D_p
35	200	50	0.32	0.31	0.96	4.0	58.1	170	133.7	2.67

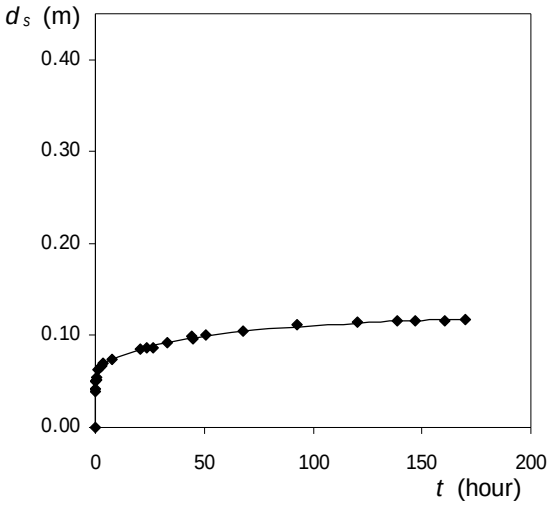

Test 35

t (hour)	d_s (m)	t (hour)	d_s (m)	t (hour)	d_s (m)
0.00	0.000	20.42	0.085	147.15	0.116
0.07	0.040	23.60	0.086	160.33	0.116
0.13	0.042	26.40	0.087	170.10	0.118
0.25	0.051	33.32	0.092		
0.38	0.052	44.45	0.099		
0.53	0.055	44.77	0.097		
1.43	0.063	50.78	0.100		
2.12	0.065	67.78	0.104		
3.00	0.067	92.82	0.111		
3.57	0.070	120.28	0.114		
7.83	0.074	138.37	0.115		

Test	d (mm)	D_p (mm)	U_c (m/s)	U (m/s)	U/U_c	d/D_p	D_p/D_{50}	t_d (hour)	d_{se} (mm)	d_{se}/D_p
36	300	75	0.34	0.33	0.98	4.0	87.2	314	197.6	2.63

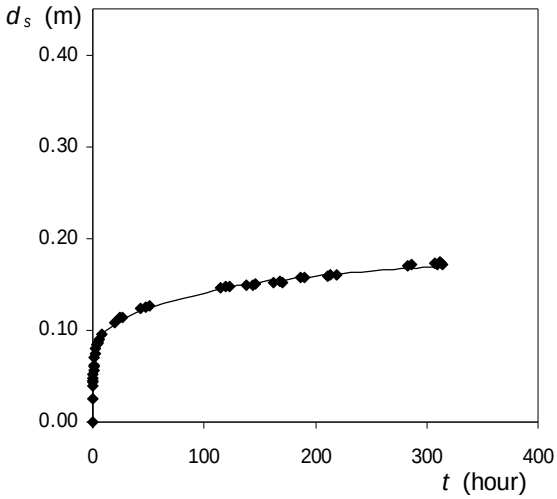

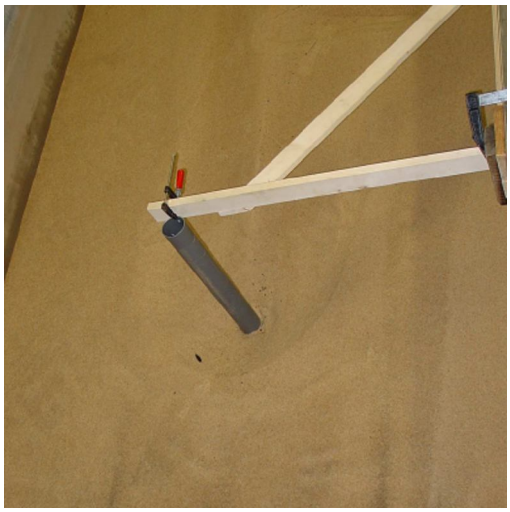

Test 36

t (hour)	d_s (m)	t (hour)	d_s (m)	t (hour)	d_s (m)	t (hour)	d_s (m)	t (hour)	d_s (m)
0.00	0.000	1.87	0.074	47.98	0.125	186.23	0.157	314.33	0.172
0.05	0.026	2.60	0.080	50.90	0.127	190.15	0.158		
0.13	0.040	3.10	0.084	114.82	0.146	210.57	0.159		
0.18	0.044	4.15	0.086	119.73	0.147	213.73	0.160		
0.23	0.045	4.87	0.087	122.90	0.147	219.40	0.160		
0.32	0.048	5.57	0.090	138.40	0.149	282.90	0.170		
0.40	0.052	7.73	0.095	143.57	0.149	285.90	0.171		
0.58	0.056	19.23	0.108	146.65	0.150	306.90	0.173		
0.75	0.061	23.90	0.114	162.82	0.152	310.05	0.171		
0.92	0.062	26.65	0.113	167.65	0.153	311.90	0.174		
1.47	0.070	43.32	0.124	170.65	0.152	312.67	0.173		

Test	d (mm)	D_p (mm)	U_c (m/s)	U (m/s)	U/U_c	d/D_p	D_p/D_{50}	t_d (hour)	d_{se} (mm)	d_{se}/D_p
37	250	50	0.33	0.33	1.00	5.0	58.1	237	116.6	2.33

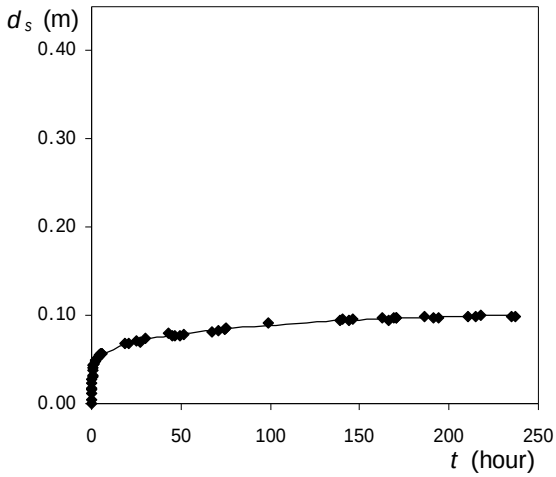

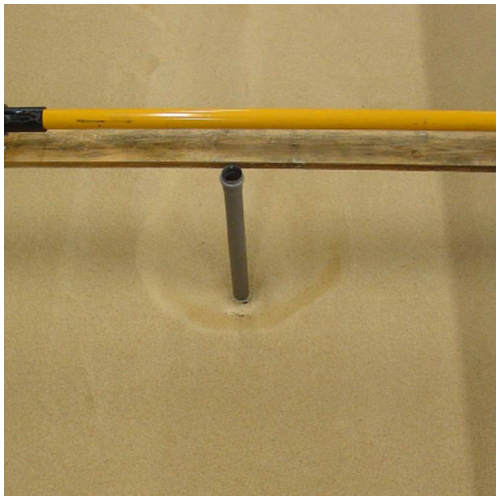

Test 37

t (hour)	d_s (m)	t (hour)	d_s (m)	t (hour)	d_s (m)	t (hour)	d_s (m)	t (hour)	d_s (m)
0.00	0.000	0.97	0.043	5.97	0.057	67.38	0.082	168.80	0.098
0.03	0.005	1.47	0.046	18.75	0.068	70.85	0.082	170.15	0.097
0.07	0.012	1.97	0.047	21.05	0.068	74.75	0.084	170.17	0.097
0.12	0.016	2.47	0.049	25.40	0.071	75.42	0.085	186.47	0.099
0.13	0.018	2.80	0.051	27.08	0.070	98.85	0.091	191.03	0.098
0.22	0.023	2.88	0.051	30.03	0.075	138.72	0.095	193.97	0.098
0.30	0.028	3.47	0.052	43.30	0.080	140.47	0.096	210.62	0.099
0.38	0.030	3.97	0.054	45.08	0.077	144.30	0.095	215.07	0.099
0.47	0.031	4.47	0.055	46.80	0.077	146.38	0.096	218.05	0.100
0.63	0.037	4.97	0.056	49.37	0.077	162.93	0.097	234.63	0.099
0.80	0.040	5.47	0.057	51.33	0.078	165.97	0.095	236.87	0.099

Test	d (mm)	D_p (mm)	U_c (m/s)	U (m/s)	U/U_c	d/D_p	D_p/D_{50}	t_d (hour)	d_{se} (mm)	d_{se}/D_p
38	375	75	0.34	0.33	0.96	5.0	87.2	315	184.3	2.46

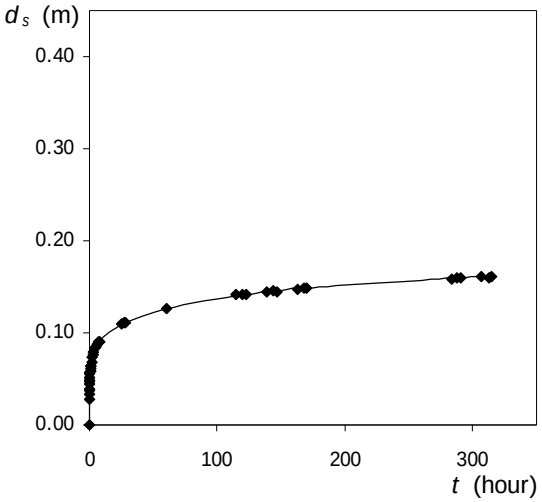

Test 38

t (hour)	d_s (m)	t (hour)	d_s (m)	t (hour)	d_s (m)	t (hour)	d_s (m)
0.00	0.000	0.60	0.058	6.77	0.090	147.17	0.145
0.05	0.028	0.77	0.061	7.58	0.091	162.83	0.148
0.08	0.034	0.92	0.064	25.13	0.110	167.67	0.149
0.12	0.038	1.08	0.065	27.32	0.111	170.25	0.148
0.15	0.039	1.58	0.068	28.18	0.111	283.25	0.158
0.18	0.044	2.08	0.074	60.00	0.126	287.83	0.160
0.22	0.047	2.78	0.077	115.08	0.141	290.75	0.160
0.25	0.049	3.27	0.079	119.50	0.142	306.75	0.162
0.38	0.051	4.08	0.084	123.00	0.142	312.83	0.160
0.42	0.055	4.58	0.085	138.92	0.144	314.67	0.161
0.50	0.057	5.58	0.088	143.58	0.146		

Reference tests at single cylindrical piers

Test	d (mm)	D_p (mm)	D_{50} (m/s)	U (m/s)	U/U_c	d/D_p	D_p/D_{50}	t_d (hour)	d_{se} (mm)	d_{se}/D_p
R1	50	110	0.86	0.27	0.97	0.45	127.9	168	157	1.43

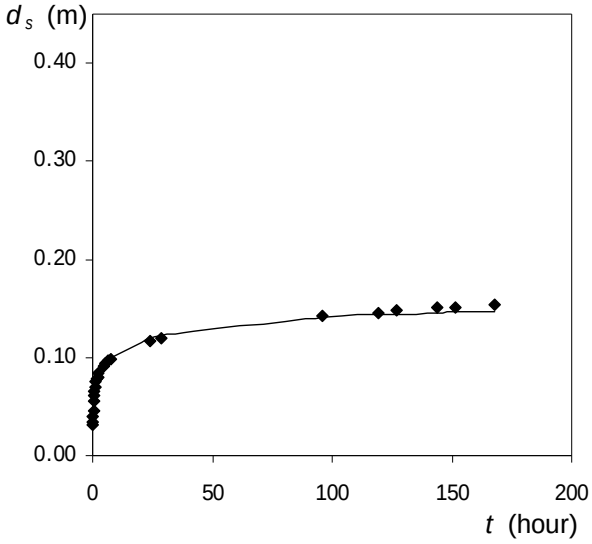

Test R1

t (hour)	d_s (m)	t (hour)	d_s (m)	t (hour)	d_s (m)
0.00	0.000	2.07	0.080	143.68	0.151
0.03	0.031	2.53	0.084	151.43	0.151
0.13	0.034	4.63	0.091	167.98	0.154
0.25	0.040	5.35	0.094		
0.33	0.046	6.32	0.096		
0.47	0.055	7.48	0.099		
0.68	0.061	23.92	0.117		
0.87	0.066	28.50	0.120		
1.05	0.070	96.07	0.142		
1.33	0.075	119.53	0.145		
1.53	0.078	126.82	0.148		

Test	d (mm)	D_p (mm)	D_{50} (m/s)	U (m/s)	U/U_c	d/D_p	D_p/D_{50}	t_d (hour)	d_{se} (mm)	d_{se}/D_p
R2	80	75	0.86	0.29	0.97	1.07	87.2	168	160	2.13

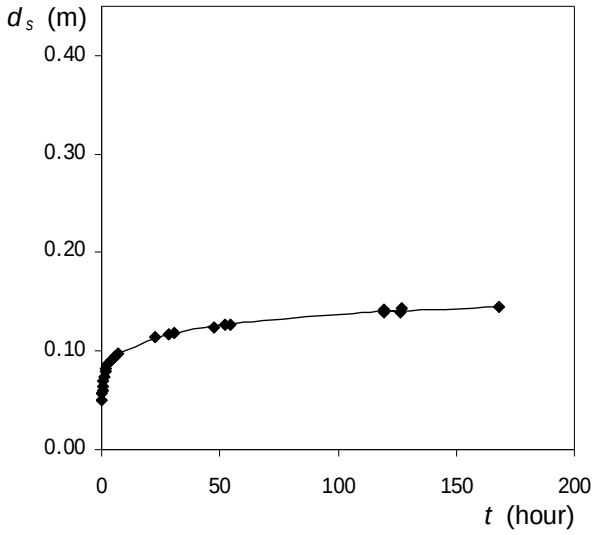

Test R2

t (hour)	d_s (m)	t (hour)	d_s (m)	t (hour)	d_s (m)
0.00	0.000	5.03	0.094	119.13	0.142
0.12	0.051	6.00	0.095	126.93	0.143
0.20	0.057	6.90	0.098	167.97	0.144
0.32	0.060	22.85	0.114		
0.40	0.064	28.17	0.117		
0.68	0.069	30.87	0.118		
0.93	0.074	47.40	0.124		
1.55	0.079	52.20	0.127		
1.95	0.082	54.67	0.127		
2.45	0.086	119.18	0.139		
3.78	0.090	126.62	0.139		

Test	d (mm)	D_p (mm)	D_{50} (m/s)	U (m/s)	U/U_c	d/D_p	D_p/D_{50}	t_d (hour)	d_{se} (mm)	d_{se}/D_p
R3	110	75	0.86	0.29	0.97	1.47	87.2	168	155	2.07

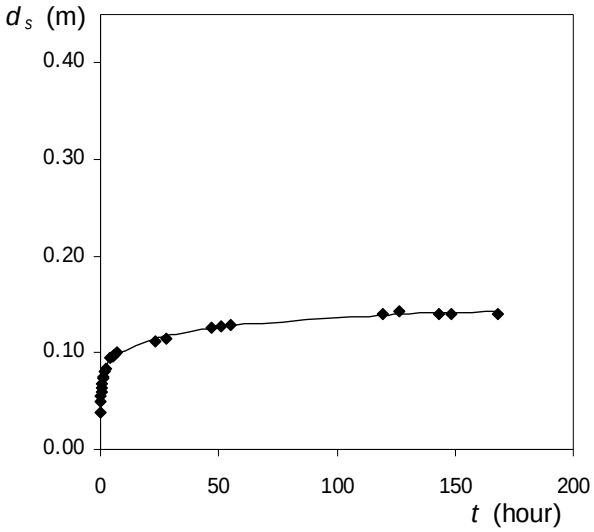

Test R3

t (hour)	d_s (m)	t (hour)	d_s (m)	t (hour)	d_s (m)
0.00	0.000	4.28	0.094	143.10	0.141
0.08	0.039	4.98	0.096	148.67	0.141
0.17	0.049	5.98	0.098	167.95	0.141
0.27	0.055	7.07	0.100		
0.35	0.059	23.23	0.112		
0.45	0.063	28.10	0.115		
0.70	0.068	47.22	0.126		
1.00	0.073	51.25	0.128		
1.18	0.075	55.00	0.129		
1.73	0.080	119.70	0.140		
2.20	0.084	126.47	0.142		

Test	d (mm)	D_p (mm)	D_{50} (m/s)	U (m/s)	U/U_c	d/D_p	D_p/D_{50}	t_d (hour)	d_{se} (mm)	d_{se}/D_p
R4	113	250	0.86	0.30	0.97	0.45	290.7	168	282	1.13

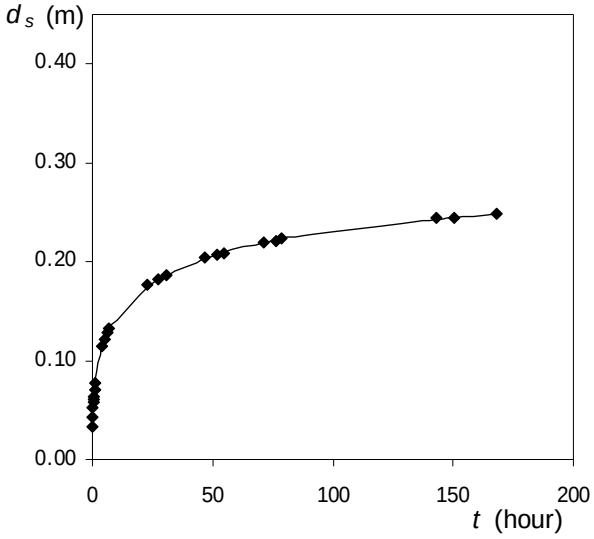

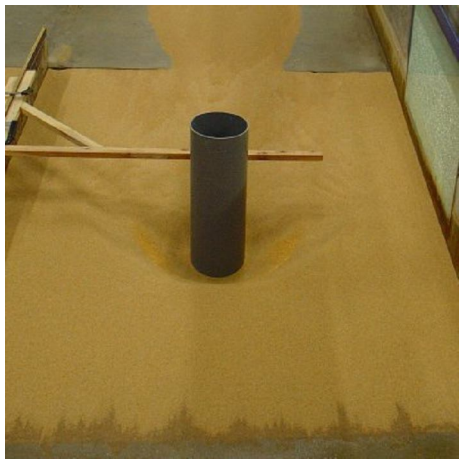

Test R4

t (hour)	d_s (m)	t (hour)	d_s (m)	t (hour)	d_s (m)
0.00	0.000	6.07	0.128	143.10	0.244
0.08	0.033	6.90	0.132	150.40	0.245
0.18	0.043	22.93	0.176	168.20	0.249
0.28	0.052	27.50	0.182		
0.43	0.057	30.50	0.187		
0.55	0.060	46.78	0.204		
0.68	0.064	51.82	0.207		
0.93	0.070	54.58	0.208		
1.40	0.077	70.97	0.219		
3.90	0.114	76.08	0.221		
5.07	0.121	78.73	0.223		

Test	d (mm)	D_p (mm)	D_{50} (m/s)	U (m/s)	U/U_c	d/D_p	D_p/D_{50}	t_d (hour)	d_{se} (mm)	d_{se}/D_p
R5	75	160	0.86	0.28	0.97	0.47	186.0	168	240	1.50

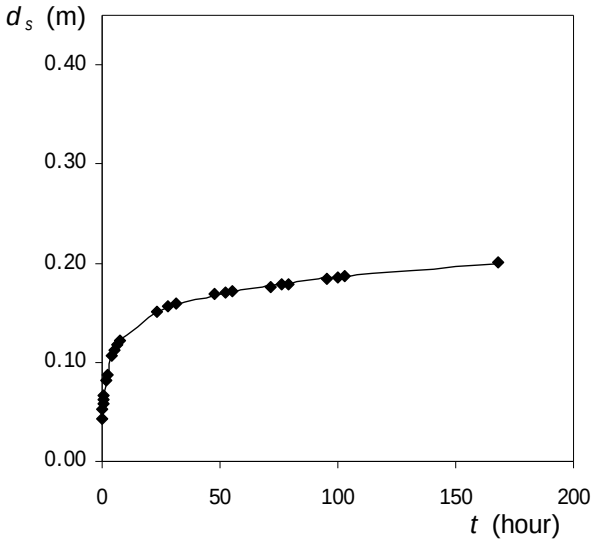

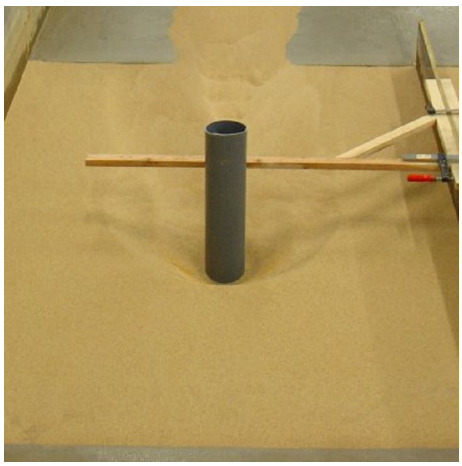

Test R5

t (hour)	d_s (m)	t (hour)	d_s (m)	t (hour)	d_s (m)
0.00	0.000	7.30	0.122	100.17	0.185
0.07	0.042	23.22	0.151	103.18	0.186
0.17	0.052	28.15	0.157	168.03	0.201
0.30	0.058	31.32	0.159		
0.52	0.063	47.48	0.169		
0.67	0.067	52.08	0.170		
1.65	0.082	55.18	0.172		
2.07	0.087	71.52	0.177		
4.25	0.107	76.17	0.179		
5.32	0.112	79.30	0.179		
6.43	0.118	95.53	0.184		

Test	d (mm)	D_p (mm)	D_{50} (m/s)	U (m/s)	U/U_c	d/D_p	D_p/D_{50}	t_d (hour)	d_{se} (mm)	d_{se}/D_p
R6	200	100	0.86	0.31	0.96	2.00	116.3	168	218	2.18

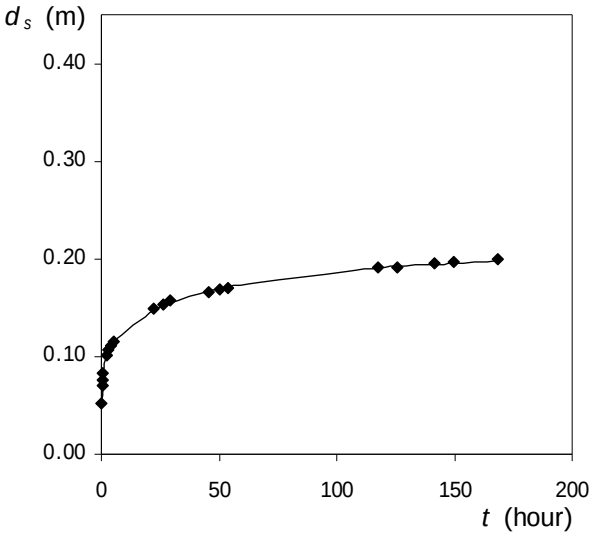

Test R6

t (hour)	d_s (m)	t (hour)	d_s (m)
0.00	0.000	29.12	0.157
0.10	0.052	45.58	0.166
0.33	0.070	50.20	0.169
0.53	0.076	53.72	0.171
0.82	0.083	117.53	0.191
2.30	0.101	125.62	0.192
3.07	0.107	141.72	0.195
4.12	0.111	149.65	0.196
5.32	0.116	168.43	0.199
22.05	0.149		
26.50	0.154		

Test	d (mm)	D_p (mm)	D_{50} (m/s)	U (m/s)	U/U_c	d/D_p	D_p/D_{50}	t_d (hour)	d_{se} (mm)	d_{se}/D_p
R7	200	150	0.86	0.31	0.96	1.33	174.4	168	252	1.68

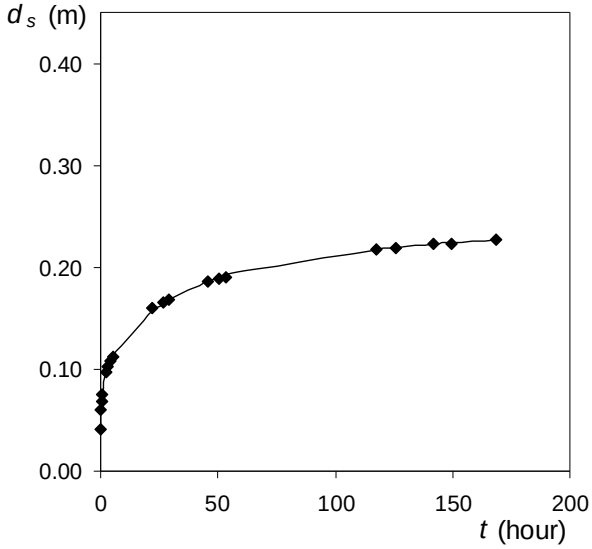

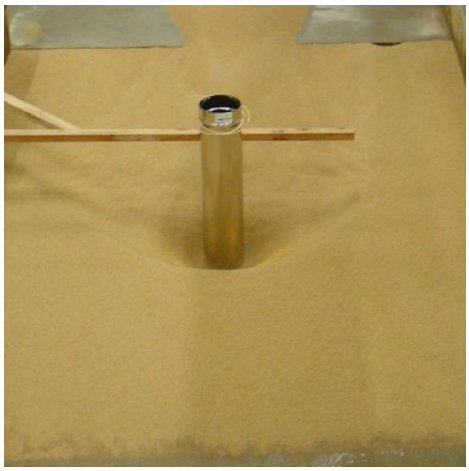

Test R7

t (hour)	d_s (m)	t (hour)	d_s (m)
0.00	0.000	29.10	0.168
0.08	0.041	45.53	0.186
0.28	0.060	50.18	0.189
0.52	0.068	53.67	0.191
0.77	0.075	117.52	0.218
2.28	0.097	125.57	0.219
3.02	0.102	141.70	0.223
4.10	0.108	149.60	0.224
5.27	0.113	168.42	0.228
22.03	0.160		
26.45	0.165		

APENDIX B – TESTS AT PILE GROUPS

Test	α (º)	s (m)	s/D_p	n	W_g (m)	t_d (day)	d_{sge} (m)	d_{sge}/d_{se1}
1	0	0.050	1.0	1	0.050	11.01	0.153	1.13

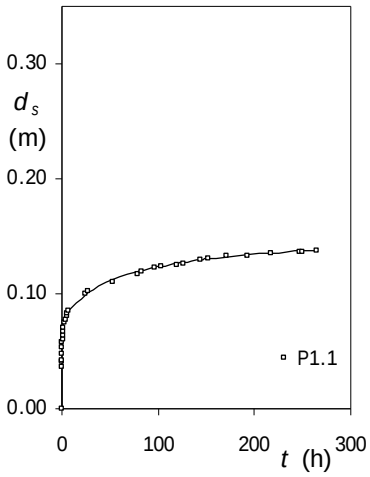

Test 1

P1.1		P2.1		P3.1		P4.1	
t (h)	d_s (m)	t (h)	d_s (m)	t (h)	d_s (m)	t (h)	d_s (m)
0.00	0.000						
0.02	0.037						
0.05	0.041						
0.08	0.043						
0.17	0.048						
0.33	0.054						
0.50	0.059						
0.75	0.061						
1.00	0.064						
1.50	0.068						
2.00	0.071						
3.00	0.075						
5.00	0.081						
6.00	0.083						
7.00	0.086						
24.00	0.100						
27.00	0.103						
52.70	0.111						
78.62	0.118						
96.00	0.123						
103.28	0.124						
120.00	0.126						
125.88	0.127						
144.00	0.130						
152.23	0.131						
170.70	0.133						
192.65	0.134						
216.87	0.136						
246.80	0.137						
250.37	0.137						
264.20	0.138						

Test	α (º)	s (m)	s/D_p	n	W_g (m)	t_d (day)	d_{sge} (m)	d_{sge}/d_{se1}
2	0	0.100	2.0	1	0.050	16.00	0.160	1.18

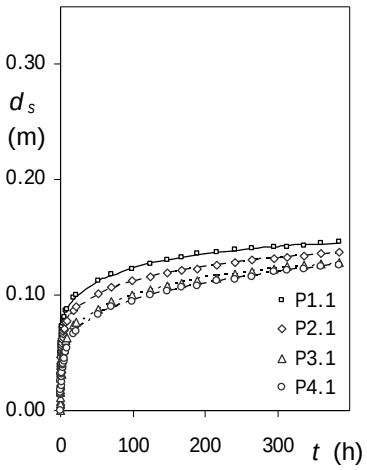

Test 2

P1.1		P2.1		P3.1		P4.1	
t (h)	d_s (m)	t (h)	d_s (m)	t (h)	d_s (m)	t (h)	d_s (m)
0.00	0.000	0.00	0.000	0.00	0.000	0.00	0.000
0.02	0.033	0.02	0.018	0.02	0.008	0.02	0.032
0.05	0.038	0.05	0.021	0.05	0.006	0.05	0.031
0.08	0.041	0.08	0.026	0.08	0.006	0.08	0.026
0.17	0.046	0.17	0.029	0.17	0.011	0.17	0.016
0.25	0.049	0.25	0.036	0.25	0.016	0.25	0.013
0.33	0.051	0.33	0.038	0.33	0.018	0.33	0.015
0.50	0.055	0.50	0.041	0.50	0.022	0.50	0.016
1.33	0.065	1.33	0.054	1.33	0.036	1.33	0.025
2.00	0.071	2.00	0.059	2.00	0.042	2.00	0.031
3.00	0.075	3.00	0.063	3.00	0.047	3.00	0.037
4.00	0.079	4.00	0.069	4.00	0.052	4.00	0.041
5.00	0.081	5.00	0.071	5.00	0.055	5.00	0.045
8.50	0.088	8.50	0.078	8.50	0.063	8.50	0.054
18.50	0.098	18.50	0.087	18.50	0.074	18.50	0.066
21.50	0.100	21.50	0.090	21.50	0.077	21.50	0.069
51.75	0.113	51.75	0.101	51.75	0.088	51.75	0.083
69.50	0.118	69.50	0.107	69.50	0.094	69.50	0.090
99.50	0.123	99.50	0.112	99.50	0.100	99.50	0.095
124.50	0.127	124.50	0.116	124.50	0.105	124.50	0.100
148.00	0.130	148.00	0.119	148.00	0.108	148.00	0.104
168.00	0.133	168.00	0.121	168.00	0.110	168.00	0.107
189.00	0.136	189.00	0.123	189.00	0.113	189.00	0.108
216.00	0.137	216.00	0.126	216.00	0.115	216.00	0.112
240.00	0.139	240.00	0.128	240.00	0.118	240.00	0.114
264.00	0.141	264.00	0.130	264.00	0.120	264.00	0.116
294.00	0.142	294.00	0.132	294.00	0.123	294.00	0.120
312.00	0.142	312.00	0.133	312.00	0.125	312.00	0.122
336.00	0.143	336.00	0.134	336.00	0.126	336.00	0.123
360.00	0.145	360.00	0.136	360.00	0.127	360.00	0.125
384.00	0.146	384.00	0.137	384.00	0.128	384.00	0.126

Test	α (º)	s (m)	s/D_p	n	W_g (m)	t_d (day)	d_{sge} (m)	d_{sge}/d_{se1}
3	0	0.150	3.0	1	0.050	13.66	0.152	1.12

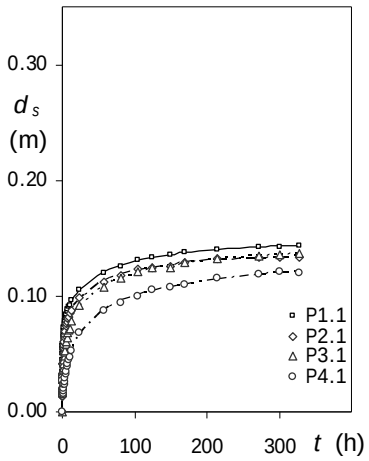

Test 3

P1.1		P2.1		P3.1		P4.1	
t (h)	d_s (m)	t (h)	d_s (m)	t (h)	d_s (m)	t (h)	d_s (m)
0.00	0.000	0.00	0.000	0.00	0.000	0.00	0.000
0.02	0.031	0.02	0.014	0.02	0.024	0.02	0.031
0.05	0.035	0.05	0.013	0.05	0.022	0.05	0.030
0.08	0.040	0.08	0.014	0.08	0.019	0.08	0.029
0.17	0.045	0.17	0.014	0.17	0.018	0.17	0.027
0.33	0.050	0.33	0.028	0.33	0.019	0.33	0.017
0.50	0.055	0.50	0.033	0.50	0.022	0.50	0.015
0.75	0.057	0.75	0.041	0.75	0.028	0.75	0.015
1.00	0.062	1.00	0.045	1.00	0.032	1.00	0.015
1.67	0.066	1.67	0.055	1.67	0.038	1.67	0.018
2.00	0.069	2.00	0.057	2.00	0.041	2.00	0.020
2.50	0.073	2.50	0.061	2.50	0.045	2.50	0.023
3.00	0.075	3.00	0.064	3.00	0.048	3.00	0.024
4.00	0.079	4.00	0.069	4.00	0.053	4.00	0.029
5.00	0.081	5.00	0.074	5.00	0.058	5.00	0.032
6.00	0.084	6.00	0.076	6.00	0.061	6.00	0.035
7.00	0.086	7.00	0.077	7.00	0.064	7.00	0.039
8.00	0.089	8.00	0.081	8.00	0.068	8.00	0.042
9.00	0.091	9.00	0.082	9.00	0.071	9.00	0.045
10.00	0.092	10.00	0.085	10.00	0.072	10.00	0.047
13.00	0.096	13.00	0.088	13.00	0.078	13.00	0.053
24.00	0.105	24.00	0.099	24.00	0.092	24.00	0.068
56.72	0.120	56.72	0.112	56.72	0.108	56.72	0.088
80.38	0.126	80.38	0.118	80.38	0.115	80.38	0.094
104.13	0.131	104.13	0.123	104.13	0.121	104.13	0.100
124.38	0.134	124.38	0.125	124.38	0.124	124.38	0.105
169.80	0.138	169.80	0.129	169.80	0.129	169.80	0.110
214.38	0.140	214.38	0.132	214.38	0.132	214.38	0.116
271.22	0.142	271.22	0.133	271.22	0.135	271.22	0.119
299.88	0.143	299.88	0.133	299.88	0.136	299.88	0.121
327.88	0.144	327.88	0.134	327.88	0.137	327.88	0.120

Test	α (º)	s (m)	s/D_p	n	W_g (m)	t_d (day)	d_{sge} (m)	d_{sge}/d_{se1}
4	0	0.225	4.5	1	0.050	16.23	0.149	1.09

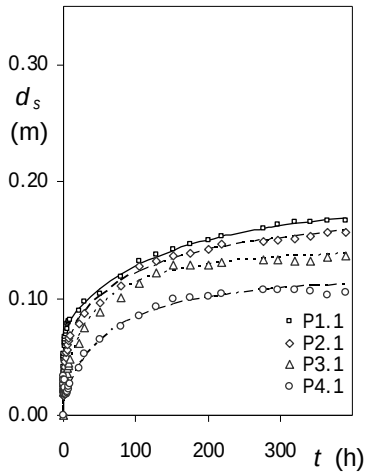

Test 4

P1.1		P2.1		P3.1		P4.1	
t (h)	d_s (m)	t (h)	d_s (m)	t (h)	d_s (m)	t (h)	d_s (m)
0.00	0.000	0.00	0.000	0.00	0.000	0.00	0.000
0.05	0.033	0.05	0.021	0.05	0.022	0.05	0.026
0.08	0.037	0.08	0.021	0.08	0.023	0.08	0.027
0.17	0.041	0.17	0.017	0.17	0.025	0.17	0.030
0.33	0.048	0.33	0.017	0.33	0.028	0.33	0.033
0.50	0.050	0.50	0.020	0.50	0.026	0.50	0.030
1.00	0.059	1.00	0.029	1.00	0.020	1.00	0.030
1.33	0.061	1.33	0.036	1.33	0.020	1.33	0.023
1.67	0.063	1.67	0.038	1.67	0.022	1.67	0.018
2.00	0.065	2.00	0.041	2.00	0.024	2.00	0.018
3.00	0.069	3.00	0.049	3.00	0.027	3.00	0.018
4.00	0.072	4.00	0.054	4.00	0.031	4.00	0.018
5.00	0.074	5.00	0.056	5.00	0.036	5.00	0.019
7.00	0.079	7.00	0.064	7.00	0.043	7.00	0.022
9.00	0.082	9.00	0.068	9.00	0.048	9.00	0.027
22.18	0.090	22.18	0.078	22.18	0.062	22.18	0.040
29.43	0.097	29.43	0.087	29.43	0.075	29.43	0.052
50.00	0.104	50.00	0.096	50.00	0.088	50.00	0.065
79.68	0.119	79.68	0.111	79.68	0.101	79.68	0.076
104.18	0.132	104.18	0.128	104.18	0.113	104.18	0.085
128.00	0.137	128.00	0.132	128.00	0.122	128.00	0.093
151.70	0.142	151.70	0.136	151.70	0.129	151.70	0.100
176.00	0.146	176.00	0.139	176.00	0.129	176.00	0.101
200.18	0.150	200.18	0.142	200.18	0.129	200.18	0.102
218.38	0.153	218.38	0.146	218.38	0.131	218.38	0.104
275.43	0.160	275.43	0.149	275.43	0.133	275.43	0.107
296.00	0.163	296.00	0.150	296.00	0.133	296.00	0.107
319.47	0.165	319.47	0.151	319.47	0.132	319.47	0.107
341.47	0.165	341.47	0.153	341.47	0.132	341.47	0.106
365.47	0.167	365.47	0.157	365.47	0.135	365.47	0.103
389.47	0.167	389.47	0.157	389.47	0.136	389.47	0.105

Test	α (º)	s (m)	s/D_p	n	W_g (m)	t_d (day)	d_{sge} (m)	d_{sge}/d_{se1}
5	0	0.300	6.0	1	0.050	11.23	0.136	1.00

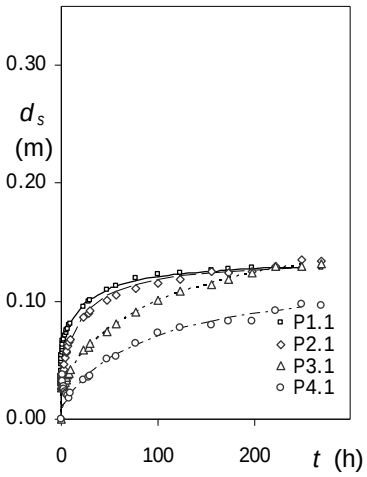

Test 5

P1.1		P2.1		P3.1		P4.1	
t (h)	d_s (m)	t (h)	d_s (m)	t (h)	d_s (m)	t (h)	d_s (m)
0.00	0.000	0.00	0.000	0.00	0.000	0.00	0.000
0.03	0.036	0.03	0.026	0.03	0.027	0.03	0.033
0.08	0.041	0.08	0.029	0.08	0.029	0.08	0.034
0.17	0.046	0.17	0.031	0.17	0.032	0.17	0.035
0.25	0.049	0.25	0.032	0.25	0.033	0.25	0.036
0.33	0.051	0.33	0.032	0.33	0.033	0.33	0.036
0.50	0.054	0.50	0.031	0.50	0.035	0.50	0.036
0.75	0.056	0.75	0.033	0.75	0.034	0.75	0.037
1.00	0.059	1.00	0.035	1.00	0.035	1.00	0.038
1.67	0.063	1.67	0.039	1.67	0.028	1.67	0.031
2.00	0.066	2.00	0.040	2.00	0.028	2.00	0.032
3.00	0.068	3.00	0.046	3.00	0.029	3.00	0.025
3.75	0.071	3.75	0.052	3.75	0.031	3.75	0.023
4.75	0.073	4.75	0.056	4.75	0.033	4.75	0.022
7.00	0.076	7.00	0.062	7.00	0.038	7.00	0.020
8.00	0.080	8.00	0.065	8.00	0.039	8.00	0.018
10.00	0.081	10.00	0.068	10.00	0.042	10.00	0.022
23.50	0.095	23.50	0.086	23.50	0.059	23.50	0.033
28.50	0.100	28.50	0.090	28.50	0.061	28.50	0.035
30.00	0.101	30.00	0.092	30.00	0.064	30.00	0.037
47.50	0.110	47.50	0.101	47.50	0.074	47.50	0.051
57.00	0.113	57.00	0.105	57.00	0.081	57.00	0.053
76.50	0.120	76.50	0.111	76.50	0.091	76.50	0.064
100.50	0.123	100.50	0.115	100.50	0.101	100.50	0.073
123.00	0.124	123.00	0.119	123.00	0.108	123.00	0.077
155.50	0.126	155.50	0.125	155.50	0.114	155.50	0.080
173.50	0.127	173.50	0.124	173.50	0.119	173.50	0.083
197.50	0.128	197.50	0.125	197.50	0.124	197.50	0.083
221.50	0.127	221.50	0.130	221.50	0.130	221.50	0.092
248.50	0.127	248.50	0.135	248.50	0.130	248.50	0.097
269.50	0.128	269.50	0.134	269.50	0.132	269.50	0.096

Test	α (º)	s (m)	s/D_p	n	W_g (m)	t_d (day)	d_{sge} (m)	d_{sge}/d_{se1}
6	15	0.050	1.0	1	0.089	11.18	0.157	1.15

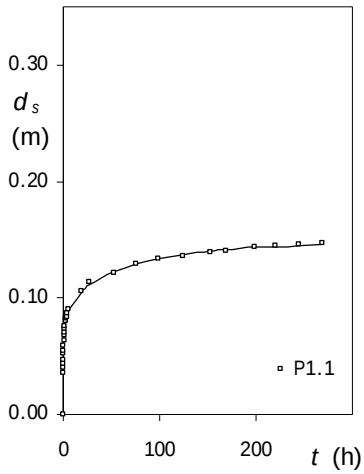

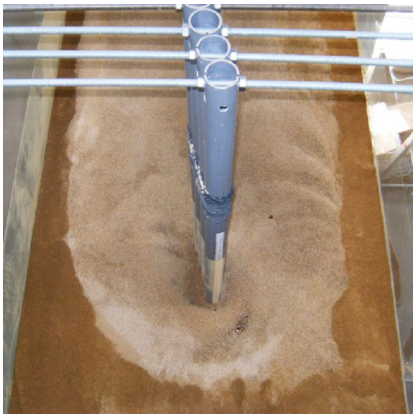

Test 6

P1.1		P2.1		P3.1		P4.1	
t (h)	d_s (m)	t (h)	d_s (m)	t (h)	d_s (m)	t (h)	d_s (m)
0.00	0.000						
0.02	0.036						
0.05	0.040						
0.08	0.044						
0.17	0.047						
0.25	0.052						
0.33	0.055						
0.50	0.059						
0.75	0.063						
1.00	0.068						
1.33	0.070						
1.67	0.074						
2.00	0.076						
2.50	0.080						
3.00	0.082						
3.75	0.084						
4.50	0.087						
5.50	0.090						
18.50	0.106						
27.00	0.114						
52.00	0.121						
75.83	0.129						
98.00	0.134						
124.00	0.136						
152.17	0.139						
168.92	0.141						
198.17	0.144						
220.00	0.145						
244.42	0.146						
268.42	0.147						

Test	α (º)	s (m)	s/D_p	n	W_g (m)	t_d (day)	d_{sge} (m)	d_{sge}/d_{se1}
7	15	0.100	2.0	1	0.128	13.19	0.152	1.12

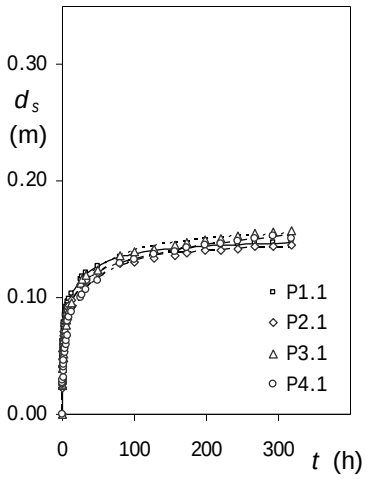

Test 7

P1.1		P2.1		P3.1		P4.1	
t (h)	d_s (m)	t (h)	d_s (m)	t (h)	d_s (m)	t (h)	d_s (m)
0.00	0.000	0.00	0.000	0.00	0.000	0.00	0.000
0.02	0.039	0.02	0.022	0.02	0.025	0.02	0.026
0.05	0.041	0.05	0.027	0.05	0.025	0.05	0.028
0.08	0.043	0.08	0.029	0.08	0.026	0.08	0.028
0.17	0.048	0.17	0.030	0.17	0.029	0.17	0.027
0.25	0.051	0.25	0.040	0.25	0.031	0.25	0.027
0.33	0.054	0.33	0.042	0.33	0.033	0.33	0.026
0.50	0.058	0.50	0.047	0.50	0.039	0.50	0.027
1.00	0.067	1.00	0.057	1.00	0.048	1.00	0.031
1.33	0.071	1.33	0.061	1.33	0.052	1.33	0.037
2.00	0.077	2.00	0.068	2.00	0.060	2.00	0.043
4.00	0.086	4.00	0.079	4.00	0.073	4.00	0.056
5.00	0.090	5.00	0.082	5.00	0.077	5.00	0.060
7.00	0.094	7.00	0.089	7.00	0.084	7.00	0.067
8.00	0.097	8.00	0.092	8.00	0.087	8.00	0.080
9.00	0.099	9.00	0.093	9.00	0.090	9.00	0.083
13.00	0.104	13.00	0.098	13.00	0.096	13.00	0.088
24.50	0.116	24.50	0.111	24.50	0.113	24.50	0.100
26.83	0.118	26.83	0.112	26.83	0.116	26.83	0.102
48.33	0.127	48.33	0.121	48.33	0.124	48.33	0.115
79.67	0.135	79.67	0.129	79.67	0.136	79.67	0.129
100.50	0.137	100.50	0.131	100.50	0.139	100.50	0.133
127.00	0.139	127.00	0.134	127.00	0.142	127.00	0.137
155.50	0.141	155.50	0.136	155.50	0.145	155.50	0.140
172.50	0.142	172.50	0.138	172.50	0.147	172.50	0.143
198.50	0.144	198.50	0.141	198.50	0.150	198.50	0.145
219.50	0.145	219.50	0.141	219.50	0.151	219.50	0.146
243.50	0.146	243.50	0.142	243.50	0.153	243.50	0.148
267.50	0.147	267.50	0.144	267.50	0.155	267.50	0.151
292.50	0.147	292.50	0.144	292.50	0.156	292.50	0.153
316.50	0.148	316.50	0.145	316.50	0.157	316.50	0.151

Test	α (º)	s (m)	s/D_p	n	W_g (m)	t_d (day)	d_{sge} (m)	d_{sge}/d_{se1}
8	15	0.150	3.0	1	0.167	15.39	0.162	1.19

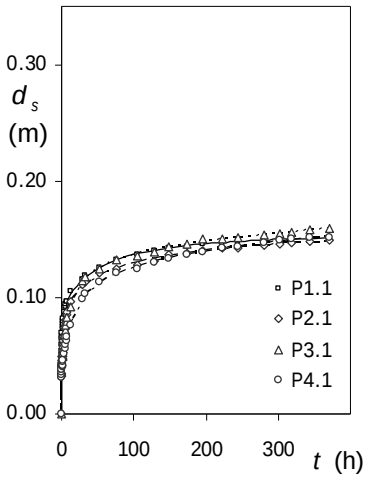

Test 8

P1.1		P2.1		P3.1		P4.1	
t (h)	d_s (m)	t (h)	d_s (m)	t (h)	d_s (m)	t (h)	d_s (m)
0.00	0.000	0.00	0.000	0.00	0.000	0.00	0.000
0.02	0.044	0.02	0.034	0.02	0.044	0.02	0.031
0.05	0.046	0.05	0.033	0.05	0.045	0.05	0.032
0.08	0.050	0.08	0.032	0.08	0.047	0.08	0.031
0.17	0.054	0.17	0.035	0.17	0.045	0.17	0.034
0.33	0.060	0.33	0.040	0.33	0.045	0.33	0.036
0.75	0.069	0.75	0.049	0.75	0.046	0.75	0.038
1.00	0.073	1.00	0.053	1.00	0.049	1.00	0.040
1.33	0.075	1.33	0.056	1.33	0.050	1.33	0.041
2.00	0.080	2.00	0.063	2.00	0.056	2.00	0.045
2.50	0.082	2.50	0.066	2.50	0.059	2.50	0.046
4.00	0.088	4.00	0.074	4.00	0.068	4.00	0.052
6.00	0.094	6.00	0.081	6.00	0.076	6.00	0.060
7.00	0.096	7.00	0.085	7.00	0.080	7.00	0.063
8.00	0.097	8.00	0.087	8.00	0.083	8.00	0.066
13.00	0.105	13.00	0.097	13.00	0.092	13.00	0.076
28.33	0.115	28.33	0.111	28.33	0.114	28.33	0.099
33.00	0.119	33.00	0.113	33.00	0.118	33.00	0.103
52.00	0.126	52.00	0.121	52.00	0.124	52.00	0.113
76.00	0.132	76.00	0.125	76.00	0.132	76.00	0.121
105.00	0.137	105.00	0.128	105.00	0.136	105.00	0.125
129.00	0.140	129.00	0.131	129.00	0.139	129.00	0.130
148.67	0.142	148.67	0.137	148.67	0.144	148.67	0.134
172.67	0.144	172.67	0.138	172.67	0.146	172.67	0.137
195.67	0.146	195.67	0.140	195.67	0.150	195.67	0.139
222.33	0.146	222.33	0.142	222.33	0.150	222.33	0.142
243.67	0.148	243.67	0.143	243.67	0.151	243.67	0.144
279.00	0.150	279.00	0.145	279.00	0.154	279.00	0.147
318.17	0.150	318.17	0.147	318.17	0.156	318.17	0.150
342.17	0.152	342.17	0.148	342.17	0.158	342.17	0.151
369.33	0.152	369.33	0.149	369.33	0.159	369.33	0.152

Test	α (º)	s (m)	s/D_p	n	W_g (m)	t_d (day)	d_{sge} (m)	d_{sge}/d_{se1}
9	15	0.225	4.5	1	0.200	8.93	0.183	1.35

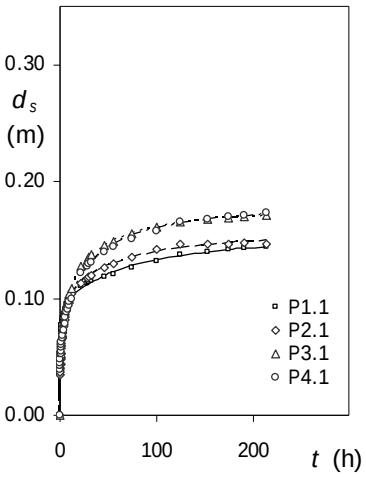

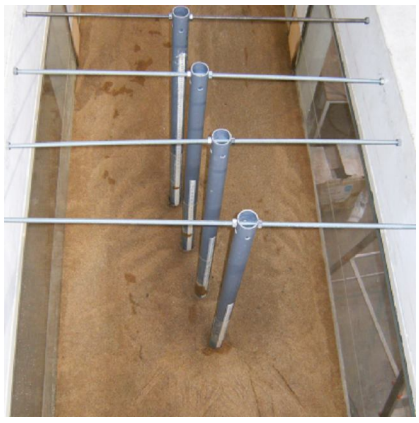

Test 9

P1.1		P2.1		P3.1		P4.1	
t (h)	d_s (m)	t (h)	d_s (m)	t (h)	d_s (m)	t (h)	d_s (m)
0.00	0.000	0.00	0.000	0.00	0.000	0.00	0.000
0.02	0.039	0.02	0.035	0.02	0.042	0.02	0.042
0.05	0.043	0.05	0.038	0.05	0.044	0.05	0.039
0.08	0.046	0.08	0.035	0.08	0.044	0.08	0.042
0.17	0.051	0.17	0.035	0.17	0.047	0.17	0.042
0.33	0.058	0.33	0.037	0.33	0.047	0.33	0.048
0.50	0.061	0.50	0.040	0.50	0.050	0.50	0.052
0.75	0.065	0.75	0.044	0.75	0.053	0.75	0.053
1.00	0.068	1.00	0.048	1.00	0.056	1.00	0.055
1.33	0.071	1.33	0.053	1.33	0.060	1.33	0.058
2.00	0.077	2.00	0.061	2.00	0.067	2.00	0.063
3.00	0.083	3.00	0.070	3.00	0.074	3.00	0.068
5.00	0.089	5.00	0.082	5.00	0.087	5.00	0.078
6.00	0.091	6.00	0.086	6.00	0.092	6.00	0.084
8.00	0.098	8.00	0.094	8.00	0.097	8.00	0.091
9.00	0.100	9.00	0.096	9.00	0.100	9.00	0.094
10.00	0.101	10.00	0.099	10.00	0.104	10.00	0.097
12.00	0.104	12.00	0.104	12.00	0.109	12.00	0.099
22.00	0.111	22.00	0.113	22.00	0.127	22.00	0.122
28.00	0.113	28.00	0.117	28.00	0.133	28.00	0.128
30.00	0.114	30.00	0.118	30.00	0.135	30.00	0.130
32.00	0.115	32.00	0.120	32.00	0.137	32.00	0.131
46.50	0.118	46.50	0.126	46.50	0.145	46.50	0.140
55.00	0.121	55.00	0.130	55.00	0.149	55.00	0.144
75.00	0.126	75.00	0.135	75.00	0.155	75.00	0.151
99.50	0.132	99.50	0.142	99.50	0.161	99.50	0.158
125.00	0.138	125.00	0.146	125.00	0.165	125.00	0.166
153.50	0.140	153.50	0.147	153.50	0.168	153.50	0.168
175.00	0.142	175.00	0.147	175.00	0.169	175.00	0.170
190.30	0.143	190.30	0.148	190.30	0.170	190.30	0.171
214.30	0.144	214.30	0.147	214.30	0.171	214.30	0.173

Test	α (º)	s (m)	s/D_p	n	W_g (m)	t_d (day)	d_{sge} (m)	d_{sge}/d_{se1}
10	15	0.300	6.0	1	0.200	11.18	0.170	1.25

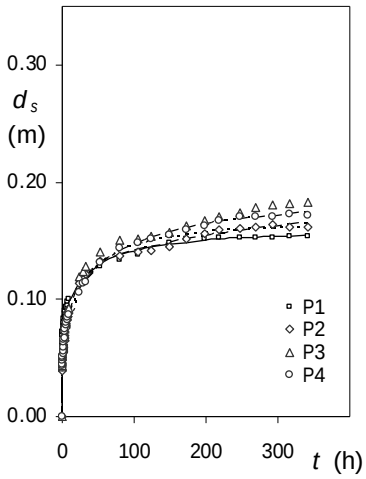

Test 10

P1.1		P2.1		P3.1		P4.1	
t (h)	d_s (m)	t (h)	d_s (m)	t (h)	d_s (m)	t (h)	d_s (m)
0.00	0.000	0.00	0.000	0.00	0.000	0.00	0.000
0.02	0.046	0.02	0.039	0.02	0.042	0.02	0.044
0.05	0.049	0.05	0.042	0.05	0.044	0.05	0.045
0.08	0.053	0.08	0.046	0.08	0.047	0.08	0.050
0.17	0.058	0.17	0.048	0.17	0.048	0.17	0.049
0.25	0.061	0.25	0.049	0.25	0.051	0.25	0.048
0.33	0.064	0.33	0.049	0.33	0.053	0.33	0.050
0.50	0.069	0.50	0.051	0.50	0.054	0.50	0.050
1.00	0.075	1.00	0.055	1.00	0.059	1.00	0.054
1.33	0.077	1.33	0.056	1.33	0.060	1.33	0.056
1.67	0.079	1.67	0.058	1.67	0.062	1.67	0.059
3.00	0.085	3.00	0.065	3.00	0.068	3.00	0.067
3.75	0.088	3.75	0.069	3.75	0.070	3.75	0.072
4.50	0.090	4.50	0.072	4.50	0.075	4.50	0.075
6.00	0.094	6.00	0.078	6.00	0.083	6.00	0.080
8.00	0.098	8.00	0.086	8.00	0.091	8.00	0.085
9.00	0.100	9.00	0.088	9.00	0.092	9.00	0.087
23.00	0.116	23.00	0.114	23.00	0.119	23.00	0.106
32.25	0.122	32.25	0.121	32.25	0.128	32.25	0.115
53.00	0.128	53.00	0.133	53.00	0.140	53.00	0.131
80.08	0.134	80.08	0.137	80.08	0.150	80.08	0.144
105.00	0.138	105.00	0.140	105.00	0.152	105.00	0.148
123.50	0.142	123.50	0.142	123.50	0.154	123.50	0.152
148.50	0.148	148.50	0.145	148.50	0.157	148.50	0.155
173.00	0.152	173.00	0.152	173.00	0.163	173.00	0.159
197.00	0.152	197.00	0.156	197.00	0.167	197.00	0.163
218.50	0.153	218.50	0.159	218.50	0.170	218.50	0.167
268.25	0.153	268.25	0.162	268.25	0.178	268.25	0.170
292.25	0.153	292.25	0.164	292.25	0.181	292.25	0.171
316.25	0.154	316.25	0.162	316.25	0.182	316.25	0.173
340.25	0.154	340.25	0.162	340.25	0.183	340.25	0.172

Test	α (º)	s (m)	s/D_p	n	W_g (m)	t_d (day)	d_{sge} (m)	d_{sge}/d_{se1}
11	30	0.050	1.0	1	0.125	6.92	0.246	1.81

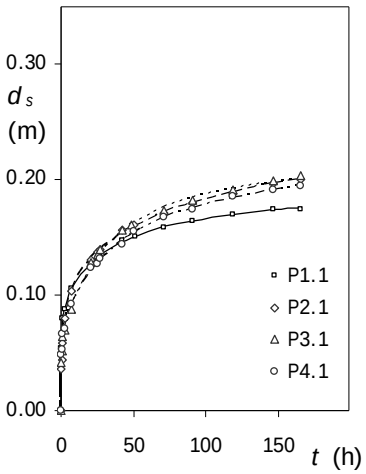

Test 11

P1.1		P2.1		P3.1		P4.1	
t (h)	d_s (m)	t (h)	d_s (m)	t (h)	d_s (m)	t (h)	d_s (m)
0.00	0.000	0.00	0.000	0.00	0.000	0.00	0.000
0.23	0.054	0.25	0.036	0.27	0.042	0.27	0.048
0.52	0.066	0.53	0.044	0.55	0.052	0.55	0.053
1.30	0.080	1.30	0.059	1.32	0.064	1.32	0.066
2.47	0.088	2.47	0.080	2.48	0.070	2.48	0.071
7.00	0.106	7.02	0.104	7.02	0.088	7.03	0.092
20.83	0.128	20.83	0.131	20.85	0.128	20.85	0.124
25.55	0.132	25.55	0.137	25.57	0.136	25.57	0.127
26.97	0.136	26.97	0.140	26.98	0.140	26.98	0.132
41.92	0.147	41.95	0.157	41.97	0.156	41.98	0.144
50.88	0.151	50.87	0.161	48.85	0.161	50.83	0.156
71.08	0.159	71.10	0.171	71.12	0.173	71.13	0.168
90.73	0.165	90.72	0.180	90.70	0.182	90.68	0.175
118.50	0.170	118.52	0.188	118.55	0.192	118.58	0.185
146.50	0.175	146.48	0.197	146.47	0.200	146.45	0.191
166.05	0.175	165.90	0.201	165.92	0.204	165.93	0.195

Test	α (º)	s (m)	s/D_p	n	W_g (m)	t_d (day)	d_{sge} (m)	d_{sge}/d_{se1}
12	30	0.100	2.0	1	0.200	6.92	0.242	1.78

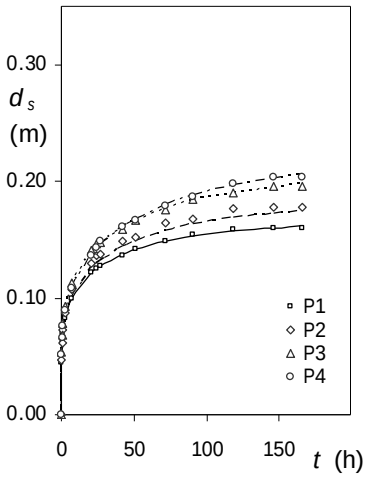

Test 12

P1.1		P2.1		P3.1		P4.1	
t (h)	d_s (m)	t (h)	d_s (m)	t (h)	d_s (m)	t (h)	d_s (m)
0.00	0.000	0.00	0.000	0.00	0.000	0.00	0.000
0.17	0.045	0.18	0.047	0.20	0.054	0.22	0.051
0.65	0.062	0.67	0.062	0.67	0.068	0.68	0.066
1.25	0.071	1.27	0.073	1.27	0.078	1.28	0.076
2.58	0.083	2.60	0.087	2.60	0.093	2.62	0.089
6.98	0.100	7.00	0.107	7.00	0.113	7.02	0.109
20.92	0.122	20.92	0.130	20.93	0.141	20.93	0.136
24.48	0.126	24.50	0.137	24.50	0.146	24.52	0.143
26.90	0.128	26.90	0.138	26.92	0.148	26.93	0.149
42.03	0.136	42.05	0.149	42.07	0.159	42.08	0.161
50.83	0.142	50.82	0.152	50.80	0.167	50.78	0.166
71.28	0.149	71.32	0.165	71.33	0.176	71.35	0.179
90.68	0.154	90.67	0.168	90.65	0.185	90.62	0.187
118.63	0.159	118.65	0.177	118.67	0.191	118.68	0.198
146.42	0.160	146.40	0.178	146.38	0.195	146.37	0.204
166.03	0.160	166.05	0.178	166.07	0.196	166.08	0.204

Test	α (º)	s (m)	s/D_p	n	W_g (m)	t_d (day)	d_{sge} (m)	d_{sge}/d_{se1}
13	30	0.150	3.0	1	0.200	7.67	0.212	1.56

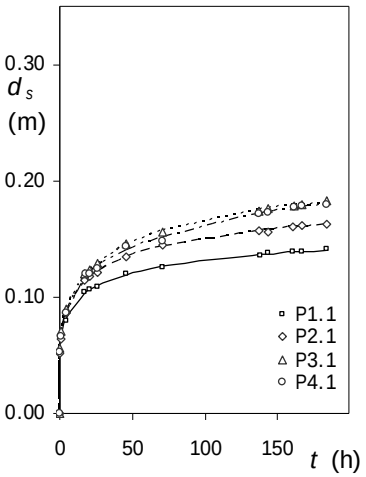

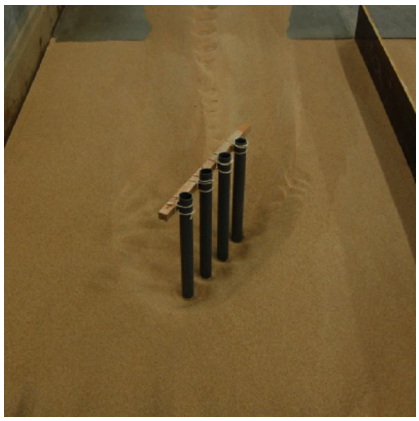

Test 13

P1.1		P2.1		P3.1		P4.1	
t (h)	d_s (m)	t (h)	d_s (m)	t (h)	d_s (m)	t (h)	d_s (m)
0.00	0.000	0.00	0.000	0.00	0.000	0.00	0.000
0.28	0.053	0.32	0.051	0.32	0.056	0.35	0.053
1.17	0.065	1.18	0.064	1.18	0.070	1.20	0.066
4.40	0.080	4.42	0.086	4.42	0.090	4.43	0.086
17.43	0.104	17.45	0.115	17.47	0.120	17.48	0.120
20.62	0.107	20.63	0.118	20.63	0.124	20.65	0.120
25.70	0.109	25.70	0.121	25.72	0.129	25.73	0.125
45.45	0.120	45.45	0.134	45.43	0.146	45.43	0.143
70.42	0.126	70.42	0.145	70.40	0.156	70.40	0.148
137.60	0.136	137.58	0.157	137.57	0.174	137.55	0.172
143.32	0.138	143.33	0.156	143.35	0.176	143.37	0.173
160.88	0.139	160.90	0.160	160.92	0.179	160.93	0.177
166.83	0.139	166.85	0.162	166.87	0.180	166.88	0.178
184.00	0.141	184.02	0.163	184.03	0.183	184.05	0.179

Test	α (º)	s (m)	s/D_p	n	W_g (m)	t_d (day)	d_{sge} (m)	d_{sge}/d_{se1}
14	30	0.225	4.5	1	0.200	7.24	0.198	1.46

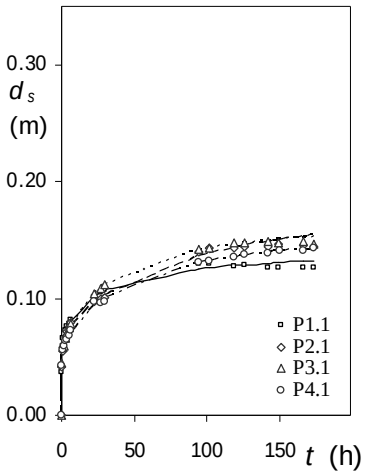

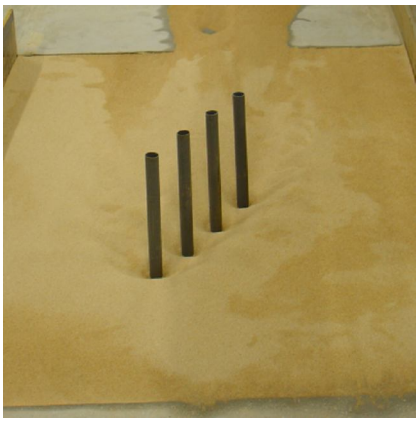

Tests 14

P1.1		P2.1		P3.1		P4.1	
t (h)	d_s (m)	t (h)	d_s (m)	t (h)	d_s (m)	t (h)	d_s (m)
0.00	0.000	0.00	0.000	0.00	0.000	0.00	0.000
0.08	0.037	0.08	0.041	0.10	0.045	0.12	0.043
0.82	0.059	0.82	0.055	0.83	0.058	0.83	0.056
1.35	0.066	1.35	0.059	1.37	0.060	1.37	0.059
2.88	0.072	2.88	0.067	2.90	0.066	2.92	0.063
3.87	0.076	3.88	0.072	3.88	0.071	3.90	0.065
5.03	0.079	5.05	0.076	5.05	0.075	5.07	0.068
5.92	0.081	5.93	0.079	5.93	0.079	5.95	0.073
22.42	0.100	22.42	0.097	22.43	0.104	22.43	0.097
26.87	0.105	26.88	0.099	26.90	0.109	26.90	0.097
29.95	0.107	29.95	0.100	29.97	0.112	29.97	0.097
94.50	0.130	94.50	0.140	94.52	0.142	94.52	0.131
101.95	0.130	101.97	0.143	101.97	0.144	101.98	0.133
118.43	0.127	118.43	0.143	118.45	0.147	118.47	0.135
125.83	0.128	125.83	0.144	125.85	0.147	125.87	0.137
142.45	0.126	142.45	0.145	142.47	0.149	142.48	0.139
149.90	0.126	149.92	0.146	149.92	0.148	149.93	0.140
166.15	0.126	166.15	0.145	166.17	0.149	166.18	0.141
173.65	0.126	173.67	0.144	173.68	0.147	173.68	0.143

Test	α (º)	s (m)	s/D_p	n	W_g (m)	t_d (day)	d_{sge} (m)	d_{sge}/d_{se1}
15	30	0.300	6.0	1	0.200	7.67	0.177	1.30

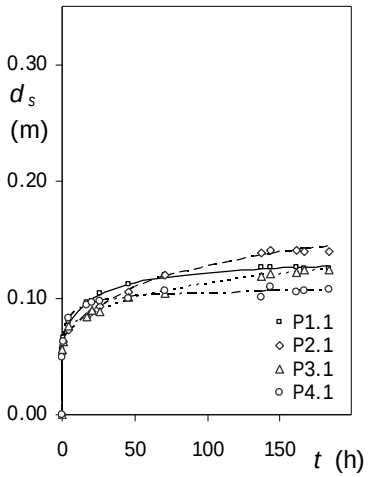

Tets 15

P1.1		P2.1		P3.1		P4.1	
t (h)	d_s (m)	t (h)	d_s (m)	t (h)	d_s (m)	t (h)	d_s (m)
0.00	0.000	0.00	0.000	0.00	0.000	0.00	0.000
0.20	0.056	0.23	0.052	0.25	0.056	0.27	0.049
1.03	0.066	1.05	0.063	1.07	0.063	1.08	0.063
4.50	0.079	4.50	0.073	4.52	0.076	4.55	0.083
17.35	0.096	17.37	0.084	17.38	0.083	17.40	0.094
20.73	0.097	20.75	0.088	20.77	0.089	20.80	0.097
25.65	0.104	25.67	0.093	25.67	0.088	25.68	0.097
45.43	0.112	45.42	0.105	45.42	0.101	45.40	0.099
70.40	0.120	70.40	0.120	70.38	0.104	70.38	0.106
136.73	0.126	136.75	0.139	136.77	0.119	136.78	0.100
143.28	0.126	143.27	0.141	143.25	0.121	143.23	0.110
160.98	0.126	161.02	0.141	161.03	0.122	161.05	0.105
166.75	0.125	166.77	0.140	166.75	0.124	166.73	0.107
184.07	0.125	184.08	0.140	184.10	0.124	184.12	0.107

Test	α (º)	s (m)	s/D_p	n	W_g (m)	t_d (day)	d_{sge} (m)	d_{sge}/d_{se1}
16	45	0.050	1.0	1	0.156	7.94	0.316	2.33

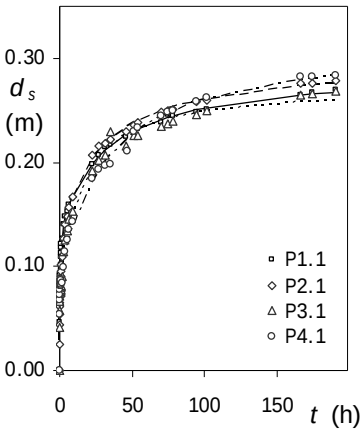

Test 16

P1.1		P2.1		P3.1		P4.1	
t (h)	d_s (m)	t (h)	d_s (m)	t (h)	d_s (m)	t (h)	d_s (m)
0.00	0.000	0.00	0.000	0.00	0.000	0.00	0.000
0.05	0.046	0.07	0.026	0.08	0.041	0.10	0.054
0.13	0.070	0.15	0.044	0.17	0.058	0.18	0.068
0.22	0.078	0.23	0.054	0.25	0.067	0.27	0.073
0.30	0.086	0.32	0.061	0.33	0.071	0.35	0.077
0.47	0.097	0.48	0.071	0.50	0.076	0.52	0.081
0.55	0.101	0.57	0.076	0.58	0.078	0.60	0.082
0.70	0.109	0.72	0.085	0.73	0.080	0.75	0.083
0.87	0.114	0.88	0.090	0.90	0.081	0.92	0.086
1.03	0.119	1.05	0.095	1.07	0.082	1.08	0.088
1.28	0.122	1.30	0.101	1.32	0.082	1.33	0.087
1.53	0.127	1.55	0.109	1.57	0.090	1.58	0.084
2.88	0.141	2.90	0.127	2.92	0.115	2.93	0.099
3.98	0.148	4.00	0.141	4.02	0.126	4.03	0.115
5.10	0.153	5.12	0.148	5.13	0.135	5.15	0.126
6.47	0.160	6.48	0.156	6.50	0.145	6.52	0.136
8.72	0.165	8.73	0.167	8.73	0.153	8.75	0.143
22.23	0.198	22.25	0.207	22.27	0.193	22.28	0.185
26.90	0.207	26.92	0.216	26.93	0.202	26.95	0.194
31.53	0.215	31.55	0.219	31.57	0.207	31.57	0.197
34.92	0.217	34.93	0.222	34.93	0.229	34.95	0.198
46.33	0.225	46.35	0.230	46.37	0.216	46.38	0.211
51.53	0.229	51.55	0.236	51.57	0.225	51.58	0.230
54.13	0.232	54.15	0.238	54.17	0.226	54.18	0.234
70.23	0.238	70.25	0.248	70.27	0.235	70.28	0.245
75.10	0.246	75.12	0.250	75.13	0.238	75.15	0.248
78.08	0.244	78.10	0.251	78.12	0.239	78.13	0.250
94.15	0.249	94.17	0.258	94.18	0.245	94.20	0.258
101.57	0.250	101.58	0.260	101.60	0.250	101.62	0.262
166.23	0.265	166.25	0.276	166.27	0.265	166.28	0.282
174.50	0.267	174.52	0.276	174.53	0.266	174.55	0.282
190.47	0.270	190.48	0.278	190.50	0.268	190.52	0.283

Test	α (º)	s (m)	s/D_p	n	W_g (m)	t_d (day)	d_{sge} (m)	d_{sge}/d_{se1}
17	45	0.100	2.0	1	0.200	6.95	0.175	1.29

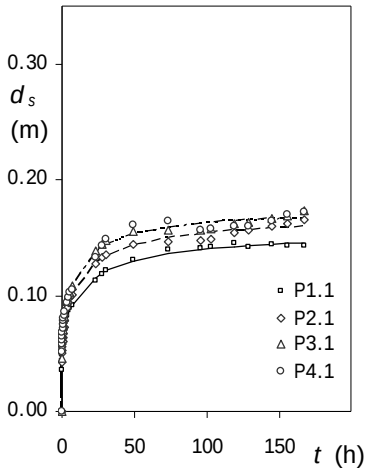

Test 17

P1.1		P2.1		P3.1		P4.1	
t (h)	d_s (m)	t (h)	d_s (m)	t (h)	d_s (m)	t (h)	d_s (m)
0.00	0.000	0.00	0.000	0.00	0.000	0.00	0.000
0.03	0.035	0.05	0.042	0.07	0.046	0.08	0.052
0.12	0.043	0.13	0.050	0.15	0.056	0.17	0.058
0.20	0.050	0.22	0.053	0.23	0.062	0.25	0.062
0.28	0.052	0.30	0.056	0.32	0.065	0.33	0.065
0.37	0.053	0.38	0.058	0.40	0.067	0.42	0.069
0.50	0.057	0.52	0.061	0.53	0.070	0.55	0.071
0.67	0.061	0.68	0.063	0.70	0.074	0.72	0.075
0.83	0.064	0.85	0.067	0.87	0.076	0.88	0.078
1.10	0.067	1.12	0.070	1.13	0.079	1.15	0.081
1.33	0.070	1.35	0.072	1.37	0.081	1.38	0.083
1.83	0.074	1.85	0.078	1.87	0.087	1.88	0.086
3.65	0.083	3.67	0.089	3.68	0.095	3.70	0.094
4.73	0.087	4.75	0.094	4.77	0.101	4.62	0.099
5.73	0.089	5.75	0.098	5.77	0.103	5.78	0.103
6.82	0.091	6.83	0.101	6.85	0.108	6.87	0.105
22.77	0.113	22.78	0.127	22.80	0.138	22.82	0.134
27.63	0.118	27.65	0.134	27.67	0.144	27.68	0.143
30.73	0.122	30.75	0.135	30.77	0.148	30.78	0.149
48.72	0.131	48.73	0.144	48.75	0.155	48.78	0.161
73.00	0.140	73.02	0.147	73.03	0.157	73.05	0.164
95.22	0.141	95.23	0.147	95.25	0.156	95.27	0.156
102.78	0.142	102.80	0.149	102.82	0.158	102.83	0.158
118.83	0.145	118.85	0.155	118.87	0.163	118.88	0.160
128.33	0.142	128.35	0.157	128.37	0.163	128.38	0.160
144.90	0.144	144.92	0.160	144.92	0.166	144.93	0.165
154.88	0.143	154.90	0.162	154.90	0.169	154.92	0.170
166.70	0.143	166.72	0.166	166.73	0.174	166.75	0.173

Test	α (º)	s (m)	s/D_p	n	W_g (m)	t_d (day)	d_{sge} (m)	d_{sge}/d_{se1}
18	45	0.150	3.0	1	0.200	9.92	0.156	1.15

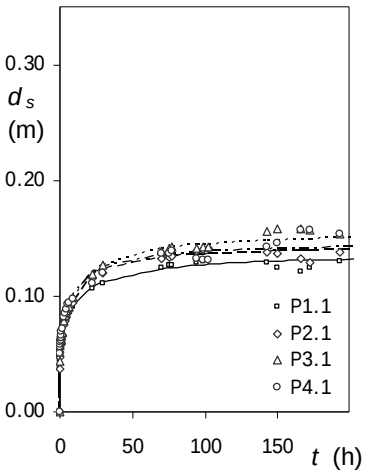

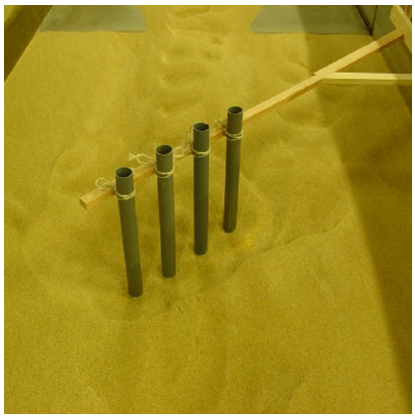

Test 18

P1.1		P2.1		P3.1		P4.1	
t (h)	d_s (m)	t (h)	d_s (m)	t (h)	d_s (m)	t (h)	d_s (m)
0.00	0.000	0.00	0.000	0.00	0.000	0.00	0.000
0.03	0.038	0.05	0.037	0.07	0.044	0.08	0.050
0.30	0.045	0.15	0.047	0.17	0.052	0.18	0.056
0.23	0.051	0.25	0.052	0.27	0.057	0.28	0.059
0.32	0.055	0.33	0.055	0.35	0.060	0.37	0.060
0.42	0.056	0.43	0.057	0.45	0.061	0.47	0.062
0.53	0.059	0.55	0.059	0.57	0.063	0.58	0.063
0.70	0.062	0.72	0.063	0.73	0.063	0.75	0.065
0.87	0.064	0.88	0.064	0.90	0.065	0.92	0.066
1.12	0.067	1.13	0.066	1.15	0.067	1.17	0.070
1.37	0.068	1.38	0.067	1.40	0.068	1.42	0.072
2.95	0.076	2.97	0.075	2.98	0.078	3.00	0.082
3.63	0.079	3.65	0.079	3.67	0.083	3.68	0.085
4.63	0.082	4.65	0.082	4.67	0.087	4.68	0.089
5.62	0.085	5.63	0.085	5.65	0.090	5.67	0.093
6.17	0.087	6.18	0.087	6.20	0.091	6.22	0.094
8.97	0.091	8.98	0.094	9.00	0.099	9.03	0.098
22.40	0.107	22.42	0.115	22.43	0.118	22.45	0.112
29.93	0.112	29.95	0.120	29.97	0.127	29.98	0.120
70.32	0.124	70.33	0.132	70.35	0.139	70.37	0.137
75.12	0.127	75.13	0.133	75.15	0.141	75.17	0.137
77.05	0.127	77.07	0.134	77.08	0.143	77.10	0.139
94.20	0.129	94.22	0.140	94.23	0.141	94.25	0.133
98.83	0.130	98.85	0.141	98.87	0.142	98.88	0.131
101.82	0.131	101.83	0.142	101.85	0.142	101.87	0.131
142.27	0.129	142.28	0.138	142.30	0.155	142.32	0.142
166.20	0.122	166.22	0.133	166.23	0.158	166.25	0.157
171.87	0.125	171.88	0.129	171.90	0.157	171.92	0.157
192.87	0.130	192.88	0.138	192.90	0.153	192.92	0.153
215.98	0.136	216.00	0.145	216.02	0.137	216.03	0.134
238.13	0.139	238.15	0.149	238.17	0.141	238.18	0.127

Test	α (º)	s (m)	s/D_p	n	W_g (m)	t_d (day)	d_{sge} (m)	d_{sge}/d_{se1}
19	45	0.225	4.5	1	0.250	8.23	0.158	1.16

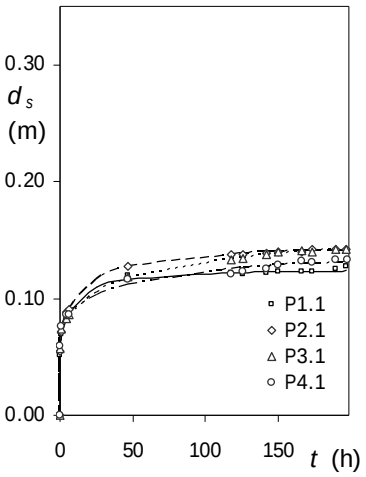

Test 19

P1.1		P2.1		P3.1		P4.1	
t (h)	d_s (m)	t (h)	d_s (m)	t (h)	d_s (m)	t (h)	d_s (m)
0.00	0.000	0.00	0.000	0.00	0.000	0.00	0.000
0.22	0.052	0.23	0.055	0.23	0.057	0.25	0.059
1.23	0.069	1.25	0.072	1.25	0.074	1.27	0.076
4.25	0.083	4.27	0.088	4.27	0.083	4.28	0.086
6.10	0.088	6.10	0.091	6.12	0.086	6.12	0.086
25.00	0.110	25.00	0.117	25.00	0.105	25.00	0.103
46.83	0.120	46.83	0.128	46.85	0.118	46.85	0.116
118.22	0.122	118.23	0.137	118.23	0.133	118.25	0.121
126.25	0.120	126.25	0.138	126.27	0.135	126.27	0.123
142.40	0.122	142.42	0.138	142.42	0.138	142.43	0.126
150.15	0.123	150.17	0.139	150.17	0.139	150.18	0.129
166.62	0.123	166.63	0.140	166.63	0.141	166.65	0.131
174.02	0.123	174.02	0.142	174.03	0.140	174.03	0.130
190.28	0.125	190.28	0.142	190.30	0.142	190.30	0.133
197.62	0.128	197.63	0.142	197.63	0.142	197.65	0.134

Test	α (º)	s (m)	s/D_p	n	W_g (m)	t_d (day)	d_{sge} (m)	d_{sge}/d_{se1}
20	45	0.300	6.0	1	0.200	7.95	0.144	1.06

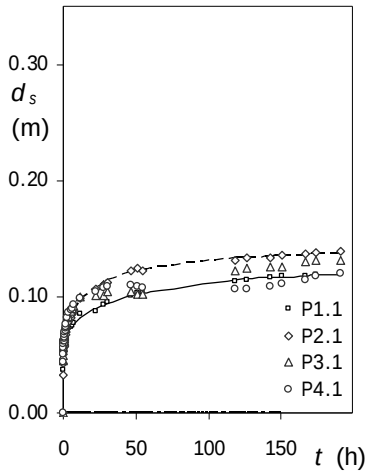

Test 20

P1.1		P2.1		P3.1		P4.1	
t (h)	d_s (m)	t (h)	d_s (m)	t (h)	d_s (m)	t (h)	d_s (m)
0.00	0.000	0.00	0.000	0.00	0.000	0.00	0.000
0.03	0.037	0.05	0.033	0.07	0.044	0.08	0.044
0.12	0.046	0.13	0.043	0.15	0.050	0.17	0.051
0.22	0.050	0.23	0.051	0.25	0.056	0.27	0.056
0.30	0.053	0.32	0.053	0.33	0.057	0.35	0.059
0.47	0.058	0.48	0.057	0.50	0.062	0.52	0.062
0.55	0.057	0.57	0.057	0.58	0.062	0.60	0.064
0.72	0.061	0.73	0.060	0.75	0.065	0.77	0.065
0.88	0.063	0.90	0.063	0.92	0.066	0.93	0.068
1.05	0.063	1.07	0.064	1.08	0.068	1.10	0.069
1.55	0.066	1.57	0.068	1.58	0.073	1.60	0.073
1.80	0.067	1.82	0.070	1.83	0.075	1.85	0.074
2.05	0.067	2.07	0.072	2.08	0.077	2.10	0.076
3.08	0.071	3.10	0.076	3.12	0.082	3.13	0.082
3.90	0.073	3.92	0.079	3.93	0.083	3.95	0.087
5.87	0.076	5.88	0.085	5.90	0.090	5.92	0.090
6.88	0.077	6.90	0.088	6.92	0.092	6.93	0.093
12.00	0.085	12.02	0.099	12.02	0.100	12.03	0.098
22.37	0.088	22.38	0.107	22.40	0.101	22.42	0.105
27.53	0.093	27.55	0.109	27.57	0.102	27.58	0.107
30.72	0.095	30.73	0.112	30.75	0.104	30.77	0.109
46.82	0.101	46.83	0.123	46.85	0.104	46.87	0.110
51.28	0.103	51.30	0.124	51.32	0.102	51.33	0.109
54.23	0.103	54.25	0.123	54.27	0.103	54.28	0.108
118.67	0.114	118.68	0.131	118.70	0.123	118.72	0.106
126.50	0.114	126.52	0.133	126.53	0.124	126.55	0.107
142.58	0.116	142.60	0.134	142.62	0.125	142.63	0.109
150.45	0.118	150.47	0.136	150.48	0.126	150.50	0.111
166.35	0.118	166.37	0.136	166.38	0.131	166.40	0.114
174.13	0.119	174.15	0.138	174.17	0.131	174.18	0.117
190.72	0.120	190.73	0.139	190.75	0.131	190.77	0.120

Test	α (º)	s (m)	s/D_p	n	W_g (m)	t_d (day)	d_{sge} (m)	d_{sge}/d_{se1}
21	90	0.050	1.0	1	0.200	10.34	0.354	2.61

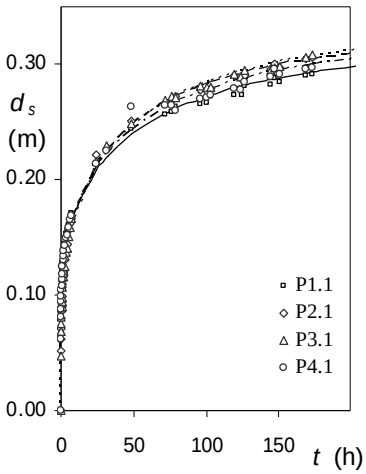

Test 21

P1.1		P2.1		P3.1		P4.1	
t (h)	d_s (m)	t (h)	d_s (m)	t (h)	d_s (m)	t (h)	d_s (m)
0.00	0.000	0.00	0.000	0.00	0.000	0.00	0.000
0.05	0.061	0.03	0.052	0.02	0.048	0.02	0.062
0.13	0.085	0.12	0.062	0.10	0.069	0.08	0.081
0.22	0.092	0.20	0.071	0.18	0.069	0.17	0.088
0.30	0.099	0.28	0.079	0.27	0.076	0.25	0.094
0.38	0.104	0.37	0.080	0.35	0.081	0.33	0.099
0.47	0.105	0.45	0.087	0.43	0.089	0.42	0.104
1.05	0.121	1.03	0.107	1.02	0.107	1.00	0.125
1.30	0.129	1.28	0.113	1.27	0.112	1.25	0.125
1.55	0.133	1.53	0.117	1.52	0.116	1.50	0.130
1.80	0.134	1.78	0.120	1.77	0.119	1.75	0.134
2.05	0.139	2.03	0.122	2.02	0.122	2.00	0.139
2.55	0.144	2.53	0.130	2.52	0.125	2.50	0.143
3.05	0.149	3.03	0.135	3.02	0.133	3.00	0.149
4.17	0.156	4.15	0.145	4.13	0.141	4.12	0.152
5.08	0.161	5.07	0.156	5.05	0.151	5.03	0.159
6.08	0.164	6.07	0.162	6.05	0.159	6.03	0.165
7.12	0.171	7.10	0.167	7.08	0.166	7.07	0.169
24.17	0.214	24.15	0.222	24.13	0.216	24.12	0.214
48.22	0.244	48.20	0.251	48.18	0.248	48.17	0.264
71.50	0.256	71.48	0.267	71.47	0.269	71.45	0.264
76.17	0.259	76.15	0.269	76.13	0.272	76.12	0.264
79.32	0.263	79.30	0.272	79.28	0.271	79.27	0.261
95.58	0.265	95.57	0.278	95.55	0.281	95.53	0.271
124.18	0.274	124.17	0.287	124.15	0.289	124.13	0.278
144.10	0.282	144.08	0.296	144.07	0.295	144.05	0.289
168.43	0.291	168.42	0.305	168.40	0.306	168.38	0.296
172.83	0.292	172.82	0.307	172.80	0.309	172.78	0.297
239.22	0.313	239.20	0.323	239.18	0.323	239.17	0.319
244.42	0.308	244.40	0.318	244.38	0.323	244.37	0.315
248.20	0.308	248.18	0.314	248.17	0.322	248.13	0.321

Test	α (º)	s (m)	s/D_p	n	W_g (m)	t_d (day)	d_{sge} (m)	d_{sge}/d_{se1}
22	90	0.100	2.0	1	0.200	9.56	0.190	1.40

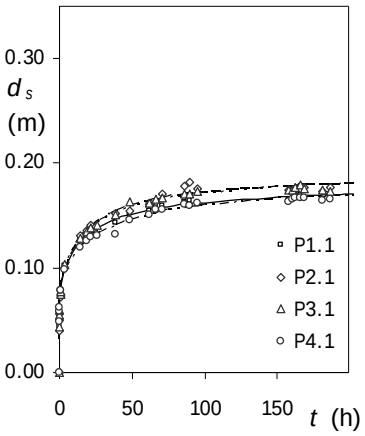

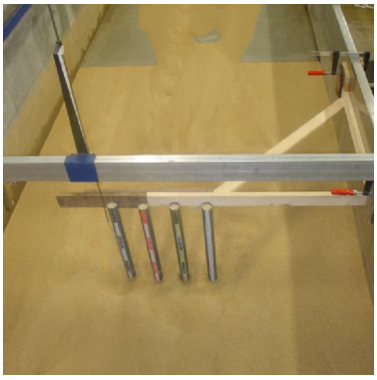

Test 22

P1.1		P2.1		P3.1		P4.1	
t (h)	d_s (m)	t (h)	d_s (m)	t (h)	d_s (m)	t (h)	d_s (m)
0.00	0.000	0.00	0.000	0.00	0.000	0.00	0.000
0.07	0.043	0.07	0.040	0.08	0.043	0.08	0.049
0.20	0.053	0.22	0.050	0.22	0.054	0.23	0.059
0.35	0.060	0.35	0.056	0.37	0.059	0.37	0.063
0.77	0.075	0.78	0.072	0.78	0.075	0.80	0.078
1.02	0.078	1.02	0.075	1.03	0.077	1.03	0.078
3.97	0.102	3.97	0.100	4.02	0.104	4.02	0.098
14.70	0.127	14.68	0.131	14.67	0.129	14.65	0.120
18.73	0.130	18.72	0.136	18.70	0.135	18.68	0.126
21.30	0.134	21.28	0.140	21.27	0.138	21.25	0.129
25.52	0.135	25.53	0.139	25.55	0.140	25.55	0.131
38.77	0.143	38.77	0.152	38.75	0.150	38.73	0.132
48.18	0.152	48.17	0.155	48.15	0.163	48.12	0.146
61.55	0.155	61.53	0.161	61.52	0.162	61.50	0.151
65.98	0.158	65.97	0.163	65.95	0.166	65.93	0.156
70.83	0.160	70.82	0.171	70.80	0.167	70.78	0.156
86.08	0.163	86.07	0.178	86.05	0.171	86.03	0.161
89.93	0.164	89.92	0.182	89.90	0.171	89.88	0.160
94.87	0.161	94.85	0.175	94.83	0.173	94.82	0.161
158.15	0.165	158.13	0.175	158.12	0.175	158.10	0.163
160.65	0.166	160.63	0.174	160.62	0.175	160.60	0.166
162.35	0.170	162.33	0.176	162.32	0.177	162.30	0.167
165.75	0.169	165.73	0.176	165.72	0.179	165.70	0.167
168.65	0.174	168.63	0.176	168.62	0.176	168.60	0.167
181.53	0.169	181.52	0.173	181.50	0.175	181.48	0.165
186.55	0.171	186.53	0.177	186.52	0.173	186.50	0.166
206.27	0.175	206.25	0.180	206.23	0.178	206.22	0.167
208.15	0.176	208.13	0.181	208.12	0.183	208.10	0.167
213.70	0.180	213.68	0.182	213.67	0.183	213.65	0.168
229.37	0.176	229.35	0.180	229.33	0.179	229.32	0.167

Test	α (º)	s (m)	s/D_p	n	W_g (m)	t_d (day)	d_{sge} (m)	d_{sge}/d_{se1}
23	90	0.150	3.0	1	0.200	9.44	0.175	1.29

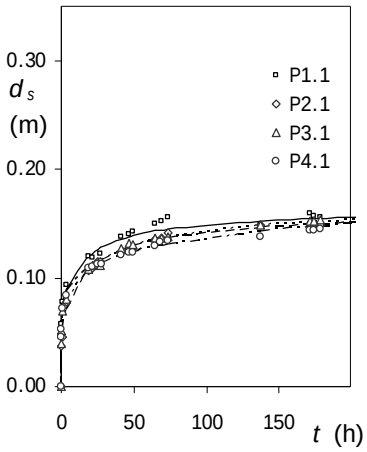

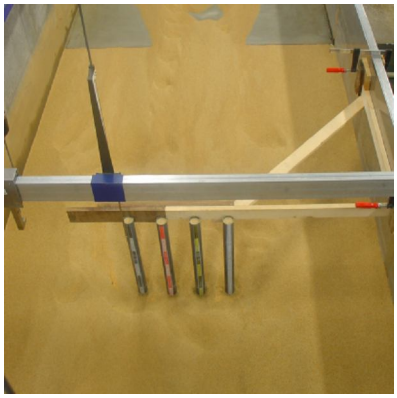

Test 23

P1.1		P2.1		P3.1		P4.1	
t (h)	d_s (m)	t (h)	d_s (m)	t (h)	d_s (m)	t (h)	d_s (m)
0.00	0.000	0.00	0.000	0.00	0.000	0.00	0.000
0.07	0.046	0.12	0.037	0.13	0.040	0.15	0.045
0.20	0.058	0.25	0.047	0.27	0.052	0.28	0.052
1.23	0.078	1.25	0.045	1.27	0.070	1.28	0.072
3.60	0.094	3.62	0.078	3.63	0.081	3.65	0.084
18.67	0.119	18.65	0.107	18.63	0.108	18.62	0.110
21.08	0.119	21.10	0.109	21.12	0.111	21.13	0.111
25.03	0.114	25.05	0.115	25.07	0.112	25.08	0.113
27.30	0.122	27.32	0.115	27.33	0.111	27.35	0.113
40.88	0.138	40.87	0.124	40.85	0.127	40.83	0.121
46.73	0.141	46.75	0.126	46.77	0.132	46.78	0.123
49.18	0.142	49.20	0.127	49.22	0.131	49.23	0.123
64.90	0.149	64.88	0.135	64.87	0.137	64.85	0.130
68.62	0.153	68.60	0.137	68.58	0.137	68.57	0.133
73.15	0.155	73.13	0.142	73.12	0.138	73.10	0.134
137.50	0.149	137.52	0.148	137.53	0.148	137.55	0.138
171.30	0.160	171.28	0.150	171.27	0.152	171.25	0.144
173.75	0.157	173.73	0.150	173.72	0.153	173.70	0.144
178.70	0.156	178.72	0.149	178.73	0.154	178.75	0.145
202.28	0.149	202.27	0.149	202.25	0.155	202.23	0.152
218.93	0.149	218.95	0.149	218.97	0.152	218.98	0.156
226.57	0.148	226.55	0.150	226.53	0.151	226.52	0.155

Test	α (º)	s (m)	s/D_p	n	W_g (m)	t_d (day)	d_{sge} (m)	d_{sge}/d_{se1}
24	90	0.225	4.5	1	0.200	7.23	0.159	1.17

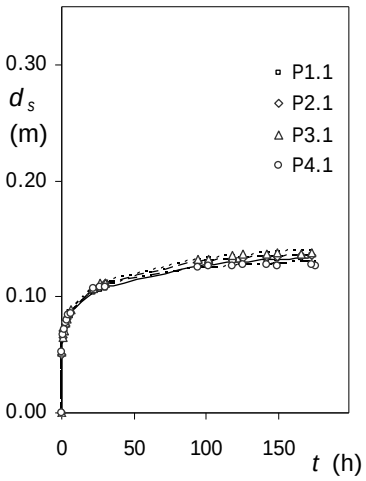

Test 24

P1.1		P2.1		P3.1		P4.1	
t (h)	d_s (m)	t (h)	d_s (m)	t (h)	d_s (m)	t (h)	d_s (m)
0.00	0.000	0.00	0.000	0.00	0.000	0.00	0.000
0.10	0.051	0.12	0.051	0.13	0.052	0.13	0.052
0.73	0.065	0.73	0.065	0.75	0.065	0.75	0.068
1.37	0.070	1.37	0.070	1.38	0.070	1.38	0.072
2.80	0.077	2.80	0.076	2.82	0.077	2.82	0.077
3.88	0.082	3.90	0.081	3.90	0.081	3.92	0.080
4.95	0.084	4.97	0.083	4.97	0.085	4.98	0.084
5.95	0.087	5.95	0.086	5.97	0.089	5.97	0.085
22.32	0.104	22.33	0.106	22.33	0.108	22.35	0.107
26.90	0.106	26.90	0.110	26.92	0.111	26.92	0.108
29.85	0.107	29.87	0.111	29.87	0.112	29.88	0.109
94.52	0.127	94.52	0.131	94.53	0.132	94.53	0.125
101.85	0.127	101.87	0.130	101.87	0.133	101.88	0.126
118.45	0.130	118.47	0.131	118.47	0.135	118.48	0.127
125.75	0.131	125.75	0.133	125.77	0.137	125.77	0.128
142.47	0.131	142.48	0.135	142.48	0.137	142.50	0.127
149.82	0.132	149.82	0.135	149.83	0.138	149.83	0.126
166.17	0.134	166.18	0.136	166.18	0.137	176.20	0.126
173.57	0.136	173.58	0.136	173.58	0.138	173.60	0.127

Test	α (º)	s (m)	s/D_p	n	W_g (m)	t_d (day)	d_{sge} (m)	d_{sge}/d_{se1}
25	90	0.300	6.0	1	0.200	7.76	0.127	0.94

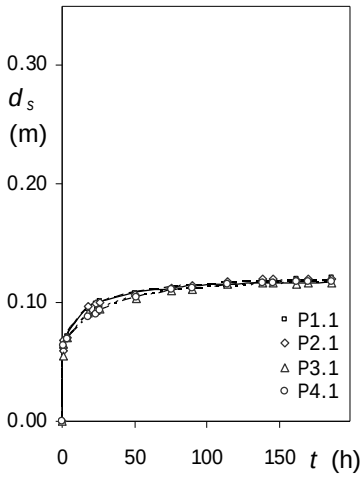

Test 25

P1.1		P2.1		P3.1		P4.1	
t (h)	d_s (m)	t (h)	d_s (m)	t (h)	d_s (m)	t (h)	d_s (m)
0.00	0.000	0.00	0.000	0.00	0.000	0.00	0.000
0.03	0.058	0.03	0.061	0.03	0.057	0.03	0.061
0.15	0.059	0.15	0.062	0.15	0.058	0.15	0.061
0.67	0.059	0.62	0.059	0.60	0.055	0.60	0.063
1.23	0.062	1.25	0.068	1.27	0.064	1.28	0.064
3.38	0.072	3.42	0.070	3.47	0.071	3.48	0.069
6.00	0.080	6.00	0.079	6.00	0.074	6.00	0.073
18.32	0.095	18.30	0.097	18.28	0.092	18.27	0.088
23.32	0.100	23.33	0.099	23.35	0.093	23.37	0.091
25.75	0.102	25.73	0.100	25.72	0.094	25.70	0.093
50.85	0.108	50.87	0.107	50.88	0.104	50.90	0.105
75.48	0.111	75.47	0.112	75.45	0.110	75.43	0.112
89.88	0.112	89.90	0.114	89.92	0.111	89.93	0.112
114.23	0.115	114.22	0.118	114.20	0.115	114.18	0.116
138.67	0.118	138.68	0.120	138.70	0.117	138.72	0.116
145.57	0.118	145.55	0.120	145.53	0.116	145.52	0.117
162.15	0.120	162.17	0.119	162.18	0.116	162.20	0.118
170.43	0.118	170.42	0.120	170.40	0.116	170.38	0.117
186.17	0.121	186.18	0.120	186.20	0.117	186.22	0.118

Test	α (º)	s (m)	s/D_p	n	W_g (m)	t_d (day)	d_{sge} (m)	d_{sge}/d_{se1}
26	0	0.050	1.0	2	0.100	13.2	0.261	1.92

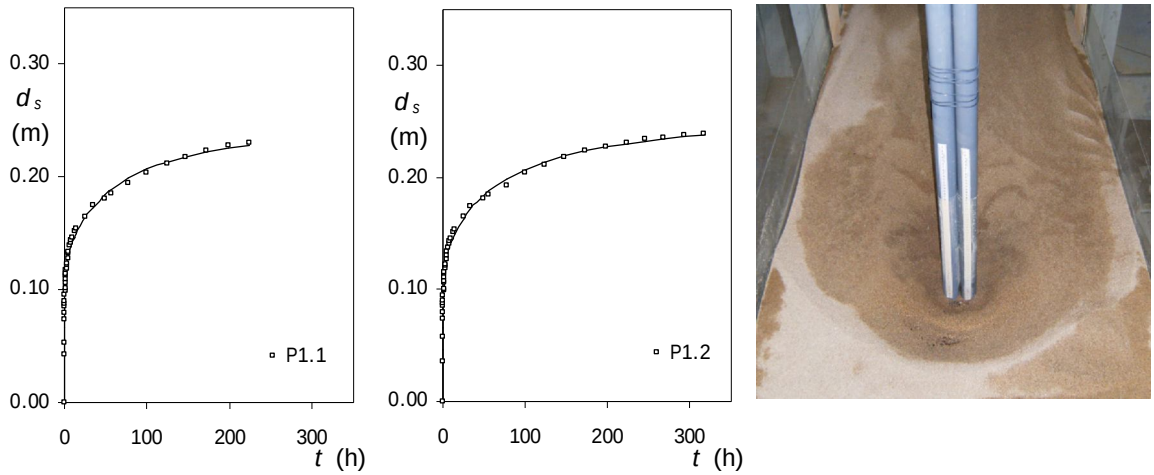

Test 26

P1.1		P2.1		P3.1		P4.1		P1.2	
t (h)	d_s (m)	t (h)	d_s (m)	t (h)	d_s (m)	t (h)	d_s (m)	t (h)	d_s (m)
0.00	0.000							0.00	0.000
0.03	0.043							0.03	0.036
0.17	0.074							0.17	0.074
0.25	0.080							0.25	0.080
0.33	0.085							0.33	0.085
0.42	0.088							0.42	0.088
0.50	0.090							0.50	0.090
0.83	0.099							0.83	0.099
1.00	0.101							1.00	0.101
1.50	0.109							1.50	0.108
2.00	0.114							2.00	0.114
2.67	0.119							2.67	0.119
3.00	0.122							3.00	0.121
4.00	0.128							4.00	0.127
5.50	0.134							5.50	0.134
8.50	0.144							8.50	0.143
10.00	0.146							10.00	0.146
14.00	0.154							14.00	0.154
25.00	0.165							25.00	0.165
49.00	0.181							49.00	0.181
56.00	0.185							56.00	0.185
77.00	0.194							77.00	0.193
99.50	0.204							99.50	0.204
124.00	0.212							124.00	0.211
146.50	0.218							146.50	0.218
172.50	0.223							172.50	0.224
198.17	0.228							198.17	0.228
223.50	0.230							223.50	0.231
268.33								268.33	0.236
292.33								292.33	0.238
316.33								316.33	0.239

Test	α (º)	s (m)	s/D_p	n	W_g (m)	t_d (day)	d_{sge} (m)	d_{sge}/d_{se1}
27	0	0.100	2.0	2	0.100	15.2	0.185	1.36

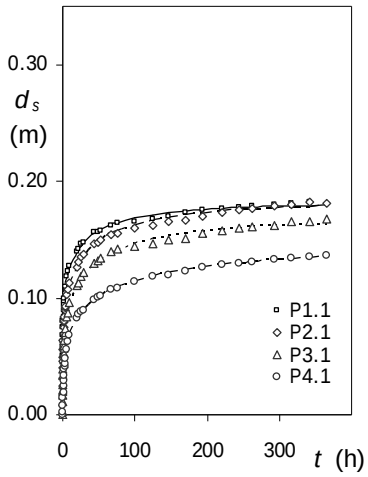

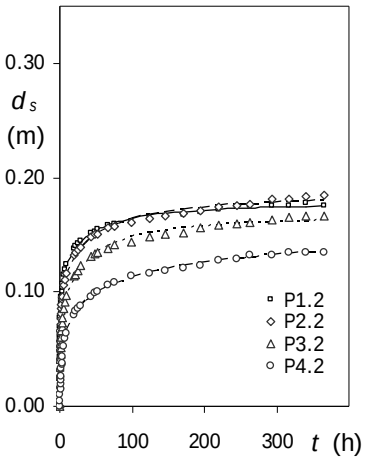

Test 27

P1.1		P2.1		P3.1		P4.1		P1.2	
t (h)	d_s (m)	t (h)	d_s (m)	t (h)	d_s (m)	t (h)	d_s (m)	t (h)	d_s (m)
0.00	0.000	0.00	0.000	0.00	0.000	0.00	0.000	0.00	0.000
0.03	0.045	0.03	0.025	0.03	0.011	0.03	-0.004	0.03	0.048
0.08	0.050	0.08	0.031	0.08	0.020	0.08	-0.009	0.08	0.043
0.25	0.063	0.25	0.046	0.25	0.021	0.25	-0.001	0.25	0.059
0.33	0.068	0.33	0.049	0.33	0.026	0.33	0.002	0.33	0.063
0.75	0.081	0.75	0.064	0.75	0.039	0.75	0.014	0.75	0.077
1.00	0.084	1.00	0.069	1.00	0.044	1.00	0.019	1.00	0.081
1.67	0.094	1.67	0.079	1.67	0.057	1.67	0.029	1.67	0.090
2.00	0.097	2.00	0.081	2.00	0.059	2.00	0.033	2.00	0.093
3.00	0.104	3.00	0.089	3.00	0.068	3.00	0.041	3.00	0.100
3.50	0.108	3.50	0.092	3.50	0.071	3.50	0.044	3.50	0.104
6.00	0.119	6.00	0.103	6.00	0.084	6.00	0.056	6.00	0.115
9.50	0.128	9.50	0.113	9.50	0.096	9.50	0.068	9.50	0.124
19.50	0.140	19.50	0.126	19.50	0.111	19.50	0.083	19.50	0.138
24.50	0.146	24.50	0.135	24.50	0.118	24.50	0.088	24.50	0.142
28.00	0.148	28.00	0.137	28.00	0.122	28.00	0.089	28.00	0.145
48.00	0.157	48.00	0.148	48.00	0.132	48.00	0.101	48.00	0.153
52.33	0.158	52.33	0.150	52.33	0.134	52.33	0.102	52.33	0.155
67.17	0.162	67.17	0.154	67.17	0.140	67.17	0.107	67.17	0.158
75.25	0.164	75.25	0.155	75.25	0.142	75.25	0.109	75.25	0.160
98.92	0.166	98.92	0.160	98.92	0.144	98.92	0.114	98.92	0.162
123.92	0.168	123.92	0.162	123.92	0.147	123.92	0.119	123.92	0.164
145.42	0.170	145.42	0.165	145.42	0.150	145.42	0.120	145.42	0.166
169.92	0.173	169.92	0.167	169.92	0.151	169.92	0.123	169.92	0.168
220.08	0.177	220.08	0.173	220.08	0.158	220.08	0.129	220.08	0.172
244.58	0.178	244.58	0.176	244.58	0.160	244.58	0.130	244.58	0.174
262.00	0.179	262.00	0.177	262.00	0.161	262.00	0.131	262.00	0.175
293.17	0.180	293.17	0.179	293.17	0.162	293.17	0.133	293.17	0.176
316.33	0.181	316.33	0.180	316.33	0.165	316.33	0.134	316.33	0.176
340.33	0.182	340.33	0.182	340.33	0.165	340.33	0.135	340.33	0.178
364.33		364.33	0.181	364.33	0.168	364.33	0.136	364.33	0.176

Test	α (º)	s (m)	s/D_p	n	W_g (m)	t_d (day)	d_{sge} (m)	d_{sge}/d_{se1}
28	0	0.150	3.0	2	0.100	14.1	0.183	1.35

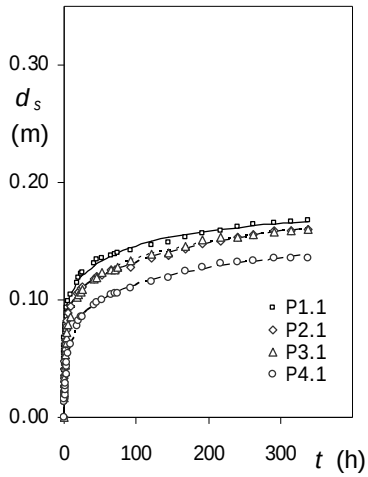

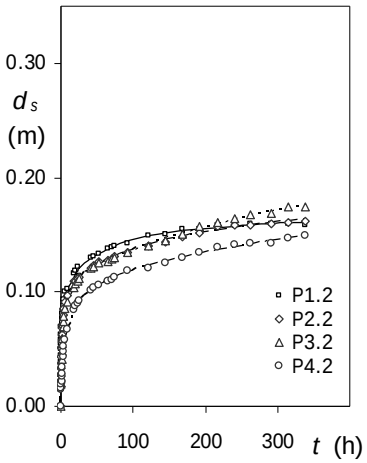

Test 28

P1.1		P2.1		P3.1		P4.1		P1.2	
t (h)	d_s (m)	t (h)	d_s (m)	t (h)	d_s (m)	t (h)	d_s (m)	t (h)	d_s (m)
0.00	0.000	0.00	0.000	0.00	0.000	0.00	0.000	0.00	0.000
0.03	0.040	0.03	0.018	0.03	0.019	0.03	0.018	0.03	0.039
0.08	0.045	0.08	0.021	0.08	0.017	0.08	0.018	0.08	0.045
0.17	0.050	0.17	0.027	0.17	0.020	0.17	0.015	0.17	0.050
0.25	0.054	0.25	0.033	0.25	0.021	0.25	0.014	0.25	0.055
0.50	0.061	0.50	0.041	0.50	0.029	0.50	0.013	0.50	0.063
1.33	0.074	1.33	0.058	1.33	0.044	1.33	0.023	1.33	0.076
1.67	0.077	1.67	0.062	1.67	0.048	1.67	0.027	1.67	0.079
3.00	0.085	3.00	0.074	3.00	0.063	3.00	0.037	3.00	0.088
4.50	0.093	4.50	0.082	4.50	0.072	4.50	0.047	4.50	0.094
8.17	0.104	8.17	0.094	8.17	0.086	8.17	0.062	8.17	0.103
17.17	0.115	17.17	0.105	17.17	0.102	17.17	0.078	17.17	0.116
20.00	0.119	20.00	0.107	20.00	0.104	20.00	0.082	20.00	0.119
26.00	0.123	26.00	0.111	26.00	0.109	26.00	0.086	26.00	0.114
41.33	0.131	41.33	0.118	41.33	0.118	41.33	0.095	41.33	0.130
44.67	0.134	44.67	0.120	44.67	0.119	44.67	0.098	44.67	0.131
51.83	0.135	51.83	0.121	51.83	0.123	51.83	0.100	51.83	0.133
65.00	0.138	65.00	0.125	65.00	0.125	65.00	0.104	65.00	0.138
70.17	0.139	70.17	0.126	70.17	0.126	70.17	0.105	70.17	0.139
74.67	0.140	74.67	0.126	74.67	0.128	74.67	0.106	74.67	0.140
92.17	0.142	92.17	0.128	92.17	0.133	92.17	0.110	92.17	0.142
121.33	0.147	121.33	0.135	121.33	0.139	121.33	0.116	121.33	0.149
144.00	0.149	144.00	0.138	144.00	0.140	144.00	0.119	144.00	0.151
168.00	0.153	168.00	0.143	168.00	0.146	168.00	0.124	168.00	0.155
192.17	0.157	192.17	0.148	192.17	0.151	192.17	0.128	192.17	0.155
216.17	0.159	216.17	0.150	216.17	0.153	216.17	0.131	216.17	0.158
240.17	0.162	240.17	0.153	240.17	0.153	240.17	0.132	240.17	0.159
261.17	0.164	261.17	0.155	261.17	0.156	261.17	0.133	261.17	0.160
290.83	0.166	290.83	0.159	290.83	0.158	290.83	0.135	290.83	0.160
313.83	0.167	313.83	0.159	313.83	0.159	313.83	0.135	313.83	0.160
337.83	0.168	337.83	0.160	337.83	0.160	337.83	0.136	337.83	0.158

Test	α (º)	s (m)	s/D_p	n	W_g (m)	t_d (day)	d_{sge} (m)	d_{sge}/d_{se1}
29	0	0.225	4.5	2	0.100	9.1	0.146	1.08

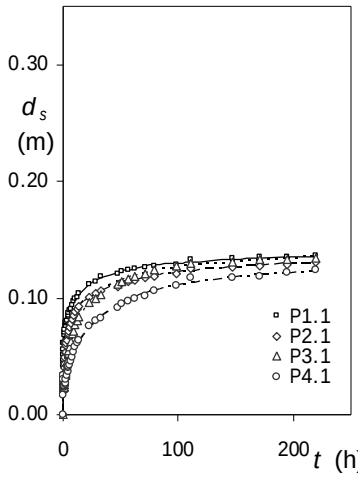

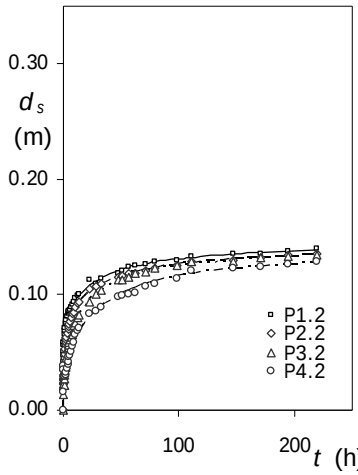

Test 29

P1.1		P2.1		P3.1		P4.1		P1.2	
t (h)	d_s (m)	t (h)	d_s (m)	t (h)	d_s (m)	t (h)	d_s (m)	t (h)	d_s (m)
0.00	0.000	0.00	0.000	0.00	0.000	0.00	0.000	0.00	0.000
0.03	0.032	0.03	0.020	0.03	0.029	0.03	0.017	0.03	0.039
0.08	0.042	0.08	0.021	0.08	0.028	0.08	0.031	0.08	0.042
0.17	0.047	0.17	0.022	0.17	0.030	0.17	0.033	0.17	0.047
0.25	0.051	0.25	0.023	0.25	0.025	0.25	0.032	0.25	0.051
0.50	0.061	0.50	0.029	0.50	0.024	0.50	0.030	0.50	0.059
0.83	0.068	0.83	0.040	0.83	0.026	0.83	0.025	0.83	0.066
1.17	0.071	1.17	0.044	1.17	0.028	1.17	0.025	1.17	0.069
1.75	0.076	1.75	0.052	1.75	0.033	1.75	0.026	1.75	0.074
2.00	0.076	2.00	0.054	2.00	0.035	2.00	0.027	2.00	0.075
4.00	0.084	4.00	0.068	4.00	0.051	4.00	0.037	4.00	0.083
5.75	0.090	5.75	0.075	5.75	0.058	5.75	0.043	5.75	0.087
7.50	0.094	7.50	0.082	7.50	0.069	7.50	0.049	7.50	0.091
9.00	0.097	9.00	0.085	9.00	0.072	9.00	0.054	9.00	0.094
10.50	0.099	10.50	0.088	10.50	0.077	10.50	0.058	10.50	0.097
12.50	0.101	12.50	0.091	12.50	0.081	12.50	0.062	12.50	0.099
14.00	0.104	14.00	0.093	14.00	0.084	14.00	0.064	14.00	0.100
23.00	0.112	23.00	0.101	23.00	0.096	23.00	0.076	23.00	0.113
28.00	0.114	28.00	0.104	28.00	0.100	28.00	0.081	28.00	0.110
47.00	0.121	47.00	0.110	47.00	0.112	47.00	0.092	47.00	0.119
51.00	0.123	51.00	0.113	51.00	0.114	51.00	0.095	51.00	0.121
57.00	0.124	57.00	0.114	57.00	0.116	57.00	0.097	57.00	0.124
62.00	0.125	62.00	0.115	62.00	0.119	62.00	0.099	62.00	0.125
71.00	0.126	71.00	0.117	71.00	0.121	71.00	0.102	71.00	0.127
79.00	0.127	79.00	0.118	79.00	0.124	79.00	0.106	79.00	0.129
98.50	0.129	98.50	0.121	98.50	0.127	98.50	0.111	98.50	0.130
111.33	0.133	111.33	0.125	111.33	0.130	111.33	0.117	111.33	0.133
147.00	0.134	147.00	0.126	147.00	0.131	147.00	0.117	147.00	0.135
171.00	0.135	171.00	0.127	171.00	0.133	171.00	0.118	171.00	0.136
195.00	0.135	195.00	0.129	195.00	0.133	195.00	0.122	195.00	0.138
219.00	0.136	219.00	0.131	219.00	0.134	219.00	0.124	219.00	0.140

Test	α (º)	s (m)	s/D_p	n	W_g (m)	t_d (day)	d_{sge} (m)	d_{sge}/d_{se1}
30	0	0.300	6.0	2	0.100	7.1	0.156	1.15

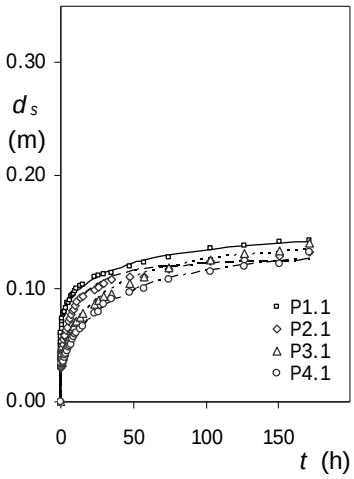

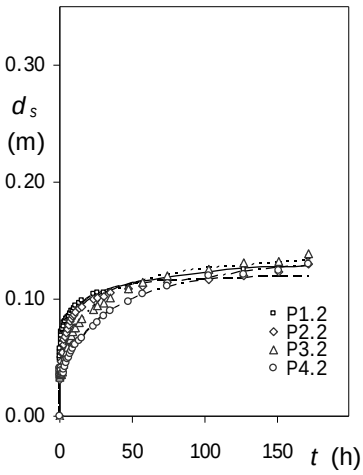

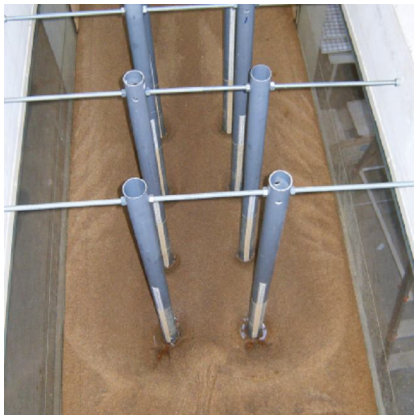

Test 30

P1.1		P2.1		P3.1		P4.1		P1.2	
t (h)	d_s (m)	t (h)	d_s (m)	t (h)	d_s (m)	t (h)	d_s (m)	t (h)	d_s (m)
0.00	0.000	0.00	0.000	0.00	0.000	0.00	0.000	0.00	0.000
0.05	0.045	0.05	0.030	0.05	0.033	0.05	0.035	0.05	0.036
0.10	0.050	0.10	0.032	0.10	0.036	0.10	0.039	0.10	0.049
0.17	0.053	0.17	0.031	0.17	0.037	0.17	0.041	0.17	0.051
0.25	0.057	0.25	0.031	0.25	0.041	0.25	0.043	0.25	0.055
0.50	0.064	0.50	0.036	0.50	0.035	0.50	0.041	0.50	0.062
1.00	0.071	1.00	0.042	1.00	0.039	1.00	0.037	1.00	0.069
1.33	0.074	1.33	0.047	1.33	0.039	1.33	0.037	1.33	0.072
1.67	0.077	1.67	0.051	1.67	0.040	1.67	0.035	1.67	0.073
2.00	0.078	2.00	0.055	2.00	0.042	2.00	0.036	2.00	0.075
2.50	0.079	2.50	0.057	2.50	0.044	2.50	0.039	2.50	0.077
3.00	0.080	3.00	0.059	3.00	0.047	3.00	0.041	3.00	0.080
3.75	0.083	3.75	0.063	3.75	0.050	3.75	0.043	3.75	0.081
4.50	0.087	4.50	0.066	4.50	0.052	4.50	0.045	4.50	0.083
5.25	0.088	5.25	0.071	5.25	0.055	5.25	0.048	5.25	0.084
6.00	0.090	6.00	0.074	6.00	0.058	6.00	0.049	6.00	0.085
7.00	0.093	7.00	0.077	7.00	0.060	7.00	0.051	7.00	0.088
8.00	0.094	8.00	0.081	8.00	0.065	8.00	0.055	8.00	0.090
9.00	0.096	9.00	0.082	9.00	0.067	9.00	0.057	9.00	0.090
10.00	0.098	10.00	0.085	10.00	0.070	10.00	0.060	10.00	0.092
11.00	0.100	11.00	0.089	11.00	0.071	11.00	0.061	11.00	0.094
23.00	0.111	23.00	0.099	23.00	0.086	23.00	0.078	23.00	0.104
30.00	0.113	30.00	0.105	30.00	0.093	30.00	0.086	30.00	0.105
35.00	0.114	35.00	0.108	35.00	0.096	35.00	0.091	35.00	0.107
47.67	0.120	47.67	0.110	47.67	0.105	47.67	0.097	47.67	0.110
57.00	0.123	57.00	0.111	57.00	0.111	57.00	0.100	57.00	0.113
74.00	0.128	74.00	0.118	74.00	0.119	74.00	0.108	74.00	0.116
102.67	0.136	102.67	0.124	102.67	0.126	102.67	0.115	102.67	0.121
126.67	0.138	126.67	0.126	126.67	0.131	126.67	0.120	126.67	0.125
150.67	0.142	150.67	0.129	150.67	0.133	150.67	0.122	150.67	0.129
171.00	0.143	171.00	0.132	171.00	0.141	171.00	0.132	171.00	0.135

Test	α (º)	s (m)	s/D_p	n	W_g (m)	t_d (day)	d_{sge} (m)	d_{sge}/d_{se1}
31	15	0.050	1.0	2	0.137	7.0	0.299	2.20

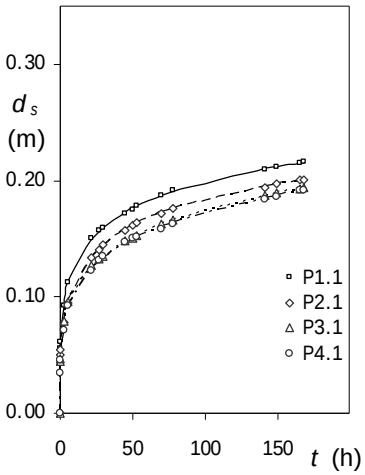

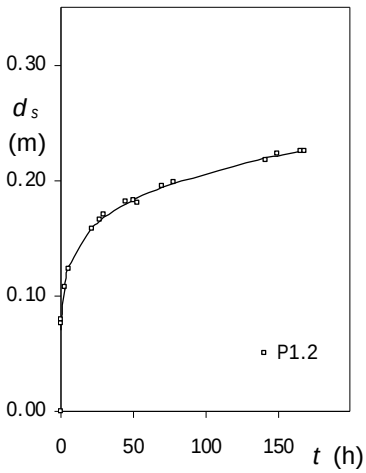

Test 31

P1.1		P2.1		P3.1		P4.1		P1.2	
t (h)	d_s (m)	t (h)	d_s (m)	t (h)	d_s (m)	t (h)	d_s (m)	t (h)	d_s (m)
0.00	0.000	0.00	0.000	0.00	0.000	0.00	0.000	0.00	0.000
0.20	0.055	0.22	0.050	0.23	0.044	0.23	0.035	0.25	0.076
0.37	0.062	0.38	0.055	0.38	0.047	0.40	0.046	0.42	0.080
2.25	0.093	2.25	0.078	2.27	0.079	2.27	0.071	2.28	0.108
5.35	0.112	5.37	0.095	5.38	0.096	5.38	0.093	5.40	0.123
21.18	0.151	21.20	0.134	21.20	0.127	21.22	0.123	21.23	0.159
26.35	0.157	26.37	0.141	26.38	0.132	26.38	0.131	26.40	0.166
29.27	0.160	29.27	0.145	29.28	0.135	29.30	0.135	29.32	0.170
45.00	0.172	45.00	0.157	45.02	0.148	45.02	0.147	45.03	0.182
50.28	0.175	50.30	0.162	50.32	0.150	50.32	0.151	50.33	0.182
52.80	0.179	52.83	0.164	52.83	0.152	52.88	0.152	52.92	0.180
69.20	0.187	69.22	0.172	69.23	0.163	69.23	0.159	69.25	0.195
77.38	0.192	77.40	0.177	77.42	0.167	77.42	0.162	77.43	0.198
141.25	0.210	141.27	0.193	141.27	0.187	141.28	0.184	141.30	0.218
149.13	0.212	149.15	0.197	149.15	0.190	149.17	0.187	149.18	0.223
165.22	0.215	165.23	0.201	165.23	0.193	165.25	0.192	165.25	0.226
167.97	0.216	167.98	0.201	168.00	0.194	168.00	0.192	168.02	0.225

Test	α (º)	s (m)	s/D_p	n	W_g (m)	t_d (day)	d_{sge} (m)	d_{sge}/d_{se1}
32	15	0.100	2.0	2	0.204	7.0	0.240	1.76

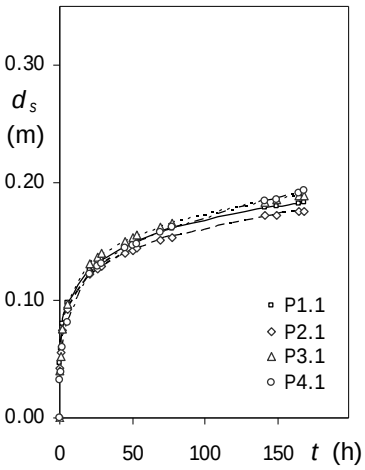

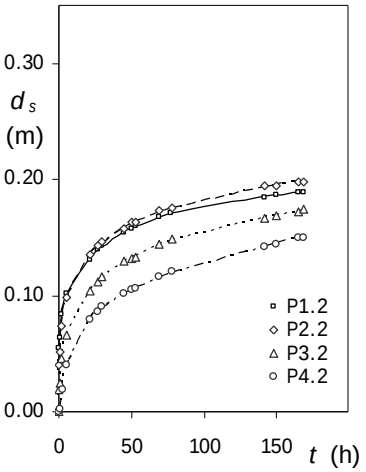

Test 32

P1.1		P2.1		P3.1		P4.1		P1.2	
t (h)	d_s (m)	t (h)	d_s (m)	t (h)	d_s (m)	t (h)	d_s (m)	t (h)	d_s (m)
0.00	0.000	0.00	0.000	0.00	0.000	0.00	0.000	0.00	0.000
0.12	0.046	0.13	0.043	0.13	0.040	0.15	0.032	0.17	0.055
0.57	0.059	0.58	0.056	0.58	0.052	0.60	0.039	0.62	0.064
2.17	0.080	2.18	0.075	2.20	0.075	2.20	0.060	2.22	0.084
5.45	0.098	5.47	0.092	5.48	0.096	5.50	0.081	5.52	0.102
21.08	0.126	21.10	0.122	21.12	0.131	21.13	0.122	21.15	0.131
26.45	0.132	26.47	0.127	26.48	0.136	26.50	0.129	26.52	0.140
29.18	0.135	29.20	0.129	29.22	0.141	29.22	0.131	29.23	0.143
45.10	0.146	45.10	0.140	45.12	0.150	45.13	0.145	45.13	0.155
50.20	0.149	50.22	0.143	50.23	0.153	50.23	0.147	50.25	0.158
53.02	0.150	53.03	0.144	53.05	0.155	53.05	0.148	53.07	0.160
69.10	0.158	69.12	0.152	69.12	0.162	69.13	0.158	69.15	0.168
77.48	0.162	77.50	0.153	77.52	0.166	77.52	0.162	77.53	0.171
141.17	0.178	141.17	0.172	141.18	0.184	141.18	0.184	141.20	0.185
149.23	0.180	149.25	0.173	149.25	0.186	149.27	0.186	149.28	0.187
165.15	0.182	165.17	0.176	165.17	0.189	165.18	0.192	165.20	0.189
168.08	0.184	168.08	0.175	168.10	0.189	168.12	0.193	168.12	0.189

Test	α (º)	s (m)	s/D_p	n	W_g (m)	t_d (day)	d_{sge} (m)	d_{sge}/d_{se1}
33	15	0.150	3.0	2	0.255	7.0	0.183	1.35

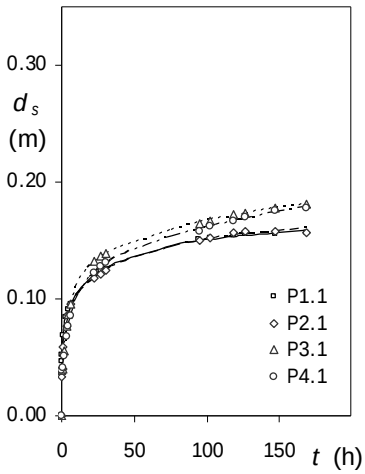

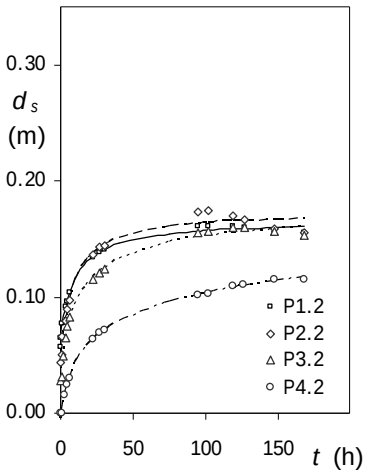

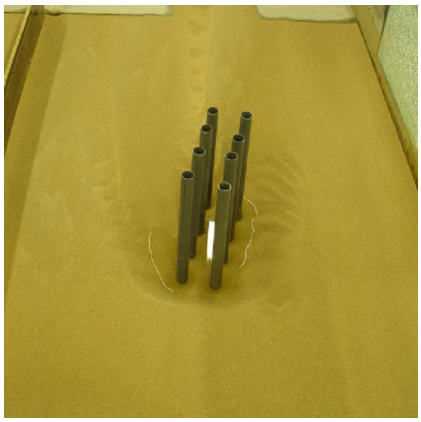

Test 33

P1.1		P2.1		P3.1		P4.1		P1.2	
t (h)	d_s (m)	t (h)	d_s (m)	t (h)	d_s (m)	t (h)	d_s (m)	t (h)	d_s (m)
0.00	0	0.00	0	0.00	0	0.00	0	0.00	0.000
0.23	0.047	0.25	0.034	0.27	0.039	0.28	0.039	0.23	0.057
0.43	0.052	0.45	0.04	0.47	0.04	0.48	0.041	0.43	0.065
1.32	0.069	1.33	0.059	1.35	0.056	1.38	0.051	1.32	0.077
3.13	0.085	3.15	0.077	3.17	0.077	3.18	0.068	3.13	0.091
4.40	0.091	4.42	0.086	4.43	0.087	4.45	0.077	4.40	0.097
6.08	0.096	6.10	0.095	6.12	0.096	6.13	0.085	6.08	0.104
10.00	0.1047	10.00	0.102	10.00	0.1113	10.00	0.0997	10.00	0.116
18.00	0.116	18.00	0.1136	18.00	0.1268	18.00	0.1166	18.00	0.131
22.55	0.12	22.57	0.117	22.58	0.132	22.60	0.122	22.55	0.134
27.17	0.124	27.18	0.121	27.20	0.137	27.23	0.128	27.18	0.139
30.15	0.126	30.17	0.124	30.18	0.139	30.20	0.131	30.17	0.141
40.00	0.1327	40.00	0.1307	40.00	0.145	40.00	0.1374	40.00	0.146
75.00	0.1455	75.00	0.1447	75.00	0.1594	75.00	0.1535	75.00	0.155
94.57	0.151	94.58	0.15	94.60	0.164	94.62	0.158	94.57	0.161
102.05	0.152	102.07	0.152	102.08	0.167	102.10	0.163	102.07	0.162
118.57	0.154	118.58	0.156	118.60	0.172	118.62	0.167	118.57	0.161
126.40	0.156	126.42	0.158	126.43	0.174	126.45	0.17	126.40	0.160
147.20	0.156	147.22	0.158	147.25	0.178	147.27	0.176	147.22	0.155
168.10	0.156	168.12	0.157	168.13	0.181	168.15	0.178	168.10	0.156

Test	α (º)	s (m)	s/D_p	n	W_g (m)	t_d (day)	d_{sge} (m)	d_{sge}/d_{se1}
34	15	0.225	4.5	2	0.300	7.2	0.205	1.51

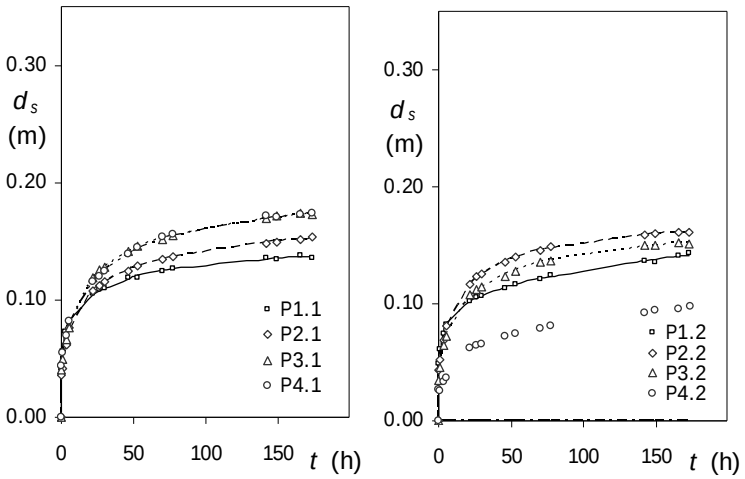

Test 34

P1.1		P2.1		P3.1		P4.1		P1.2	
t (h)	d_s (m)	t (h)	d_s (m)	t (h)	d_s (m)	t (h)	d_s (m)	t (h)	d_s (m)
0.00	0.000	0.00	0.000	0.00	0.000	0.00	0.000	0.00	0.000
0.23	0.042	0.27	0.036	0.28	0.040	0.32	0.044	0.25	0.049
0.95	0.056	0.97	0.042	0.98	0.049	1.02	0.055	0.95	0.062
3.17	0.073	3.18	0.061	3.22	0.066	3.23	0.070	3.18	0.074
5.53	0.081	5.55	0.076	5.57	0.077	5.58	0.082	5.53	0.083
21.80	0.105	21.82	0.107	21.83	0.119	21.87	0.115	21.80	0.103
26.02	0.109	26.03	0.113	26.07	0.125	26.08	0.120	26.02	0.105
29.62	0.110	29.63	0.116	29.67	0.128	30.35	0.125	29.62	0.107
45.92	0.119	45.93	0.125	45.97	0.142	45.98	0.140	45.92	0.113
53.08	0.119	53.10	0.129	53.13	0.146	53.15	0.144	53.08	0.117
70.12	0.124	70.13	0.135	70.17	0.151	70.18	0.153	70.12	0.122
77.18	0.127	77.20	0.137	77.22	0.155	77.23	0.155	77.18	0.124
141.88	0.136	141.90	0.149	141.92	0.170	141.97	0.171	141.90	0.137
149.37	0.135	149.38	0.149	149.40	0.171	149.43	0.170	149.37	0.136
165.63	0.138	165.65	0.151	165.68	0.174	165.70	0.172	165.63	0.141
173.28	0.136	173.30	0.154	173.33	0.173	173.35	0.174	173.28	0.143

Test	α (º)	s (m)	s/D_p	n	W_g (m)	t_d (day)	d_{sge} (m)	d_{sge}/d_{se1}
35	15	0.300	6.0	2	0.300	8.9	0.204	1.51

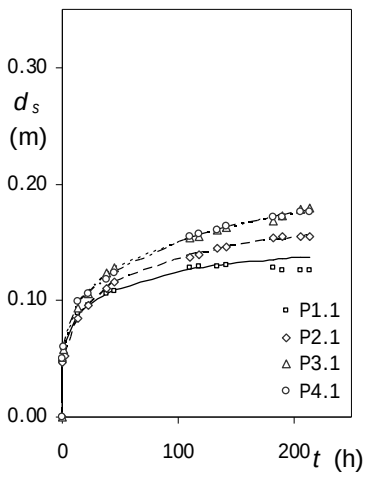

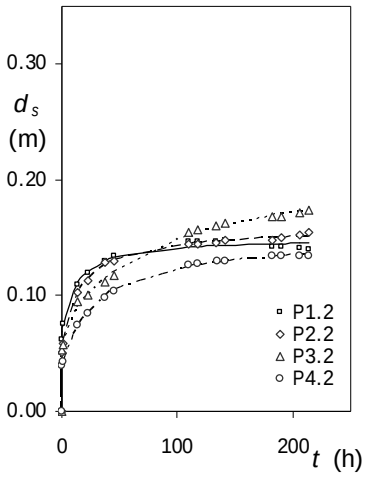

Test 35

P1.1		P2.1		P3.1		P4.1		P1.2	
t (h)	d_s (m)	t (h)	d_s (m)	t (h)	d_s (m)	t (h)	d_s (m)	t (h)	d_s (m)
0.00	0.000	0.00	0.000	0.00	0.000	0.00	0.000	0.00	0.000
0.32	0.047	0.33	0.047	0.35	0.052	0.38	0.051	0.40	0.062
1.28	0.059	1.73	0.053	1.33	0.058	1.35	0.060	1.30	0.075
14.02	0.089	14.02	0.085	14.05	0.094	14.05	0.099	14.08	0.110
22.03	0.095	22.05	0.096	22.07	0.106	22.07	0.106	22.10	0.120
37.73	0.106	37.75	0.111	37.77	0.123	37.78	0.118	37.82	0.130
45.52	0.109	45.53	0.116	45.55	0.128	45.57	0.123	45.58	0.134
110.02	0.128	110.03	0.138	110.05	0.154	110.07	0.155	110.08	0.147
117.80	0.130	117.82	0.140	117.83	0.155	117.85	0.157	117.87	0.146
133.95	0.129	133.97	0.144	133.97	0.161	133.98	0.160	134.00	0.147
141.63	0.130	141.65	0.146	141.67	0.163	141.67	0.164	141.68	0.148
182.55	0.128	182.57	0.154	182.58	0.168	182.60	0.171	182.63	0.142
190.02	0.127	190.03	0.155	190.05	0.173	190.07	0.172	190.08	0.142
206.23	0.126	206.23	0.155	206.27	0.178	206.27	0.176	206.30	0.141
213.43	0.126	213.45	0.154	213.47	0.179	213.47	0.176	213.40	0.140

Test	α (º)	s (m)	s/D_p	n	W_g (m)	t_d (day)	d_{sge} (m)	d_{sge}/d_{se1}
36	30	0.050	1.0	2	0.168	6.8	0.316	2.33

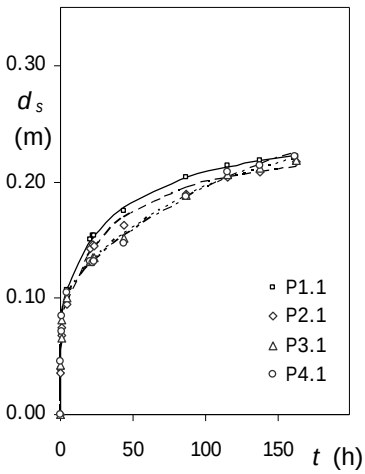

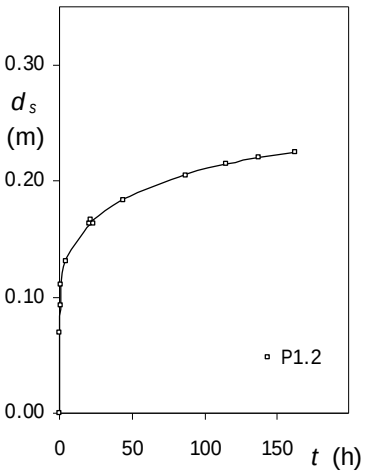

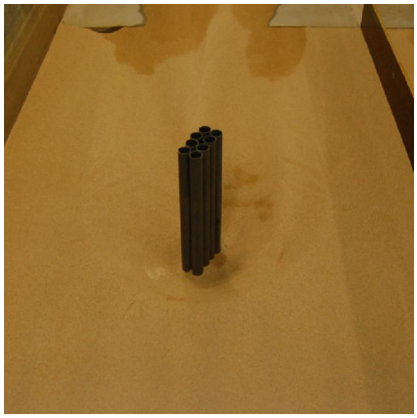

Test 36

P1.1		P2.1		P3.1		P4.1		P1.2	
t (h)	d_s (m)	t (h)	d_s (m)	t (h)	d_s (m)	t (h)	d_s (m)	t (h)	d_s (m)
0.00	0.000	0.00	0.000	0.00	0.000	0.00	0.000	0.00	0.000
0.08	0.039	0.10	0.036	0.12	0.043	0.13	0.046	0.13	0.069
0.52	0.069	0.53	0.069	0.55	0.066	0.55	0.071	0.57	0.093
1.18	0.085	1.18	0.075	1.20	0.081	1.20	0.085	1.22	0.111
4.12	0.107	4.13	0.095	4.13	0.101	4.15	0.105	4.18	0.131
20.25	0.150	20.25	0.143	20.27	0.132	20.27	0.132	20.28	0.164
21.90	0.154	21.90	0.146	21.92	0.135	21.93	0.131	21.93	0.167
23.22	0.154	23.23	0.145	23.23	0.135	23.25	0.131	23.25	0.164
43.73	0.175	43.75	0.163	43.78	0.152	43.83	0.147	43.70	0.184
86.80	0.204	86.78	0.190	86.77	0.189	86.75	0.188	86.82	0.205
114.93	0.214	114.95	0.204	114.98	0.206	115.02	0.209	114.92	0.215
137.27	0.218	137.25	0.208	137.22	0.212	137.20	0.215	137.28	0.221
162.25	0.222	162.28	0.218	162.30	0.219	161.83	0.222	162.22	0.225

Test	α (º)	s (m)	s/D_p	n	W_g (m)	t_d (day)	d_{sge} (m)	d_{sge}/d_{se1}
37	30	0.100	2.0	2	0.287	6.8	0.331	2.44

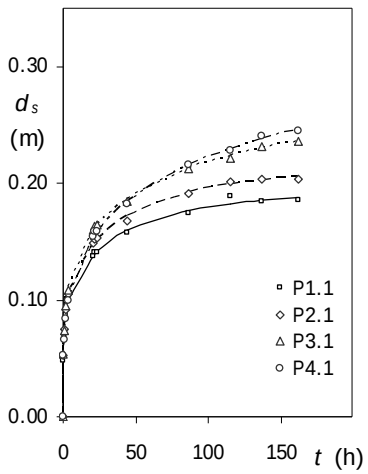

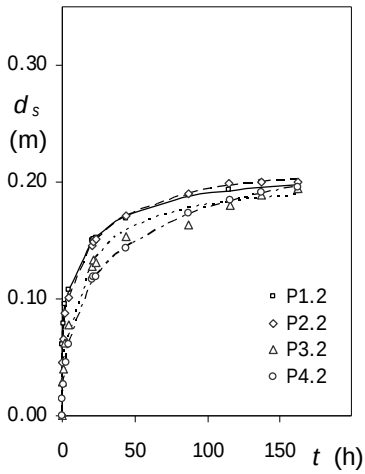

Test 37

P1.1		P2.1		P3.1		P4.1		P1.2	
t (h)	d_s (m)	t (h)	d_s (m)	t (h)	d_s (m)	t (h)	d_s (m)	t (h)	d_s (m)
0.00	0.000	0.00	0.000	0.00	0.000	0.00	0.000	0.00	0.000
0.23	0.048	0.25	0.053	0.25	0.054	0.27	0.053	0.28	0.061
0.82	0.069	0.83	0.075	0.83	0.074	0.85	0.066	0.87	0.079
2.15	0.088	2.17	0.092	2.18	0.095	2.20	0.084	2.22	0.096
4.02	0.100	4.03	0.105	4.03	0.109	4.05	0.100	4.07	0.108
20.40	0.138	20.40	0.149	20.42	0.160	20.42	0.154	20.43	0.150
21.85	0.141	21.85	0.152	21.87	0.164	21.87	0.159	21.88	0.152
23.20	0.141	23.22	0.153	23.22	0.164	23.23	0.159	23.23	0.152
43.92	0.158	43.95	0.168	43.97	0.185	44.07	0.183	43.88	0.169
86.78	0.175	86.73	0.191	86.72	0.213	86.63	0.216	86.77	0.189
115.12	0.189	115.13	0.201	115.23	0.221	115.27	0.229	115.08	0.193
137.03	0.184	137.00	0.204	136.95	0.232	136.92	0.240	137.05	0.200
162.47	0.186	162.48	0.204	162.50	0.236	162.52	0.245	162.47	0.192

Test	α (º)	s (m)	s/D_p	n	W_g (m)	t_d (day)	d_{sge} (m)	d_{sge}/d_{se1}
38	30	0.150	3.0	2	0.300	7.8	0.278	2.04

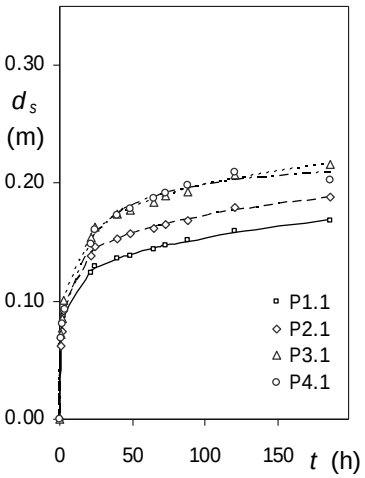

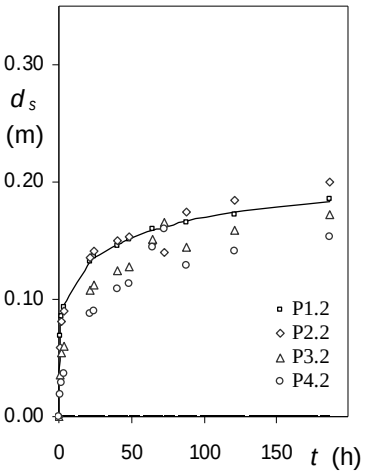

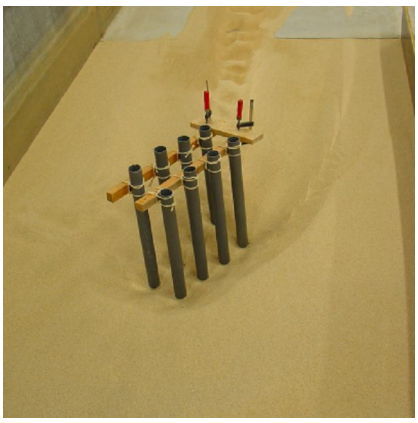

Test 38

P1.1		P2.1		P3.1		P4.1		P1.2	
t (h)	d_s (m)	t (h)	d_s (m)	t (h)	d_s (m)	t (h)	d_s (m)	t (h)	d_s (m)
0.00	0.000	0.00	0.000	0.00	0.000	0.00	0.000	0.00	0.000
0.68	0.062	0.70	0.062	0.72	0.072	0.72	0.069	0.77	0.069
1.58	0.074	1.58	0.074	1.60	0.085	1.62	0.081	1.67	0.085
3.13	0.087	3.15	0.092	3.15	0.101	3.17	0.093	3.18	0.093
21.30	0.125	21.27	0.139	21.23	0.154	21.22	0.149	21.33	0.132
24.43	0.130	24.45	0.146	24.47	0.163	24.48	0.161	24.52	0.137
39.87	0.136	39.85	0.153	39.83	0.174	39.80	0.173	39.90	0.146
48.67	0.139	48.65	0.157	48.63	0.178	48.60	0.178	48.68	0.151
64.60	0.144	64.62	0.162	64.63	0.184	64.67	0.187	64.68	0.160
72.72	0.147	72.68	0.165	72.67	0.189	72.63	0.192	72.60	0.162
88.00	0.152	87.98	0.168	87.97	0.193	87.93	0.199	88.02	0.166
120.65	0.159	120.63	0.180	120.63	0.207	120.62	0.210	120.65	0.172
186.22	0.169	186.10	0.188	186.08	0.216	186.07	0.203	186.13	0.185

Test	α (º)	s (m)	s/D_p	n	W_g (m)	t_d (day)	d_{sge} (m)	d_{sge}/d_{se1}
39	30	0.225	4.5	2	0.300	6.9	0.217	1.60

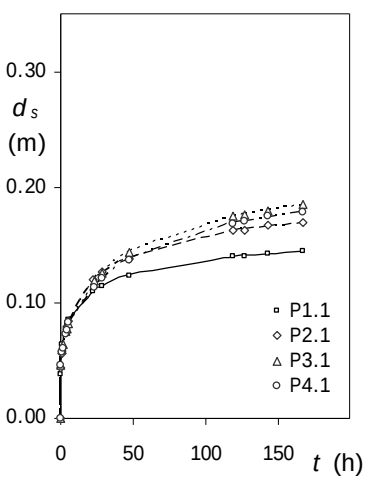

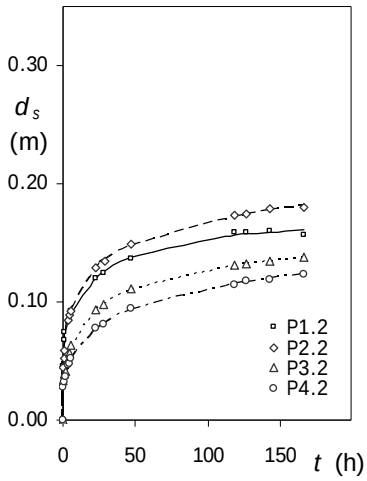

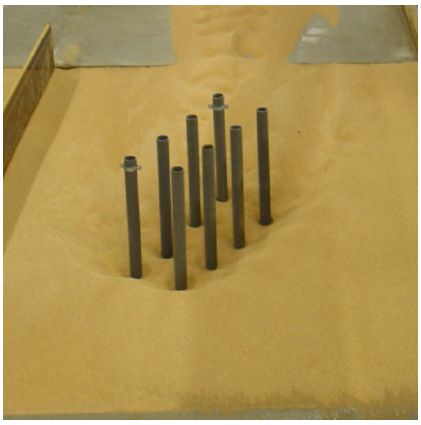

Test 39

P1.1		P2.1		P3.1		P4.1		P1.2	
t (h)	d_s (m)	t (h)	d_s (m)	t (h)	d_s (m)	t (h)	d_s (m)	t (h)	d_s (m)
0.00	0.000	0.00	0.000	0.00	0.000	0.00	0.000	0.00	0.000
0.08	0.038	0.12	0.044	0.13	0.046	0.15	0.046	0.10	0.046
0.77	0.059	0.78	0.056	0.82	0.059	0.83	0.058	0.77	0.068
1.32	0.065	1.33	0.058	1.37	0.064	1.38	0.061	1.32	0.075
3.43	0.078	3.45	0.074	3.48	0.075	3.50	0.073	3.43	0.084
4.25	0.082	4.28	0.079	4.30	0.078	4.32	0.077	4.27	0.087
5.32	0.085	5.33	0.084	5.35	0.082	5.38	0.083	5.32	0.093
22.73	0.110	22.75	0.120	22.78	0.118	22.80	0.114	22.73	0.120
28.28	0.115	28.30	0.126	28.33	0.126	28.35	0.121	28.30	0.124
47.33	0.124	47.35	0.138	47.38	0.144	47.40	0.137	47.35	0.137
118.87	0.140	118.88	0.163	118.92	0.175	118.93	0.169	118.87	0.159
126.42	0.141	126.43	0.163	126.45	0.177	126.48	0.170	126.43	0.159
142.52	0.143	142.53	0.167	142.57	0.180	142.58	0.175	142.53	0.160
166.60	0.145	166.62	0.169	166.65	0.185	166.68	0.179	166.62	0.157

Test	α (º)	s (m)	s/D_p	n	W_g (m)	t_d (day)	d_{sge} (m)	d_{sge}/d_{se1}
40	30	0.300	6.0	2	0.300	7.7	0.200	1.47

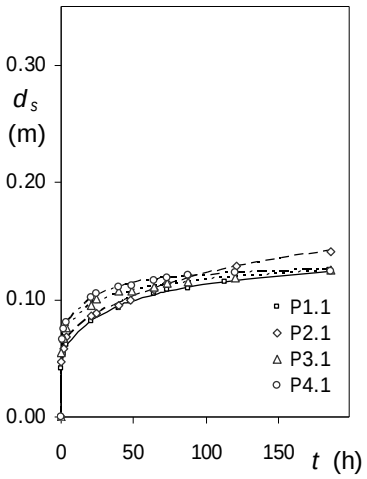

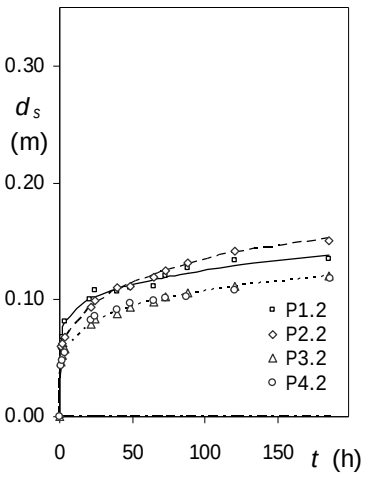

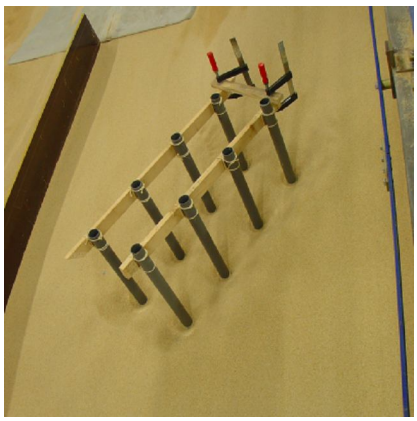

Test 40

P1.1		P2.1		P3.1		P4.1		P1.2	
t (h)	d_s (m)	t (h)	d_s (m)	t (h)	d_s (m)	t (h)	d_s (m)	t (h)	d_s (m)
0.00	0.000	0.00	0.000	0.00	0.000	0.00	0.000	0.00	0.000
0.27	0.042	0.28	0.047	0.30	0.055	0.48	0.066	0.50	0.059
1.38	0.053	1.40	0.058	1.42	0.067	1.43	0.075	1.47	0.068
3.30	0.061	3.30	0.069	3.33	0.076	3.35	0.080	3.37	0.081
21.12	0.082	20.98	0.086	21.00	0.095	20.95	0.102	21.13	0.101
24.30	0.087	24.33	0.088	24.37	0.100	24.38	0.105	24.40	0.108
40.15	0.093	40.13	0.096	40.12	0.107	40.08	0.111	40.00	0.107
48.33	0.099	48.38	0.099	48.40	0.108	48.42	0.112	48.52	0.110
64.42	0.105	64.43	0.109	64.45	0.110	64.48	0.117	64.52	0.112
72.85	0.109	72.88	0.114	72.90	0.114	72.95	0.119	72.68	0.120
87.87	0.109	87.85	0.121	87.82	0.115	87.83	0.121	87.88	0.127
112.77	0.115	120.77	0.128	120.75	0.118	120.75	0.123	120.73	0.134
185.88	0.125	185.90	0.141	186.00	0.126	185.98	0.124	185.87	0.135

Test	α (º)	s (m)	s/D_p	n	W_g (m)	t_d (day)	d_{sge} (m)	d_{sge}/d_{se1}
41	45	0.050	1.0	2	0.191	12.0	0.335	2.47

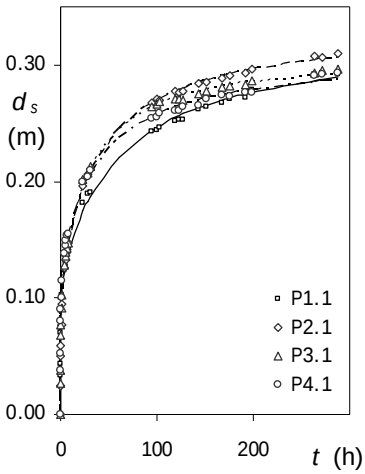

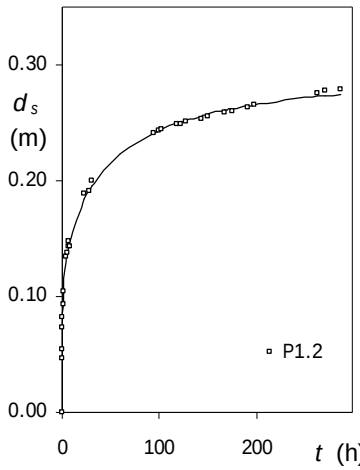

Test 41

P1.1		P2.1		P3.1		P4.1		P1.2	
t (h)	d_s (m)	t (h)	d_s (m)	t (h)	d_s (m)	t (h)	d_s (m)	t (h)	d_s (m)
0.00	0.000	0.00	0.000	0.00	0.000	0.00	0.000	0.00	0.000
0.02	0.033	0.03	0.025	0.03	0.027	0.05	0.038	0.05	0.047
0.08	0.044	0.08	0.025	0.10	0.038	0.10	0.053	0.12	0.055
0.32	0.070	0.32	0.050	0.33	0.068	0.33	0.080	0.35	0.073
0.47	0.075	0.47	0.059	0.48	0.077	0.48	0.090	0.50	0.082
0.92	0.091	0.92	0.077	0.93	0.091	0.93	0.100	0.95	0.093
1.70	0.102	1.70	0.094	1.72	0.102	1.72	0.115	1.73	0.104
4.37	0.123	4.37	0.126	4.38	0.128	4.38	0.138	4.40	0.134
5.27	0.127	5.27	0.133	5.28	0.136	5.28	0.145	5.30	0.138
6.03	0.132	6.03	0.138	6.05	0.140	6.05	0.149	6.07	0.143
6.72	0.136	6.72	0.142	6.73	0.143	6.73	0.154	6.75	0.148
7.47	0.139	7.47	0.147	7.48	0.147	7.48	0.155	7.50	0.144
23.10	0.181	23.10	0.197	23.12	0.201	23.12	0.200	23.13	0.189
27.72	0.189	27.68	0.207	27.68	0.207	27.70	0.204	27.70	0.191
30.77	0.191	30.77	0.211	30.78	0.213	30.78	0.210	30.80	0.200
60.00	0.221	60.00	0.245	60.00	0.246	60.00	0.237	60.00	0.223
94.60	0.243	94.60	0.268	94.62	0.264	94.62	0.254	94.63	0.241
99.58	0.245	99.58	0.270	99.60	0.266	99.60	0.255	99.62	0.243
102.72	0.247	102.72	0.270	102.73	0.268	102.73	0.259	102.75	0.244
118.65	0.252	118.65	0.278	118.67	0.271	118.67	0.261	118.68	0.249
122.35	0.253	122.35	0.277	122.37	0.271	122.37	0.261	122.38	0.249
126.90	0.253	126.90	0.277	126.92	0.270	126.92	0.264	126.93	0.251
143.05	0.262	143.05	0.284	143.07	0.276	143.07	0.265	143.08	0.253
150.50	0.265	150.50	0.286	150.52	0.278	150.52	0.271	150.53	0.255
167.08	0.268	167.08	0.288	167.10	0.281	167.10	0.274	167.12	0.259
174.72	0.271	174.72	0.291	174.73	0.282	174.73	0.274	174.75	0.260
191.33	0.272	191.33	0.293	191.35	0.283	191.35	0.277	191.37	0.263
197.63	0.279	197.63	0.297	197.65	0.286	197.65	0.276	197.67	0.265
262.68	0.292	262.68	0.308	262.70	0.293	262.70	0.291	262.72	0.276
270.53	0.293	270.53	0.307	270.55	0.295	270.55	0.293	270.57	0.277
287.02	0.292	287.02	0.310	287.03	0.297	287.03	0.293	287.05	0.279

Test	α (º)	s (m)	s/D_p	n	W_g (m)	t_d (day)	d_{sge} (m)	d_{sge}/d_{se1}
42	45	0.100	2.0	2	0.250	9.0	0.257	1.90

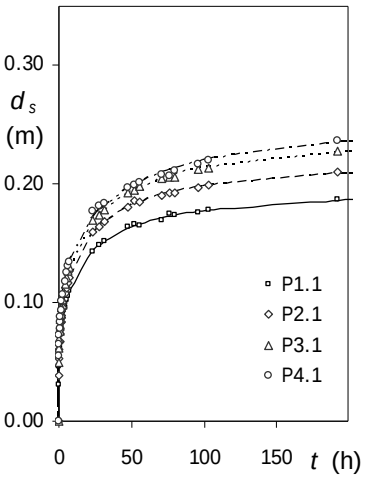

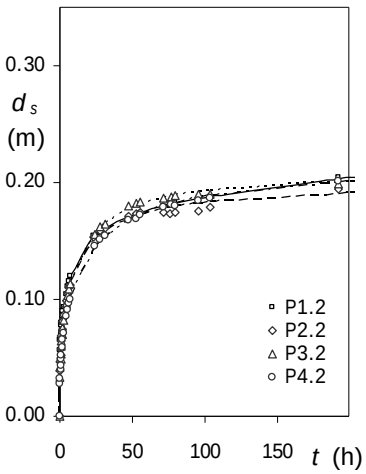

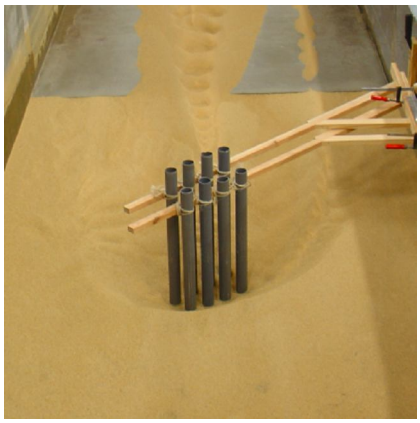

Test 42

P1.1		P2.1		P3.1		P4.1		P1.2	
t (h)	d_s (m)	t (h)	d_s (m)	t (h)	d_s (m)	t (h)	d_s (m)	t (h)	d_s (m)
0.00	0.000	0.00	0.000	0.00	0.000	0.00	0.000	0.00	0.000
0.03	0.031	0.05	0.039	0.07	0.050	0.08	0.055	0.10	0.048
0.18	0.046	0.20	0.053	0.22	0.062	0.23	0.065	0.25	0.057
0.37	0.054	0.38	0.061	0.40	0.070	0.42	0.073	0.43	0.066
0.57	0.062	0.58	0.067	0.60	0.076	0.62	0.078	0.63	0.071
0.82	0.066	0.83	0.073	0.85	0.081	0.87	0.084	0.88	0.078
1.07	0.072	1.08	0.077	1.10	0.086	1.12	0.088	1.13	0.080
1.45	0.077	1.47	0.084	1.48	0.091	1.50	0.094	1.52	0.086
1.90	0.082	1.92	0.089	1.93	0.096	1.95	0.101	1.97	0.090
2.43	0.087	2.45	0.096	2.47	0.102	2.48	0.107	2.50	0.093
4.28	0.096	4.30	0.108	4.32	0.115	4.33	0.118	4.35	0.104
5.35	0.103	5.37	0.113	5.38	0.121	5.40	0.125	5.42	0.111
6.20	0.105	6.22	0.117	6.23	0.126	6.25	0.131	6.27	0.116
7.30	0.110	7.32	0.121	7.33	0.130	7.35	0.135	7.37	0.120
23.55	0.143	23.57	0.160	23.58	0.170	23.60	0.177	23.62	0.155
27.98	0.149	28.00	0.164	28.02	0.174	28.03	0.182	28.05	0.158
31.07	0.152	31.08	0.168	31.10	0.178	31.12	0.183	31.13	0.163
47.33	0.164	47.35	0.180	47.37	0.193	47.38	0.197	47.40	0.170
52.15	0.166	52.17	0.186	52.18	0.195	52.20	0.200	52.22	0.173
55.22	0.165	55.23	0.185	55.25	0.198	55.27	0.202	55.28	0.173
71.15	0.170	71.17	0.190	71.18	0.205	71.20	0.208	71.22	0.180
76.20	0.175	76.22	0.192	76.23	0.205	76.25	0.207	76.27	0.182
79.62	0.174	79.63	0.193	79.65	0.206	79.67	0.211	79.18	0.183
95.48	0.176	95.50	0.197	95.52	0.212	95.53	0.217	95.55	0.186
103.10	0.179	103.12	0.199	103.13	0.214	103.15	0.220	103.17	0.188
192.00	0.187	192.02	0.210	192.03	0.228	192.05	0.237	192.07	0.205
199.48	0.187	199.50	0.210	199.52	0.228	199.53	0.237	199.55	0.205
215.28	0.187	215.30	0.211	215.32	0.231	215.33	0.240	215.35	0.204

Test	α (º)	s (m)	s/D_p	n	W_g (m)	t_d (day)	d_{sge} (m)	d_{sge}/d_{se1}
43	45	0.150	3.0	2	0.250	9.0	0.244	1.80

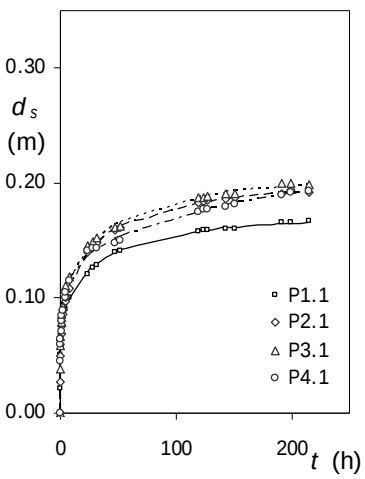

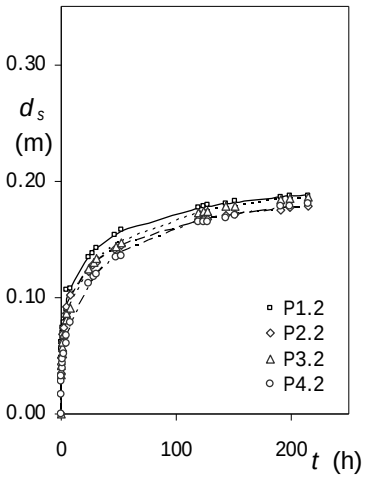

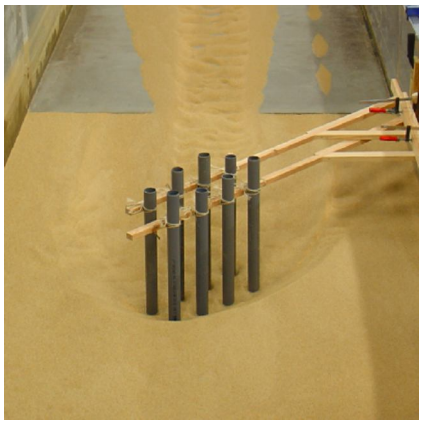

Test 43

P1.1		P2.1		P3.1		P4.1		P1.2	
t (h)	d_s (m)	t (h)	d_s (m)	t (h)	d_s (m)	t (h)	d_s (m)	t (h)	d_s (m)
0.00	0.000	0.00	0.000	0.00	0.000	0.00	0.000	0.00	0.000
0.03	0.021	0.03	0.027	0.05	0.038	0.07	0.046	0.10	0.048
0.22	0.050	0.23	0.050	0.23	0.059	0.25	0.060	0.27	0.056
0.43	0.051	0.45	0.060	0.47	0.067	0.47	0.064	0.48	0.062
0.73	0.058	0.75	0.069	0.77	0.079	0.77	0.071	0.78	0.066
1.10	0.066	1.12	0.076	1.13	0.079	1.15	0.080	1.15	0.069
1.58	0.071	1.60	0.080	1.62	0.085	1.63	0.085	1.65	0.074
2.17	0.076	2.18	0.085	2.20	0.092	2.22	0.089	2.23	0.078
4.00	0.090	4.02	0.097	4.03	0.104	4.05	0.101	4.07	0.090
4.97	0.100	4.98	0.101	5.00	0.111	5.02	0.105	5.03	0.107
7.48	0.100	7.50	0.109	7.50	0.119	7.52	0.115	7.53	0.107
23.25	0.121	23.27	0.140	23.28	0.146	23.30	0.141	23.32	0.135
27.75	0.127	27.77	0.145	27.78	0.149	27.80	0.143	27.82	0.138
30.98	0.129	31.00	0.148	31.02	0.152	31.03	0.143	31.05	0.143
47.07	0.140	47.08	0.159	47.10	0.161	47.12	0.148	47.13	0.153
51.90	0.142	51.92	0.161	51.93	0.163	51.95	0.151	51.97	0.158
119.22	0.158	119.23	0.183	119.25	0.188	119.27	0.175	119.28	0.177
124.10	0.159	124.12	0.184	124.13	0.188	124.15	0.177	124.17	0.178
127.00	0.159	127.02	0.185	127.03	0.188	127.05	0.178	127.07	0.180
143.27	0.160	143.28	0.187	143.30	0.190	143.32	0.180	143.33	0.181
150.92	0.160	150.93	0.188	150.95	0.191	150.97	0.182	150.98	0.183
191.32	0.166	191.33	0.191	191.35	0.199	191.37	0.190	191.38	0.186
199.13	0.166	199.15	0.194	199.17	0.200	199.18	0.191	199.20	0.187
214.92	0.167	214.93	0.192	214.95	0.199	214.97	0.193	214.98	0.187

Test	α (º)	s (m)	s/D_p	n	W_g (m)	t_d (day)	d_{sge} (m)	d_{sge}/d_{se1}
44	45	0.225	4.5	2	0.250	8.1	0.189	1.39

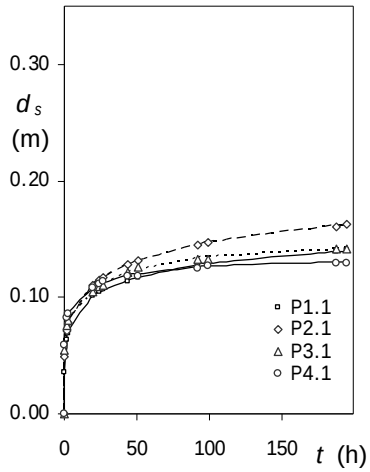

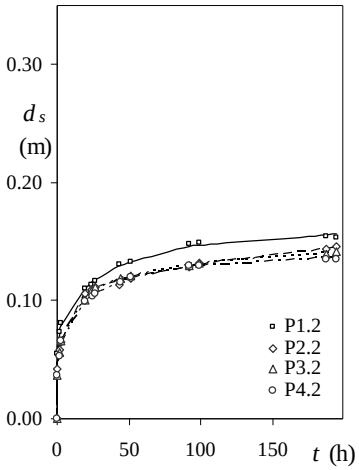

Test 44

P1.1		P2.1		P3.1		P4.1		P1.2	
t (h)	d_s (m)	t (h)	d_s (m)	t (h)	d_s (m)	t (h)	d_s (m)	t (h)	d_s (m)
0.00	0.000	0.00	0.000	0.00	0.000	0.00	0.000	0.00	0.000
0.20	0.036	0.22	0.049	0.25	0.055	0.27	0.059	0.22	0.055
1.72	0.063	1.73	0.072	1.75	0.076	1.78	0.083	1.72	0.073
2.85	0.070	2.87	0.078	2.88	0.080	2.92	0.086	2.85	0.081
19.27	0.101	19.28	0.111	19.32	0.104	19.33	0.108	19.27	0.110
24.27	0.105	24.28	0.115	24.32	0.109	24.33	0.112	24.27	0.114
26.83	0.107	26.85	0.117	26.88	0.110	26.90	0.113	26.83	0.117
43.75	0.114	43.77	0.128	43.78	0.121	43.80	0.118	43.75	0.130
50.88	0.117	50.90	0.131	50.93	0.126	50.95	0.118	50.90	0.133
91.75	0.128	91.77	0.145	91.80	0.133	91.82	0.125	91.75	0.149
98.92	0.130	98.93	0.147	98.97	0.133	98.98	0.127	98.92	0.150
187.73	0.139	187.75	0.161	187.78	0.141	187.80	0.130	187.75	0.155
194.43	0.140	194.45	0.162	194.48	0.142	194.52	0.130	194.45	0.153

Test	α (º)	s (m)	s/D_p	n	W_g (m)	t_d (day)	d_{sge} (m)	d_{sge}/d_{se1}
45	45	0.300	6.0	2	0.250	8.9	0.177	1.30

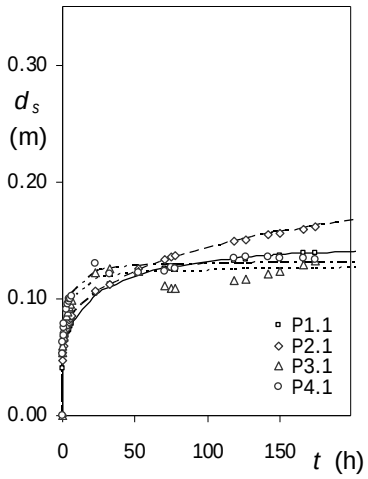

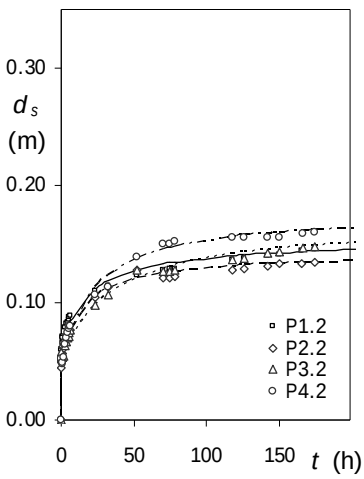

Test 45

P1.1		P2.1		P3.1		P4.1		P1.2	
t (h)	d_s (m)	t (h)	d_s (m)	t (h)	d_s (m)	t (h)	d_s (m)	t (h)	d_s (m)
0.00	0.000	0.00	0.000	0.00	0.000	0.00	0.000	0.00	0.000
0.07	0.040	0.08	0.047	0.10	0.054	0.12	0.053	0.13	0.053
0.30	0.051	0.32	0.054	0.33	0.060	0.35	0.063	0.37	0.061
0.65	0.057	0.67	0.060	0.68	0.067	0.70	0.069	0.72	0.065
0.97	0.059	0.98	0.064	1.00	0.071	1.02	0.075	1.03	0.071
1.28	0.062	1.30	0.065	1.32	0.074	1.33	0.079	1.35	0.070
3.02	0.069	3.03	0.074	3.05	0.085	3.07	0.091	3.08	0.079
3.67	0.072	3.68	0.077	3.70	0.089	3.72	0.095	3.73	0.082
4.28	0.073	4.30	0.080	4.32	0.092	4.33	0.098	4.35	0.084
4.90	0.075	4.92	0.082	4.93	0.093	4.95	0.100	4.97	0.086
5.43	0.077	5.45	0.083	5.47	0.096	5.48	0.100	5.50	0.088
6.07	0.078	6.08	0.085	6.10	0.098	6.12	0.102	6.13	0.089
22.97	0.105	22.98	0.107	23.00	0.122	23.02	0.130	23.03	0.110
32.18	0.112	32.20	0.112	32.22	0.125	32.23	0.121	32.25	0.115
52.05	0.121	52.07	0.125	52.08	0.123	52.10	0.122	52.12	0.123
70.35	0.125	70.37	0.133	70.38	0.111	70.40	0.123	70.42	0.128
75.03	0.126	75.05	0.135	75.07	0.109	75.08	0.126	75.10	0.129
78.02	0.127	78.03	0.136	78.05	0.109	78.07	0.126	78.08	0.129
118.28	0.132	118.30	0.150	118.32	0.115	118.33	0.135	118.35	0.137
126.20	0.134	126.22	0.151	126.23	0.117	126.25	0.136	126.27	0.137
142.40	0.135	142.42	0.155	142.43	0.121	142.45	0.136	142.47	0.140
150.08	0.136	150.10	0.156	150.12	0.124	150.13	0.135	150.15	0.141
166.05	0.139	166.07	0.159	166.08	0.129	166.10	0.135	166.12	0.145
174.18	0.139	174.20	0.161	174.22	0.132	174.23	0.134	174.25	0.145
214.38	0.143	214.40	0.170	214.42	0.140	214.43	0.128	214.45	0.153
222.15	0.144	222.17	0.170	222.18	0.140	222.20	0.130	222.22	0.152
214.02	0.144	214.03	0.172	214.05	0.142	214.07	0.127	214.08	0.155

Test	α (º)	s (m)	s/D_p	n	W_g (m)	t_d (day)	d_{sge} (m)	d_{sge}/d_{se1}
46	90	0.050	1.0	2	0.200	8.8	0.369	2.71

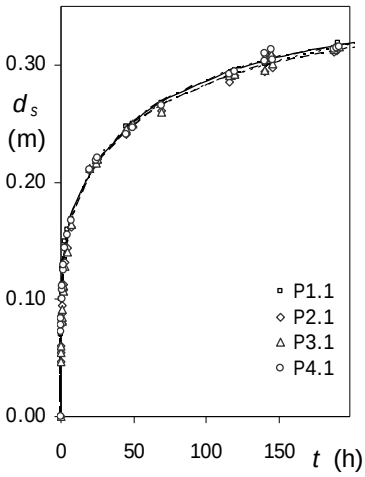

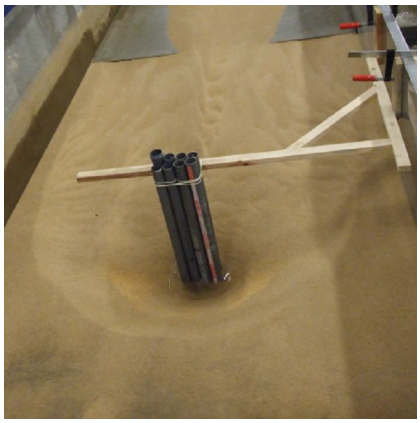

Test 46

P1.1		P2.1		P3.1		P4.1		P1.2	
t (h)	d_s (m)	t (h)	d_s (m)	t (h)	d_s (m)	t (h)	d_s (m)	t (h)	d_s (m)
0.00	0.000	0.00	0.000	0.00	0.000	0.00	0.000		
0.07	0.070	0.08	0.047	0.10	0.047	0.10	0.072		
0.13	0.079	0.13	0.054	0.15	0.055	0.17	0.079		
0.18	0.085	0.20	0.060	0.20	0.060	0.22	0.084		
0.45	0.100	0.47	0.079	0.47	0.081	0.48	0.101		
0.65	0.106	0.67	0.088	0.68	0.084	0.70	0.108		
0.92	0.112	0.90	0.094	0.90	0.091	0.92	0.111		
1.35	0.127	1.37	0.108	1.37	0.107	1.38	0.125		
1.60	0.131	1.62	0.113	1.62	0.112	1.63	0.129		
2.80	0.149	2.82	0.132	2.82	0.128	2.83	0.144		
4.07	0.159	4.08	0.144	4.08	0.141	4.10	0.155		
7.47	0.168	7.47	0.162	7.48	0.164	7.48	0.167		
20.00	0.209	20.02	0.211	20.02	0.212	20.03	0.211		
24.00	0.215	24.00	0.217	24.02	0.217	24.02	0.219		
25.52	0.221	25.53	0.220	25.55	0.220	25.55	0.221		
44.70	0.247	44.72	0.241	44.72	0.245	44.73	0.241		
49.25	0.250	49.27	0.247	49.27	0.250	49.42	0.247		
69.00	0.267	69.02	0.261	69.02	0.259	69.03	0.266		
116.48	0.292	116.50	0.286	116.50	0.291	116.52	0.292		
119.72	0.293	119.73	0.291	119.75	0.293	119.75	0.294		
140.52	0.302	140.53	0.294	140.53	0.295	140.55	0.303		
145.72	0.303	145.73	0.298	145.75	0.300	145.75	0.305		
140.52	0.309	140.53	0.304	140.55	0.306	140.55	0.310		
144.63	0.310	144.65	0.308	144.67	0.309	144.67	0.314		
188.35	0.314	188.37	0.311	188.38	0.313	188.40	0.313		
189.85	0.315	189.87	0.313	189.88	0.315	189.90	0.315		
191.32	0.319	191.33	0.313	191.35	0.316	191.37	0.315		
211.90	0.321	211.92	0.320	211.93	0.318	211.95	0.320		

Test	α (º)	s (m)	s/D_p	n	W_g (m)	t_d (day)	d_{sge} (m)	d_{sge}/d_{se1}
47	90	0.100	2.0	2	0.200	12.1	0.212	1.56

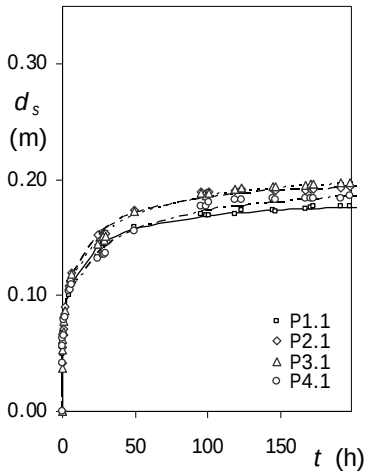

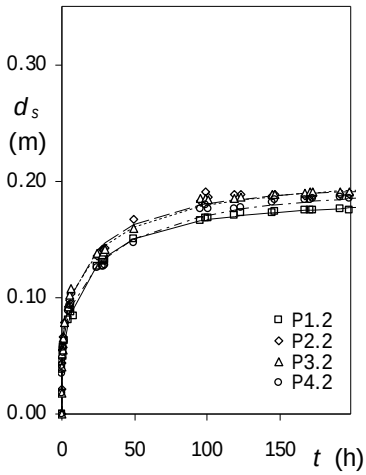

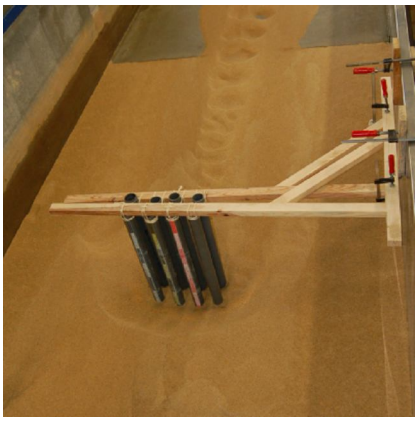

Test 47

P1.1		P2.1		P3.1		P4.1		P1.2	
t (h)	d_s (m)	t (h)	d_s (m)	t (h)	d_s (m)	t (h)	d_s (m)	t (h)	d_s (m)
0.00	0.000	0.00	0.000	0.00	0.000	0.00	0.000	0.00	0.000
0.10	0.050	0.08	0.042	0.07	0.038	0.07	0.042	0.05	0.018
0.27	0.061	0.25	0.055	0.23	0.053	0.23	0.057	0.20	0.038
0.43	0.068	0.42	0.067	0.40	0.062	0.40	0.063	0.37	0.045
0.58	0.071	0.57	0.072	0.55	0.069	0.55	0.066	0.53	0.049
0.98	0.083	0.97	0.082	0.97	0.078	0.95	0.080	0.93	0.057
1.65	0.087	1.63	0.090	1.63	0.087	1.62	0.081	1.60	0.063
4.55	0.101	4.53	0.108	4.53	0.108	4.52	0.104	4.65	0.081
5.42	0.106	5.40	0.113	5.40	0.115	5.38	0.105	8.37	0.084
6.58	0.113	6.57	0.120	6.57	0.118	6.55	0.110	6.53	0.088
24.20	0.142	24.18	0.152	24.18	0.145	24.17	0.133	24.15	0.127
27.77	0.145	27.77	0.154	27.75	0.151	27.73	0.136	27.72	0.131
28.70	0.146	28.70	0.153	28.68	0.148	28.68	0.136	28.67	0.132
29.47	0.147	29.45	0.154	29.45	0.152	29.43	0.137	29.42	0.132
49.45	0.159	49.47	0.174	49.48	0.173	49.40	0.156	49.45	0.151
95.67	0.170	95.65	0.190	95.65	0.188	95.63	0.178	95.60	0.166
99.02	0.169	99.00	0.188	99.05	0.186	99.03	0.178	99.02	0.168
100.85	0.169	100.83	0.190	100.82	0.189	100.80	0.181	100.78	0.168
119.15	0.171	119.13	0.191	119.12	0.192	119.10	0.182	119.07	0.171
123.63	0.174	123.62	0.192	123.60	0.193	123.58	0.183	123.57	0.173
144.95	0.174	144.93	0.192	144.92	0.194	144.90	0.184	144.88	0.173
147.03	0.173	147.02	0.191	146.97	0.194	146.95	0.183	146.93	0.174
167.62	0.175	167.60	0.191	167.58	0.195	167.57	0.184	167.55	0.175
171.40	0.176	171.37	0.192	171.35	0.196	171.33	0.184	171.32	0.175
172.73	0.177	172.72	0.192	172.70	0.197	172.68	0.184	172.67	0.176
191.88	0.177	191.87	0.193	191.85	0.197	191.83	0.184	191.82	0.176
198.25	0.177	198.23	0.194	198.22	0.198	198.20	0.186	198.25	0.175
239.85	0.176	239.87	0.188	239.88	0.193	239.90	0.180	239.78	0.174
287.55	0.177	287.53	0.193	287.52	0.199	287.50	0.183	287.48	0.181
289.58	0.174	289.60	0.194	289.62	0.198	289.63	0.182	289.65	0.175

Test	α (º)	s (m)	s/D_p	n	W_g (m)	t_d (day)	d_{sge} (m)	d_{sge}/d_{se1}
48	90	0.150	3.0	2	0.200	8.3	0.189	1.39

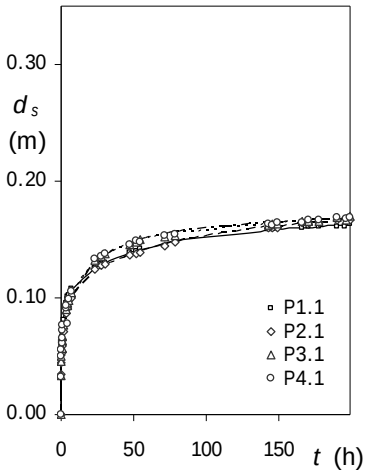

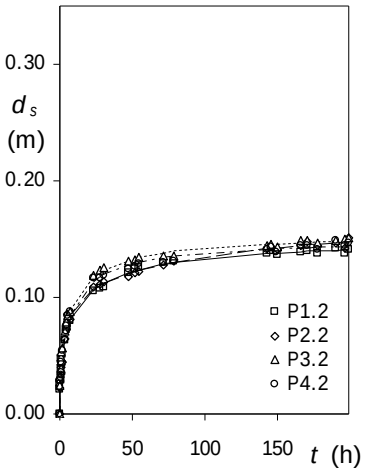

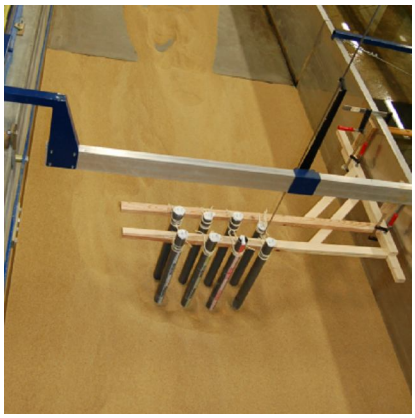

Test 48

P1.1		P2.1		P3.1		P4.1		P1.2	
t (h)	d_s (m)	t (h)	d_s (m)	t (h)	d_s (m)	t (h)	d_s (m)	t (h)	d_s (m)
0.00	0.000	0.00	0.000	0.00	0.000	0.00	0.000	0.00	0.000
0.12	0.044	0.10	0.034	0.08	0.033	0.07	0.033	0.18	0.021
0.27	0.055	0.25	0.044	0.23	0.045	0.22	0.050	0.33	0.027
0.43	0.063	0.42	0.051	0.40	0.050	0.38	0.055	0.50	0.029
0.60	0.067	0.58	0.054	0.57	0.056	0.55	0.062	0.67	0.033
0.77	0.071	0.75	0.059	0.73	0.063	0.72	0.066	0.83	0.039
1.05	0.075	1.03	0.064	1.02	0.067	1.00	0.072	1.12	0.048
1.38	0.081	1.37	0.071	1.35	0.076	1.33	0.076	1.45	0.051
3.18	0.095	3.17	0.087	3.23	0.090	3.13	0.091	3.25	0.064
4.07	0.099	4.05	0.091	4.03	0.094	4.02	0.094	4.13	0.072
4.82	0.101	4.80	0.094	4.78	0.096	4.77	0.078	4.88	0.072
5.60	0.102	5.58	0.098	5.43	0.098	5.55	0.099	5.67	0.077
7.13	0.108	7.12	0.100	7.10	0.105	7.08	0.106	7.20	0.080
23.53	0.125	23.52	0.124	23.50	0.133	23.48	0.133	23.60	0.106
27.67	0.129	27.65	0.128	27.63	0.135	27.62	0.135	27.73	0.108
30.70	0.130	30.68	0.129	30.67	0.138	30.65	0.138	30.77	0.109
46.93	0.138	46.92	0.137	46.90	0.146	46.88	0.146	47.00	0.121
51.58	0.140	51.57	0.138	51.55	0.148	51.53	0.149	51.65	0.125
54.75	0.142	54.73	0.139	54.72	0.150	54.70	0.148	54.82	0.125
71.13	0.145	71.12	0.145	71.10	0.152	71.08	0.153	71.20	0.130
78.90	0.149	78.88	0.148	78.87	0.153	78.85	0.154	78.97	0.132
142.88	0.159	142.87	0.160	142.85	0.162	142.83	0.164	142.95	0.138
145.55	0.158	145.53	0.160	145.52	0.163	145.50	0.163	145.62	0.140
149.45	0.160	149.43	0.160	149.42	0.164	149.40	0.164	149.52	0.136
166.27	0.160	166.25	0.165	166.23	0.165	166.22	0.165	166.33	0.139
170.70	0.161	170.68	0.165	170.67	0.166	170.65	0.167	170.77	0.140
177.42	0.161	177.43	0.164	177.45	0.165	177.47	0.167	177.48	0.138
190.30	0.161	190.28	0.166	190.27	0.169	190.25	0.169	190.37	0.142
195.87	0.161	195.88	0.168	195.90	0.167	195.92	0.168	195.93	0.138
199.08	0.163	199.07	0.167	199.05	0.170	199.03	0.169	199.12	0.141

Test	α (º)	s (m)	s/D_p	n	W_g (m)	t_d (day)	d_{sge} (m)	d_{sge}/d_{se1}
49	90	0.225	4.5	2	0.200	6.9	0.178	1.31

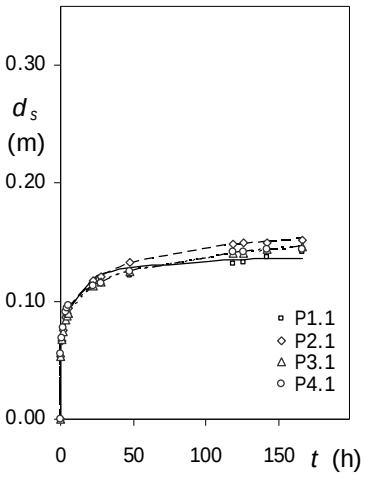

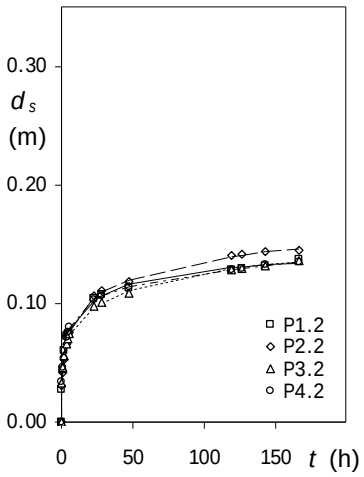

Test 49

P1.1		P2.1		P3.1		P4.1		P1.2	
t (h)	d_s (m)	t (h)	d_s (m)	t (h)	d_s (m)	t (h)	d_s (m)	t (h)	d_s (m)
0.00	0.000	0.00	0.000	0.00	0.000	0.00	0.000	0.00	0.000
0.15	0.052	0.15	0.054	0.17	0.053	0.17	0.056	0.18	0.028
0.63	0.068	0.63	0.067	0.65	0.067	0.65	0.069	0.67	0.044
1.38	0.076	1.38	0.076	1.40	0.074	1.40	0.077	1.42	0.060
3.28	0.086	3.28	0.086	3.30	0.084	3.30	0.091	3.33	0.072
4.32	0.088	4.32	0.090	4.33	0.088	4.33	0.094	4.35	0.074
5.17	0.092	5.17	0.094	5.18	0.090	5.18	0.096	5.20	0.075
22.80	0.112	22.80	0.117	22.82	0.113	22.83	0.113	22.85	0.104
28.15	0.117	28.15	0.120	28.17	0.116	28.17	0.115	28.18	0.108
47.38	0.122	47.38	0.132	47.40	0.125	47.40	0.125	47.43	0.113
118.70	0.132	118.70	0.149	118.72	0.140	118.72	0.142	118.75	0.129
126.47	0.133	126.48	0.150	126.48	0.141	126.50	0.142	126.33	0.130
142.37	0.137	142.37	0.150	142.38	0.144	142.38	0.144	142.42	0.132
166.67	0.142	166.68	0.151	166.68	0.146	166.70	0.144	166.72	0.137

Test	α (º)	s (m)	s/D_p	n	W_g (m)	t_d (day)	d_{sge} (m)	d_{sge}/d_{se1}
50	90	0.300	6.0	2	0.200	7.7	0.141	1.04

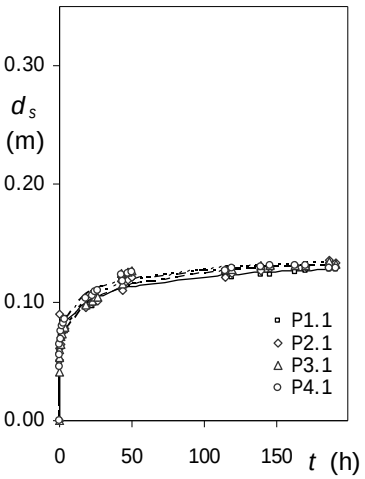

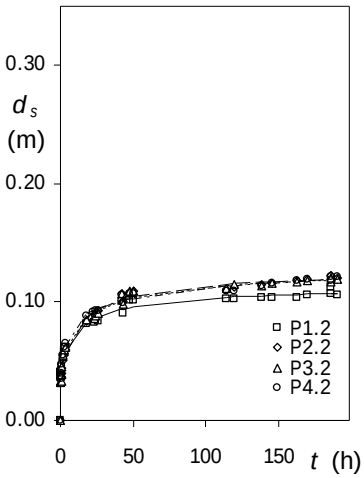

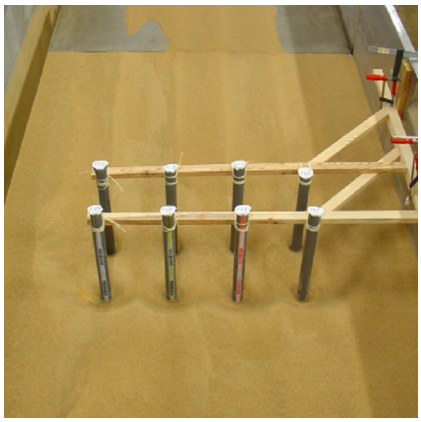

Test 50

P1.1		P2.1		P3.1		P4.1		P1.2	
t (h)	d_s (m)	t (h)	d_s (m)	t (h)	d_s (m)	t (h)	d_s (m)	t (h)	d_s (m)
0.00	0.000	0.00	0.000	0.00	0.000	0.00	0.000	0.00	0.000
0.08	0.048	0.07	0.090	0.05	0.042	0.03	0.045	0.15	0.041
0.27	0.059	0.25	0.051	0.23	0.054	0.22	0.056	0.33	0.038
0.47	0.065	0.45	0.061	0.43	0.060	0.42	0.065	0.53	0.039
0.73	0.071	0.72	0.065	0.72	0.065	0.68	0.069	0.78	0.042
1.18	0.075	1.17	0.070	1.13	0.071	1.12	0.076	1.23	0.045
2.03	0.081	2.02	0.075	2.00	0.073	1.98	0.080	2.07	0.053
2.72	0.083	2.72	0.076	2.70	0.078	2.70	0.082	2.77	0.058
3.30	0.086	3.30	0.078	3.28	0.079	3.27	0.085	3.35	0.062
18.22	0.095	18.20	0.095	18.18	0.098	18.17	0.103	18.28	0.081
22.93	0.097	22.92	0.100	22.90	0.101	22.88	0.106	23.00	0.083
24.52	0.101	24.50	0.102	24.48	0.104	24.47	0.109	24.58	0.085
26.10	0.102	26.08	0.102	26.07	0.105	26.05	0.110	26.17	0.083
43.60	0.111	43.58	0.110	43.57	0.115	43.55	0.118	43.67	0.091
42.70	0.118	42.68	0.118	42.67	0.124	42.65	0.123	42.77	0.100
47.28	0.121	47.27	0.118	47.25	0.125	47.23	0.125	47.35	0.102
50.22	0.120	50.20	0.121	50.18	0.127	50.17	0.125	50.28	0.101
114.13	0.121	114.12	0.122	114.10	0.128	114.08	0.127	114.20	0.103
119.47	0.121	119.45	0.124	119.43	0.128	119.42	0.129	119.53	0.103
138.73	0.123	138.72	0.127	138.70	0.131	138.68	0.130	138.80	0.103
145.68	0.124	145.67	0.128	145.65	0.131	145.63	0.132	145.75	0.104
162.57	0.125	162.55	0.131	162.53	0.131	162.52	0.131	162.63	0.104
170.05	0.127	170.03	0.131	170.02	0.132	170.00	0.131	170.12	0.106
186.47	0.128	186.45	0.133	186.43	0.134	186.42	0.129	186.53	0.107
191.13	0.128	191.12	0.133	191.10	0.132	191.08	0.129	191.20	0.106
185.97	0.130	185.95	0.135	185.93	0.135	185.92	0.129	186.03	0.113

Test	α (º)	s (m)	s/D_p	n	W_g (m)	t_d (day)	d_{sge} (m)	d_{sge}/d_{se1}
51	0	0.050	1.0	3	0.150	8.1	0.327	2.41

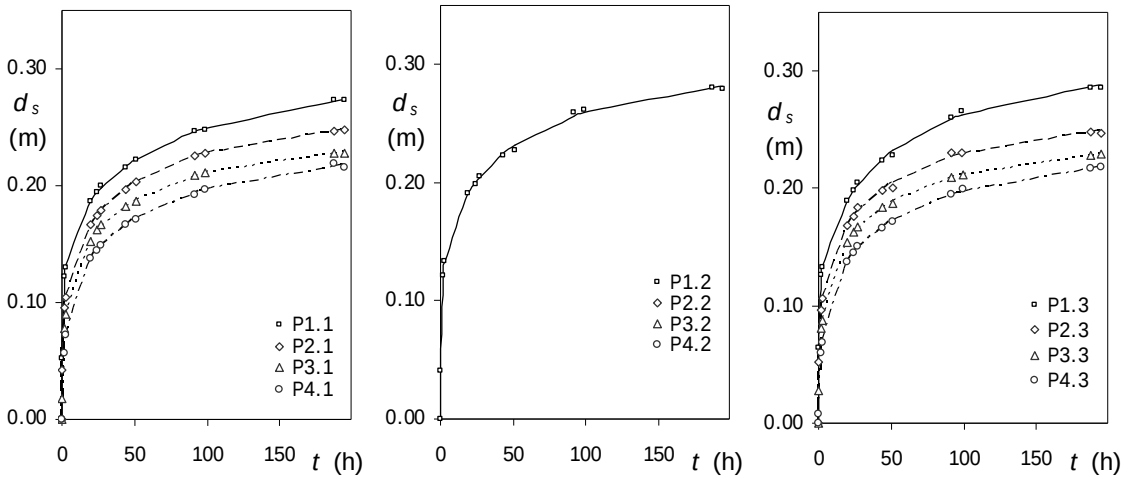

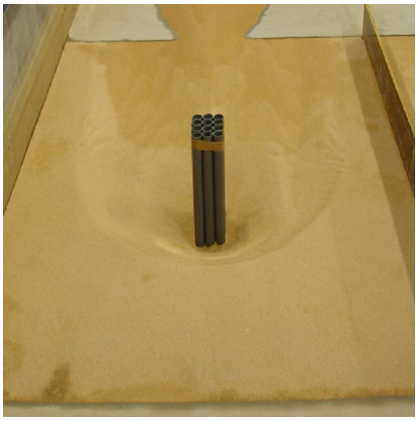

Test 51

P1.1		P2.1		P3.1		P4.1		P1.2		P1.3	
t (h)	d_s (m)	t (h)	d_s (m)	t (h)	d_s (m)	t (h)	d_s (m)	t (h)	d_s (m)	t (h)	d_s (m)
0.00	0.000	0.00	0.000	0.00	0.000	0.00	0.000	0.00	0.000	0.00	0.000
0.03	0.052	0.07	0.042	0.08	0.017	0.08	0.000	0.05	0.041	0.05	0.064
1.78	0.122	1.82	0.095	1.83	0.078	1.83	0.057	1.80	0.121	1.80	0.126
2.68	0.130	2.72	0.104	2.73	0.090	2.73	0.072	2.70	0.134	2.70	0.133
19.33	0.187	19.38	0.166	19.38	0.153	19.38	0.138	19.35	0.192	19.35	0.190
24.12	0.194	24.15	0.175	24.17	0.163	24.17	0.145	24.13	0.199	24.13	0.199
26.90	0.200	26.95	0.178	26.97	0.166	26.97	0.149	26.92	0.205	26.92	0.205
43.58	0.216	43.62	0.197	43.63	0.182	43.63	0.166	43.60	0.224	43.60	0.223
50.97	0.222	51.00	0.204	51.02	0.187	51.02	0.172	50.97	0.228	50.98	0.228
91.58	0.247	91.62	0.225	91.63	0.209	91.63	0.193	91.58	0.260	91.60	0.261
98.98	0.248	99.02	0.228	99.03	0.211	99.03	0.197	99.00	0.262	99.00	0.266
187.57	0.273	187.60	0.247	187.60	0.228	187.62	0.219	187.57	0.280	187.58	0.286
194.52	0.273	194.55	0.248	194.57	0.228	194.58	0.216	194.53	0.280	194.55	0.286

Test	α (º)	s (m)	s/D_p	n	W_g (m)	t_d (day)	d_{sge} (m)	d_{sge}/d_{se1}
52	0	0.100	2.0	3	0.150	7.0	0.211	1.56

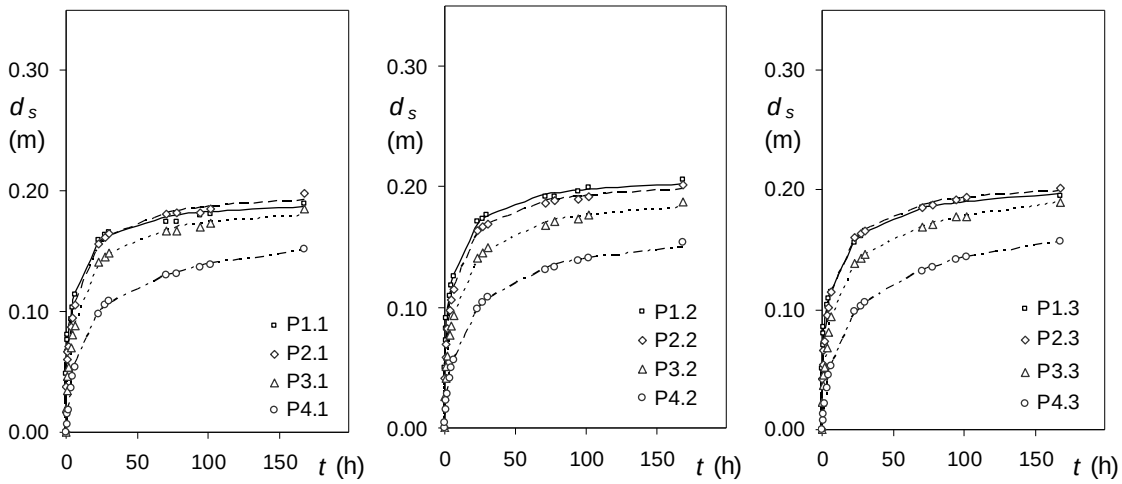

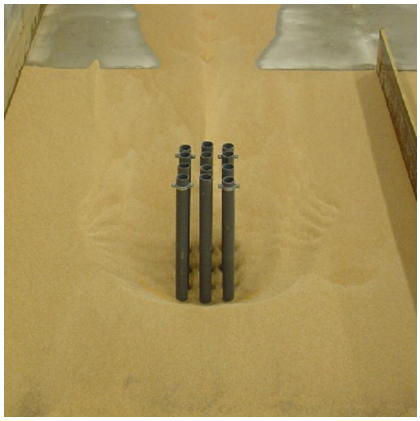

Test 52

P1.1		P2.1		P3.1		P4.1		P1.2		P1.3	
t (h)	d_s (m)	t (h)	d_s (m)	t (h)	d_s (m)	t (h)	d_s (m)	t (h)	d_s (m)	t (h)	d_s (m)
0.00	0.000	0.00	0.000	0.00	0.000	0.00	0.000	0.00	0.000	0.00	0.000
0.10	0.048	0.13	0.037	0.17	0.019	0.20	-0.007	0.10	0.050	0.12	0.051
0.52	0.067	0.55	0.060	0.58	0.034	0.62	0.007	0.53	0.072	0.53	0.071
0.98	0.077	1.02	0.067	1.05	0.046	1.08	0.015	1.00	0.083	1.00	0.080
1.35	0.081	1.38	0.072	1.42	0.054	1.45	0.019	1.37	0.091	1.37	0.086
3.27	0.094	3.30	0.087	3.33	0.070	3.38	0.037	3.27	0.110	3.28	0.104
4.45	0.103	4.48	0.095	4.52	0.081	4.57	0.046	4.47	0.118	4.47	0.109
6.18	0.115	6.22	0.106	6.25	0.088	6.28	0.054	6.20	0.126	6.20	0.115
22.93	0.159	22.97	0.156	23.00	0.141	23.03	0.098	22.95	0.171	22.95	0.156
27.13	0.164	27.17	0.162	27.20	0.146	27.23	0.105	27.13	0.173	27.15	0.162
30.05	0.165	30.08	0.165	30.12	0.148	30.15	0.109	30.07	0.177	30.07	0.165
70.92	0.175	70.95	0.181	70.98	0.167	71.02	0.130	70.92	0.192	70.93	0.186
77.75	0.175	77.78	0.182	77.82	0.167	77.85	0.132	77.75	0.192	77.77	0.188
94.70	0.180	94.73	0.182	94.77	0.171	94.80	0.137	94.70	0.196	94.72	0.190
101.75	0.181	101.78	0.185	101.82	0.173	101.85	0.139	101.75	0.199	101.77	0.192
168.07	0.190	168.10	0.198	168.13	0.185	168.17	0.152	168.07	0.206	168.08	0.195

Test	α (º)	s (m)	s/D_p	n	W_g (m)	t_d (day)	d_{sge} (m)	d_{sge}/d_{se1}
53	0	0.150	3.0	3	0.150	7.2	0.208	1.53

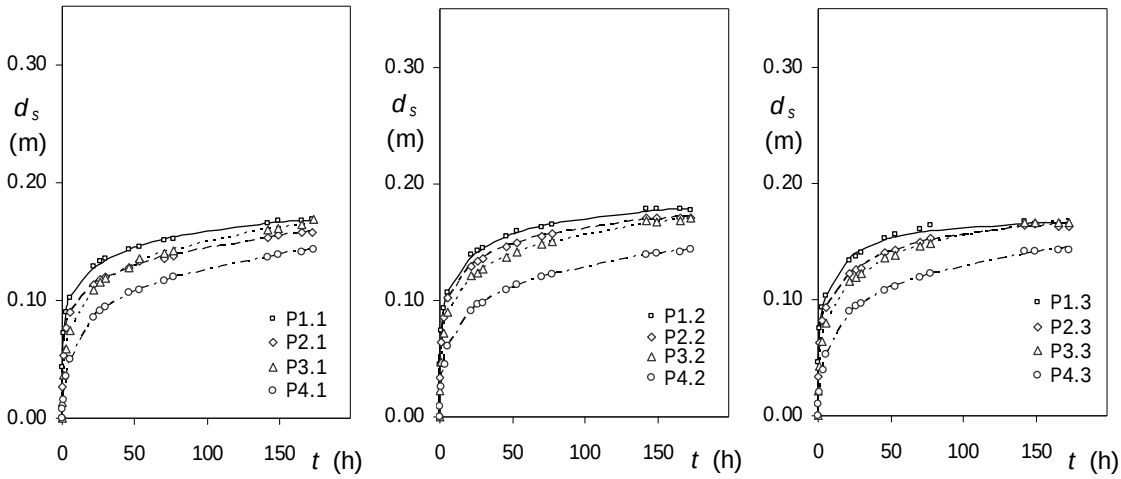

Test 53

P1.1		P2.1		P3.1		P4.1		P1.2		P1.3	
t (h)	d_s (m)	t (h)	d_s (m)	t (h)	d_s (m)	t (h)	d_s (m)	t (h)	d_s (m)	t (h)	d_s (m)
0.00	0.000	0.00	0.000	0.00	0.000	0.00	0.000	0.00	0.000	0.00	0.000
0.10	0.044	0.15	0.027	0.18	0.013	0.22	0.008	0.12	0.045	0.13	0.046
1.08	0.072	1.12	0.053	1.15	0.037	1.18	0.016	1.10	0.074	1.10	0.075
3.03	0.091	3.07	0.077	3.10	0.059	3.15	0.035	3.05	0.094	3.07	0.093
5.67	0.102	5.68	0.090	5.72	0.075	5.75	0.050	5.67	0.107	5.68	0.104
21.68	0.128	21.72	0.113	21.75	0.109	21.78	0.086	21.68	0.139	21.70	0.134
26.17	0.134	26.20	0.118	26.23	0.115	26.27	0.091	26.17	0.142	26.18	0.137
29.50	0.135	29.53	0.120	29.57	0.119	29.60	0.094	29.52	0.144	29.52	0.140
46.07	0.143	46.10	0.128	46.13	0.128	46.17	0.107	46.08	0.155	46.08	0.153
52.97	0.145	53.00	0.134	53.03	0.135	53.07	0.109	52.98	0.159	52.98	0.156
70.25	0.152	70.28	0.136	70.32	0.141	70.35	0.117	70.27	0.163	70.27	0.160
77.07	0.152	77.10	0.138	77.13	0.142	77.17	0.120	77.08	0.165	77.08	0.164
142.03	0.165	142.07	0.154	142.10	0.160	142.13	0.136	142.05	0.178	142.05	0.167
149.25	0.168	149.28	0.155	149.32	0.161	149.35	0.139	149.27	0.178	149.27	0.165
165.78	0.167	165.82	0.158	165.87	0.165	165.90	0.142	165.80	0.178	165.80	0.164
173.18	0.169	173.22	0.158	173.25	0.168	173.28	0.143	173.20	0.177	173.20	0.163

Test	α (º)	s (m)	s/D_p	n	W_g (m)	t_d (day)	d_{sge} (m)	d_{sge}/d_{se1}
54	0	0.225	4.5	3	0.150	8.2	0.218	1.60

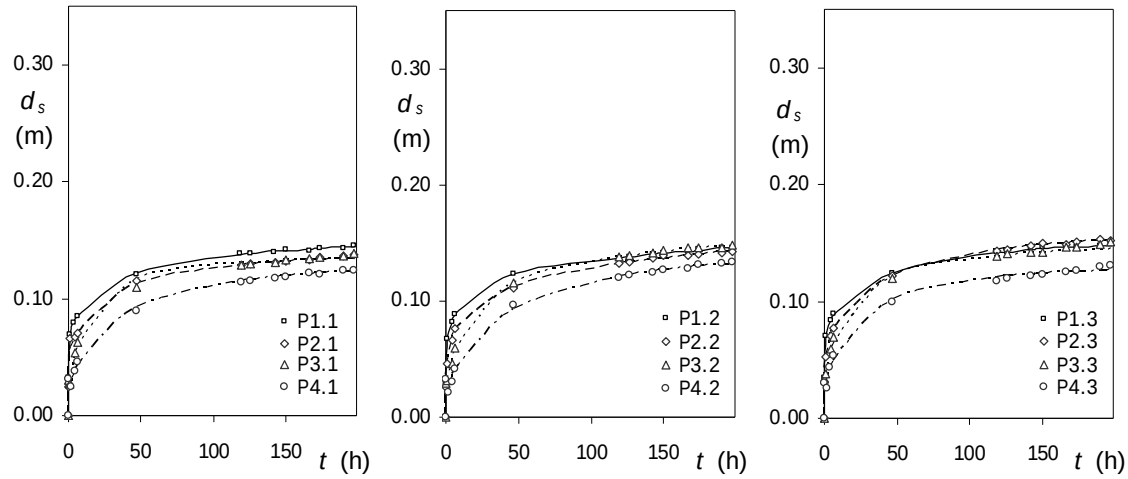

Test 54

P1.1		P2.1		P3.1		P4.1		P1.2		P1.3	
t (h)	d_s (m)	t (h)	d_s (m)	t (h)	d_s (m)	t (h)	d_s (m)	t (h)	d_s (m)	t (h)	d_s (m)
0.00	0.000	0.00	0.000	0.00	0.000	0.00	0.000	0.00	0.000	0.00	0.000
0.03	0.032	0.07	0.025	0.10	0.030	0.13	0.031	0.03	0.029	0.05	0.035
1.25	0.069	1.28	0.066	1.33	0.027	1.37	0.025	1.27	0.068	1.27	0.071
4.05	0.080	4.08	0.067	4.13	0.053	4.17	0.038	4.07	0.082	4.07	0.084
6.10	0.085	6.13	0.071	6.18	0.062	6.22	0.046	6.12	0.088	6.12	0.089
46.63	0.121	46.67	0.115	46.70	0.110	46.73	0.090	46.63	0.123	46.65	0.124
118.25	0.139	119.03	0.129	119.07	0.129	119.10	0.114	119.02	0.137	119.02	0.142
126.05	0.139	126.08	0.130	126.12	0.129	126.15	0.115	126.07	0.138	126.07	0.142
142.43	0.140	142.47	0.131	142.50	0.131	142.53	0.117	142.43	0.140	142.45	0.145
149.95	0.142	149.98	0.132	150.02	0.133	150.05	0.118	149.97	0.141	149.97	0.146
166.63	0.141	166.67	0.133	166.70	0.135	166.73	0.122	166.65	0.142	166.65	0.146
173.82	0.143	173.85	0.135	173.88	0.136	173.92	0.121	173.83	0.145	173.83	0.146
190.28	0.143	190.32	0.136	190.35	0.137	190.38	0.124	190.30	0.146	190.30	0.148
197.43	0.145	197.47	0.138	197.48	0.139	197.53	0.124	197.43	0.145	197.45	0.149

Test	α (º)	s (m)	s/D_p	n	W_g (m)	t_d (day)	d_{sge} (m)	d_{sge}/d_{se1}
55	0	0.300	6.0	3	0.150	8.5	0.139	1.03

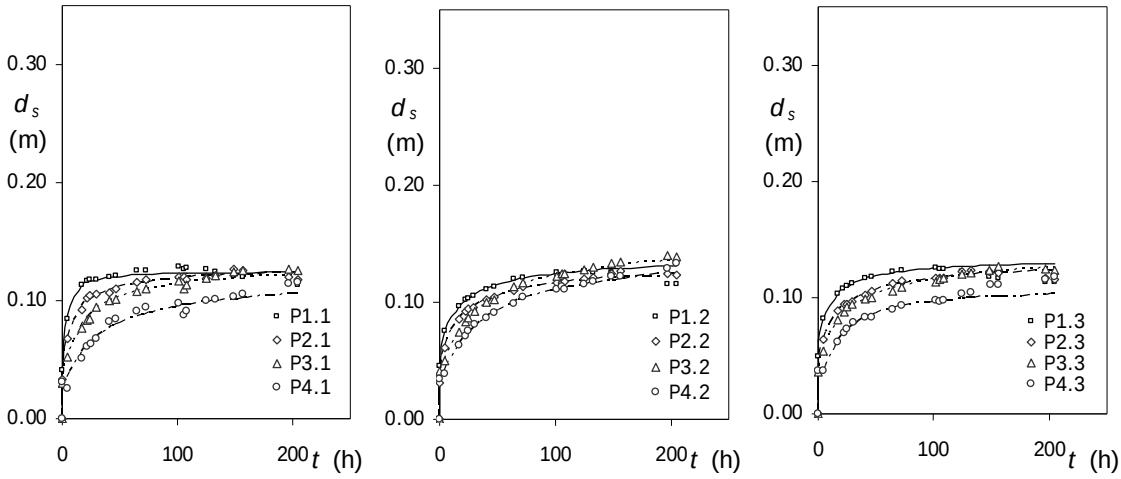

Test 55

P1.1		P2.1		P3.1		P4.1		P1.2		P1.3	
t (h)	d_s (m)	t (h)	d_s (m)	t (h)	d_s (m)	t (h)	d_s (m)	t (h)	d_s (m)	t (h)	d_s (m)
0.00	0.000	0.00	0.000	0.00	0.000	0.00	0.000	0.00	0.000	0.00	0.000
0.05	0.042	0.08	0.033	0.10	0.030	0.10	0.032	0.12	0.046	0.13	0.049
4.27	0.085	4.37	0.068	4.37	0.052	4.43	0.026	4.30	0.076	4.32	0.082
16.88	0.114	16.95	0.092	17.00	0.077	17.05	0.051	16.92	0.097	16.93	0.103
22.02	0.116	22.07	0.102	22.10	0.084	22.13	0.061	22.05	0.102	22.05	0.108
24.32	0.118	24.37	0.104	24.42	0.085	24.45	0.064	24.35	0.103	24.37	0.110
29.73	0.118	29.83	0.105	29.93	0.094	30.02	0.068	29.77	0.105	29.78	0.112
40.50	0.120	40.55	0.106	40.58	0.100	40.63	0.082	40.52	0.112	40.53	0.116
46.75	0.122	46.82	0.110	46.85	0.101	46.88	0.085	46.78	0.114	46.78	0.117
64.45	0.125	64.50	0.115	64.55	0.108	64.58	0.091	64.48	0.120	64.48	0.123
72.40	0.125	72.45	0.118	72.48	0.110	72.52	0.094	72.42	0.121	72.43	0.124
101.42	0.128	101.43	0.120	101.43	0.117	101.43	0.098	101.43	0.126	101.43	0.126
105.28	0.127	105.33	0.120	105.38	0.110	105.43	0.088	105.32	0.124	105.32	0.124
107.98	0.127	108.05	0.118	108.08	0.113	108.13	0.091	108.02	0.125	108.03	0.125
124.82	0.127	124.87	0.119	124.90	0.119	124.95	0.100	124.85	0.127	124.85	0.123
132.40	0.125	132.45	0.121	132.48	0.121	132.52	0.101	132.43	0.125	132.43	0.122
148.60	0.121	148.67	0.126	148.70	0.125	148.75	0.104	148.63	0.125	148.65	0.118
156.37	0.120	156.42	0.126	156.45	0.125	156.48	0.106	156.40	0.124	156.40	0.116
196.67	0.114	196.72	0.120	196.77	0.127	196.82	0.114	196.70	0.116	196.70	0.114
204.38	0.114	204.45	0.118	204.48	0.126	204.52	0.116	204.42	0.116	204.43	0.113

Test	α (º)	s (m)	s/D_p	n	W_g (m)	t_d (day)	d_{sge} (m)	d_{sge}/d_{se1}
56	15	0.050	1.0	3	0.185	8.2	0.334	2.46

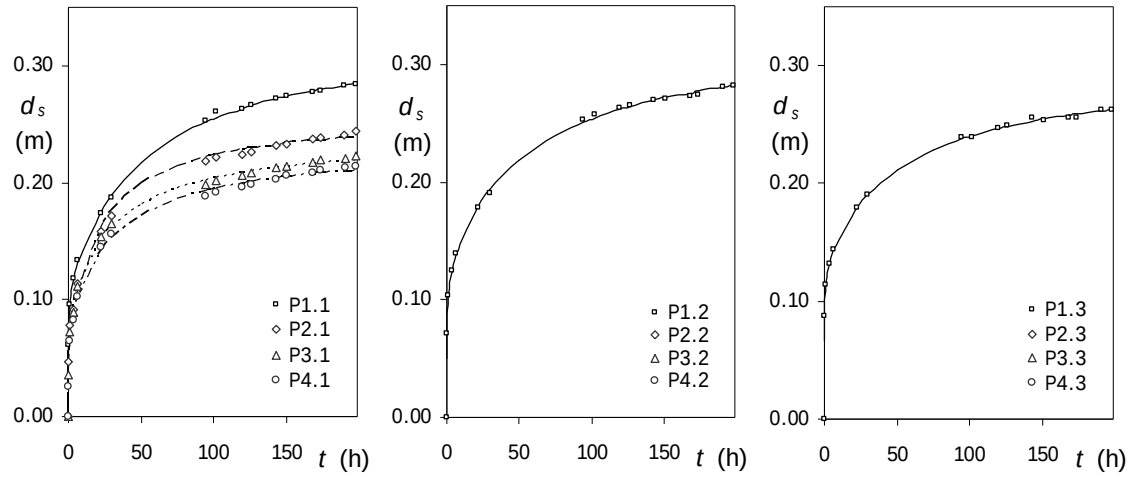

Test 56

P1.1		P2.1		P3.1		P4.1		P1.2		P1.3	
t (h)	d_s (m)	t (h)	d_s (m)	t (h)	d_s (m)	t (h)	d_s (m)	t (h)	d_s (m)	t (h)	d_s (m)
0.00	0.000	0.00	0.000	0.00	0.000	0.00	0.000	0.00	0.000	0.00	0.000
0.20	0.061	0.20	0.047	0.22	0.036	0.23	0.026	0.25	0.072	0.27	0.088
1.27	0.096	1.27	0.078	1.28	0.072	1.28	0.065	1.30	0.103	1.30	0.115
3.35	0.118	3.35	0.092	3.37	0.090	3.37	0.082	3.38	0.125	3.38	0.131
6.32	0.133	6.33	0.113	6.35	0.111	6.37	0.102	6.37	0.139	6.38	0.144
22.08	0.174	22.10	0.158	22.12	0.154	22.13	0.145	22.15	0.179	22.17	0.179
29.95	0.187	29.97	0.172	29.98	0.165	30.00	0.156	30.02	0.190	30.03	0.190
50.00	0.217	50.00	0.199	50.00	0.182	50.00	0.172	50.00	0.219	50.00	0.212
75.00	0.240	75.00	0.215	75.00	0.195	75.00	0.186	75.00	0.240	75.00	0.229
94.23	0.253	94.25	0.219	94.27	0.198	94.27	0.189	94.28	0.253	94.30	0.239
101.97	0.261	101.97	0.222	101.98	0.202	102.00	0.192	102.02	0.257	102.02	0.239
119.70	0.263	119.72	0.224	119.73	0.206	119.73	0.196	119.75	0.263	119.77	0.247
126.23	0.266	126.25	0.227	126.25	0.209	126.27	0.198	126.28	0.266	126.28	0.249
142.77	0.272	142.77	0.232	142.78	0.213	142.80	0.203	142.82	0.270	142.83	0.256
150.78	0.274	150.80	0.233	150.82	0.214	150.82	0.206	150.85	0.271	150.87	0.254
168.28	0.277	168.30	0.237	168.32	0.217	168.33	0.208	168.33	0.273	168.35	0.256
173.93	0.279	173.95	0.239	173.97	0.219	173.97	0.210	173.98	0.274	174.00	0.256
190.42	0.284	190.43	0.241	190.45	0.220	190.45	0.213	190.47	0.281	190.48	0.263
197.83	0.284	197.85	0.245	197.87	0.223	197.87	0.214	197.88	0.282	197.90	0.263

Test	α (º)	s (m)	s/D_p	n	W_g (m)	t_d (day)	d_{sge} (m)	d_{sge}/d_{se1}
57	15	0.100	2.0	3	0.279	8.2	0.305	2.25

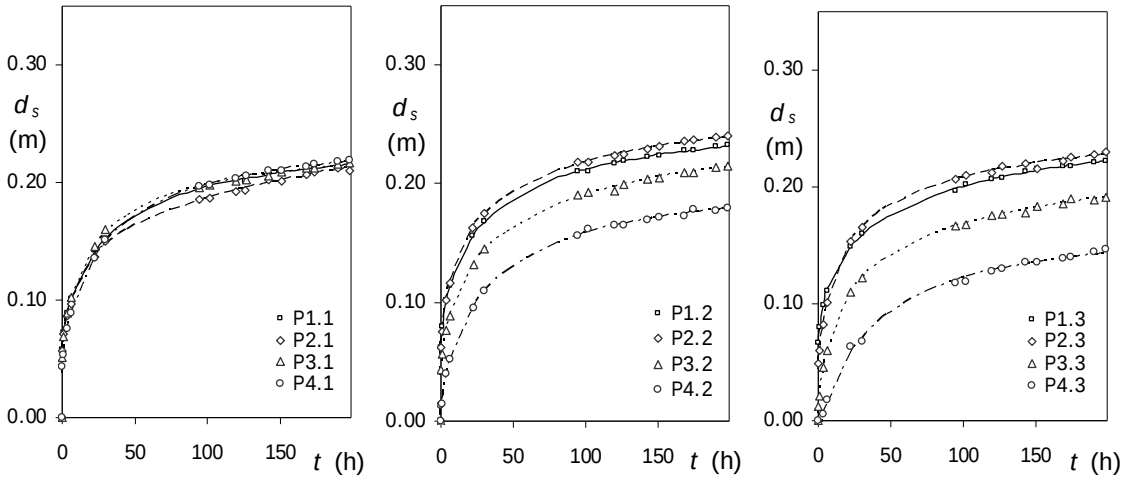

Test 57

P1.1		P2.1		P3.1		P4.1		P1.2		P1.3	
t (h)	d_s (m)	t (h)	d_s (m)	t (h)	d_s (m)	t (h)	d_s (m)	t (h)	d_s (m)	t (h)	d_s (m)
0.00	0.000	0.00	0.000	0.00	0.000	0.00	0.000	0.00	0.000	0.00	0.000
0.27	0.058	0.28	0.057	0.28	0.051	0.30	0.043	0.30	0.062	0.35	0.066
1.10	0.072	1.10	0.071	1.12	0.069	1.12	0.054	1.13	0.080	1.18	0.080
3.40	0.089	3.40	0.087	3.42	0.089	3.42	0.076	3.43	0.102	3.48	0.099
6.08	0.101	6.10	0.097	6.12	0.102	6.13	0.089	6.15	0.114	6.23	0.111
22.18	0.142	22.20	0.137	22.22	0.145	22.23	0.135	22.23	0.156	22.30	0.149
30.03	0.152	30.05	0.150	30.07	0.160	30.08	0.151	30.10	0.169	30.13	0.160
45.00	0.168	45.00	0.160	45.00	0.172	45.00	0.166	45.00	0.183	45.00	0.172
75.00	0.187	75.00	0.177	75.00	0.190	75.00	0.188	75.00	0.202	75.00	0.191
94.32	0.195	94.33	0.186	94.35	0.196	94.37	0.196	94.37	0.210	94.43	0.197
102.03	0.197	102.03	0.186	102.05	0.198	102.07	0.198	102.08	0.211	102.12	0.202
119.77	0.201	119.78	0.192	119.80	0.202	119.80	0.203	119.82	0.217	119.87	0.206
126.50	0.201	126.50	0.193	126.53	0.202	126.55	0.206	126.55	0.219	126.62	0.207
142.57	0.209	142.58	0.202	142.60	0.206	142.62	0.210	142.63	0.223	142.68	0.214
150.87	0.209	150.90	0.201	150.90	0.209	150.92	0.210	150.92	0.224	150.97	0.216
168.12	0.212	168.13	0.207	168.13	0.212	168.15	0.213	168.17	0.228	168.22	0.218
174.00	0.211	174.02	0.209	174.03	0.213	174.03	0.215	174.05	0.228	174.12	0.218
190.23	0.216	190.23	0.212	190.25	0.216	190.27	0.218	190.27	0.232	190.33	0.221
197.92	0.216	197.92	0.210	197.93	0.216	197.95	0.219	197.97	0.233	198.02	0.222

Test	α (º)	s (m)	s/D_p	n	W_g (m)	t_d (day)	d_{sge} (m)	d_{sge}/d_{se1}
58	15	0.150	3.0	3	0.342	7.8	0.250	1.84

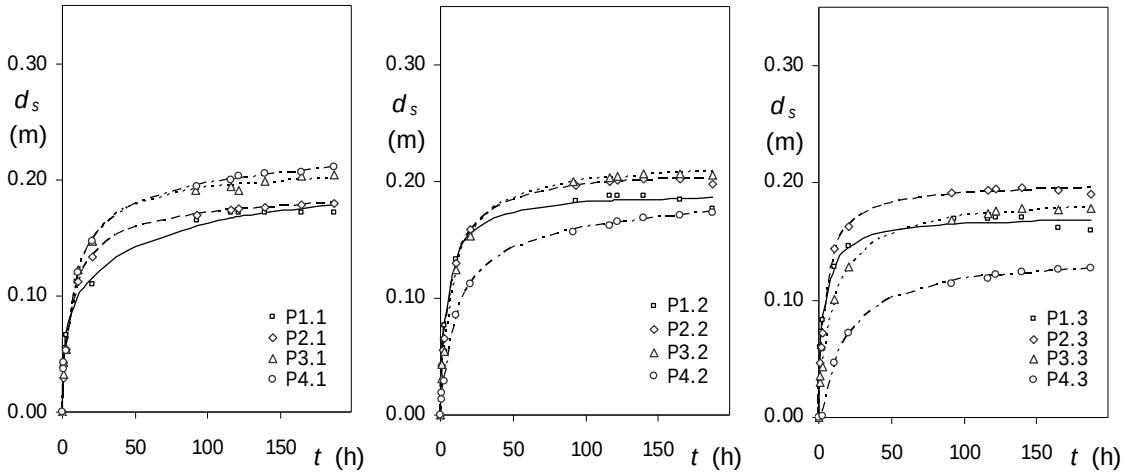

Test 58

P1.1		P2.1		P3.1		P4.1		P1.2		P1.3	
t (h)	d_s (m)	t (h)	d_s (m)	t (h)	d_s (m)	t (h)	d_s (m)	t (h)	d_s (m)	t (h)	d_s (m)
0.00	0.000	0.00	0.000	0.00	0.000	0.00	0.000	0.00	0.000	0.00	0.000
0.47	0.043	0.57	0.030	0.57	0.032	0.65	0.037	0.52	0.042	0.53	0.060
1.40	0.055	1.35	0.043	1.33	0.043	1.27	0.043	1.40	0.064	1.38	0.073
2.67	0.067	2.62	0.054	2.62	0.054	2.55	0.053	2.67	0.077	2.65	0.083
10.32	0.112	10.38	0.112	10.42	0.122	10.47	0.120	10.35	0.134	10.37	0.129
20.85	0.110	20.90	0.133	20.98	0.147	21.00	0.147	20.87	0.154	20.88	0.146
45.00	0.139	45.00	0.157	45.00	0.176	45.00	0.176	45.00	0.173	45.00	0.158
92.90	0.165	92.88	0.170	91.80	0.191	92.78	0.194	92.92	0.183	92.93	0.170
116.35	0.172	116.43	0.174	116.45	0.194	116.55	0.200	116.37	0.188	116.38	0.170
121.82	0.172	121.90	0.175	121.92	0.191	122.00	0.203	121.83	0.188	121.85	0.170
139.88	0.172	139.80	0.176	139.78	0.199	139.70	0.205	139.87	0.188	139.85	0.171
164.67	0.172	164.75	0.179	164.77	0.203	164.85	0.206	164.68	0.184	164.70	0.162
187.38	0.172	187.30	0.180	187.28	0.204	187.20	0.211	187.37	0.177	187.35	0.159

Test	α (º)	s (m)	s/D_p	n	W_g (m)	t_d (day)	d_{sge} (m)	d_{sge}/d_{se1}
59	15	0.225	4.5	3	0.400	8.5	0.208	1.53

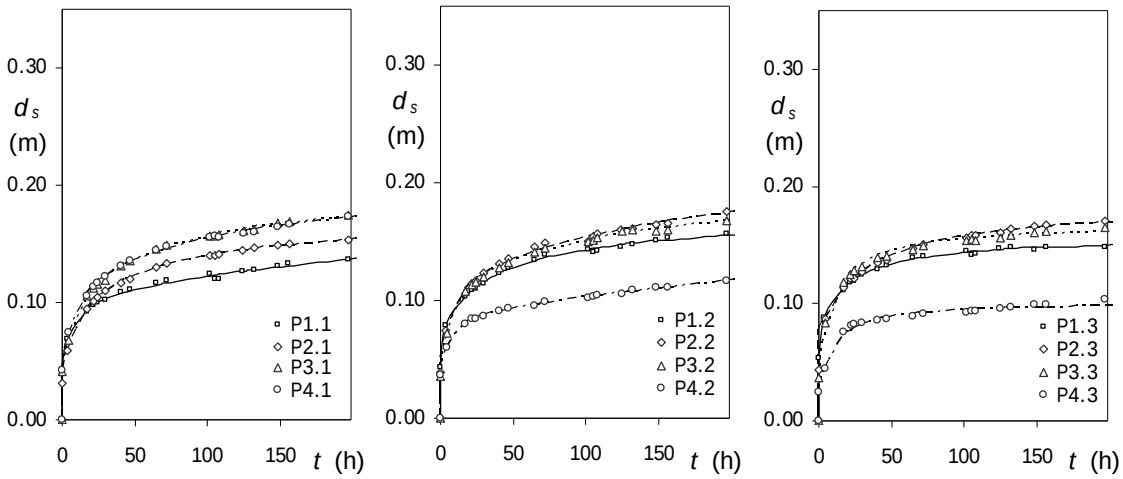

Test 59

P1.1		P2.1		P3.1		P4.1		P1.2		P1.3	
t (h)	d_s (m)	t (h)	d_s (m)	t (h)	d_s (m)	t (h)	d_s (m)	t (h)	d_s (m)	t (h)	d_s (m)
0.00	0.000	0.00	0.000	0.00	0.000	0.00	0.000	0.00	0.000	0.00	0.000
0.20	0.039	0.23	0.031	0.25	0.041	0.28	0.042	0.22	0.043	0.22	0.053
3.92	0.069	3.93	0.059	4.15	0.068	4.20	0.075	3.93	0.079	3.95	0.088
17.10	0.093	17.15	0.094	17.20	0.105	17.23	0.106	17.12	0.104	17.13	0.111
21.90	0.098	21.95	0.101	22.00	0.113	22.03	0.114	21.92	0.109	21.93	0.118
24.50	0.100	24.53	0.104	24.58	0.115	24.62	0.117	24.52	0.110	24.52	0.120
29.48	0.102	29.53	0.110	29.58	0.119	29.63	0.122	29.50	0.115	29.52	0.125
40.68	0.109	40.72	0.117	40.77	0.131	40.80	0.132	40.70	0.123	40.70	0.130
46.60	0.111	46.65	0.120	46.68	0.136	46.72	0.136	46.62	0.128	46.63	0.133
64.65	0.117	64.68	0.130	64.75	0.146	64.80	0.144	64.65	0.135	64.67	0.139
72.23	0.119	72.28	0.133	72.32	0.149	72.35	0.148	72.25	0.138	72.27	0.141
101.43	0.124	101.43	0.140	101.43	0.157	101.43	0.155	101.43	0.144	101.43	0.145
105.15	0.120	105.17	0.140	105.22	0.157	105.27	0.157	105.15	0.141	105.17	0.142
108.18	0.120	108.22	0.142	108.27	0.157	108.30	0.155	108.20	0.143	108.20	0.143
124.65	0.127	124.68	0.145	124.72	0.161	124.77	0.159	124.67	0.146	124.68	0.147
132.27	0.128	132.30	0.147	132.33	0.163	132.37	0.161	132.27	0.148	132.28	0.148
148.82	0.131	148.85	0.148	148.88	0.168	148.92	0.164	148.83	0.152	148.83	0.146
156.22	0.133	156.25	0.150	156.30	0.169	156.33	0.167	156.23	0.153	156.23	0.149
196.88	0.136	196.92	0.153	196.95	0.174	197.00	0.174	196.88	0.156	196.90	0.148
204.23	0.138	204.27	0.154	204.32	0.175	204.35	0.175	204.25	0.156	204.25	0.148

Test	α (º)	s (m)	s/D_p	n	W_g (m)	t_d (day)	d_{sge} (m)	d_{sge}/d_{se1}
60	15	0.300	6.0	3	0.400	7.8	0.170	1.26

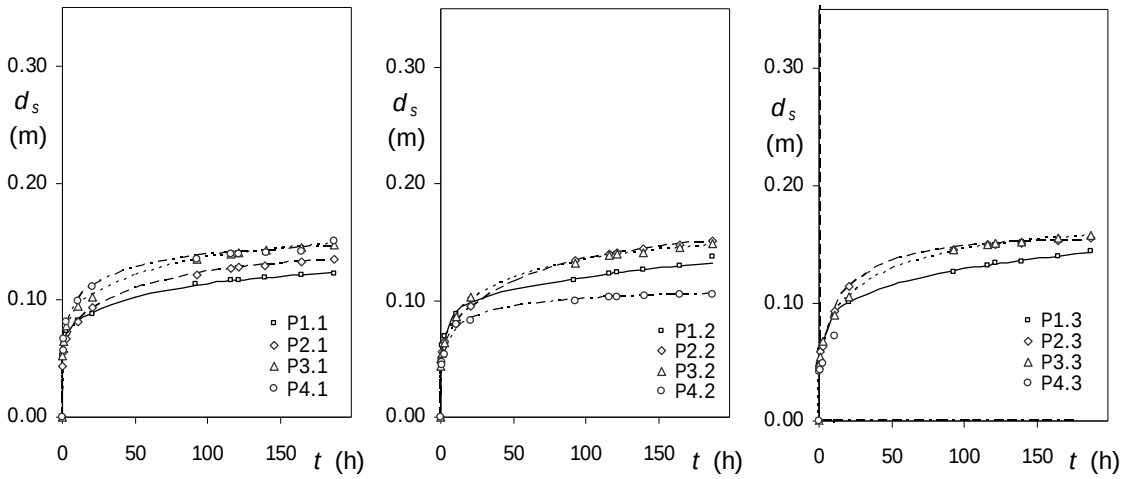

Test 60

P1.1		P2.1		P3.1		P4.1		P1.2		P1.3	
t (h)	d_s (m)	t (h)	d_s (m)	t (h)	d_s (m)	t (h)	d_s (m)	t (h)	d_s (m)	t (h)	d_s (m)
0.00	0.000	0.00	0.000	0.00	0.000	0.00	0.000	0.00	0.000	0.00	0.000
0.25	0.053	0.37	0.044	0.38	0.053	0.48	0.057	0.35	0.049	0.32	0.048
1.18	0.065	1.17	0.056	1.10	0.064	1.08	0.067	1.18	0.062	1.20	0.060
2.38	0.074	2.45	0.067	2.53	0.078	2.52	0.082	2.40	0.069	2.42	0.067
10.55	0.082	10.65	0.081	10.67	0.095	10.70	0.099	10.57	0.088	10.58	0.091
20.83	0.088	20.82	0.094	20.73	0.103	20.70	0.112	20.85	0.101	20.87	0.101
50.00	0.102	50.00	0.110	50.00	0.121	50.00	0.129	50.00	0.109	50.00	0.115
91.98	0.114	93.07	0.122	93.08	0.135	93.15	0.135	92.00	0.118	93.02	0.127
116.27	0.117	116.25	0.127	116.18	0.139	116.15	0.139	116.28	0.123	116.30	0.133
121.58	0.117	121.67	0.128	121.68	0.141	121.73	0.139	121.60	0.124	121.62	0.134
139.93	0.120	139.95	0.130	140.03	0.143	140.05	0.140	139.92	0.126	139.90	0.136
164.60	0.121	164.58	0.133	164.50	0.145	164.47	0.142	164.62	0.130	164.63	0.140
187.47	0.123	187.48	0.135	187.57	0.147	187.55	0.150	187.45	0.138	187.43	0.144

Test	α (º)	s (m)	s/D_p	n	W_g (m)	t_d (day)	d_{sge} (m)	d_{sge}/d_{se1}
61	30	0.050	1.0	3	0.212	7.0	0.347	2.55

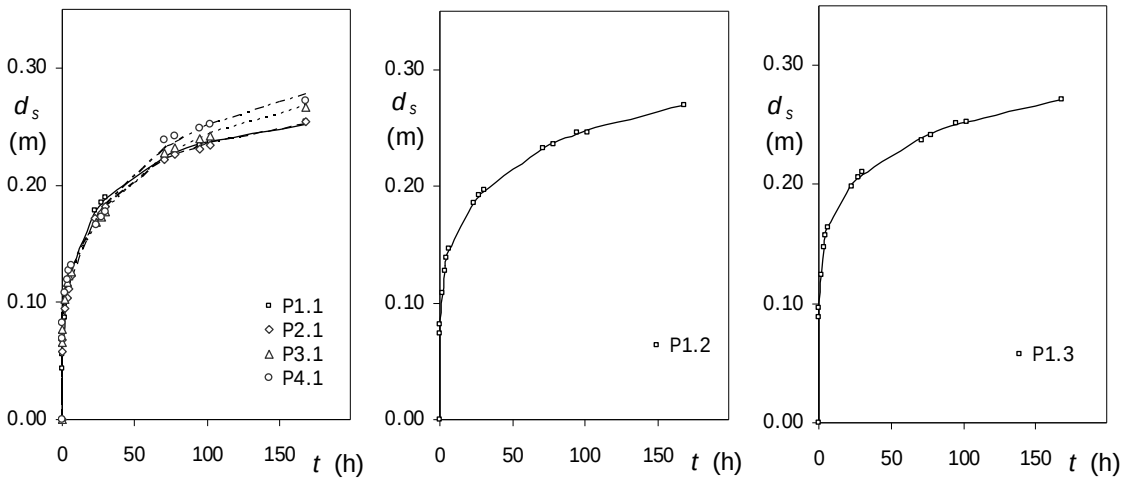

Test 61

P1.1		P2.1		P3.1		P4.1		P1.2		P1.3	
t (h)	d_s (m)	t (h)	d_s (m)	t (h)	d_s (m)	t (h)	d_s (m)	t (h)	d_s (m)	t (h)	d_s (m)
0.00	0.000	0.00	0.000	0.00	0.000	0.00	0.000	0.00	0.000	0.00	0.000
0.23	0.043	0.27	0.058	0.27	0.066	0.28	0.069	0.30	0.074	0.30	0.089
0.40	0.055	0.42	0.068	0.42	0.077	0.43	0.083	0.45	0.082	0.45	0.096
1.47	0.087	1.47	0.095	1.48	0.103	1.48	0.108	1.50	0.108	1.50	0.124
3.15	0.109	3.17	0.104	3.17	0.117	3.18	0.119	3.87	0.128	3.20	0.147
4.58	0.118	4.58	0.111	4.60	0.123	4.60	0.127	4.62	0.138	4.62	0.158
6.07	0.129	6.07	0.123	6.08	0.126	6.08	0.132	6.10	0.146	6.10	0.164
23.05	0.178	23.05	0.172	23.07	0.168	23.07	0.166	23.08	0.186	23.08	0.198
27.03	0.185	27.03	0.176	27.05	0.173	27.05	0.173	27.07	0.192	27.07	0.206
30.15	0.190	30.15	0.181	30.17	0.177	30.18	0.177	30.20	0.197	30.20	0.210
70.80	0.223	70.80	0.222	70.82	0.228	70.82	0.238	70.83	0.232	70.83	0.238
77.87	0.227	77.87	0.227	77.88	0.232	77.88	0.242	77.90	0.236	77.90	0.242
94.58	0.234	94.58	0.231	94.60	0.240	94.60	0.249	94.62	0.246	94.62	0.251
101.87	0.237	101.87	0.234	101.88	0.242	101.88	0.251	101.90	0.247	101.90	0.252
167.95	0.254	167.97	0.254	167.98	0.266	167.98	0.272	168.00	0.270	168.00	0.271

Test	α (º)	s (m)	s/D_p	n	W_g (m)	t_d (day)	d_{sge} (m)	d_{sge}/d_{se1}
62	30	0.100	2.0	3	0.373	8.0	0.378	2.78

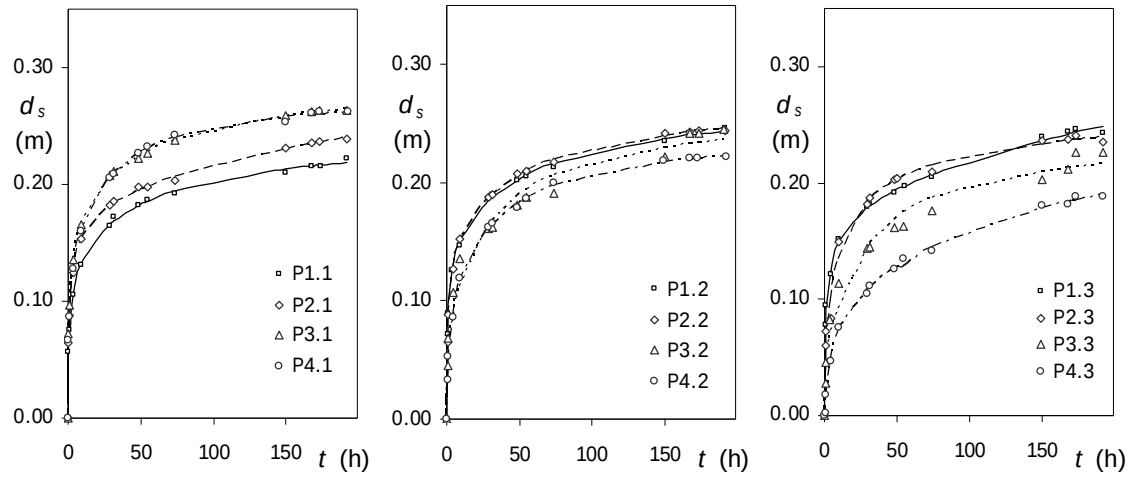

Test 62

P1.1		P2.1		P3.1		P4.1		P1.2		P1.3	
t (h)	d_s (m)	t (h)	d_s (m)	t (h)	d_s (m)	t (h)	d_s (m)	t (h)	d_s (m)	t (h)	d_s (m)
0.00	0.000	0.00	0.000	0.00	0.000	0.00	0.000	0.00	0.000	0.00	0.000
0.37	0.057	0.40	0.064	0.42	0.072	0.43	0.067	0.47	0.072	0.53	0.078
1.03	0.075	1.08	0.088	1.12	0.097	1.13	0.087	1.15	0.090	1.22	0.094
3.97	0.106	3.98	0.124	4.00	0.135	4.02	0.128	4.05	0.126	4.08	0.121
9.25	0.131	9.27	0.153	9.28	0.166	9.30	0.160	9.33	0.147	9.40	0.152
28.87	0.164	28.88	0.182	28.90	0.208	28.92	0.206	28.95	0.187	29.08	0.180
31.45	0.173	31.25	0.185	31.28	0.211	31.32	0.209	31.12	0.190	31.15	0.182
48.15	0.183	48.25	0.197	48.32	0.222	48.45	0.226	48.18	0.202	48.22	0.191
54.95	0.187	54.90	0.198	54.68	0.227	54.65	0.233	54.98	0.206	55.02	0.197
73.72	0.192	73.82	0.204	73.85	0.237	73.93	0.242	73.73	0.214	73.75	0.206
150.10	0.210	149.98	0.231	149.95	0.259	149.82	0.253	150.12	0.235	150.15	0.239
167.45	0.215	167.58	0.235	167.60	0.263	167.68	0.261	167.48	0.241	167.52	0.245
173.58	0.216	173.42	0.237	173.40	0.263	173.28	0.262	173.57	0.241	173.53	0.246
191.95	0.223	192.15	0.239	192.18	0.264	192.28	0.262	191.98	0.246	192.00	0.243

Test	α (º)	s (m)	s/D_p	n	W_g (m)	t_d (day)	d_{sge} (m)	d_{sge}/d_{se1}
63	30	0.150	3.0	3	0.400	8.3	0.280	2.06

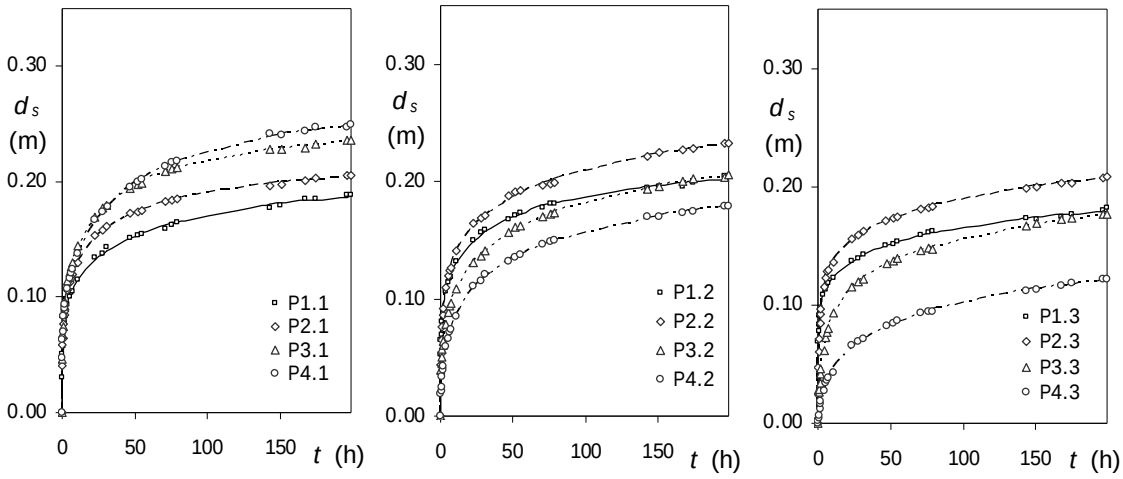

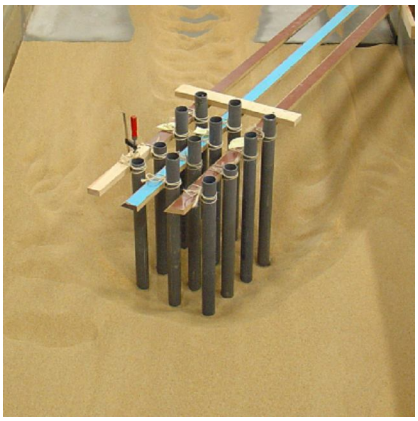

Test 63

P1.1		P2.1		P3.1		P4.1		P1.2		P1.3	
t (h)	d_s (m)	t (h)	d_s (m)	t (h)	d_s (m)	t (h)	d_s (m)	t (h)	d_s (m)	t (h)	d_s (m)
0.00	0.000	0.00	0.000	0.00	0.000	0.00	0.000	0.00	0.000	0.00	0.000
0.07	0.031	0.08	0.040	0.10	0.046	0.12	0.047	0.22	0.053	0.28	0.069
0.38	0.050	0.40	0.058	0.42	0.068	0.43	0.063	0.45	0.065	0.52	0.077
0.62	0.058	0.63	0.064	0.65	0.074	0.67	0.070	0.68	0.070	0.75	0.084
1.67	0.077	1.68	0.084	1.70	0.092	1.72	0.090	1.73	0.088	1.80	0.096
1.98	0.080	2.00	0.088	2.02	0.096	2.03	0.094	2.05	0.091	2.12	0.097
3.90	0.094	3.92	0.106	3.93	0.114	3.95	0.108	3.97	0.106	4.03	0.108
6.32	0.104	6.33	0.116	6.35	0.126	6.37	0.121	6.38	0.117	6.45	0.117
6.97	0.105	6.98	0.120	7.00	0.130	7.02	0.125	7.03	0.119	7.10	0.119
10.77	0.115	10.77	0.130	10.78	0.145	10.80	0.138	10.82	0.132	10.93	0.123
22.90	0.134	22.92	0.154	22.93	0.169	22.95	0.167	22.97	0.150	23.03	0.137
31.02	0.143	31.03	0.161	31.05	0.179	31.07	0.178	31.08	0.158	31.15	0.143
51.82	0.153	51.83	0.174	51.85	0.198	51.87	0.199	51.88	0.171	51.95	0.152
70.85	0.159	70.87	0.183	70.88	0.209	70.90	0.214	70.92	0.178	70.98	0.159
78.83	0.165	78.85	0.185	78.87	0.212	78.88	0.218	78.90	0.182	78.97	0.162
142.97	0.178	142.98	0.197	143.00	0.228	143.02	0.242	143.03	0.195	143.10	0.173
167.47	0.185	167.48	0.201	167.50	0.230	167.52	0.244	167.53	0.196	167.60	0.174
174.90	0.186	174.92	0.203	174.93	0.233	174.95	0.247	174.97	0.199	175.03	0.177
195.97	0.188	195.98	0.205	196.00	0.236	196.02	0.247	196.03	0.204	196.10	0.180
198.80	0.188	198.82	0.206	198.83	0.236	198.85	0.249	198.87	0.205	198.93	0.182

Test	α (º)	s (m)	s/D_p	n	W_g (m)	t_d (day)	d_{sge} (m)	d_{sge}/d_{se1}
64	30	0.225	4.5	3	0.400	7.2	0.237	1.75

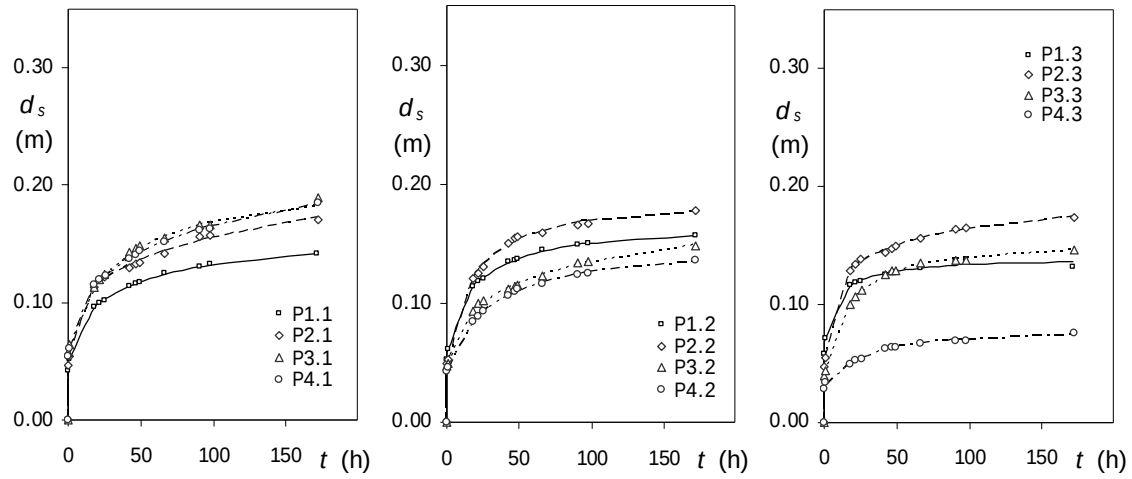

Test 64

P1.1		P2.1		P3.1		P4.1		P1.2		P1.3	
t (h)	d_s (m)	t (h)	d_s (m)	t (h)	d_s (m)	t (h)	d_s (m)	t (h)	d_s (m)	t (h)	d_s (m)
0.00	0.000	0.00	0.000	0.00	0.000	0.00	0.000	0.00	0.000	0.00	0.000
0.22	0.042	0.25	0.047	0.28	0.058	0.32	0.054	0.23	0.052	0.23	0.059
0.68	0.052	0.72	0.055	0.75	0.064	0.78	0.061	0.68	0.061	0.70	0.071
17.98	0.096	18.02	0.113	18.07	0.113	18.10	0.115	18.00	0.114	18.00	0.116
21.83	0.100	21.87	0.119	21.90	0.119	21.93	0.119	21.83	0.119	21.85	0.119
25.47	0.102	25.50	0.122	25.53	0.124	25.57	0.123	25.48	0.121	25.48	0.120
42.20	0.114	42.23	0.130	42.27	0.142	42.32	0.137	42.22	0.135	42.22	0.125
46.70	0.116	46.73	0.133	46.77	0.146	46.80	0.141	46.72	0.136	46.72	0.127
48.90	0.117	48.93	0.135	48.95	0.148	48.97	0.144	48.90	0.137	48.92	0.128
66.00	0.125	66.03	0.142	66.07	0.155	66.10	0.152	66.02	0.145	66.02	0.132
90.67	0.131	90.70	0.156	90.73	0.166	90.77	0.162	90.68	0.149	90.68	0.136
97.28	0.132	97.30	0.157	97.33	0.166	97.35	0.163	97.28	0.150	97.30	0.138
171.63	0.142	171.67	0.171	171.70	0.189	171.72	0.185	171.65	0.157	171.65	0.132

Test	α (º)	s (m)	s/D_p	n	W_g (m)	t_d (day)	d_{sge} (m)	d_{sge}/d_{se1}
65	30	0.300	6.0	3	0.400	7.9	0.228	1.68

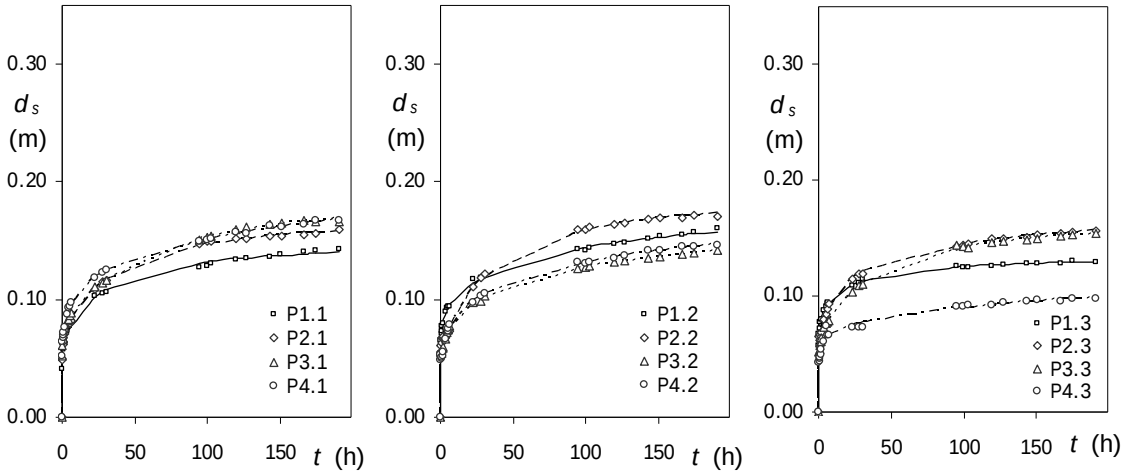

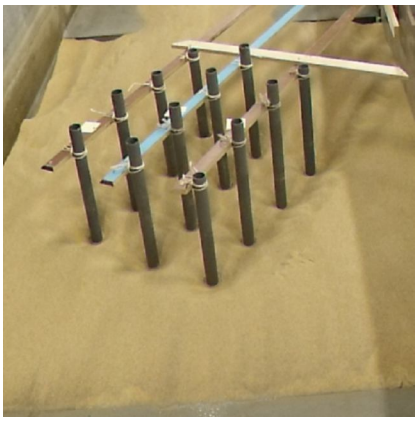

Test 65

P1.1		P2.1		P3.1		P4.1		P1.2		P1.3	
t (h)	d_s (m)	t (h)	d_s (m)	t (h)	d_s (m)	t (h)	d_s (m)	t (h)	d_s (m)	t (h)	d_s (m)
0.00	0.000	0.00	0.000	0.00	0.000	0.00	0.000	0.00	0.000	0.00	0.000
0.05	0.041	0.07	0.049	0.08	0.052	0.10	0.052	0.12	0.055	0.18	0.057
0.32	0.048	0.33	0.049	0.35	0.061	0.37	0.064	0.38	0.065	0.43	0.068
0.62	0.058	0.63	0.062	0.65	0.067	0.67	0.067	0.68	0.071	0.75	0.073
0.97	0.062	0.98	0.064	1.00	0.073	1.02	0.070	1.03	0.074	1.10	0.078
1.28	0.064	1.30	0.068	1.32	0.074	1.33	0.072	1.35	0.077	1.42	0.080
3.83	0.073	3.85	0.079	3.87	0.082	3.88	0.087	3.90	0.090	3.97	0.087
4.85	0.076	4.87	0.079	4.88	0.083	4.90	0.093	4.92	0.093	4.98	0.091
5.73	0.078	5.75	0.080	5.77	0.086	5.78	0.094	5.80	0.094	5.87	0.094
6.58	0.081	6.60	0.082	6.62	0.088	6.63	0.097	6.65	0.094	6.72	0.094
22.77	0.103	22.78	0.109	22.80	0.110	22.82	0.119	22.83	0.117	22.90	0.110
30.28	0.106	30.30	0.117	30.32	0.116	30.33	0.125	30.35	0.120	30.42	0.114
94.68	0.128	94.70	0.147	94.72	0.150	94.73	0.149	94.75	0.143	94.82	0.126
102.77	0.131	102.78	0.149	102.80	0.154	102.82	0.151	102.83	0.144	102.90	0.125
119.32	0.134	119.33	0.152	119.35	0.160	119.37	0.157	119.38	0.147	119.45	0.126
126.88	0.135	126.90	0.151	126.92	0.162	126.93	0.157	126.95	0.148	127.02	0.127
150.82	0.139	150.83	0.155	150.85	0.165	150.87	0.161	150.88	0.154	150.95	0.129
166.72	0.141	166.73	0.155	166.75	0.167	166.77	0.164	166.78	0.156	166.85	0.129
174.82	0.142	174.83	0.156	174.85	0.167	174.87	0.167	174.88	0.157	174.95	0.130
190.70	0.143	190.72	0.159	190.73	0.167	190.75	0.168	190.77	0.160	190.83	0.130

Test	α (º)	s (m)	s/D_p	n	W_g (m)	t_d (day)	d_{sge} (m)	d_{sge}/d_{se1}
66	45	0.050	1.0	3	0.227	8.9	0.359	2.65

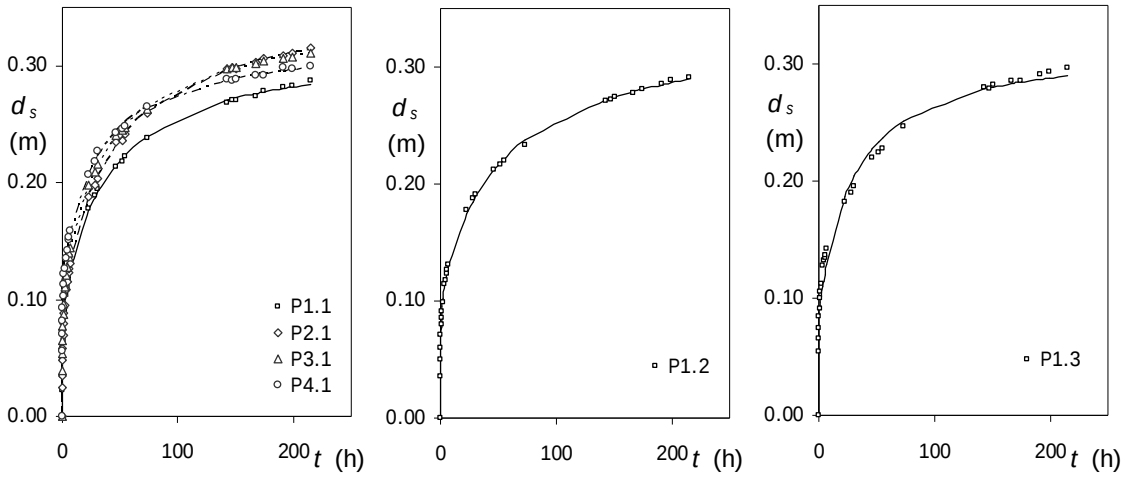

Test 66

P1.1		P2.1		P3.1		P4.1		P1.2		P1.3	
t (h)	d_s (m)	t (h)	d_s (m)	t (h)	d_s (m)	t (h)	d_s (m)	t (h)	d_s (m)	t (h)	d_s (m)
0.00	0.000	0.00	0.000	0.00	0.000	0.00	0.000	0.00	0.000	0.00	0.000
0.02	0.023	0.03	0.025	0.05	0.039	0.07	0.056	0.08	0.036	0.10	0.055
0.13	0.035	0.15	0.035	0.17	0.054	0.18	0.070	0.20	0.050	0.22	0.066
0.28	0.048	0.30	0.048	0.32	0.065	0.33	0.082	0.35	0.060	0.37	0.075
0.67	0.065	0.68	0.070	0.70	0.088	0.72	0.103	0.73	0.080	0.75	0.092
1.02	0.074	1.03	0.079	1.05	0.096	1.07	0.113	1.08	0.086	1.10	0.100
1.48	0.083	1.50	0.089	1.52	0.107	1.53	0.122	1.55	0.092	1.57	0.106
2.00	0.091	2.02	0.095	2.03	0.111	2.05	0.126	2.07	0.099	2.08	0.112
3.42	0.104	3.43	0.108	3.45	0.120	3.47	0.135	3.48	0.114	3.50	0.128
5.13	0.117	5.15	0.123	5.17	0.137	5.18	0.151	5.20	0.123	5.22	0.134
5.82	0.122	5.83	0.126	5.85	0.140	5.87	0.153	5.88	0.126	5.90	0.137
6.72	0.129	6.73	0.131	6.75	0.144	6.77	0.159	6.78	0.131	6.80	0.142
27.93	0.190	27.95	0.198	27.97	0.209	27.98	0.218	28.00	0.187	28.02	0.190
30.82	0.194	30.83	0.204	30.85	0.216	30.87	0.227	30.88	0.192	30.90	0.195
51.55	0.218	51.57	0.236	51.58	0.244	51.60	0.246	51.62	0.216	51.63	0.225
73.52	0.239	73.53	0.259	73.55	0.263	73.57	0.265	73.60	0.233	73.63	0.247
142.98	0.269	143.00	0.297	143.02	0.297	143.03	0.288	143.05	0.271	143.07	0.280
166.97	0.274	166.98	0.303	167.00	0.302	167.02	0.292	167.03	0.278	167.05	0.285
191.05	0.281	191.07	0.308	191.08	0.307	191.10	0.298	191.12	0.286	191.13	0.292
214.75	0.288	214.77	0.315	214.78	0.311	214.80	0.299	214.82	0.291	214.83	0.296

Test	α (º)	s (m)	s/D_p	n	W_g (m)	t_d (day)	d_{sge} (m)	d_{sge}/d_{se1}
67	45	0.100	2.0	3	0.300	12.0	0.329	2.42

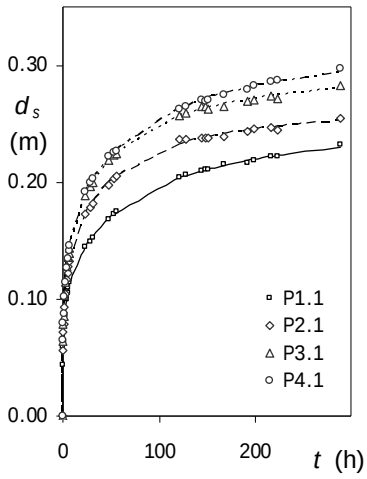

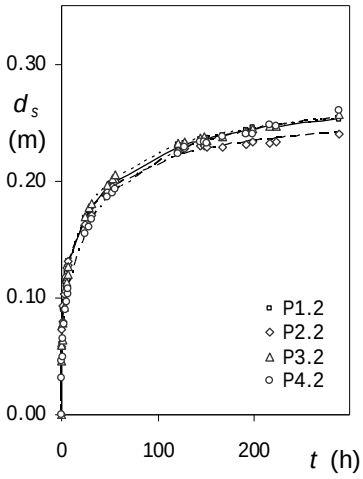

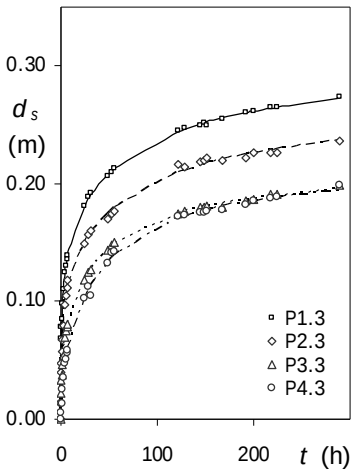

Test 67

P1.1		P2.1		P3.1		P4.1		P1.2		P1.3	
t (h)	d_s (m)	t (h)	d_s (m)	t (h)	d_s (m)	t (h)	d_s (m)	t (h)	d_s (m)	t (h)	d_s (m)
0.00	0.000	0.00	0.000	0.00	0.000	0.00	0.000	0.00	0.000	0.00	0.000
0.10	0.044	0.12	0.056	0.13	0.064	0.15	0.065	0.17	0.060	0.23	0.068
0.48	0.060	0.50	0.072	0.52	0.079	0.53	0.080	0.55	0.072	0.62	0.078
0.75	0.064	0.77	0.078	0.78	0.085	0.80	0.087	0.82	0.079	0.88	0.086
2.38	0.087	2.40	0.105	2.42	0.114	2.43	0.115	2.45	0.100	2.52	0.111
4.08	0.100	4.10	0.117	4.12	0.128	4.13	0.127	4.15	0.114	4.22	0.125
5.08	0.106	5.10	0.122	5.12	0.135	5.13	0.134	5.15	0.121	5.22	0.130
7.08	0.114	7.10	0.132	7.12	0.144	7.13	0.146	7.15	0.131	7.22	0.139
23.73	0.145	23.75	0.173	23.77	0.189	23.78	0.192	23.80	0.169	23.87	0.181
31.25	0.153	31.27	0.182	31.28	0.200	31.30	0.203	31.32	0.178	31.38	0.192
47.78	0.168	47.80	0.198	47.82	0.218	47.83	0.222	47.85	0.191	47.92	0.207
55.18	0.175	55.20	0.205	55.22	0.224	55.23	0.227	55.25	0.199	55.32	0.213
121.42	0.205	121.43	0.237	121.45	0.257	121.47	0.262	121.48	0.231	121.55	0.245
143.80	0.210	143.82	0.238	143.83	0.265	143.85	0.271	143.87	0.235	143.93	0.250
148.18	0.211	148.20	0.238	148.22	0.265	148.23	0.270	148.25	0.236	148.32	0.251
167.48	0.215	167.50	0.239	167.52	0.264	167.53	0.275	167.55	0.240	167.62	0.255
198.55	0.219	198.57	0.246	198.58	0.270	198.60	0.282	198.62	0.245	198.68	0.262
216.08	0.223	216.10	0.247	216.12	0.274	216.13	0.286	216.15	0.245	216.22	0.265
223.30	0.222	223.32	0.245	223.33	0.272	223.35	0.287	223.37	0.247	223.43	0.265
287.78	0.232	287.80	0.255	287.82	0.283	287.83	0.297	287.85	0.252	287.92	0.273

Test	α (º)	s (m)	s/D_p	n	W_g (m)	t_d (day)	d_{sge} (m)	d_{sge}/d_{se1}
68	45	0.150	3.0	3	0.300	8.9	0.279	2.05

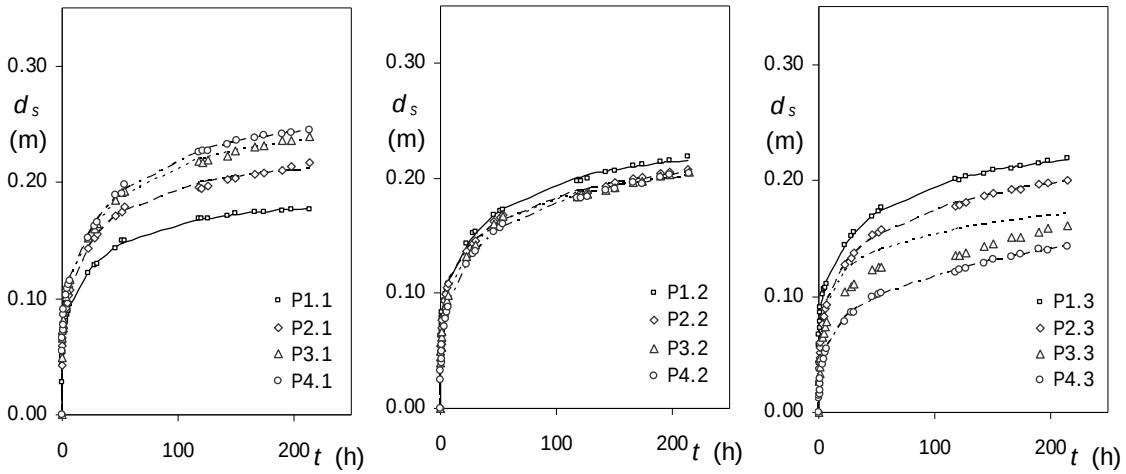

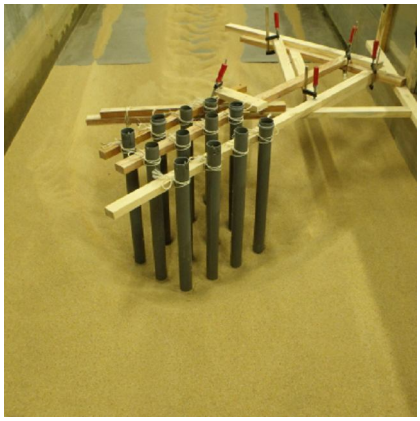

Test 68

P1.1		P2.1		P3.1		P4.1		P1.2		P1.3	
t (h)	d_s (m)	t (h)	d_s (m)	t (h)	d_s (m)	t (h)	d_s (m)	t (h)	d_s (m)	t (h)	d_s (m)
0.00	0.000	0.00	0.000	0.00	0.000	0.00	0.000	0.00	0.000	0.00	0.000
0.05	0.028	0.07	0.042	0.08	0.049	0.10	0.055	0.12	0.048	0.18	0.059
0.30	0.042	0.32	0.059	0.33	0.066	0.35	0.066	0.37	0.063	0.43	0.067
0.52	0.050	0.53	0.066	0.55	0.072	0.57	0.073	0.58	0.068	0.65	0.073
1.07	0.061	1.08	0.075	1.10	0.082	1.12	0.086	1.13	0.079	1.20	0.086
1.45	0.065	1.47	0.079	1.48	0.089	1.50	0.090	1.52	0.083	1.58	0.091
3.13	0.080	3.15	0.092	3.17	0.102	3.18	0.103	3.20	0.094	3.27	0.102
4.13	0.086	4.15	0.097	4.17	0.107	4.18	0.109	4.20	0.099	4.27	0.106
5.13	0.090	5.15	0.103	5.17	0.112	5.18	0.112	5.20	0.104	5.27	0.108
6.70	0.095	6.72	0.107	6.73	0.116	6.75	0.115	6.77	0.108	6.83	0.111
22.10	0.122	22.12	0.143	22.13	0.152	22.15	0.152	22.17	0.144	22.23	0.145
46.47	0.144	46.48	0.171	46.50	0.184	46.52	0.189	46.53	0.168	46.60	0.169
53.88	0.150	53.90	0.179	53.92	0.192	53.93	0.198	53.95	0.173	54.02	0.176
118.55	0.169	118.57	0.195	118.58	0.218	118.60	0.226	118.62	0.197	118.68	0.201
121.03	0.169	121.05	0.194	121.07	0.217	121.08	0.227	121.10	0.198	121.17	0.201
142.92	0.172	142.93	0.202	142.95	0.223	142.97	0.233	142.98	0.206	143.05	0.205
150.30	0.173	150.32	0.203	150.33	0.227	150.35	0.235	150.37	0.206	150.43	0.209
174.30	0.174	174.32	0.208	174.33	0.232	174.35	0.240	174.37	0.213	174.43	0.213
190.22	0.176	190.23	0.210	190.25	0.236	190.27	0.242	190.28	0.215	190.35	0.215
214.43	0.177	214.45	0.217	214.47	0.240	214.48	0.245	214.50	0.219	214.57	0.219

Test	α (º)	s (m)	s/D_p	n	W_g (m)	t_d (day)	d_{sge} (m)	d_{sge}/d_{se1}
69	45	0.225	4.5	3	0.300	7.2	0.182	1.34

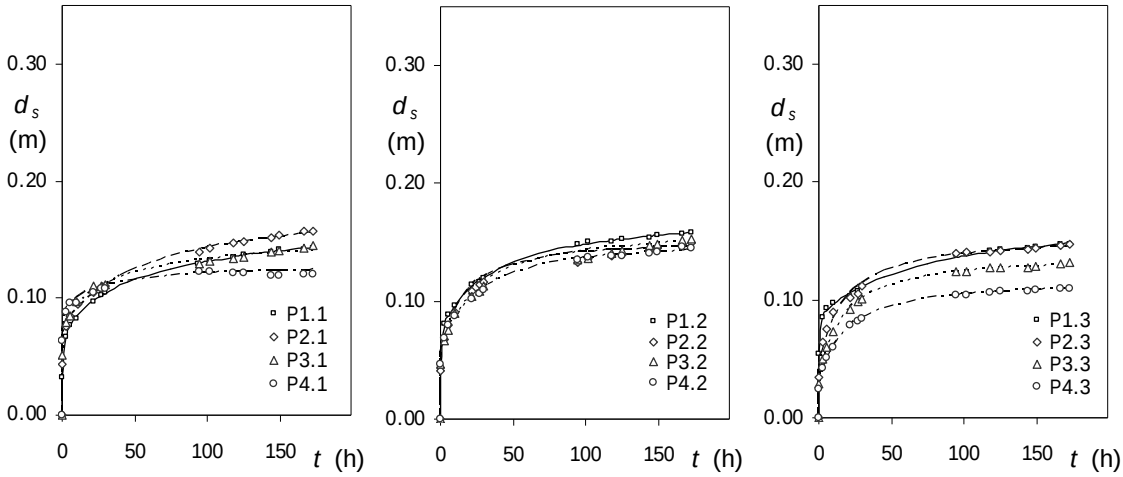

Test 69

P1.1		P2.1		P3.1		P4.1		P1.2		P1.3	
t (h)	d_s (m)	t (h)	d_s (m)	t (h)	d_s (m)	t (h)	d_s (m)	t (h)	d_s (m)	t (h)	d_s (m)
0.00	0.000	0.00	0.000	0.00	0.000	0.00	0.000	0.00	0.000	0.00	0.000
0.12	0.032	0.17	0.044	0.20	0.051	0.23	0.063	0.13	0.042	0.15	0.055
2.87	0.067	2.90	0.075	2.92	0.079	2.95	0.088	2.87	0.081	2.88	0.085
5.30	0.077	5.33	0.084	5.37	0.085	5.40	0.096	5.30	0.089	5.32	0.093
9.85	0.083	10.90	0.095	9.95	0.097	10.00	0.096	9.87	0.096	9.88	0.098
21.80	0.097	21.83	0.105	21.87	0.110	21.92	0.105	21.82	0.114	21.82	0.103
26.68	0.103	26.72	0.108	26.75	0.111	26.78	0.108	26.70	0.116	26.70	0.108
29.32	0.104	29.35	0.111	29.38	0.111	29.42	0.108	29.33	0.120	29.33	0.112
45.00	0.113	45.00	0.122	45.00	0.121	45.00	0.115	45.00	0.131	45.00	0.120
75.00	0.125	75.00	0.136	75.00	0.130	75.00	0.120	75.00	0.143	75.00	0.131
94.08	0.130	94.12	0.139	94.15	0.129	94.20	0.123	94.10	0.149	94.10	0.138
101.50	0.132	101.52	0.143	101.57	0.131	101.60	0.123	101.50	0.150	101.52	0.140
117.98	0.134	118.02	0.147	118.07	0.134	118.10	0.122	118.00	0.151	118.00	0.141
124.80	0.137	124.83	0.148	124.88	0.135	124.92	0.122	124.82	0.153	124.82	0.143
144.28	0.140	144.32	0.152	144.35	0.139	144.38	0.119	144.30	0.154	144.30	0.144
149.55	0.141	149.58	0.153	149.62	0.140	149.65	0.119	149.55	0.156	149.57	0.145
166.18	0.142	166.22	0.157	166.27	0.143	166.30	0.121	166.20	0.157	166.20	0.147
172.70	0.143	172.73	0.157	172.77	0.144	173.30	0.120	172.72	0.158	172.72	0.147

Test	α (º)	s (m)	s/D_p	n	W_g (m)	t_d (day)	d_{sge} (m)	d_{sge}/d_{se1}
70	45	0.300	6.0	3	0.300	11.6	0.160	1.18

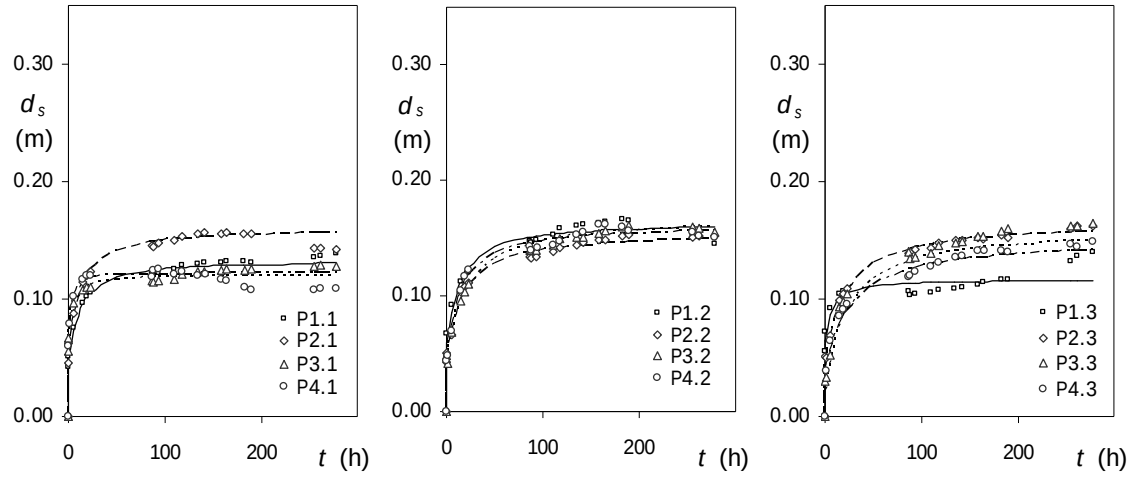

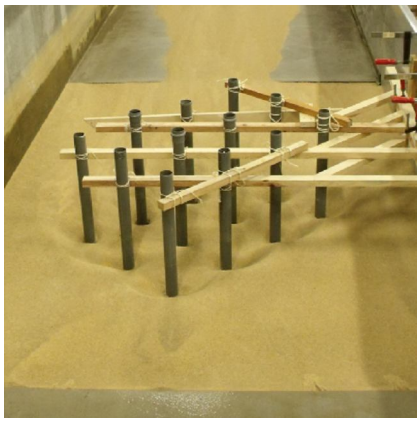

Test 70

P1.1		P2.1		P3.1		P4.1		P1.2		P1.3	
t (h)	d_s (m)	t (h)	d_s (m)	t (h)	d_s (m)	t (h)	d_s (m)	t (h)	d_s (m)	t (h)	d_s (m)
0.00	0.000	0.00	0.000	0.00	0.000	0.00	0.000	0.00	0.000	0.00	0.000
0.07	0.042	0.12	0.046	0.22	0.056	0.28	0.060	0.08	0.047	0.10	0.056
0.45	0.051	0.48	0.063	0.67	0.067	0.77	0.079	0.47	0.068	0.52	0.072
4.75	0.076	4.77	0.088	4.82	0.097	4.88	0.102	4.75	0.092	4.78	0.092
14.40	0.097	14.42	0.115	14.45	0.108	14.50	0.116	14.43	0.112	14.48	0.104
22.33	0.105	22.33	0.124	22.37	0.110	22.38	0.120	22.35	0.121	22.38	0.107
50.00	0.119	50.00	0.142	50.00	0.117	50.00	0.121	50.00	0.143	50.00	0.111
86.17	0.122	86.18	0.146	86.20	0.115	86.22	0.119	86.18	0.147	86.22	0.106
93.52	0.122	93.52	0.148	93.55	0.115	93.58	0.126	93.53	0.148	93.57	0.104
109.92	0.126	109.92	0.150	109.95	0.117	109.98	0.121	109.93	0.153	109.97	0.106
117.18	0.129	117.18	0.153	117.22	0.121	117.27	0.123	117.20	0.158	117.25	0.108
134.52	0.130	134.52	0.155	134.57	0.123	134.60	0.120	134.53	0.160	134.58	0.109
141.33	0.131	141.33	0.156	141.37	0.123	141.40	0.121	141.35	0.163	141.38	0.110
158.00	0.131	158.00	0.156	158.03	0.124	158.08	0.117	158.02	0.164	158.05	0.113
164.25	0.132	164.25	0.156	164.27	0.126	164.32	0.115	164.27	0.165	164.30	0.114
181.93	0.132	181.93	0.156	181.98	0.125	182.03	0.110	181.95	0.167	182.00	0.117
188.82	0.131	188.82	0.155	188.85	0.125	188.88	0.107	188.83	0.165	188.88	0.117
254.50	0.135	254.52	0.143	254.55	0.128	254.60	0.108	254.53	0.152	254.57	0.133
261.33	0.137	261.35	0.143	261.37	0.129	261.42	0.109	261.35	0.152	261.38	0.136
277.77	0.139	277.78	0.142	277.82	0.128	277.88	0.109	277.80	0.145	277.83	0.140

Test	α (º)	s (m)	s/D_p	n	W_g (m)	t_d (day)	d_{sge} (m)	d_{sge}/d_{se1}
71	90	0.050	1.0	3	0.200	7.4	0.328	2.42

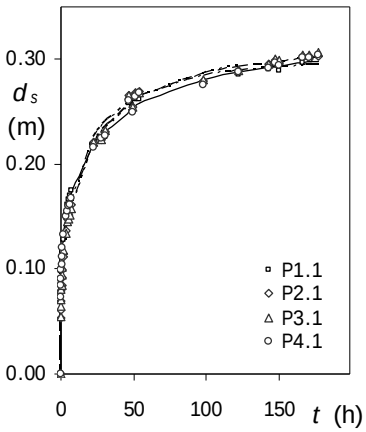

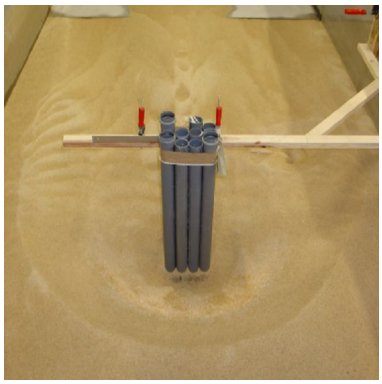

Test 71

P1.1		P2.1		P3.1		P4.1		P1.2		P1.3	
t (h)	d_s (m)	t (h)	d_s (m)	t (h)	d_s (m)	t (h)	d_s (m)	t (h)	d_s (m)	t (h)	d_s (m)
0.00	0.000	0.00	0.000	0.00	0.000	0.00	0.000				
0.12	0.075	0.10	0.053	0.08	0.054	0.07	0.073				
0.20	0.084	0.18	0.061	0.17	0.065	0.15	0.085				
0.30	0.090	0.28	0.069	0.27	0.071	0.25	0.091				
0.42	0.099	0.40	0.080	0.38	0.080	0.37	0.099				
0.53	0.104	0.52	0.085	0.50	0.085	0.48	0.105				
0.70	0.108	0.68	0.092	0.67	0.094	0.65	0.111				
1.03	0.117	1.02	0.099	1.00	0.102	0.98	0.120				
1.62	0.128	1.60	0.112	1.58	0.118	1.57	0.132				
3.72	0.151	3.70	0.137	3.68	0.134	3.67	0.150				
4.92	0.162	4.90	0.148	4.88	0.145	4.87	0.155				
5.57	0.167	5.55	0.151	5.53	0.148	5.52	0.160				
6.05	0.170	6.03	0.155	6.02	0.152	6.00	0.162				
6.83	0.175	6.82	0.161	6.80	0.158	6.78	0.168				
22.57	0.218	22.55	0.221	22.53	0.221	22.52	0.216				
27.57	0.222	27.55	0.224	27.53	0.224	27.52	0.225				
30.28	0.226	30.27	0.231	30.25	0.232	30.23	0.228				
49.45	0.250	49.43	0.255	49.42	0.254	49.40	0.250				
47.13	0.258	47.12	0.266	47.10	0.266	47.08	0.261				
51.62	0.262	51.60	0.268	51.58	0.268	51.57	0.265				
54.42	0.262	54.40	0.269	54.38	0.269	54.37	0.268				
98.00	0.276	97.98	0.279	97.97	0.280	97.95	0.275				
122.10	0.285	122.08	0.289	122.07	0.289	122.05	0.288				
143.07	0.291	143.05	0.295	143.03	0.295	143.02	0.292				
147.62	0.294	147.60	0.299	147.58	0.300	147.57	0.297				
150.32	0.290	150.30	0.297	150.28	0.300	150.27	0.295				
166.80	0.297	166.78	0.303	166.77	0.304	166.75	0.301				
171.55	0.299	171.53	0.303	171.52	0.304	171.50	0.301				
177.20	0.303	177.22	0.303	177.23	0.306	177.25	0.304				

Test	α (º)	s (m)	s/D_p	n	W_g (m)	t_d (day)	d_{sge} (m)	d_{sge}/d_{se1}
72	90	0.100	2.0	3	0.200	7.8	0.255	1.87

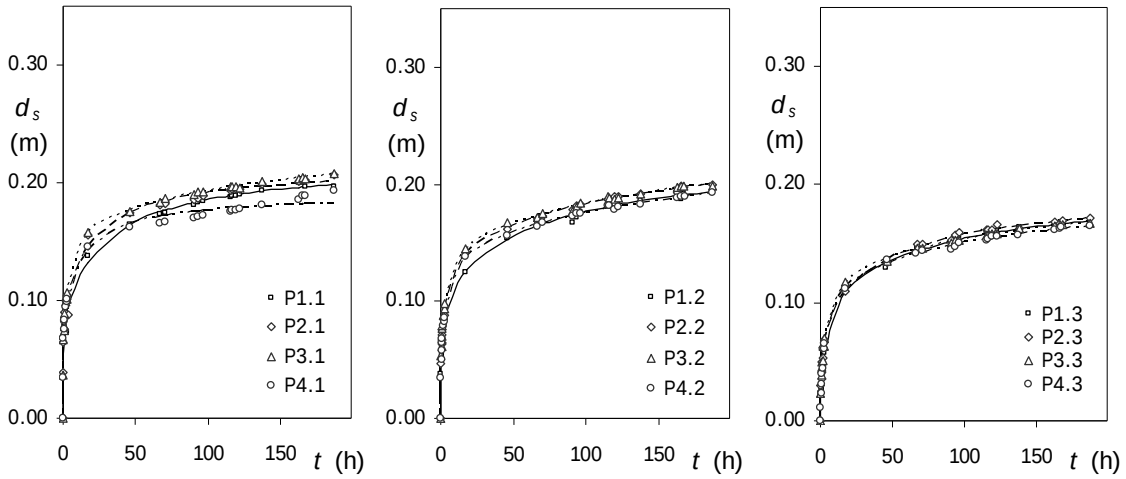

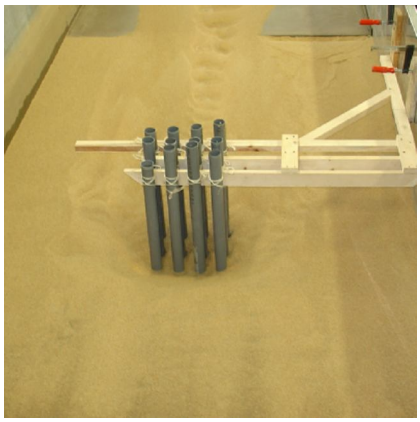

Test 72

P1.1		P2.1		P3.1		P4.1		P1.2		P1.3	
t (h)	d_s (m)	t (h)	d_s (m)	t (h)	d_s (m)	t (h)	d_s (m)	t (h)	d_s (m)	t (h)	d_s (m)
0.00	0.000	0.00	0.000	0.00	0.000	0.00	0.000	0.00	0.000	0.00	0.000
0.08	0.038	0.07	0.039	0.05	0.037	0.03	0.035	0.27	0.038	0.37	0.023
0.47	0.065	0.45	0.064	0.43	0.067	0.42	0.067	0.57	0.049	0.65	0.027
0.73	0.073	0.72	0.076	0.70	0.075	0.68	0.076	0.82	0.054	0.92	0.028
1.00	0.078	0.98	0.090	0.97	0.078	0.95	0.082	1.10	0.062	1.18	0.030
1.25	0.083	3.23	0.088	1.22	0.089	1.20	0.083	1.37	0.069	1.47	0.040
2.12	0.093	2.10	0.100	2.08	0.099	2.07	0.095	2.18	0.078	2.25	0.052
2.73	0.099	2.70	0.104	2.68	0.107	2.67	0.101	2.80	0.087	2.87	0.064
17.33	0.138	17.35	0.156	17.37	0.158	17.38	0.146	17.40	0.125	17.47	0.110
45.75	0.165	45.77	0.175	45.78	0.176	45.80	0.163	45.82	0.154	45.88	0.130
70.47	0.175	70.45	0.182	70.43	0.187	70.42	0.167	70.53	0.169	70.62	0.146
90.60	0.181	90.58	0.186	90.57	0.190	90.55	0.170	90.67	0.168	90.73	0.146
96.60	0.184	96.58	0.189	96.57	0.192	96.55	0.172	96.67	0.177	96.73	0.156
115.43	0.188	115.42	0.193	115.40	0.197	115.38	0.176	115.50	0.182	115.57	0.160
119.32	0.189	119.30	0.194	119.28	0.197	119.27	0.177	119.38	0.183	119.45	0.160
137.57	0.193	137.55	0.199	137.53	0.201	137.52	0.181	137.63	0.186	137.70	0.163
162.60	0.200	162.58	0.201	162.57	0.204	162.55	0.185	162.67	0.192	162.73	0.167
165.83	0.201	165.82	0.202	165.80	0.205	165.78	0.189	165.90	0.188	165.97	0.165
167.57	0.197	167.55	0.202	167.53	0.203	167.52	0.189	167.63	0.192	167.70	0.169
186.98	0.197	186.97	0.206	186.95	0.208	186.93	0.193	187.05	0.193	187.12	0.167

Test	α (º)	s (m)	s/D_p	n	W_g (m)	t_d (day)	d_{sge} (m)	d_{sge}/d_{se1}
73	90	0.150	3.0	3	0.200	7.3	0.187	1.37

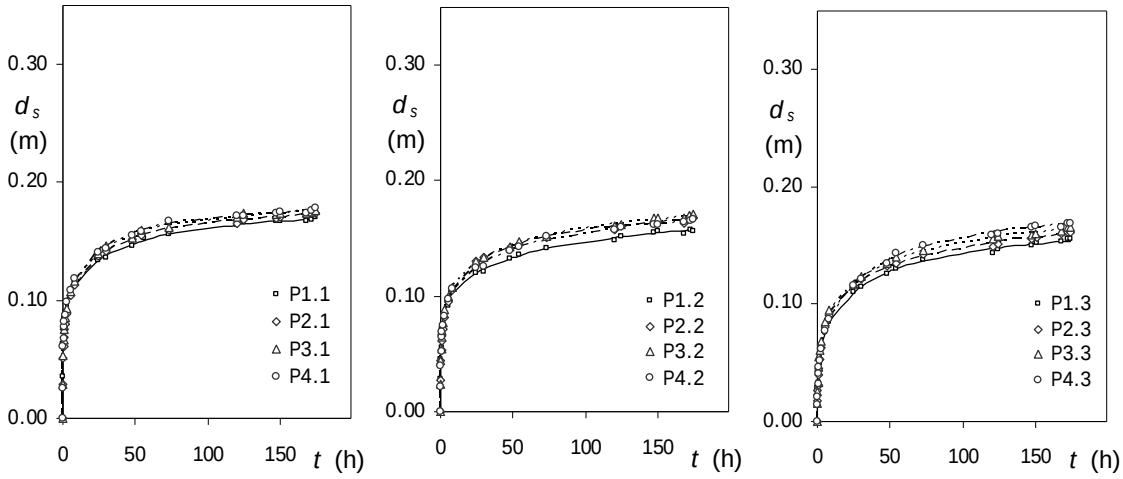

Test 73

P1.1		P2.1		P3.1		P4.1		P1.2		P1.3	
t (h)	d_s (m)	t (h)	d_s (m)	t (h)	d_s (m)	t (h)	d_s (m)	t (h)	d_s (m)	t (h)	d_s (m)
0.00	0.000	0.00	0.000	0.00	0.000	0.00	0.000	0.00	0.000	0.00	0.000
0.05	0.036	0.03	0.029	0.03	0.029	0.02	0.026	0.08	0.029	0.22	0.016
0.32	0.064	0.30	0.051	0.30	0.054	0.28	0.061	0.37	0.045	0.42	0.029
0.57	0.073	0.55	0.061	0.55	0.066	0.53	0.068	0.62	0.055	0.67	0.034
0.90	0.082	0.88	0.069	0.88	0.075	0.87	0.077	0.95	0.067	1.00	0.043
1.60	0.089	1.58	0.080	1.58	0.086	1.57	0.088	1.65	0.075	1.70	0.054
2.53	0.098	2.55	0.089	2.57	0.093	2.58	0.099	2.60	0.085	2.65	0.061
5.03	0.108	5.05	0.104	5.07	0.107	5.08	0.109	5.10	0.092	5.15	0.076
8.02	0.115	8.03	0.113	8.05	0.116	8.07	0.119	8.07	0.107	8.13	0.085
24.55	0.134	24.53	0.137	24.52	0.140	24.50	0.141	24.62	0.120	24.68	0.110
29.90	0.137	29.88	0.141	29.87	0.146	29.85	0.145	29.97	0.122	30.03	0.115
47.75	0.146	47.73	0.152	47.72	0.153	47.70	0.155	47.82	0.132	47.88	0.126
56.10	0.152	54.08	0.155	54.07	0.159	54.03	0.159	54.17	0.136	54.23	0.131
72.90	0.156	72.88	0.160	72.87	0.162	72.82	0.167	72.97	0.142	73.03	0.138
120.28	0.164	120.27	0.165	120.25	0.171	120.23	0.172	120.35	0.148	120.42	0.143
147.53	0.167	147.52	0.170	147.50	0.173	147.48	0.174	147.60	0.156	147.67	0.150
150.47	0.167	150.45	0.171	150.43	0.174	150.42	0.175	150.53	0.156	150.60	0.152
167.98	0.167	167.97	0.173	167.95	0.174	167.93	0.173	168.05	0.154	168.12	0.153
172.27	0.169	172.25	0.174	172.23	0.175	172.22	0.176	172.33	0.158	172.40	0.156
174.35	0.170	174.17	0.174	174.15	0.176	174.13	0.178	174.25	0.157	174.32	0.156

Test	α (º)	s (m)	s/D_p	n	W_g (m)	t_d (day)	d_{sge} (m)	d_{sge}/d_{se1}
74	90	0.225	4.5	3	0.200	7.2	0.151	1.11

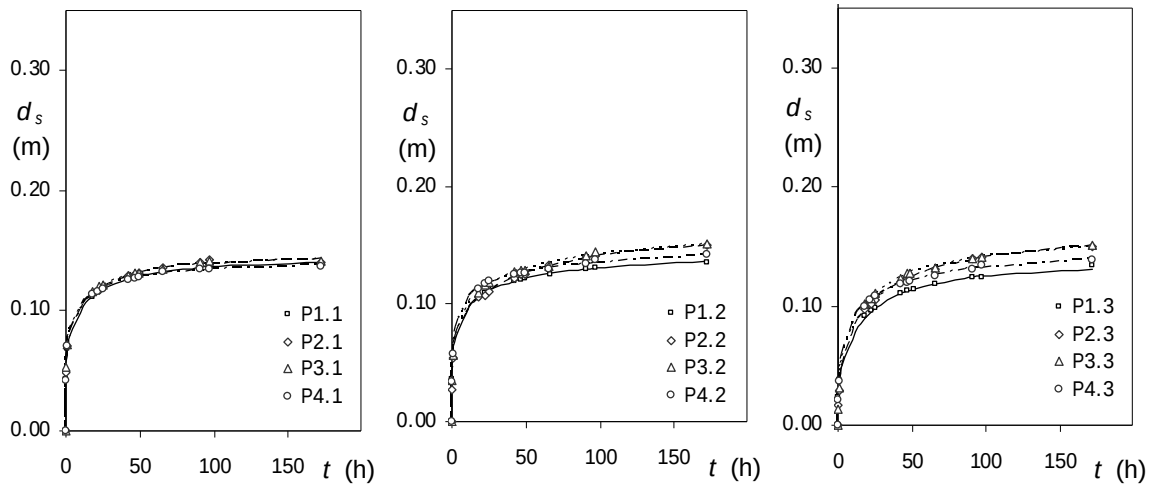

Test 74

P1.1		P2.1		P3.1		P4.1		P1.2		P1.3	
t (h)	d_s (m)	t (h)	d_s (m)	t (h)	d_s (m)	t (h)	d_s (m)	t (h)	d_s (m)	t (h)	d_s (m)
0.00	0.000	0.00	0.000	0.00	0.000	0.00	0.000	0.00	0.000	0.00	0.000
0.07	0.043	0.07	0.048	0.05	0.053	0.05	0.042	0.12	0.036	0.17	0.023
0.83	0.068	0.83	0.071	0.82	0.072	0.82	0.071	0.88	0.056	0.92	0.038
3.00	0.080	3.00	0.082	3.00	0.087	3.00	0.084	3.00	0.072	3.00	0.050
12.00	0.104	12.00	0.106	12.00	0.108	12.00	0.106	12.00	0.098	12.00	0.079
17.83	0.111	17.82	0.114	17.82	0.115	17.80	0.114	17.88	0.105	17.92	0.091
21.98	0.116	21.97	0.117	21.97	0.120	21.95	0.116	22.02	0.110	22.08	0.096
25.33	0.118	25.32	0.121	25.32	0.122	25.30	0.119	25.37	0.114	25.42	0.099
42.35	0.127	42.33	0.129	42.33	0.129	42.32	0.126	42.40	0.120	42.43	0.110
46.55	0.128	46.55	0.130	46.53	0.131	46.53	0.128	46.60	0.121	46.63	0.113
49.02	0.129	49.00	0.132	49.00	0.131	48.98	0.128	49.05	0.121	51.08	0.114
65.85	0.133	65.85	0.136	65.83	0.135	65.83	0.132	65.90	0.126	65.93	0.118
90.80	0.137	90.80	0.140	90.78	0.140	90.78	0.134	90.83	0.130	90.88	0.124
97.13	0.138	97.13	0.143	97.12	0.141	97.12	0.135	97.17	0.131	97.22	0.124
171.75	0.139	171.75	0.140	171.73	0.142	171.73	0.137	171.78	0.136	171.82	0.135

Test	α (º)	s (m)	s/D_p	n	W_g (m)	t_d (day)	d_{sge} (m)	d_{sge}/d_{se1}
75	90	0.300	6.0	3	0.200	7.0	0.145	1.07

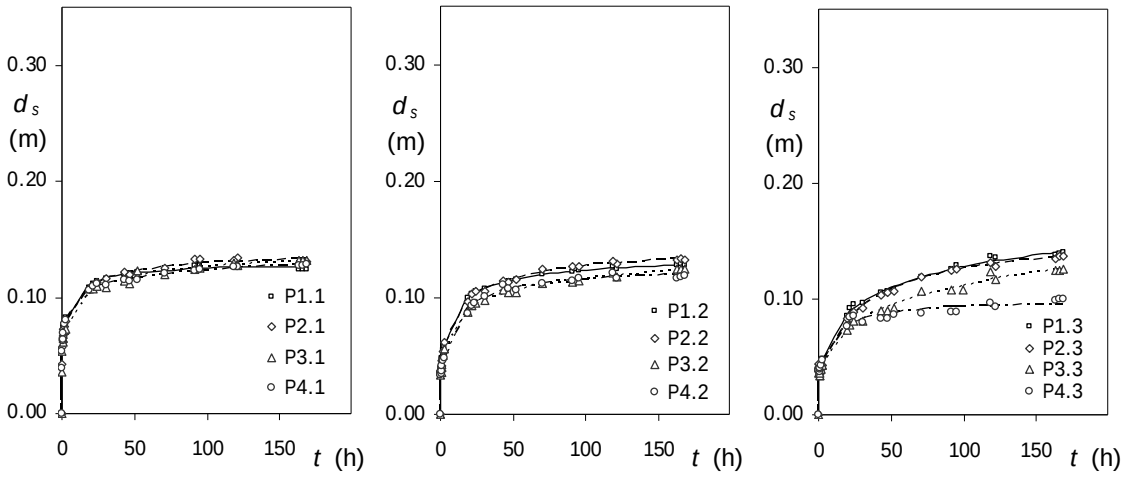

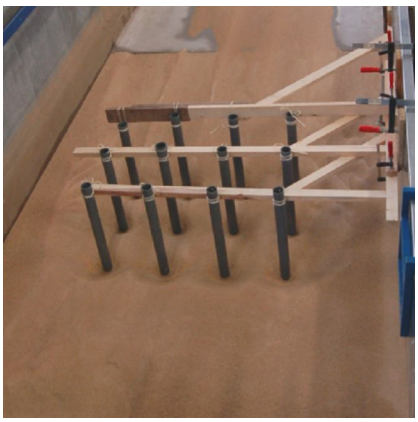

Test 75

P1.1		P2.1		P3.1		P4.1		P1.2		P1.3	
t (h)	d_s (m)	t (h)	d_s (m)	t (h)	d_s (m)	t (h)	d_s (m)	t (h)	d_s (m)	t (h)	d_s (m)
0.00	0.000	0.00	0.000	0.00	0.000	0.00	0.000	0.00	0.000	0.00	0.000
0.08	0.055	0.07	0.042	0.05	0.036	0.03	0.040	0.15	0.032	0.22	0.038
0.30	0.064	0.28	0.057	0.27	0.054	0.25	0.054	0.35	0.039	0.42	0.036
0.58	0.068	0.57	0.062	0.55	0.061	0.53	0.063	0.65	0.044	0.72	0.038
1.08	0.076	1.07	0.073	1.05	0.068	1.03	0.069	1.15	0.049	1.22	0.041
1.72	0.078	1.70	0.075	1.68	0.072	1.67	0.078	1.78	0.055	1.85	0.045
2.42	0.083	2.40	0.080	2.38	0.073	2.37	0.081	2.48	0.059	2.55	0.048
18.92	0.109	18.93	0.107	18.95	0.107	18.98	0.106	19.30	0.100	19.35	0.085
21.75	0.112	21.73	0.110	21.72	0.107	21.70	0.110	21.83	0.103	21.90	0.092
23.83	0.114	23.82	0.113	23.80	0.110	23.78	0.112	23.90	0.106	23.97	0.095
30.68	0.116	30.70	0.116	30.72	0.108	30.73	0.111	30.78	0.108	30.85	0.097
46.82	0.121	47.00	0.120	47.02	0.112	47.03	0.114	47.07	0.113	47.37	0.107
51.77	0.122	51.78	0.121	51.80	0.123	51.75	0.115	51.83	0.116	51.90	0.107
70.50	0.126	70.48	0.126	70.47	0.120	70.45	0.121	70.57	0.120	70.63	0.119
91.50	0.127	91.20	0.133	91.18	0.124	91.17	0.123	91.28	0.122	91.35	0.126
118.47	0.126	118.45	0.132	118.43	0.130	118.42	0.127	118.53	0.126	118.60	0.136
163.13	0.124	163.12	0.129	163.10	0.132	163.08	0.128	163.20	0.128	163.27	0.138
165.65	0.124	165.63	0.130	165.62	0.132	165.60	0.128	165.72	0.129	165.78	0.140
168.55	0.125	168.53	0.130	168.52	0.132	168.50	0.129	168.62	0.128	168.68	0.140

APPENDIX C – TESTS SPECIALLY DESIGNED TO ISOLATE THE EFFECT OF VISCOSITY

Test	B (m)	D_{50} (mm)	D_p (m)	d (m)	d/D_p	D_p/D_{50}	U_c (ms^{-1})	Q (ls^{-1})	U (ms^{-1})	B/d	B/D_p	u_* (ms^{-1})	t_d (hour)
1	2.00	0.86	0.050	0.050	1.0	58.1	0.281	27	0.272	40.0	40.0	0.0162	168

T (ºC)	ν ($10^{-6}m^2s^{-1}$)	u_*D_{50}/ν	UD_{50}/ν	UD_p/ν	Ud/ν	d_{se} (m)	d_{se}/D_p
15 - 20	1.156 – 1.004	12.9	217	12615	12615	0.116	2.31

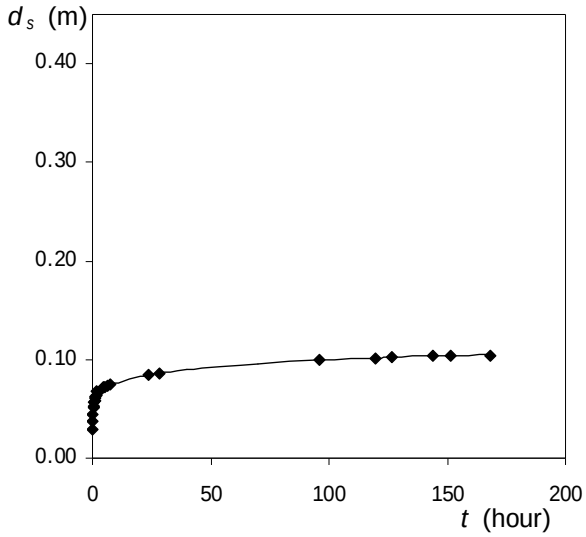

Test 1

t (hour)	d_s (m)	t (hour)	d_s (m)	t (hour)	d_s (m)
0.00	0.000	2.08	0.066	119.58	0.102
0.05	0.029	1.58	0.068	126.83	0.102
0.18	0.037	4.65	0.072	143.73	0.104
0.27	0.045	5.40	0.073	151.45	0.104
0.38	0.051	6.33	0.074	168.03	0.104
0.48	0.053	7.53	0.074		
0.73	0.057	23.93	0.084		
0.88	0.059	28.55	0.087		
1.10	0.061	40.00	0.090		
1.35	0.063	70.00	0.096		
1.58	0.064	96.08	0.099		

Test	B (m)	D_{50} (mm)	D_p (m)	d (m)	d/D_p	D_p/D_{50}	U_c (ms^{-1})	Q (m^3s^{-1})	U (ms^{-1})	B/d	B/D_p	u_* (ms^{-1})	t_d (hour)
2	2.00	0.86	0.050	0.075	1.5	58.1	0.293	43	0.284	26.7	40.0	0.0159	168

T (ºC)	ν ($10^{-6}m^2s^{-1}$)	u_*D_{50}/ν	UD_{50}/ν	UD_p/ν	Ud/ν	d_{se} (m)	d_{se}/D_p
15 - 20	1.156 – 1.004	12.7	226	13137	19705	0.119	2.38

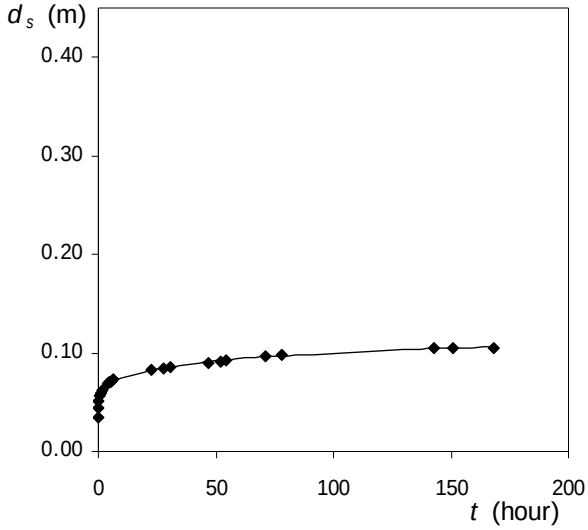

Test 2

t (hour)	d_s (m)	t (hour)	d_s (m)	t (hour)	d_s (m)
0.00	0.000	6.20	0.073	168.00	0.105
0.07	0.035	22.82	0.083		
0.20	0.044	27.50	0.084		
0.27	0.051	30.40	0.086		
0.67	0.056	46.90	0.090		
1.13	0.060	51.83	0.092		
1.45	0.062	54.53	0.092		
3.82	0.069	71.07	0.096		
4.58	0.071	77.85	0.098		
5.17	0.071	142.77	0.105		
5.82	0.072	150.67	0.105		

Test	B (m)	D_{50} (mm)	D_p (m)	d (m)	d/D_p	D_p/D_{50}	U_c (ms^{-1})	Q (m^3s^{-1})	U (ms^{-1})	B/d	B/D_p	u_* (ms^{-1})	t_d (hour)
3	4.00	1.28	0.075	0.075	1.0	58.6	0.343	100	0.333	53.3	53.3	0.0197	169

T (ºC)	ν ($10^{-6}m^2s^{-1}$)	u_*D_{50}/ν	UD_{50}/ν	UD_p/ν	Ud/ν	d_{se} (m)	d_{se}/D_p
18	1.065	23.7	400	23437	23437	0.167	2.23

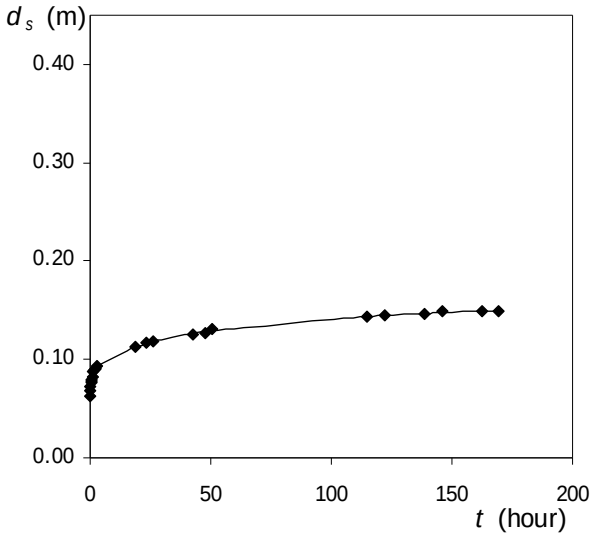

Test 3

t (hour)	d_s (m)	t (hour)	d_s (m)	t (hour)	d_s (m)
0.00	0.000	2.57	0.094	162.38	0.149
0.08	0.062	18.55	0.113	169.40	0.149
0.17	0.068	23.38	0.117		
0.27	0.072	26.32	0.119		
0.37	0.076	42.65	0.125		
0.47	0.079	47.47	0.126		
0.60	0.080	50.57	0.131		
0.97	0.083	114.70	0.144		
1.33	0.087	122.38	0.145		
1.70	0.090	138.43	0.147		
2.02	0.091	146.10	0.149		

Test	B (m)	D_{50} (mm)	D_p (m)	d (m)	d/D_p	D_p/D_{50}	U_c (ms^{-1})	Q (m^3s^{-1})	U (ms^{-1})	B/d	B/D_p	u_* (ms^{-1})	t_d (hour)
4	1.50	3.00	0.175	0.175	1.0	58.3	0.525	134	0.509	8.6	8.6	0.0325	168

T (ºC)	ν ($10^{-6}m^2s^{-1}$)	u_*D_{50}/ν	UD_{50}/ν	UD_p/ν	Ud/ν	d_{se} (m)	d_{se}/D_p
24	0.923	105.6	1655	96541	96541	0.296	1.69

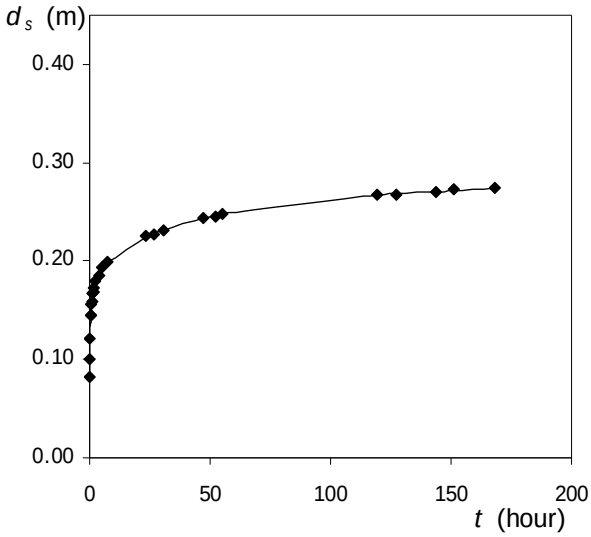

Test 4

t (hour)	d_s (m)	t (hour)	d_s (m)	t (hour)	d_s (m)
0.00	0.000	2.45	0.180	127.32	0.268
0.05	0.082	3.83	0.186	143.52	0.270
0.13	0.100	4.98	0.193	151.25	0.273
0.27	0.121	7.20	0.199	168.05	0.274
0.40	0.145	23.25	0.226		
0.53	0.145	26.98	0.228		
0.70	0.156	30.88	0.231		
0.95	0.159	47.07	0.244		
1.20	0.167	52.12	0.245		
1.45	0.169	55.10	0.248		
1.95	0.173	119.15	0.268		

Test	B (m)	D_{50} (mm)	D_p (m)	d (m)	d/D_p	D_p/D_{50}	U_c (ms^{-1})	Q (m^3s^{-1})	U (ms^{-1})	B/d	B/D_p	u_* (ms^{-1})	t_d (hour)
5	1.50	3.00	0.175	0.263	1.5	58.3	0.547	209	0.530	5.7	8.6	0.0322	193

T (ºC)	ν ($10^{-6}m^2s^{-1}$)	u_*D_{50}/ν	UD_{50}/ν	UD_p/ν	Ud/ν	d_{se} (m)	d_{se}/D_p
24	0.923	104.7	1723	100536	150804	0.324	1.85

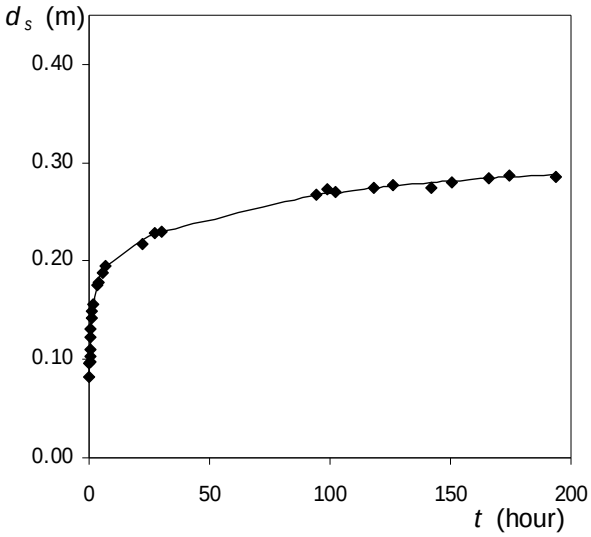

Test 5

t (hour)	d_s (m)	t (hour)	d_s (m)	t (hour)	d_s (m)
0.00	0.000	3.17	0.176	126.18	0.278
0.13	0.083	4.03	0.178	142.05	0.274
0.23	0.096	5.50	0.189	150.42	0.280
0.33	0.098	6.83	0.194	166.00	0.285
0.43	0.103	21.93	0.218	174.18	0.287
0.52	0.111	27.12	0.228	193.47	0.286
0.67	0.122	30.18	0.229		
0.83	0.131	94.50	0.268		
1.03	0.142	99.07	0.273		
1.25	0.150	102.23	0.270		
1.50	0.156	118.28	0.275		